ANALYTICAL METHODOLOGY TO PREDICT THE BEHAVIOUR OF MULTI-PANEL CLT SHEARWALLS SUBJECTED TO LATERAL LOADS

by

Vincent Nolet

A thesis submitted in partial fulfillment of the requirements for the

Master of Applied Science in Civil Engineering

University of Ottawa

September 2017

Abstract

The increasing demand for more sustainable construction has led to the development of new structural systems that include wood as building material. Cross laminated timber (CLT) has been identified as a potential system to address this need and to provide alternative options in the range of low- to medium-rise construction. The appeal in using CLT as a shearwall is driven by the combination of the rigid panels and small dimension fasteners, which allows for significant energy dissipation in the structure. However, there is currently no reliable analytical model to accurately predict the behaviour of multi-segment CLT shearwalls.

The current study aims to develop an analytical model capable of predicting the elastic and plastic phases associated with the behaviour of multi-panel CLT shearwalls. The model describes the wall behaviour as a function of the connectors' properties in terms of stiffness, strength and ductility. This dependency means that the only input required in the model is the behavioural parameters of the connections. The proposed model contains six cases with a total of 36 different failure mechanisms. Two final wall behaviours were developed, and it was found that behaviour (i.e. single wall) could be achieved if the yielding in the hold-down occurred prior to yielding in the panel joints. Inversely, the other behaviour (i.e. coupled panels) was achieved if the yielding in the vertical joint occur prior to yielding in the hold-down. The analytical model was validated using a numerical model, and the results of the comparison showed very close match between the two models.

The study proposed simplified design provisions with the aim to optimize the walls ductility (CP behaviour) or strength and stiffness (SW behaviour).

Acknowledgement

I will always be grateful for the experiences I have had throughout my studies, thinking of all the professors who taught me or supervised me in undergraduate projects and allowed me to develop my professionalism.

I would like to sincerely thank my supervisor Dr. Ghasan Doudak for is guidance, time and devotion for me to fulfill this project. I am also grateful for the opportunity he gave me to work on this project prepared in collaboration with Dr. Daniele Casagrande.

On that note, I also want to acknowledge Dr. Daniele Casagrande for his guidance and his positive work ethic throughout this project which made it very pleasant to work with.

I also want to extend my appreciation to my fiancée Véronique Fugère for her moral support throughout the years and for her understanding.

Finally, I want to thank my family and friends for their constant encouragement and belief in my potential since the beginning of my studies. Also, I am grateful for their encouragement and for sharing good moments alongside my projects.

Table of Content

List of Tables

List of Figures

List of Symbols

b	=	Width of a single panel
B	=	Total length of the wall
$d_{u,c}$	=	Ultimate displacement capacity of a fastener
$d_{u,h}$	=	Ultimate displacement capacity of the hold-down
$d_{y,c}$	=	Yielding displacement of a fastener
$d_{y,h}$	=	Yielding displacement of the hold-down
f^{pl,j^*}	=	Increase of lateral force in the plastic state of kinematic mode j^*
F	=	Lateral force applied on top of the wall
F_q	=	Activation force
F_{c,y,i,j^*}	=	Force in each fastener of a vertical joint in kinematic mode j^*
F_t^{el,j^*}	=	Value of transitional force in the elastic state between kinematic mode j^* and $j^* + 1$
F_t^{pl,j^*}	=	Value of transitional force in the plastic state between kinematic mode j^* and $j^* + 1$
h	=	Height of the panels
j^*	=	Kinematic mode of the wall
$\tilde{j}$	=	Kinematic mode achieved in the elastic state
$\hat{j}$	=	Kinematic mode achieved in the plastic state
$\widetilde{k}$	=	Dimensionless stiffness ratio
k_c	=	Elastic stiffness of a single fastener in the vertical joint
k_h	=	Elastic stiffness of the hold-down
$k_h'^{\,el,j^*}$	=	Elastic equivalent hold-down tensile stiffness in kinematic mode j^*
k_H^{el,j^*}	=	Elastic equivalent lateral stiffness of the wall in kinematic mode j^*

$k_h'^{\,\mathrm{p}l,j^*}$	=	Plastic equivalent hold-down tensile stiffness in kinematic mode j^*
k_H^{pl,j^*}	=	Plastic equivalent lateral stiffness of the wall in kinematic mode j^*
m	=	Number of panel of the wall
n	=	Number of fasteners in the vertical joint
q	=	Uniformly distributed vertical load
$\tilde{q}$	=	Dimensionless loads ratio
r_c	=	Strength of fasteners
r_h	=	Strength of the hold-down
R_{c,j^*}	=	Reaction force from the ground on panel j^*
$R_{w,c}^{el,j^*}$	=	Elastic strength related to the vertical joint in kinematic mode j^*
$R_{w,h}^{el,j^*}$	=	Elastic strength related to the hold-down in kinematic mode j^*
R_w^{pl}	=	Plastic strength of the wall
s	=	Spacing between fasteners in a vertical joint
$t^{pl,1}$	=	Increase of tension force in the hold-down in plastic state for kinematic mode 1
$T^{el,\tilde{j}}$	=	Hold-down tension force in kinematic mode $\tilde{j}$ at elastic strength
v_j^{el,j^*}	=	Elevation of panel j in the elastic state in kinematic mode j^*
$v_j'^{\,pl,j^*}$	=	Elevation of panel j in the plastic state in kinematic mode j^* after the increase of force to yield vertical joint $j^* - 1$
v_j^{pl,j^*}	=	Elevation of panel j in the plastic state in kinematic mode j^*
V_c^{el,j^*}	=	Total elongation of fasteners attained in kinematic mode j^* in the elastic state
V_0^{el,j^*}	=	Total elongation of hold-down attained in kinematic mode j^* in the elastic state
V_c^{pl,j^*}	=	Total elongation of fasteners attained in kinematic mode j^* in the plastic state

V_0^{pl,j^*}	=	Total elongation of hold-down attained in kinematic mode j^* in the plastic state
$\delta_{h,t}^{pl,j^*+1}$	=	Increase of displacement (plateau) between kinematic mode $j^* + 1$ and j^*
Δ_h^{el}	=	Displacement achieved at elastic strength
$\Delta_{h,t}^{el,j^*}$	=	Value of transitional displacement in the elastic state between kinematic mode j^* and $j^* + 1$
Δ_h^{pl}	=	Displacement achieved at plastic strength
$\Delta_{h,t}^{pl,j^*}$	=	Value of transitional displacement in the plastic state between kinematic mode j^* and $j^* + 1$
$\Delta_{h,t}^{pl,j^*+1,k}$	=	Total displacement of the wall after reattachment of panel j^* with the ground in plastic state
Δ_h^u	=	Ultimate displacement capacity of the wall
$\vartheta'^{\,j^*}$	=	Variation of angle of rotation in kinematic mode j^*
μ_w	=	Ductility of the wall

CHAPTER 1 - Introduction

1.1 General

The increasing demand for more sustainable construction has led to the development of new structural systems that include wood as building material. One of the most recent engineered wood products (EWP) in North America nowadays is cross-laminated timber (CLT), which is a simple yet innovative product that possesses high levels of strength and stiffness and allows for two-way bending action due to the layout of its laminates. The product is manufactured by gluing together lumber pieces orthogonally to one another (Figure 1-1), thereby creating slabs consisting of dimensions that are between 0.5m to 3m in width, and 72mm to 400mm in thickness (CLT Handbook). The massiveness of the slabs makes them suitable for structural floor and wall systems. In particular, the high in-plan stiffness makes CLT suitable to be used as shearwalls and diaphragms, where the panels can be considered to act as rigid bodies under lateral load while allowing energy dissipation through deformation in the connectors.

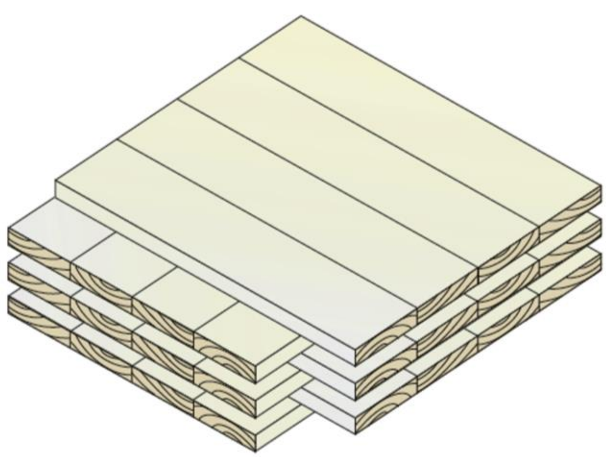

Figure 1-1: CLT Configuration (FPInnovation, 2011)

The size of the CLT panels is limited primarily by transportation restrictions. Another motivation to limiting the size of the wall segments is the need to develop some ductility in the system by introducing more joints between the wall panels. The panel-to-panel connections (also referred to in this thesis as vertical joints and panel joints) typically consist of small dimension fasteners such as nails or self-tapping screws. The combination of the rigid panels and small dimension fasteners means that the wall becomes more flexible (when compared to the stiffness of a wall of same size but consisting of a single panel) but it also provides significant amount of ductility to the structure. The wall panels are typically connected to the floor diaphragm using angle brackets that would help resist the shear and hold-down that are typically placed at the ends of each wall to resist the uplift force due to the overturning. Figure 1-2 illustrates typical multi-panel shearwall configuration, and indicates typical placement and detailing of panel joints, angle brackets and hold-downs.

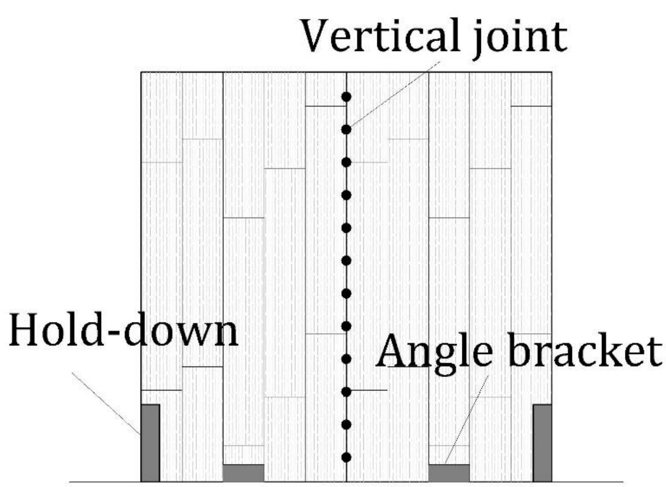

Figure 1-2: Typical CLT Shearwall Configuration

There is currently no reliable analytical model to accurately predict the behaviour of multi-segment CLT shearwalls. The capacity is typically determined by designers by means of static equilibrium considerations using simplifying assumptions or by sophisticated models, where the CLT panels are assumed as shell elements and the connections as linear or non-linear links. Current design standards in Canada (CSA O86) provides guidelines regarding the design of CLT shearwalls that require the connections to be moderately ductile. However, the standard does not yet contain any ductility classification of connections in order to clearly identify an appropriate connection system to dissipate the energy required. One way designers have addressed this issue is by under-designing the vertical joints in order to increase the wall ductility, however this may lead to design configurations that does not allow the shearwall to attain its full capacity potential. In the current version of Eurocode 8 (2013), which deals with the design of structures for earthquake resistance, there are currently no provisions for the design of CLT structures. However, the values for ductility factors and specific capacity design rules are currently being developed by the committee.

1.2 Scope of Research

The current study aims to develop an analytical model capable of predicting the elastic and plastic phases associated with the behaviour of multi-panel CLT shearwalls. The proposed model is derived based on the stiffness, strength and ductility behaviour of the connectors. The model aims to provide a full description of the wall behaviour, which could also lead to a more efficient design of CLT shearwalls. The approach will propose the solution according to possible wall behaviours and establishes expressions that can associate the ultimate displacement of the wall with the properties of connectors used. The analytical model is validated using numerical modelling for the entire force-displacement behaviour of the wall.

1.3 Research Objectives

The overarching goal of this research study is to develop an analytical procedure that can reliably describe the behaviour of CLT shearwalls in elastic and plastic regions. The aim is to derive expressions that will enable the development of the complete force-displacement curve for multi-panel wall systems. The model requires inputs such as strength, yielding displacement and ultimate displacement of both hold-down and fasteners in vertical joints. The proposed model can also help identify test matrices for experimental programs dealing with CLT shearwalls, since certain failure modes can be difficult to predict. It also provides an accurate method to determine the overall ductility of the wall according to the properties of connectors. Another objective of this study is to provide simplified design methodologies and expressions that can help the designer determine the kinematic modes and allow accurate predictions of the capacity, displacement and ductility for simple design cases.

The objectives outlined herein are achieved by following the methodology described below:

1. Conduct a detailed review of the available literature on the subject of behaviour of CLT shearwalls subjected to lateral loads. This includes a summary presentation of an analytical approach developed for elastic behaviour of multi-panel CLT wall by Casagrande et al. (2017). This study lays the foundation to the current study, where analytical expressions developed in the elastic range are extended to include the behaviour in the plastic range.
2. Develop general cases that are dominated by either the hold-downs or panel vertical joints to predict the final kinematic mode of failure for multi-panel CLT shearwalls.
3. From the developed general cases outlined in point 2 above, numerous modes of failure are established and related to behaviour the vertical joint and hold-down connections.

4. A validation of the predicted behaviour of the multi-panel shearwall is carried out by means of a numerical model developed using a commercially available finite element (FE) software.
5. Finally, implication of the proposed approach on design is discussed and design guidelines are provided to help optimize of the CLT shearwalls design according to the analytical model developed.

1.4 Thesis Organization

Chapter 1 provides a general introduction to CLT as an engineered wood product and describes the research needs, goals and how the current study aims to contribute to the state of knowledge.

Chapter 2 reviews the available literature on experimental and analytical studies dealing with the behaviour of multi-panel CLT shearwalls subjected to lateral loading.

Chapter 3 defines the variables used in the proposed model and presents general concepts required to define the behaviour of CLT shearwalls.

Chapter 4 and Chapter 5 present the proposed analytical model based on the expected kinematic mode of the wall.

Chapter 6 compares the analytical model with a numerical analysis based on a commercially available FE software.

Chapter 7 discusses the current design provisions and proposed simplified analytical provision based on the current research.

Chapter 8 presents the conclusions and future work arising from the current study.

CHAPTER 2 - Literature Review

2.1 Introduction

This chapter presents the state of the art knowledge on the behaviour of CLT shearwalls subjected to lateral loading. The majority of the existing research involves experimental studies at the building, wall or joint levels. These studies are presented in Sections 2.2. Comparison between experimental results and numerical models is presented in Section 2.3. Finally, studies suggesting analytical models are presented in Section 2.4.

2.2 Experimental Studies

2.2.1 Ceccotti et al. (2006)

The SOFIE project was a comprehensive study covering CLT building behaviour, including building physics, fire, durability and earthquake. The research was undertaken in collaboration with the Italian National Research Council - Trees and Timber Institute (CNR-IVALSA), the Karlsruhe Institute of Technology and the National Institute for Earth Science and Disaster Prevention (NIED) of Japan to design. The aim of the project was to conduct experimental testing on full-scale CLT buildings subjected to earthquake loading simulated using a shaking table. The researchers performed reverse cyclic and monotonic loading on a one-storey CLT structure with the aim to investigate the joint behaviour and to ensure ductile behaviour. Three- and seven-storey buildings were also tested using a shaking table facility. The authors concluded that no residual displacement was observed after 10 simulated earthquake events and that the fasteners behaved in a ductile manner. Also, no permanent deformation was observed after the testing. However, high accelerations were measured at upper storey of the seven-storey building and required further investigation.

2.2.2 Popovski and Karakabeyli (2012)

The main objective of this study was to determine the structural properties of typical CLT shearwalls. The focus was on developing ductility factors that can be appropriately used in design. Different variables such as panel’s aspect ratios, types of connectors and opening configurations were investigated. The study found that the stiffness of the walls increased with the increase of vertical loads. Based on the test results, the authors proposed R_d and R_o factors equal to 2.0 and 1.5, respectively. It was also concluded that using nails in discrete hold-downs would increase seismic performance by providing more ductility to the system.

2.2.3 Gavric et al. (2013)

Gavric et. al. (2013) performed cyclic loading tests on CLT walls to establish their behaviour and ability to dissipate energy. The study established that coupled wall behaviour provides lower elastic stiffness and strength capacity than single wall behaviour. However, this behaviour exhibited more displacement capacity and ductility. When the panels deflected together as a single wall it exhibited high strength and performed better in term of total dissipated energy until a certain inter-storey drift. It was found that the sliding and rocking motions are the main sources of wall displacement. It was also noted that rocking (as opposed to sliding) behavior was desirable since the walls tend to return to their initial position. The displacement related to rocking motion was reduced by including hold-downs at the wall ends and by applying a vertical load on the wall. The authors recommend that the hold-down be used as part of the energy dissipative joints while the angle bracket remains in the elastic range.

2.2.4 Sadeghi and Smith (2014)

This study focussed on experimentally investigating half-lapped and single spline CLT connections. Both type of connections used self-tapping screws and were subjected to in-plane shear forces. The failure modes of the fasteners were evaluated with and without washers. The inclusion of washer was reported to influence the failure mechanisms. For the cases with no washer, the failure mode was governed by the pull-through resistance of the head-side of the screw. By including the washer, the mode of failure was governed by the withdrawal resistance of the screw's threaded portion. The washer also caused a significant increase in the capacity of the joints.

2.2.5 Gavric et al. (2015b)

This study evaluated the strength, stiffness, and energy dissipation of CLT connections using screws and investigated configurations that mimic wall-to-wall, floor-to-floor and wall-to-floor joints. The study experimentally investigated screw connections in 5-ply CLT panels for in-plane monotonic, cyclic shear and withdrawal loading. It was concluded that the step-joints exhibited 50% higher initial stiffness compared to the spline joints. However, the spline joints had 40% higher resistance and ultimate displacement. For connections tested in tension, the half-lap joints failed in splitting or in the inner layers due to the failure of glued. Spline connection failed with pull-through of screw head forming a plastic hinge. The authors also observed that sufficient spacing, end distances and edge distances were required to avoid brittle failure mode. Finally, an over-strength factor of 1.6 was proposed for CLT connection using screws.

2.2.6 Popovski and Gavric (2016)

Popovski and Gavric (2016) performed full-scale testing of a two-storey CLT structure with the main objective to investigate its behaviour under quasi-static and cyclic loading. The study investigated different connection configuration and details. It was found that the reduction in the number of screws in perpendicular wall-to-wall connections did not have a significant effect on the overall resistance however it led to an increase in lateral displacement. Also, it was found that the number and type of fasteners and the aspect ratio of panels contribute to the behaviour and mode of deformation of CLT walls. The authors observed that the relative slip between floor panels in the test configurations was negligible according to their experiments. It is noteworthy to mention that the study found that placing the angle brackets in the middle of a wall segment meant that they were loaded mostly in shear since the rocking movement had a small effect in this area. This finding has implications on some of the assumptions made in the current study when developing the analytical model.

2.2.7 Hossain et al. (2016)

Hossain et. al. (2016) investigated the capacity of the panel-to-panel connection under pure shear loads for a 3-ply CLT panels using self-tapping screws (STS). Three connection types were tested including half-lap, surface spline and butt joints. The butt joint was considered because it does not require machining, thereby providing a cheap alternative. Vertical joints of CLT walls with butt joints connected using STS installed at an angle of 45° to the joint line and 32.5° to the face of the panel were investigated under pure shear loading. The STS fasteners were installed with different orientations at each shear plane so that half of the STS were in tension and the other half in compression. The connection was characterized as stiff and with little energy dissipation capability. The study concluded that the connection capacity can be conservatively estimated using the withdrawal resistance of the individual self-tapping screws. In terms of ductility, STS installed in double inclination exhibited high and moderate ductility classification for quasi-static monotonic and reversed cyclic test, respectively.

2.3 Comparison between Experimental Tests and Numerical Analysis

2.3.1 Shen et al. (2013)

Shen et. al. investigated the behaviour of CLT walls and connectors with the aim of comparing test results to existing commercially available numerical hysteretic models, namely SAWS (Folz, and Filiatrault, 2001) and Pinching 4 (Lowes and Mitra, 2004). Both these models consider strength and stiffness degradation of the connectors. To calibrate the numerical model, connection specimens were tested under CUREE loading protocols (ASTM E2126-11) to quantify the monotonic and cyclic envelope curves. The study concluded that under monotonic and cyclic loading, Pinching 4 developed better fit in comparison with experimental tests because it considered more degrees of freedom. Also, it was observed that increasing in the connection strength longitudinal to the grain can improve the capacity of CLT shearwalls for the boundary condition tested.

2.3.2 Yasumura et al. (2016)

This study aimed at investigating the performance of a three-storeys building under lateral loading. and compared the experimental test results with finite element model (FEM). The experimentally investigation included reverse cyclic loading of multi-panel walls and single-panel wall. 3-D nonlinear analysis was performed using a numerical software, in which elastic properties of the connectors were determined from experimental test and included in the model. The study found that the stiffness of the single-panel wall was more than twice the value of that found in the multi-panel wall. The ductility ratio of both wall configurations was found to be more than 3.0. The viscous damping of the multi-panel wall was found to be higher than that of single-panel wall. The FEM analysis was deemed capable of predicting the behaviour of the CLT structure. The displacement found for the multi-panel walls was mainly due to rocking behaviour. The q value, which accounts for ductility of the system in seismic design was found to be 2.0 regardless of the size of the CLT wall panel.

2.3.3 Pozza and Trutalli (2016)

Pozza and Trutalli (2016) developed a correlation between the capacity of the energy-dissipative connectors, the wall slenderness and the q-factor. This was done by conducting 2-D analysis of 24 walls using a numerical software. The model assumed that the angle brackets resist shear forces, and the hold-downs resist the overturning force. The CLT panels were assumed to have high in-plane stiffness and the connectors were assumed to have non-linear behaviour following Pinching 4 (Lowes and Mitra, 2004) hysteresis model. Nonlinear dynamic analysis was performed and the results were compared with experimental or numerical analysis available in literature. It was found that the energy dissipation and seismic response were dependant on the slenderness and the characteristics of the vertical joint between panels. It is also found that a q factor of 2.0 was too conservative for multi-panel CLT walls.

2.4 Existing Analytical Model

2.4.1 Gavric et al. (2015a)

This study investigated single and coupled CLT shearwall behaviours with different panel-to-panel and anchorage connection types. This analytical solution was compared with 16 cyclic tests with different connection layout. The study found that the in-plane deformation in CLT panel were almost negligible. The vertical load improved the lateral resistance, stiffness and ductility of the wall. The importance of the vertical joint was also highlighted. The number of self-tapping screws affected the wall stiffness, lateral capacity and kinematic mode. For wall design, the authors propose to design angle brackets to stay elastic in shear after a seismic event to prevent any residual slip.

An analytical model was also developed for rocking displacement for the different possible behaviours the wall. An equation was also proposed for sliding deformation regarding the angle brackets deformation with the assumption that the hold-down only resist the rocking movement and have no contribution to the horizontal slip.

2.4.2 Casagrande et al. (2017)

Casagrande et. al. (2017) proposed a mathematical model to determine the mechanical behaviour of multi-panel CLT shearwalls based on the minimum potential energy approach. The model considers the hold-down to resist rocking movement only, while the panel-to-panel joint resisted the shear force. For the different wall behaviours, an analytical model was proposed that was capable of determining the lateral displacement, forces in the hold-down, vertical joint and CLT panel, as a function of the relative connectors' stiffness. From the analytical model, the authors established that each panel of multi-segmental wall is characterized by an absolute centre of rotation when the hold-down stiffness is larger than vertical joint stiffness. The proposed analytical model was validated by the mean of a numerical modelling and the results showed a near perfect match between the two models.

CHAPTER 3 - Methodology and Definitions

3.1 Notation

A multi-panel wall is assumed to be composed of m panels with individual panel length b for a total length B $(b \cdot m)$, and of a height h as illustrated in Figure 3-1. The wall is assumed to be subjected to an external horizontal force F and to a uniformly distributed vertical load, q. A vertical joint between the CLT panels is assumed to be composed of n fasteners with a vertical spacing s. In the model, the fasteners in the vertical joint are represented by two orthogonal elastic springs, acting only in the plane of the panels. The external bottom corner of the first panel is anchored to the ground by means of a hold-down. The mechanical behaviours of the hold-down and panel-to-panel joint are represented by elastic-perfectly plastic curves (Figure 3-2). The curves are characterized by the elastic stiffnesses of k_h and k_c, strengths r_h and r_c, yield displacement $d_{y,h}$ and $d_{y,c}$, and the ultimate displacement $d_{u,h}$ and $d_{u,c}$ for the hold-down and panel joint, respectively.

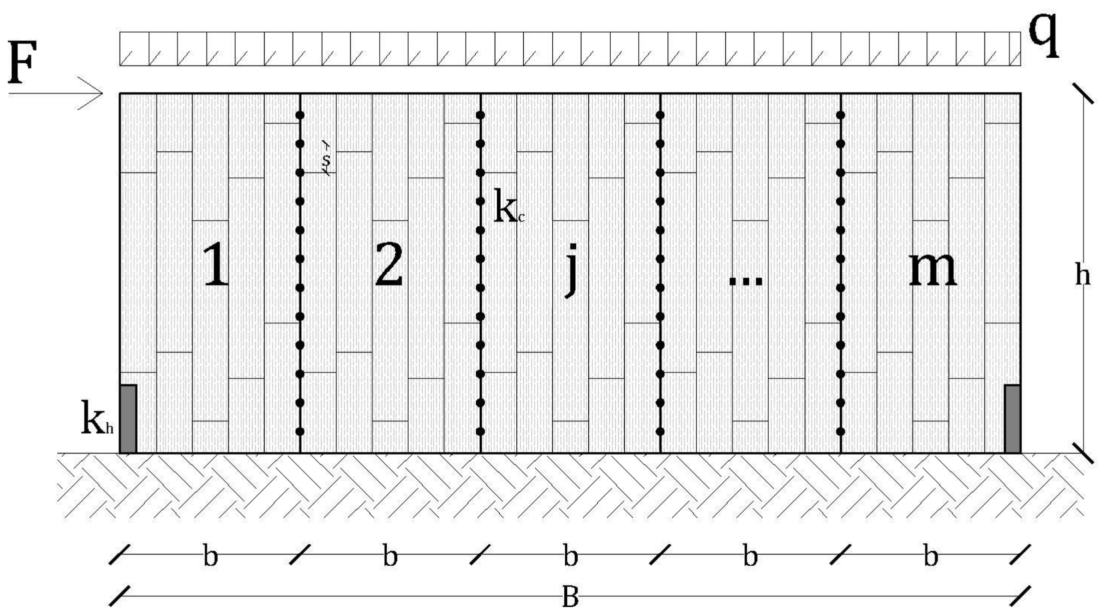

Figure 3-1: Multi-Panel CLT Wall Notation

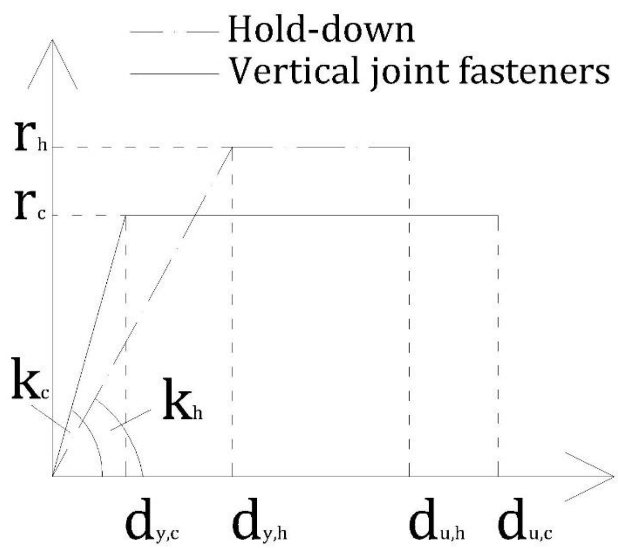

Figure 3-2: Elastic-Perfectly Plastic Curves for Hold-Down and Panel-to-Panel Joint

Theoretically, there are three types of possible rocking behaviours (Figure 3-3) providing different kinematic modes for the wall. Coupled Panel behaviour, CP, is characterized by the rotation of all panels about a point of rotation located at their lower right or left corner

(Figure 3-3a). Single Wall behaviour, SW, is achieved when there is only one global centre of rotation at the lower corner of the 1^{st} or m^{th} panel (lower right or left corner of the wall) (Figure 3-3b). Intermediate behaviour, IN, which occurs when a segment of the multi-panel wall deforms in SW behaviour and the rest in CP behaviour (Figure 3-3c).

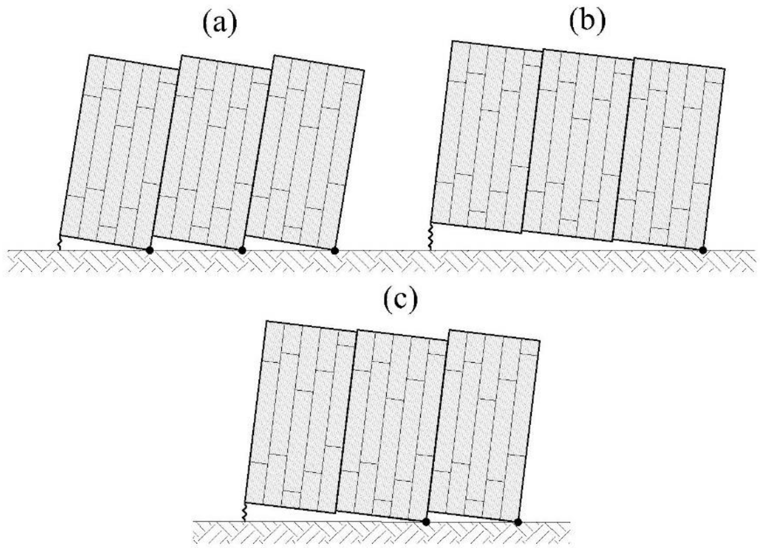

Figure 3-3: Physical Meaning to Rocking Behaviours (a) Coupled-Panel, (b) Single-Wall and (c) Intermediate

3.2 Elastic Behaviour

Casagrande et. al. (2017) developed an analytical model to establish the elastic behaviour of multi-panel CLT shearwalls. The kinematic behaviour was defined using two variables, the dimensionless stiffness ratio of the wall, $\widetilde{k} = \frac{k_h}{n \cdot k_c}$, and the dimensionless loads ratio, $\tilde{q} = \frac{q \cdot B^2}{2 \cdot F \cdot h}$. Figure 3-4 demonstrates the relationship between the dimensionless stiffness ratio as a function of the dimensionless load ratio. It can be seen from the figure that the wall can transition from one kinematic mode to another depending on the magnitude of the lateral and vertical loads.

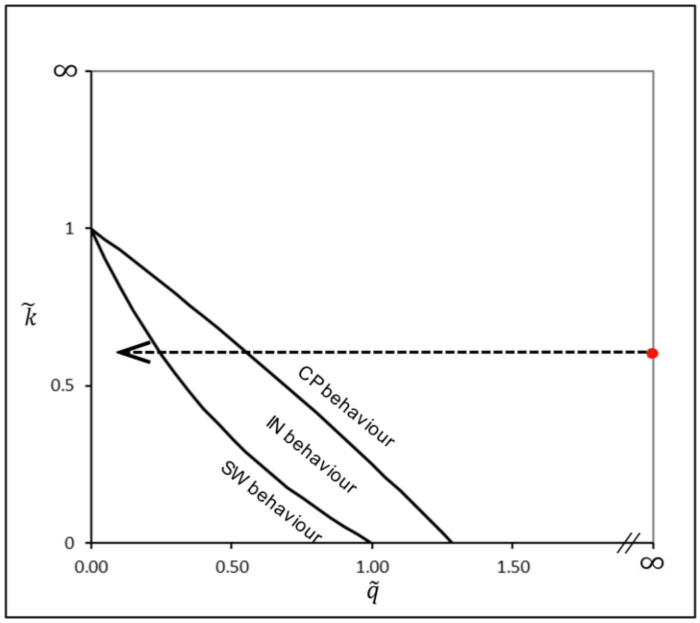

Figure 3-4: Kinematic Path of the Wall Through Different Behaviour Under Increasing Lateral Force

The behaviour of the wall is associated with a kinematic mode in relationship to the first panel that disconnects from the floor slab. The SW behaviour is associated with kinematic mode m since the m^{th} panel is the one in direct contact with the ground or floor slab. Similarly, the CP behaviour is identified as kinematic mode 1 and the IN behaviour is expressed in term of a kinematic mode attained j^*, where $2 \leq j^* \leq m-1$ (see Figure 3-5).

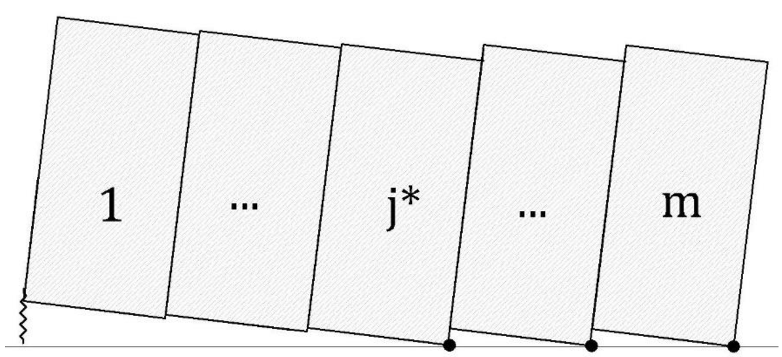

Figure 3-5: Definition of the Relation between Kinematic Mode and Behaviours

The definition of transitional force in elastic state was introduced by Casagrande et al. (2017) and the general form was presented for any kinematic mode $j^* = [1, m-1]$ as the transition between kinematic mode j^* and j^*+1. It was developed relative to small angle assumption and represents the value of lateral force applied on top of the wall. The transitional lines are shown in Figure 3-4 and they depend on the number of panels as well as the dimensionless stiffness and load ratios. They help identify the kinematic modes and allow the prediction of the wall's elastic strength, as expressed in Equation (1).

$$F_t^{el,j^*} = \frac{q \cdot B^2}{2 \cdot h} \cdot \frac{\tilde{k} \cdot \Psi^{j^*+1} + \Phi^{j^*+1}}{1 - \tilde{k}} \quad (1)$$

Where

$$\Phi^{j^*+1} = \frac{m \cdot [2 \cdot (j^*+1) - 1] - (j^*+1) \cdot j^*}{m^2} \quad (2)$$

$$\Psi^{j^*+1} = \frac{m \cdot [(j^*+1)^2 - 3 \cdot (j^*+1) + 1] + (j^*+1) \cdot j^*}{m^2} \quad (3)$$

The formulation of elastic strength in this study has been developed in term of the properties of the connectors as well as the wall geometry. The elastic strength related to the vertical joint, $R_{w,c}^{el,1}$, and to the hold-down, $R_{w,h}^{el,1}$, for a multi-panel wall in CP behaviour are presented in Equations (4) and (5), respectively.

$$R_{w,c}^{el,1} = r_c \cdot \frac{k_h'^{\,el,1} \cdot b}{k_c \cdot h} + F_q \quad (4)$$

$$R_{w,h}^{el,1} = r_h \cdot \frac{k_h'^{\,el,1} \cdot b}{k_h \cdot h} + F_q \quad (5)$$

Where r_c and r_h are the strength of the fasteners in the vertical joint and hold-down respectively. F_q is the activation force, defined as the lateral force required to overcome the effect of the vertical load applied on the wall. The activation force is derived from static equilibrium while assuming the wall as a rigid body, as expressed in Equation (6).

$$F_q = \frac{q \cdot m \cdot b^2}{2 \cdot h} \quad (6)$$

An equivalent hold-down tensile stiffness is derived based on the stiffness of the hold-down, the vertical joint, and wall geometry. Based on the assumption that for kinematic mode 1 (CP behaviour), the hold-down and vertical joint represent a system of springs in parallel. One can obtain:

$$k_h'^{\,el,1} = k_h + (m-1) \cdot n \cdot k_c \quad (7)$$

An equivalent lateral stiffness of the wall is derived from the equivalent hold-down tensile stiffness, as presented in Equation (8).

$$k_H^{el,1} = \frac{k_h'^{\,el,1} \cdot b^2}{h^2} \quad (8)$$

Always according to Casagrande et al. (2017, for the IN behaviour associated kinematic mode $j^* = [2, m-1]$, the strength related to the hold-down and vertical joint capacity takes the following forms:

$$R_{w,h}^{el,j^*} = \frac{r_h \cdot b \cdot \alpha_{(j^*)}}{h \cdot j^* \cdot \tilde{k}} + \frac{q \cdot b^2 \cdot m \cdot j^*}{2h} \quad (9)$$

$$R_{w,c}^{el,j^*} = \begin{cases} \frac{r_c \cdot n \cdot b \cdot \alpha_{(j^*)}}{h \cdot \beta_{(j^*)}} + \frac{q \cdot b^2 \cdot \gamma_{(j^*)}}{2 \cdot h \cdot \beta_{(j^*)}} \; with\, j^* = [1 : m-1] \\ \frac{r_c \cdot n \cdot b \cdot \alpha_{(m)}}{h \cdot m \cdot \tilde{k}} + \frac{q \cdot b^2 \cdot \rho_{(m)}}{2 \cdot h} \; with\, j^* = m \end{cases} \quad (10)$$

where,

$$\alpha_{(j^*)} = (j^* + m \cdot j^* - m) \cdot \tilde{k} + m - j^* \quad (11)$$

$$\beta_{(j^*)} = 1 + (j^* - 1) \cdot \tilde{k} \quad (12)$$

$$\gamma_{(j^*)} = m + j^* \cdot (j^* - 1) + (j^* - 1) \cdot (m - j^*) \cdot \tilde{k} \quad (13)$$

$$\rho_{(m)} = m^2 - \frac{2\alpha_{(m)} \cdot (m-1)}{m \cdot \tilde{k}} \quad (14)$$

The equivalent hold-down tensile stiffness for a system in kinematic mode m (SW behaviour) can be written assuming a system of springs that are in series. In Equation (15), $m - 1$ represents the number of joint in a wall consisting of m panels.

$$k_h'^{\,el,m} = \left(\frac{1}{k_h} + \frac{m-1}{n \cdot k_c}\right)^{-1} \quad (15)$$

The associated equivalent lateral stiffness in the SW behaviour can be written in the following form:

$$k_H^{el,m} = \frac{k_h'^{\,el,m} \cdot b^2 \cdot m^2}{h^2} \quad (16)$$

Finally, the equivalent hold-down tensile stiffness for IN behaviour, where the j^{*th} panel is the first to rotate about its lower corner, can be expressed as a system with springs in both parallel and series, as expressed in Equation (17):

$$k_h'^{\,el,j^*} = \frac{n \cdot k_c \cdot [(j^* + mj^* - m) \cdot k_h + (m - j^*) \cdot n \cdot k_c]}{n \cdot k_c + (j^* - 1) \cdot k_h} \quad (17)$$

The equivalent lateral stiffness of the wall in elastic state for model j^* is written as:

$$k_H^{el,j^*} = \frac{k_h'^{\,el,j^*} \cdot b^2}{h^2} \quad (18)$$

3.3 Plastic Behaviour

The current study extends the methodology described in Section 3.2 in order to establish the behaviour of CLT shearwalls past the point of elastic strength. The derivation of the proposed approach is explained in more details in Chapters 4 and 5. To help explain the methodology a general evaluation of possible kinematic paths is explained here. Figure 3-6 is also used to illustrate the approach.

At the point of yielding of the vertical joints ($k_c = 0$), the dimensionless stiffness ratio would tend toward infinity ($\widetilde{k} \approx \infty$). Similarly, at the point of hold-down yielding ($k_h = 0$), the dimensionless stiffness ratio $\widetilde{k}$ will reach the value of zero. The focus of the methodology is on the final behaviour of the wall represented by the SW or CP behaviour, as shown in Figure 3-6. Although the wall can transition from one behaviour to another in the elastic state, the final wall behaviour can be mathematically described through the behaviour of the hold-down and vertical joints. In particular, the order of yielding of the connectors plays a major role in dictating what the final failure mode of the wall will be. As will be shown in Chapter 4, irrespective of the kinematic mode of the wall in the elastic state, the SW behaviour can always be achieved as a final mode of failure if the hold-down connector yields before the panel joint connector. Contrarily, if the panel joints yield before the hold-down connection, CP behaviour can be achieved as a final mode of failure as presented in Chapter 5. For both these cases however, it is required that the system has sufficient displacement capacity in order to achieve the final kinematic mode. If the system does not possess sufficient displacement capacity, other intermediate state of behaviours may be achieved depending on when the ultimate failure of one or both connectors is attained.

The dimensionless stiffness ratio plays a major role in the behaviour the wall may attain in the elastic region. For example, it was established by Casagrande et al. (2017) that for $\tilde{k} > 1$, the elastic strength of the wall is in the region where CP behaviour governs, regardless of the lateral load value. However, as presented in Figure 3-4, the wall may achieve all behaviours in elastic state for any wall configuration with a dimensionless stiffness ratio, $\tilde{k}$, smaller than 1. Therefore, the kinematic mode attained by the wall might change in the elastic state to a different final mode in the plastic state. Figure 3-6 presents the combinations of behaviour resulting in all possible kinematic paths. The case where the dimensionless stiffness ratio is larger than 1 is covered by the case where the elastic state in achieved in CP behaviour. The elastic state is characterized by the horizontal line in Figure 3-6 and each dot represents the start point of connector yielding. The line then tends towards the final behaviour depending on which connector yields. What is of interest to the development of the proposed model is the behaviour type in the elastic and plastic states. Therefore, a notation is used to describe the failure path. For example, the failure path where the connectors yield in the CP behaviour but has SW as final behaviour is denoted CP^{EL}-SW^{PL}. Similarly, if the wall achieves yielding in the SW behaviour and failure in the CP behaviour would be denoted SW^{EL}-CP^{PL}.

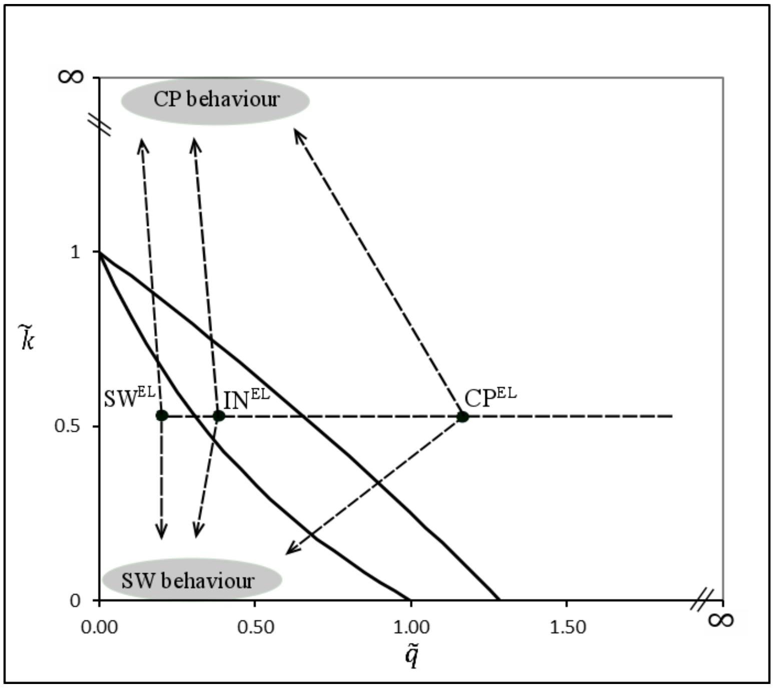

Figure 3-6: Definition of Elasto-Plastic Kinematic Path

The proposed analytical model includes cases where neither SW or CP behaviour can be acheived. This may occur due to limitation in the connectors' ductility, where the wall may fail prematurly and remain in the IN behaviour prior to acheiveing the intented final behaviour.

To better facilitate the understanding of the methodology, kinematic mode 1 (CP behaviour) and kinematic mode m (SW behaviour) will be presented first, followed by the intermediate behaviour where the elastic strength is achieved in mode $j^* = [2, m-1]$. The intermediate cases represent general cases where kinematic mode 1 and m can be obtained as special cases.

3.4 Nomenclature

The general characteristics of the force-displacement curve are defined following a specific nomenclature to facilitate identifying the various segments in the curve. This section identifies the key parameters found in the force-displacement curve (Figure 3-7) and explains the physical meaning of each variable.

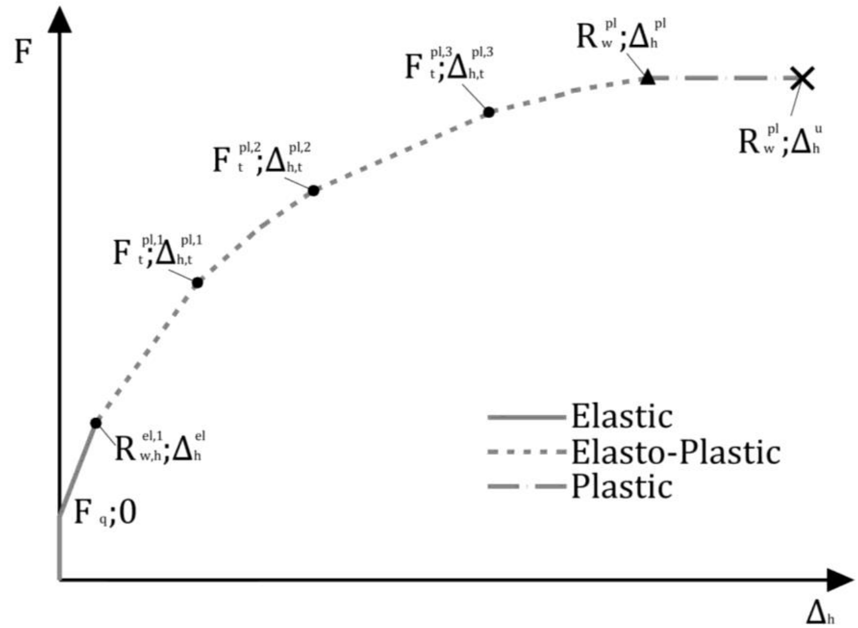

Figure 3-7: Force-Displacement Curve Nomenclature

F_q is defined as the activation force which represents the lateral force level that initiates the rocking displacement. This force depends on the relative magnitude of the horizontal and the vertical loads. $R_{w,Z}^{el,Y}$ is the strength of the wall (w) that can be achieved in the elastic (el) state. Z represents whether the wall strength is governed by a hold-down (h) or a panel joint (c) and Y relates to the kinematic model in which the strength is achieved. For example, $R_{w,c}^{el,2}$ represents the elastic strength of the wall governed by the vertical joint in kinematic mode 2. R_w^{pl} is the plastic strength of the wall, which is attained when both connectors yield.

Δ_h^X represents the displacement due to rocking motion of the wall when a specific strength is reached in state X (elastic, el , or plastic pl). Δ_h^u represents the ultimate displacement of the wall when the ultimate failure of a connectors occurs. $F_t^{X,Y}$ denotes the transition force between different kinematic behaviours. Y indicates the first panel to rotate about its own centre of rotation when this transitional force is achieved in state X. For the IN behaviour, the first panel to rotate about its own center of rotation is associated with kinematic mode j^*.

$\Delta_{h,t}^{X,Y}$ represents the transitory displacement in rocking motion, where the change in kinematic behaviour occurs, whereas $\delta_{h,t}^{X,Y}$ represents the increase of horizontal displacement leading to a change in kinematic mode in rocking without any increase in the force (resulting in a plateau).

Additionally, $T^{X,Y}$ represents the hold-down tension force. The magnitude of this variable is obtained incrementally, and at each step, the symbol used is $t^{X,Y}$, which represent the increase of force in the hold-down due to the increase of lateral force on the wall for a certain state X in kinematic mode Y. Similarly, the lateral force applied on the wall is assigned a symbol F, where the transitional force is denoted $F_t^{X,Y}$ and the symbol $f^{X,Y}$ relates to the incremental rise of lateral force in state X during kinematic mode Y.

Finally, the equations that requires more development outside the general procedures will be denoted as (Eq.)^{A} referring that more details are provided in the Appendix.

CHAPTER 4 - Development of the Analytical Model to Achieve SW as Final Behaviour

4.1 General

Figure 4-1 shows the three possible failure paths that can lead to the final SW behaviour. These include the wall achieving elastic yield in a) CP behaviour, b) SW behaviour and c) IN behaviour, after which the final SW behaviour is achieved due to yielding in the hold-down prior to yielding in the panel joints. The failure paths for cases a), b) and c) are denoted $CP^{EL}SW^{PL}$, $SW^{EL}SW^{PL}$ and $IN^{EL}SW^{PL}$, respectively, as shown in Figure 4-1. It is important to reiterate that the behaviour shown in Figure 4-1 can only be achieved if the connectors have sufficient displacement capacity post yielding. Wall failures where limited ductility is attained in the connectors are presented through the development of the model as special failure mechanisms.

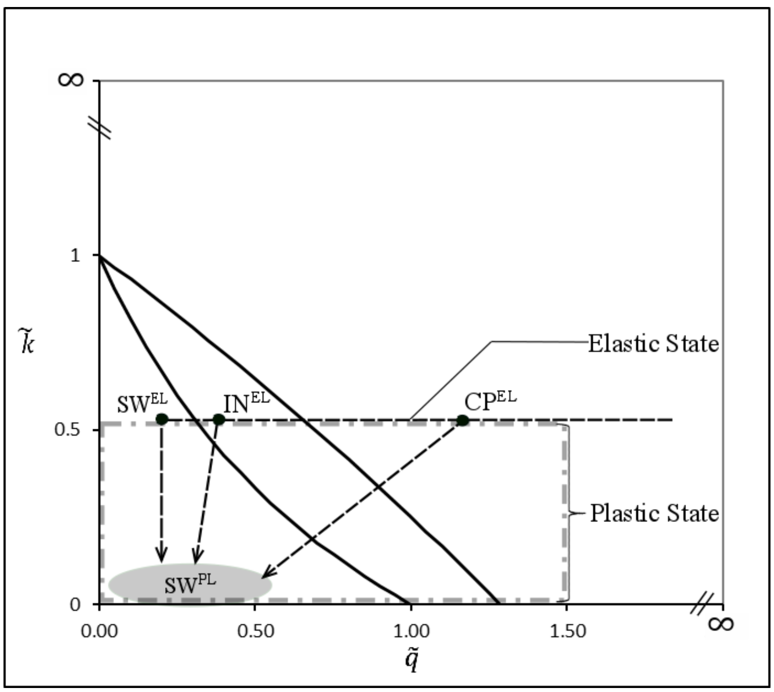

Figure 4-1: Kinematic Paths to Achieve SW Behaviour

In order to relate the point of transition between the elastic and plastic state to the point of final behaviour, variables $\tilde{j}$ and $\hat{j}$ are introduced. $\tilde{j}$ is associated with the kinematic mode in the elastic state, whereas $\hat{j}$ is associated with the final kinematic mode in the plastic state. As such, $\tilde{j}$ and $\hat{j}$ can take on values of 1 (CP behaviour), m (SW behaviour) or $2 \leq \tilde{j} \leq m-1$ (IN behaviour).

As mentioned earlier, achieving SW as the final wall behaviour can be attained when the wall strength related to the hold-down yielding is smaller than that related to the panel joint yielding. This condition is ensured by the inequality shown in Equation (19) for any kinematic mode $\tilde{j}$.

$$R_{w,h}^{el,\tilde{j}} < R_{w,c}^{el,\tilde{j}} \quad (19)$$

To achieve the CP kinematic behaviour in the elastic state, the dimensionless stiffness ratio should be larger than 1 or the elastic strength of the wall related to hold-down yielding in the CP behaviour ($\tilde{j} = 1$) is required to be less than the transition force between kinematic mode 1 and 2 in the elastic state (see Section 3.2). This requirement is ensured through the following condition.

$$R_{w,h}^{el,1} < F_t^{el,1} \ or \ \tilde{k} > 1 \quad (20)$$

Similarly, the SW kinematic behaviour in the elastic state is achieved when the elastic strength of the wall related to hold-down yielding in the SW behaviour ($\tilde{j} = m$) is larger than the final transitional force prior to attaining kinematic mode m in the elastic state.

$$R_{w,h}^{el,m} > F_t^{el,m-1} \ (21)$$

Finally, the IN behaviour in the elastic state is achieved when the elastic strength of the wall related to hold-down yielding in the IN behaviour $\tilde{j} = [2, m-1]$ is between the transitional forces defining the intermediate kinematic modes immediately before and after the mode under consideration $\tilde{j} = j^*$.

$$F_t^{el,j^*-1} < R_{w,h}^{el,j^*} < F_t^{el,j^*} \quad (22)$$

4.2 Model Development for the CP^{EL}-SW^{PL} Case

This case is achieved through the CP behaviour in the elastic state and the SW behaviour in the final plastic state and is ensured by the inequalities presented in Equations (19) and (20). When failure mechanisms VII (Figure 4-2) cannot be achieved, the behaviour of the wall depends on the limitation in the ductility of the individual connectors. Therefore, from the elastic state (represented by the line up to point CP^{EL}), the wall may possess limited ductility and therefore would remain in plastic CP region or only reach the plastic state in the IN region. The different behaviour regions for which the wall may reach its ultimate capacity are presented in the general force-displacement curve shown in Figure 4-2 and associated kinematic path in Figure 4-3.

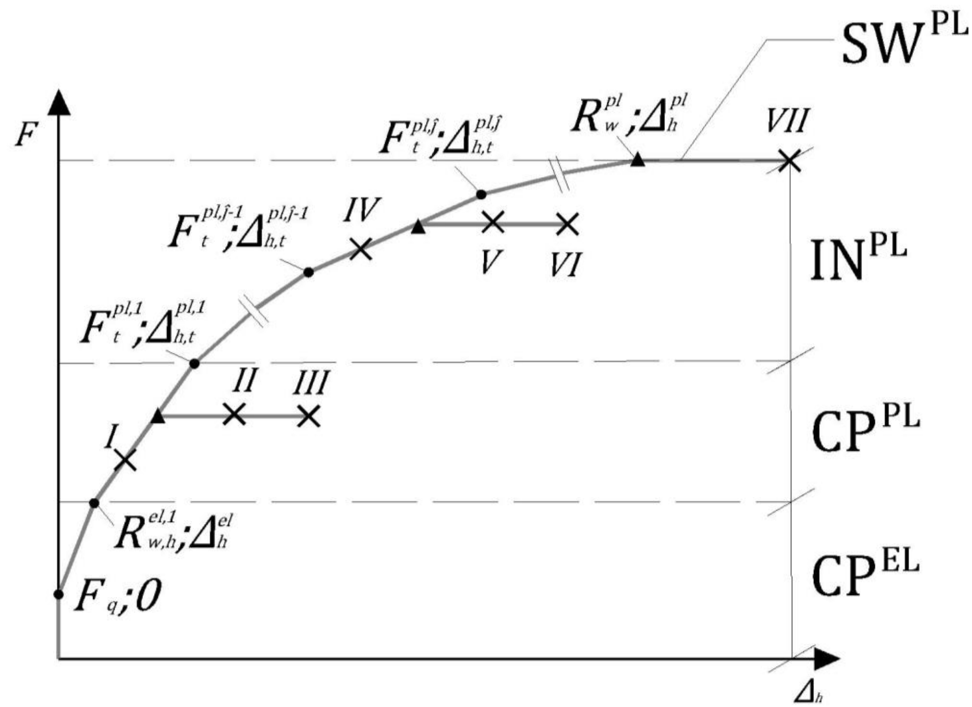

Figure 4-2: General Elasto-Plastic Force-Displacement Curve for Kinematic Path CP^{EL}-SW^{PL}

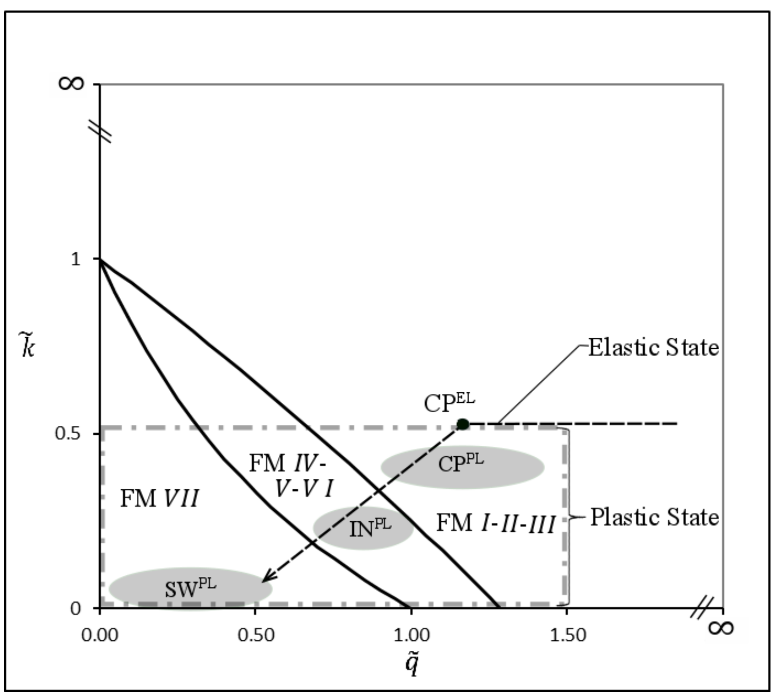

Figure 4-3: Behaviour Region of failure Mechanism for CP^{EL}-SW^{PL}

Different failure mechanisms (i.e. FM $I - VII$) can be defined depending on the kinematic mode reached in the plastic state and the sequence of failure of the connectors, including those with limited ductility. All failure mechanisms along the CP^{EL}-SW^{PL} path are illustrated in Figure 4-4. The dot at the bottom right corner of the panels represent a point of contact and rotation between the panel and ground. The spiral and the cross defines the behaviour of the individual connectors and represents yielding or complete failure, respectively.

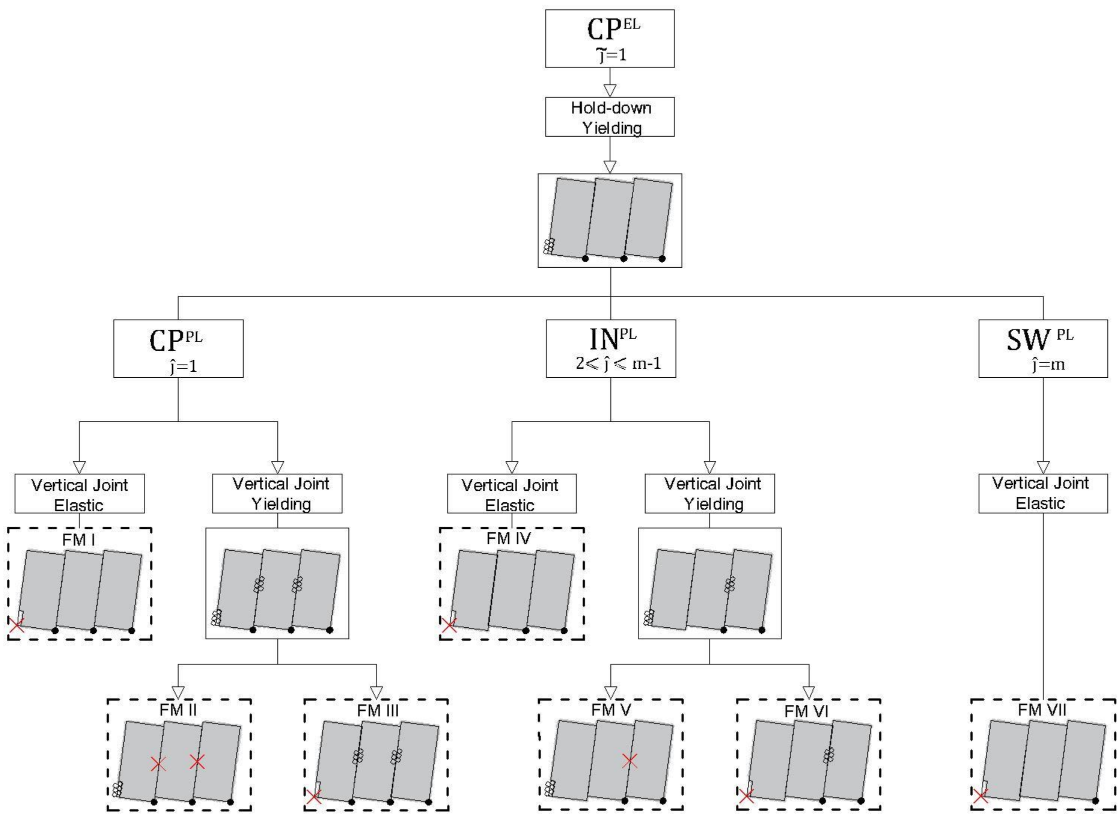

Figure 4-4: Definition of Failure Mechanism for CP^{EL}-SW^{PL}

It can be observed that when the panel joint remains elastic, the wall failure governed by failure in the hold-down. However, yielding of the vertical joint in the CP^{PL} and IN^{PL} regions would lead to ultimate failure in ether hold-down or vertical joint.

The subsequent sections will follow the structure presented in Figure 4-4, starting by describing the elastic state in CP behaviour (Section 4.2.1), followed by a description of the plastic states in the CP, IN and SW behaviour in Sections 4.2.2, 4.2.3 and 4.2.4, respectively.

4.2.1 CP Behaviour in Elastic State

The first point in the force-displacement relationship of the wall for all cases is the activation force, as defined by Equation (6) and discussed in Section 3.2.

The elastic strength of the wall associated with the hold-down yield strength in kinematic mode 1, $R_{w,h}^{el,1}$, can be described as (same as Equation 5 in Section 3.2):

$$R_{w,h}^{el,1} = r_h \cdot \frac{k_h'^{\,el,1} \cdot b}{k_h \cdot h} + F_q \quad (23)$$

The top horizontal displacement of the wall associated with the elastic strength, Δ_h^{el}, can be written as a function of the vertical elongation in the hold-down, $d_{y,h}$, and the aspect ratio of the wall panels, $\frac{h}{b}$. This displacement can initially be expressed in terms of increase in force over the equivalent lateral stiffness of the wall, $k_H^{el,1}$:

$$\Delta_h^{el} = \frac{R_{w,h}^{el,1} - F_q}{k_H^{el,1}} = \frac{r_h \cdot k_h'^{\,el,1} \cdot b}{k_h \cdot h} \cdot \frac{h^2}{k_h'^{\,el,1} \cdot b^2} = \frac{r_h \cdot h}{k_h \cdot b} = d_{y,h} \cdot \frac{h}{b} \quad (24)$$

4.2.2 Plastic CP Behaviour Region, Failure Mechanism $I - III$

As can be seen in Figure 4-5, CP^{PL} is defined by the limits represented with the yielding of the hold-down (transition from elastic to plastic state, Eq. 23), and the transitional force to achieve IN behaviour, $F_t^{pl,1}$. This transition force defines the state where the first panel is no longer in contact with the ground, i.e. the reaction of the first panel is equal to zero (Figure 4-6).

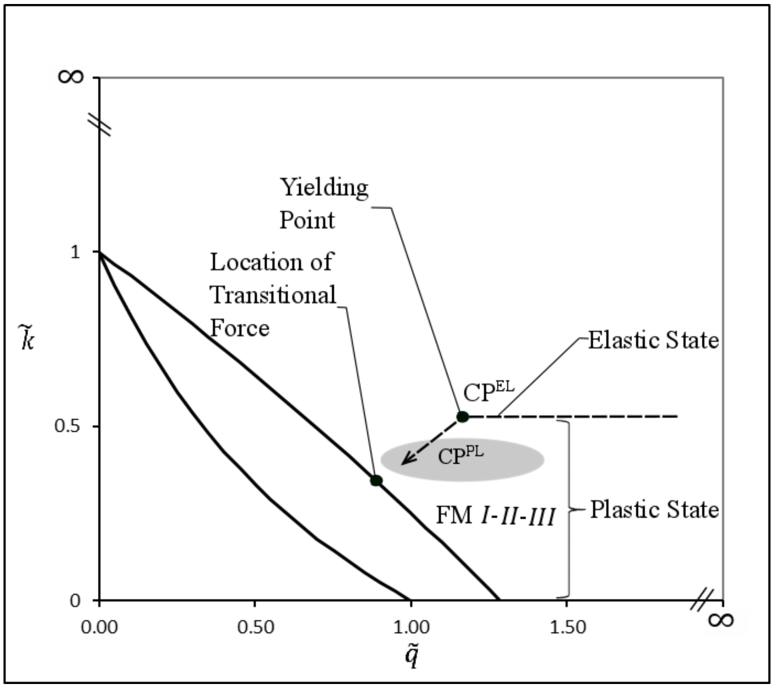

Figure 4-5: Behaviour Region CP^{PL} for Kinematic Path of Case CP^{EL}-SW^{PL}

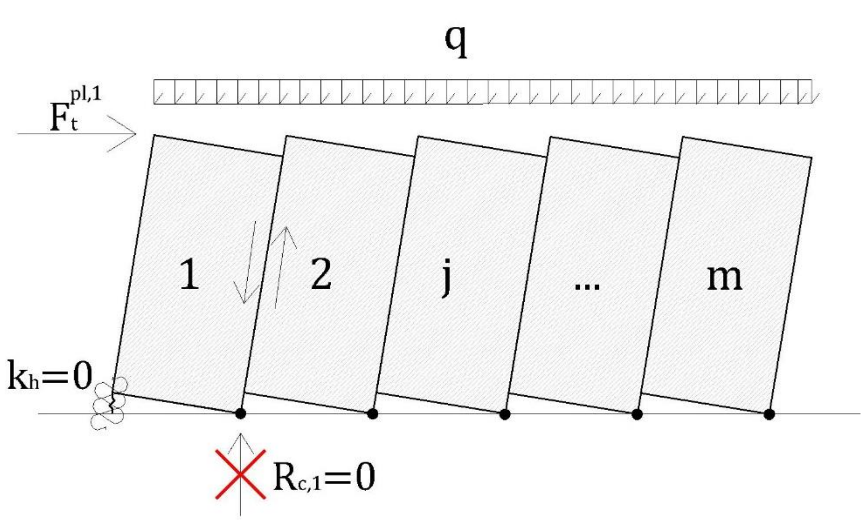

Figure 4-6: Transition from CP^{PL} to IN^{PL} Behaviour Region

The increase in lateral force, $F_t^{pl,1} - R_{w,h}^{el,1}$, that leads to kinematic mode 2 (i.e. $R_{c,1} = 0$), is expressed using static equilibrium, as shown in Equation (25):

$$F_t^{pl,1} - R_{w,h}^{el,1} = \frac{R_{c,1} \cdot b}{h} \cdot (m-1) = \frac{b \cdot (m-1)}{h} \cdot \left[r_h \cdot \left(1 - \frac{n \cdot k_c}{k_h}\right) + q \cdot b \right] \quad (25)$$

where $R_{c,1}$ is calculated considering static equilibrium of the first panel:

$$R_{c,1} = r_h \left(1 - \frac{n \cdot k_c}{k_h}\right) + q \cdot b \quad (26)$$

The total transitional force between the CP to IN behaviours is expressed in Equation (27) as the sum of the elastic strength achieved in kinematic mode 1, $R_{w,h}^{el,1}$, and the increase in force defined in Equation (25).

$$F_t^{pl,1} = R_{w,h}^{el,1} + \left(F_t^{pl,1} - R_{w,h}^{el,1}\right) = \frac{r_h \cdot b \cdot m}{h} + \frac{q \cdot b^2}{2h} \cdot (3m-2) \quad (27)^{A}$$

The total lateral displacement of the wall related to the transitional force defined in Equation (27), can be written as the sum of the elastic displacement and the displacement associated with the increase in force causing a shift to kinematic mode 2 from elastic strength:

$$\Delta_{h,t}^{pl,1} = \Delta_h^{el} + \frac{F_t^{pl,1} - R_{w,h}^{el,1}}{k_H^{pl,1}} = \frac{h}{b \cdot n \cdot k_c} \cdot (r_h + qb) \quad (28)^{A}$$

The equivalent hold-down tensile stiffness in the plastic state for kinematic mode 1 is written in a similar fashion to that in the elastic state (Equation 7 in Section 3.2) but without the contribution of the hold-down, $k_h'^{\,pl,1} = k_h'^{\,el,1}(k_h = 0)$. Therefore, the equivalent lateral stiffness of the wall can be expressed as:

$$k_H^{pl,1} = \frac{k_h'^{\,pl,1} \cdot b^2}{h^2} = \frac{(m-1) \cdot n \cdot k \cdot b^2}{h^2} \quad (29)$$

The transitional force, $F_t^{pl,1}$ and its associated displacement cannot be attained in failure mechanisms I, II and III due to limited elongation capability in the connectors (see Fig. 4-4). These failure mechanisms are achieved when the wall remains in the CP behaviour following the yielding of the hold-down. Attaining failure mechanism I is ensured by the following two conditions: a) failure of the hold-down is reached while the wall remains in CP behaviour (Eq. 30), and b) the failure of the hold-down is reached prior to the yielding of the panel joints (Eq. 31):

$$d_{u,h} < V_0^{pl,1} = b \cdot \vartheta = \frac{1}{n \cdot k_c}(r_h + qb) \quad (30)^{A}$$

$$d_{y,c} > d_{u,h} \quad (31)$$

Where $V_0^{pl,1}$ is the total displacement of the hold-down in kinematic mode 1 for the CP behaviour in the plastic state. It is expressed as the panel width, b, and the angle of rotation of all panels, ϑ, due to lateral force $F_t^{pl,1}$.

The plastic strength of the wall under these conditions can be written as an interpolation between the elastic strength and the transitional force between kinematic modes 1 and 2.

$$R_w^{pl,I} = R_w^{el} + \left(F_t^{pl,1} - R_{w,h}^{el,1}\right) \cdot \frac{d_{u,h} - d_{y,h}}{V_0^{pl,1} - d_{y,h}} \quad (32)$$

The total lateral displacement for failure mechanism I (Eq. 33) occurs in kinematic mode 1 in the plastic state and is controlled only by the ultimate displacement of the hold-down.

$$\Delta_h^{u,I} = \Delta_h^{pl} = \Delta_h^{el} + \frac{R_w^{pl,I} - R_{w,h}^{el,1}}{k_H^{pl,1}} = \frac{h}{b} \cdot d_{u,h} \quad (33)$$

The ductility of the wall for failure mechanism I is defined only by the ductility in the hold-down, and can be expressed as:

$$\mu_w{}^I = \frac{\Delta_h^{u,I}}{\Delta_h^{el}} = \frac{\frac{h}{b} \cdot d_{u,h}}{\frac{h}{b} \cdot d_{y,h}} = \mu_h \quad (34)$$

Failure mechanism II and III also occur in the CP plastic behaviour, but where the wall's plastic strength is governed by yielding in the vertical joints. It is ensured by the following two conditions: a) yielding of the panel joints in kinematic mode 1 prior to achieving the displacement in the connectors associated with the transitional force $F_t^{pl,1}$ (Eq. 35), and b) yielding displacement of the vertical joints is reached prior to the ultimate displacement of the hold-down (Eq.36):

$$d_{y,c} < V_\mathrm{c}^{pl,1} = \frac{1}{n \cdot k_c}(r_h + qb) \quad (35)^{\mathrm{A}}$$

$$d_{y,c} < d_{u,h} \quad (36)$$

The plastic strength of the wall for failure mechanisms II and III occurs when the panel joints yield. Therefore, the wall resistance can be expressed as the sum of the elastic strength and the increase of force that is governed by the yielding displacement of the panel joints:

$$R_w^{pl,II} = R_w^{pl,III} = R_{w,h}^{el,1} + \left(F_t^{pl,1} - R_{w,h}^{el,1}\right) \cdot \frac{d_{y,c} - d_{y,h}}{V_\mathrm{c}^{pl,1} - d_{y,h}} \quad (37)$$

The total displacement at the plastic strength for both failure mechanisms II and III is governed by the yield displacement of the vertical joint.

$$\Delta_h^{pl,II} = \Delta_h^{pl,III} = \Delta_h^{el} + \frac{R_w^{pl,II,III} - R_{w,h}^{el,1}}{k_H^{pl,1}} = \frac{r_c \cdot h}{k_c \cdot b} = d_{y,c} \cdot \frac{h}{b} \quad (38)$$

The ultimate displacements for failure mechanism II and III are characterized by failure in the vertical joints and in the hold-down, respectively. They can be expressed as the ultimate displacement for each connector and the wall panel aspect ratio.

$$\Delta_h^{u,II} = \frac{h}{b} \cdot d_{u,c} \quad (39)$$

$$\Delta_h^{u,III} = \frac{h}{b} \cdot d_{u,h} \quad (40)$$

The ductility for failure mechanism II and III can be expressed as:

$$\mu_w{}^{II} = \frac{\Delta_h^{u,II}}{\Delta_h^{el}} = \frac{\frac{h}{b} \cdot d_{u,c}}{\frac{h}{b} \cdot d_{y,h}} = \mu_h \cdot \frac{d_{u,c}}{d_{u,h}} \quad (41)$$

$$\mu_w{}^{III} = \frac{\Delta_h^{u,II}}{\Delta_h^{el}} = \frac{\frac{h}{b} \cdot d_{u,h}}{\frac{h}{b} \cdot d_{y,h}} = \mu_h \quad (42)$$

4.2.3 IN Behaviour Region in Plastic State, Failure Mechanisms $IV - VI$

Figure 4-7 illustrates the region for failure mechanisms $IV - VI$, which starts when the transitional force to achieve the first kinematic mode in IN behaviour, $F_t^{pl,1}$, is reached. This particular behaviour is attained when the ductility of the connectors is sufficient to extend the wall beyond CP behaviour.

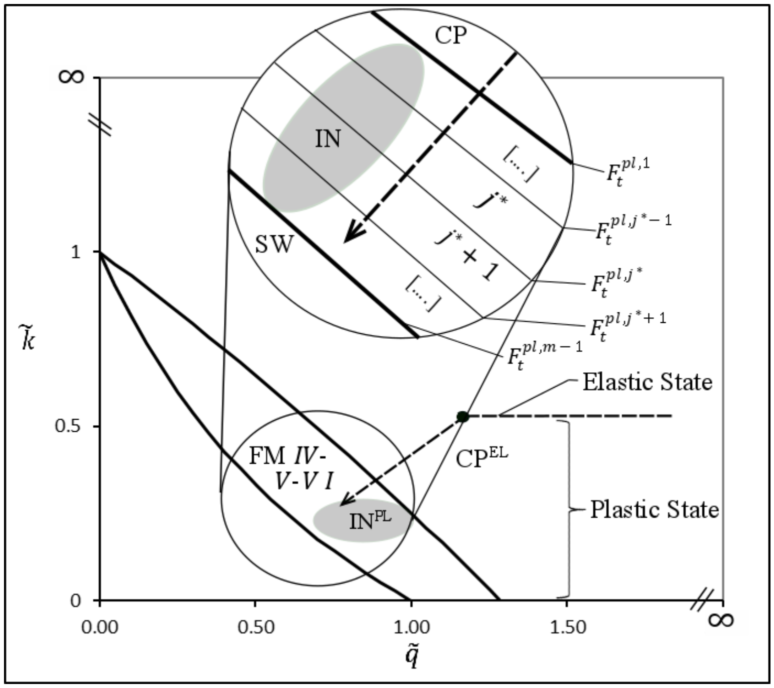

Figure 4-7: Behaviour Region IN^{PL} for Kinematic Path of Case CP^{EL}-SW^{PL}

The development of the force-displacement curve follows the procedure outlined in Figure 4-8. As indicated in Figure 4-8, the value of j^* is increased between 2 and $m-1$ (for $m > 2$).

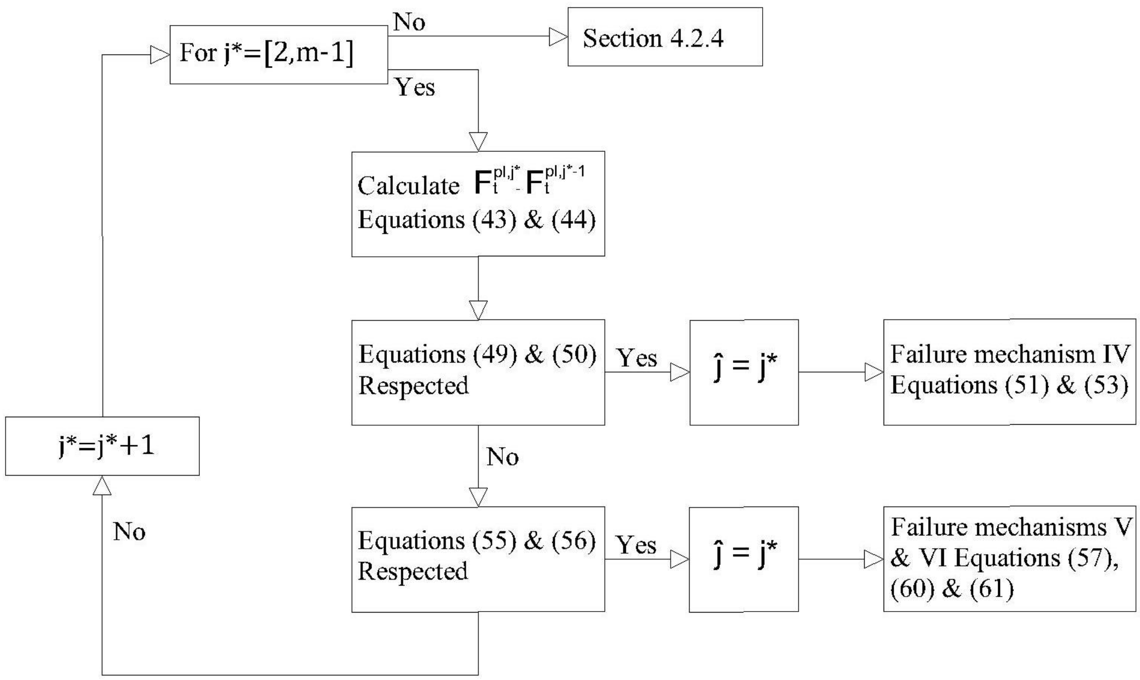

Figure 4-8: Steps to solve IN Behaviour Region of Case CP^{EL}-SW^{PL}, Failure Mechanisms IV-VI

The transitional forces and associated displacements for kinematic mode j^* and j^*+1 are calculated to define the limits surrounding kinematic mode j^*. The transitional forces to attain modes j^* and j^*+1 are denoted F_t^{pl,j^*-1} and F_t^{pl,j^*}, respectively. Through static equilibrium, the increase in lateral force between two adjacent kinematic modes can be expressed as:

$$F_t^{pl,j^*} - F_t^{pl,j^*-1} = \frac{R_{c,j^*} \cdot b}{h}(m - j^*) = \frac{q \cdot b^2}{h}(m - j^*) \quad (43)$$

Where the reaction force of the j^{*th} panel only considers the vertical load applied on the panel because the uplifted panels (from 1 to j^*) stiffness is equal to zero in this segment of the wall since the hold-down has yielded and the wall stiffness is assumed as springs in series representing the hold-down and vertical joint. Therefore, the lateral forces are transferred to the next panels in contact with the ground and the reaction force takes the following expression using static equilibrium:

$R_{c,j^*} = q \cdot b$ (44)

The total transitional force at the point where the wall changes from kinematic mode j^* to kinematic mode $j^* + 1$ is the sum of the first transitional force to the incremental increase of lateral force resulting a change in behaviour.

$F_t^{pl,j^*} = F_t^{pl,1} + \sum_{j=2}^{j^*} \left(F_t^{pl,j} - F_t^{pl,j-1} \right) = \frac{r_h \cdot b \cdot m}{h} + \frac{q \cdot b^2}{2h} [3m + 2m(j^* - 1) - j^*(j^* + 1)]$

(45)[A]

The total lateral displacement for kinematic mode j^* associated with transitional force expressed in Equation (45) takes the following form:

$\Delta_{h,t}^{pl,j^*} = \Delta_{h,t}^{pl,1} + \sum_{j=2}^{j^*} \frac{F_t^{pl,j} - F_t^{pl,j-1}}{k_H^{pl,j}} = \frac{h}{b} \cdot \frac{r_h}{n \cdot k_c} + \frac{q \cdot h \cdot j^*}{n \cdot k_c}$ (46)[A]

The equivalent lateral stiffness of the wall in kinematic mode j^* is expressed as:

$k_H^{pl,j^*} = \frac{{k'_h}^{pl,j^*} \cdot b^2}{h^2} = \frac{(m - j^*) \cdot n \cdot k_c \cdot b^2}{h^2}$ (47)

Where the equivalent hold-down stiffness is:

${k'_h}^{pl,j^*} = (m - j^*) \cdot n \cdot k_c$ (48)

Failure mechanism IV is characterized by the failure of the hold-down in kinematic mode j^* attained before the yielding of the vertical joints, as expressed in Equation (49). Equation (50) shows that the ultimate displacement of the hold-down in failure mechanism IV is bounded by the deformation achieving kinematic mode j^* and $j^* + 1$. This is expressed through the following two conditions:

$$d_{y,c} > \frac{r_h}{n \cdot k_c}\left(1 - \frac{1}{j^*}\right) + \frac{q \cdot b}{n \cdot k_c}\left[\frac{(j^*-1)}{2} + \frac{1}{j^*}\right] + \frac{d_{u,h}}{j^*} \quad (49)^{A}$$

$$\frac{1}{n \cdot k_c}\left(r_h + \frac{j^* \cdot (j^*-1) q \cdot b}{2}\right) < d_{u,h} < \frac{1}{n \cdot k_c}\left(r_h + \frac{j^* \cdot (j^*+1) q \cdot b}{2}\right) \quad (50)^{A}$$

If both conditions 49 and 50 are met, then j^* and $\hat{j}$ are equal and becomes associated with the final kinematic mode in the plastic state.

The plastic strength for failure mechanism IV is calculated by adding the first transitional force, $F_t^{pl,1}$, to the increase of force required fully develop kinematic mode $j^* = [2, \hat{j} - 1]$. The plastic strength associated with kinematic mode $\hat{j}$ resulting in the failure of the hold-down is presented in Equation (51).

$$R_w^{pl,IV} = F_t^{pl,1} + \sum_{j=2}^{\hat{j}-1} F_t^{pl,j} - F_t^{pl,j-1} + \left(\frac{d_{u,h} - V_0^{pl,\hat{j}}}{\left(\frac{\hat{j} \cdot q \cdot b}{n \cdot k_c}\right)}\right) \cdot \left(F_t^{pl,\hat{j}} - F_t^{pl,\hat{j}-1}\right) = R_w^{pl,IV} =$$

$$\frac{r_h \cdot b}{h}\left[m + 1 - \frac{m}{\hat{j}}\right] + \frac{q \cdot b^2 \cdot m \cdot \hat{j}}{2 \cdot h} + \frac{d_{u,h} \cdot n \cdot k_c \cdot b \cdot (m - \hat{j})}{\hat{j} \cdot h} \quad (51)^{A}$$

Where $V_0^{pl,\hat{j}}$ is the total hold-down elongation attained in mode $\hat{j}$.

$$V_0^{pl,\hat{j}} = \frac{1}{n \cdot k_c}(r_h + qb) + \sum_{j^*=2}^{\hat{j}-1} \frac{j \cdot q \cdot b}{n \cdot k_c} = \frac{r_h}{n \cdot k_c} + \frac{\hat{j} \cdot (\hat{j}-1) \cdot q \cdot b}{2 \cdot n \cdot k_c} \quad (52)^{A}$$

The ultimate displacement of the wall in failure mechanism IV is the sum of the lateral displacement of the wall in CP behaviour, the incremental displacement to achieve all intermediate kinematic modes (2 to $\hat{j} - 1$) and the displacement in the final kinematic mode $\hat{j}$ governed by failure in the hold-down. The expression is shown in Equation (53).

$$\Delta_h^{u,IV} = \Delta_{h,t}^{pl,1} + \sum_{j=2}^{\hat{j}-1} \frac{F_t^{pl,j} - F_t^{pl,j-1}}{k_H^{pl,j}} + \frac{h}{\hat{j} \cdot b} \cdot \left(d_{u,h} - V_0^{pl,\hat{j}}\right) = \frac{h}{b \cdot \hat{j}} \cdot \left[d_{u,h} + \frac{(\hat{j}-1) \cdot r_h}{n \cdot k_c} + \frac{q \cdot b \cdot \hat{j}}{2 \cdot n \cdot k_c}(\hat{j}-1)\right] \quad (53)^{A}$$

The ductility of the wall can be developed as:

$$\mu_w{}^{IV} = \frac{\Delta_h^{u,IV}}{\Delta_h^{el}} \quad (54)$$

Failure mechanisms V and VI occurs when the vertical joints yield in kinematic mode j^* prior the failure of the hold-down, as expressed in Equation (55). Equation (56) shows that the yielding displacement of the vertical joints in failure mechanism V and VI is bounded by the deformation to fully develop kinematic mode $j^* - 1$ and j^*.

$$d_{u,h} > \frac{r_h}{n \cdot k_c}(1 - j^*) - \frac{(j^*-1) \cdot j^* \cdot q \cdot b}{2 \cdot n \cdot k_c} + j^* \cdot d_{y,c} \quad (55)^{A}$$

$$\frac{1}{n \cdot k_c}(r_h + (j^* - 1)qb) < d_{y,c} < \frac{1}{n \cdot k_c}(r_h + j^* qb) \quad (56)^{A}$$

The plastic strength of failure mechanism V and VI is the sum of the first transitional force, $F_t^{pl,1}$, the increase of force required fully develop kinematic mode $j^* = [2, \hat{j} - 1]$ and the interpolation of the increase of force to achieve kinematic mode $\hat{j}$ that is governed by the yielding displacement of panel joints.

$$R_w^{pl,V} = R_w^{pl,VI} = F_t^{pl,1} + \sum_{j=2}^{\hat{j}-1} \frac{q \cdot b^2}{h}(m - j) + \left(\frac{d_{y,c} - V_c^{pl,\hat{j}}}{\left(\frac{q \cdot b}{n \cdot k_c}\right)}\right) \cdot \frac{q \cdot b^2}{h}(m - \hat{j}) = \frac{r_h \cdot b}{h}[\hat{j}] + \frac{n \cdot r_c \cdot b}{h}[m - \hat{j}] + \frac{\mathrm{q} \cdot b^2}{2 \cdot h}(m - \hat{j} + \hat{j}^2) \quad (57)^{A}$$

Where $V_c^{pl,\hat{j}}$ is the total elongation of fasteners in the last vertical joint ($m - 1^{th}$) attained in mode $\hat{j}$ and is shown Equation (58). The elongation in this joint is the studied as it is the vertical joint resisting the maximum force according to the analytical model developed by Casagrande et al. (2017).

$$V_c^{pl,\hat{j}} = \frac{1}{n \cdot k_c}[r_h + q \cdot b(\hat{j} - 1)] \quad (58)^{A}$$

The plastic displacement of the wall in failure mechanism V and VI is the sum of the lateral displacement of the wall in CP behaviour, the incremental displacement to develop all intermediate kinematic modes (2 to $\hat{j} - 1$) and the displacement in the final kinematic mode $\hat{j}$ governed by yielding of the vertical joints. The expression is shown in Equation (59).

$$\Delta_h^{pl,V} = \Delta_h^{pl,VI} = \frac{h}{b} \cdot d_{y,c} \quad (59)$$

The ultimate displacements for failure mechanism V and VI are characterized by failure in the vertical joints and the hold-down, respectively. It can be expressed as the ultimate displacement of the vertical joint and the wall panel aspect ratio for Equation (60). Equation (61) is developed as the sum of wall displacement in CP behaviour, the incremental displacement through kinematic modes 2 up to $\hat{j} - 1$ and the displacement in the final kinematic mode, $\hat{j}$, governed by failure in the hold-down.

$$\Delta_h^{u,V} = \frac{h}{b} \cdot d_{u,c} \quad (60)$$

$$\Delta_h^{u,VI} = \Delta_{h,t}^{pl,1} + \sum_{j=2}^{\hat{j}-1} \frac{F_t^{pl,j} - F_t^{pl,j-1}}{k_H^{pl,j}} + \frac{h}{\hat{j} \cdot b} \cdot \left(d_{u,h} - V_0^{pl,\hat{j}}\right) = \frac{h}{b \cdot \hat{j}} \cdot \Big[d_{u,h} + \tilde{k}(\hat{j} - 1)d_{y,h} +$$

$$\frac{q \cdot h}{2 \cdot n \cdot k_c}(\hat{j} - 1)\Big] \quad (61)^{A}$$

The ductility for kinematic modes V and VI are expressed in Equations (62) and (63), respectively.

$$\mu_w{}^{V} = \frac{\frac{h}{b} \cdot d_{u,c}}{\frac{h}{b} \cdot d_{y,h}} = \mu_h \cdot \frac{d_{u,c}}{d_{h,c}} \quad (62)$$

$$\mu_w{}^{VI} = \frac{\Delta_h^{u,VI}}{\Delta_h^{el}} \quad (63)$$

If failure mechanisms IV to VI are not attained, all steps in section 4.2.3 are repeated with an increase value of j^*, as shown in Figure 4-8, until $j^* = m$. The connectors are considered with sufficient ductility if kinematic mode m can be achieve.

4.2.4 SW Behaviour in Plastic State, Failure Mechanisms VII

SW behaviour is achieved when kinematic mode m is reached. To do so, the last transitional force must be resisted by the wall as shown in Figure 4-9.

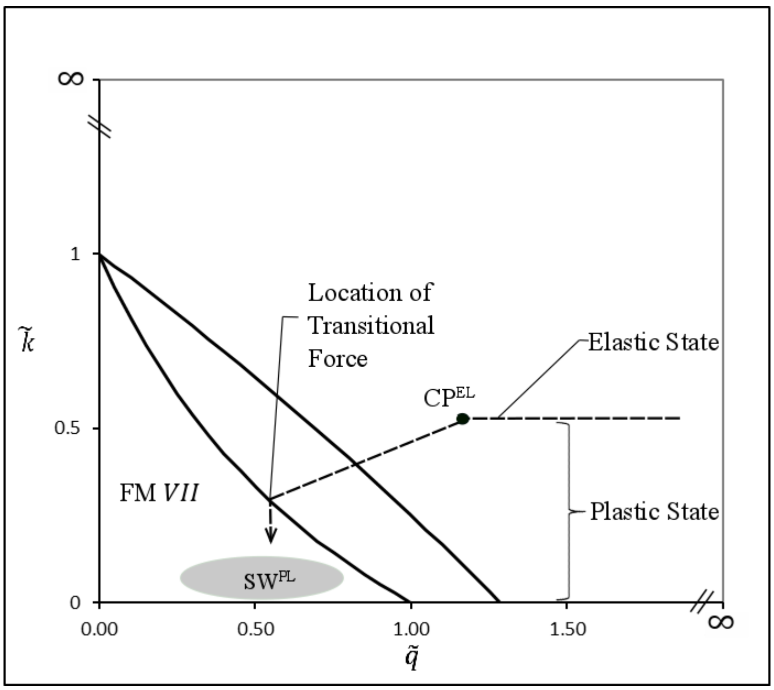

Figure 4-9: Behaviour Region SW^{PL} for Kinematic Path of Case CP^{EL}-SW^{PL}

Once SW behaviour is achieved, no additional lateral load is resisted by the wall since the hold-down has yielded and the wall stiffness is assumed as springs in series representing the hold-down and vertical joint. The plastic strength of the wall is equal to the transitional force, $F_t^{pl,m-1}$, and can be obtained by static equilibrium:

$$R_w^{pl,VII} = F_t^{pl,m-1} = \frac{r_h \cdot B}{h} + \frac{q \cdot B^2}{2 \cdot h} \quad (64)$$

The wall displacement associated with the plastic strength is the summation of the plastic deformation attained in kinematic mode 1 and the incremental displacement for each subsequent kinematic mode up to $m-1$:

$$\Delta_h^{pl,VII} = \Delta_{h,t}^{pl,1} + \sum_{j=2}^{m-1} \frac{F_t^{pl,j} - F_t^{pl,j-1}}{k_H^{pl,j}} = \frac{h}{b} \cdot \frac{r_h}{n \cdot k_c} + \frac{q \cdot h \cdot (m-1)}{n \cdot k_c} \quad (65)^{\mathrm{A}}$$

For the wall to achieve the SW behaviour in the plastic state in failure mechanism VII, the panel joint between the $m-1^{\mathrm{th}}$ and m^{th} panels must remain elastic.

$$d_{y,c} \geq \frac{1}{n \cdot k_c} [r_h + q \cdot b \cdot (m-1)] \quad (66)^{\mathrm{A}}$$

The ultimate lateral displacement of the wall is only dependant on the hold-down elongation since no additional load is applied to the elastic vertical joint. It should be noted that considering the incremental elongation of the hold-down for each kinematic mode is necessary, since they are not equal for different kinematic modes. Therefore, the elongation in hold-down for the SW behaviour, $V_0^{pl,m}$, is calculated as:

$$V_0^{pl,m} = \frac{1}{n \cdot k_c}(r_h + qb) + \sum_{j=2}^{m-1} \frac{j \cdot q \cdot b}{n \cdot k_c} = \frac{1}{n \cdot k_c}\left[r_h + \frac{q \cdot b \cdot m \cdot (m-1)}{2}\right] \quad (67)^{\mathrm{A}}$$

Ensuring the hold-down's ultimate displacement is larger than the required elongation to reach SW behaviour can be expressed as:

$$d_{u,h} \geq V_0^{pl,m} \ (68)$$

The ultimate displacement of the wall in failure mechanism VII is the sum of the lateral displacement of the wall in CP behaviour, the incremental displacement to achieve all intermediate kinematic modes (2 to $m-1$) and the displacement in the final kinematic mode m governed by failure in the hold-down. The expression is shown in Equation (69).

$$\Delta_h^{u,VII} = \Delta_{h,t}^{pl,1} + \sum_{j=2}^{m-1} \frac{F_t^{pl,j} - F_t^{pl,j-1}}{k_H^{pl,j}} + \frac{h}{m \cdot b} \cdot \left(d_{u,h} - V_0^{pl,m}\right) = \frac{h}{m \cdot b} \cdot d_{u,h} - \frac{h(m-1)}{m \cdot b} \frac{r_h}{n \cdot k_c} + \frac{q \cdot h \cdot (m-1)}{2 \cdot n \cdot k_c} \qquad (69)^{A}$$

The ductility of the wall can be expressed since the yielding and ultimate displacements are known:

$$\mu_w{}^{VII} = \frac{\Delta_h^{u,VII}}{\Delta_h^{el}} \qquad (70)$$

4.3 Model Development for the SW^{EL}-SW^{PL} Case

This case is achieved through the SW behaviour in the elastic state and the SW behaviour in the final plastic state and is ensured by the inequalities presented in Equations (19) and (21). It is assumed that the wall has transitioned through all three behaviours (CP, IN and SW) in the elastic state. This case only allows one failure mechanism because for kinematic mode m to be reached, the lateral stiffness is dominated by the yielding of the hold-down thereby disallowing the wall to take additional lateral load. This ensures that the vertical joints remain elastic. The force-displacement curve in Figure 4-10 presents the different behaviour region.

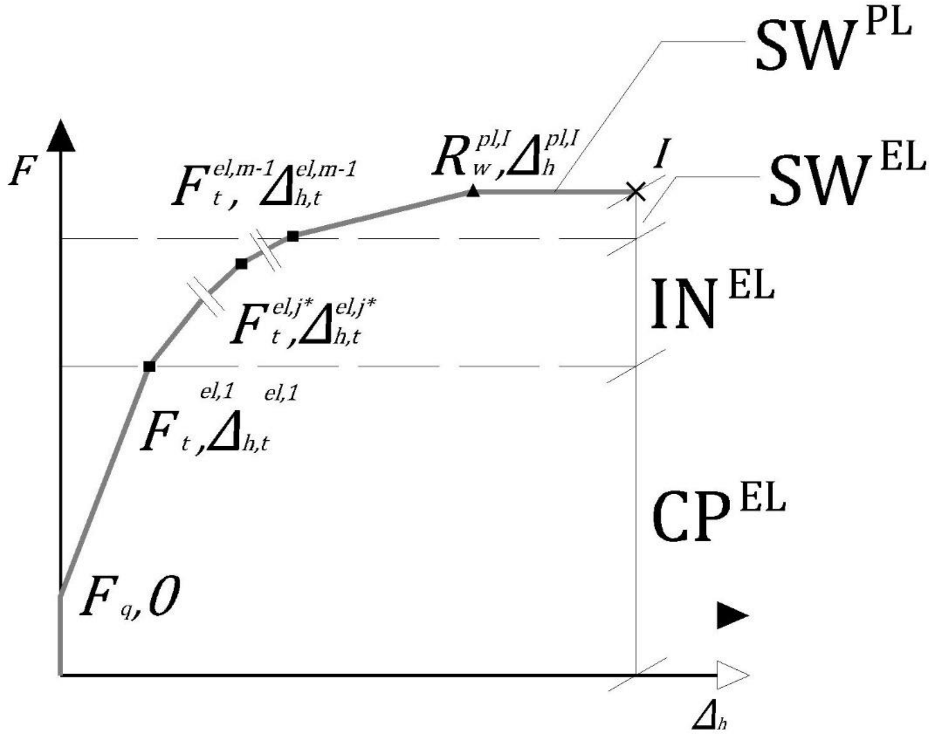

Figure 4-10: General Elasto-Plastic Force-Displacement Curve for Kinematic Path SW^{EL}-SW^{PL}

The only behaviour region where the failure occur is SW due to the fact that all other behaviour regions occurs in the elastic state. The kinematic path is presented in Figure 4-11 where it can be seen that the elastic state is represented by a line extending to point SW^{EL} where the wall attains its yielding strength. Afterward, the wall behaves without stiffness since the hold-down has yielded and the wall stiffness is assumed as springs in series representing the hold-down and vertical joint. To illustrate the lack of ability to resist additional load during the plastic state, the kinematic path between point SW^{EL} and SW^{PL} in Figure 4-11 is illustrated as a vertical line.

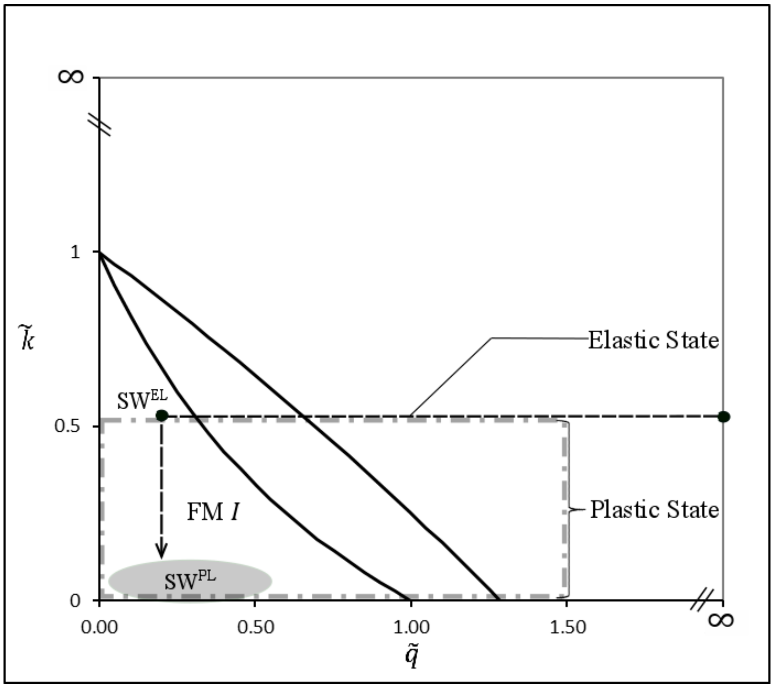

Figure 4-11: Behaviour Region of failure Mechanism for SW^{EL}-SW^{PL}

The failure mechanism is presented in Figure 4-11, while highlighting the yielding requirements and sequence to attain this failure mechanism.

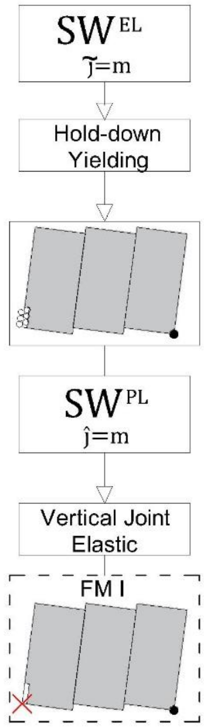

Figure 4-12: Definition of Failure Mechanism for SW^{EL}-SW^{PL}

The values for transitional force associated with kinematic mode j^* where $1 \leq j^* \leq m-1$ are presented in Equation (1). The transitional displacement achieved at the kinematic mode j^*, $\Delta_{h,t}^{el,j^*}$, is developed as the sum of displacements associated with the increase of force resulting a change of kinematic modes prior to achieving j^*.

$$\Delta_{h,t}^{el,j^*} = \frac{F_t^{el,1} - F_q}{k_H^{el,1}} + \sum_{j=2}^{j^*} \frac{F_t^{el,j} - F_t^{el,j-1}}{k_H^{el,j}} \quad (71)$$

Where equivalent lateral stiffness of the wall in the elastic state for mode j^* is written as:

$$k_H^{el,j^*} = \frac{k_h'^{\,el,j^*} \cdot b^2}{h^2} \quad (72)$$

The equivalent hold-down tensile stiffness for the elastic state of kinematic mode j^* is expressed as:

$$k_h'^{\,el,j^*} = \frac{n \cdot k_c \cdot [(j^* + mj^* - m) \cdot k_h + (m - j^*) \cdot n \cdot k_c]}{n \cdot k_c + (j^* - 1) \cdot k_h} \quad (73)$$

The plastic strength and displacement of the wall in failure mechanism I are equal to those attained at the elastic state where the hold-down yields in kinematic mode m, $R_{w,h}^{el,m}$ (as presented in Eq.8). As previously mentioned, no additional lateral forces are resisted in the plastic state which provide the following plastic characteristics for failure mechanism I:

$$R_w^{pl,I} = R_{w,h}^{el,m} \quad (74)$$

$$\Delta_h^{pl,I} = \Delta_h^{el} \quad (75)$$

Where the expression for elastic displacement has been defined in Casagrande et al. (2017) as:

$$\Delta_h^{el} = \left(\frac{R_{w,h}^{el,m} \cdot h^2}{b^2} - \frac{q \cdot m^2 \cdot h}{2} \cdot \frac{k_h'^{\,el,m}}{k_h}\right) \cdot \frac{1}{m^2 \cdot k_h'^{\,el,m}} \quad (76)$$

Also, where the equivalent hold-down tensile stiffness is expressed as a system of springs in series as:

$$k_h'^{\,el,m} = \left(\frac{1}{k_h} + \frac{m-1}{n \cdot k_c}\right)^{-1} \quad (77)$$

The ultimate displacement of the wall can be written as the sum of the elastic and plastic displacement related only to the hold-down properties. Therefore, the ultimate displacement of the wall takes the following form:

$$\Delta_h^{u,I} = \Delta_h^{el} + \frac{h}{B} \cdot \left(d_{u,h} - d_{y,h}\right) \quad (78)$$

The ductility is shown in Equation (79).

$$\mu_w{}^I = \frac{\Delta_h^{u,I}}{\Delta_h^{el}} \quad (79)$$

4.4 Model Development for the IN^{EL}-SW^{PL} Case

This case is achieved through the IN behaviour in the elastic state and the SW behaviour in the final plastic state and is ensured by the inequalities presented in Equations (19) and (22). The kinematic mode where the elastic strength is achieved, $\tilde{j}$, is found by increment of j^* until Equation (22) is validated for values of $\tilde{j}$ in the range of $[1, m-1]$. As shown in Figure 4-13, the behaviour regions are presented as CP behaviour (CP^{EL}) and IN behaviour (IN^{EL}) both in the elastic state until kinematic mode $\tilde{j}$ is achieved. From the elastic state, the wall may possess limited ductility and therefore remain in the IN behaviour for kinematic mode $\hat{j} = \tilde{j}$ or achieve a superior value of kinematic mode, $\hat{j}$, while still in the IN behaviour, in the range of $\tilde{j} + 1 \leq \hat{j} \leq m - 1$. SW behaviour and the associated failure mechanism VII is achieved if the ductility of hold-down and the yield displacement of vertical joints are sufficient. The different behaviour regions for which the wall may reach its ultimate capacity are presented in the general force-displacement curve shown in Figure 4-13 and associated kinematic path in Figure 4-14.

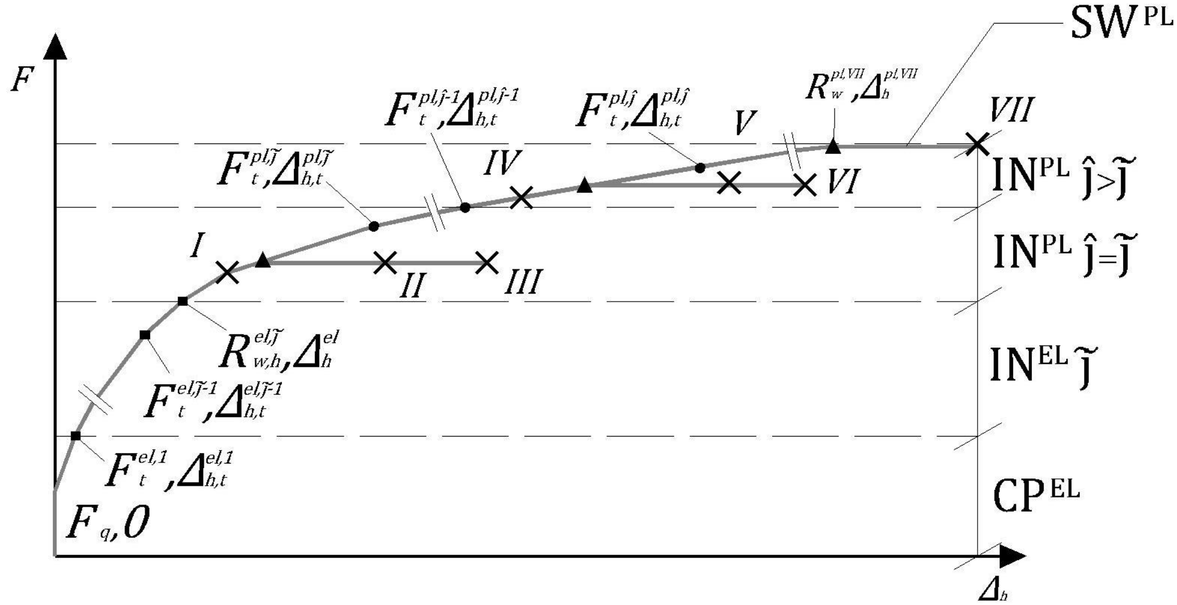

Figure 4-13: General Elasto-Plastic Force-Displacement Curve for Kinematic Path IN^{EL}-SW^{PL}

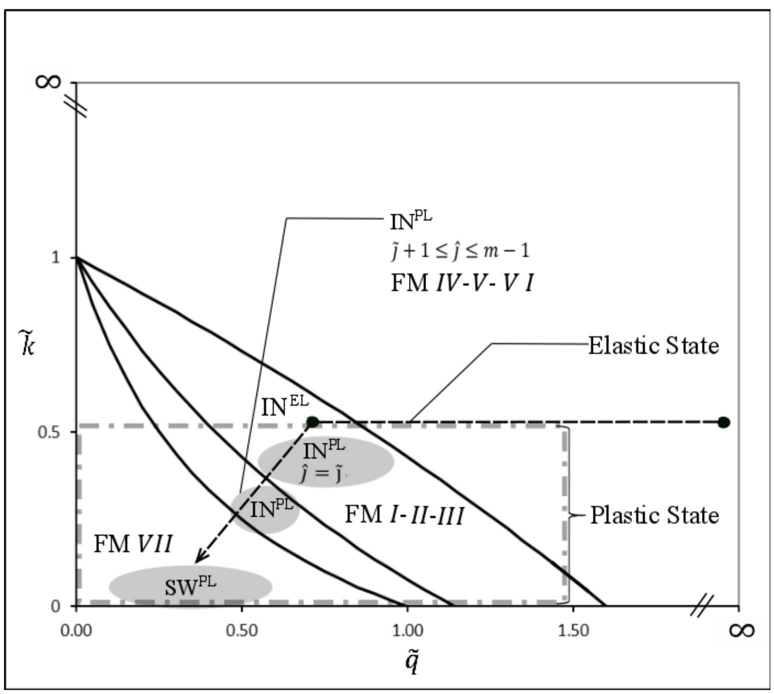

Figure 4-14: Behaviour Region of failure Mechanism for IN^{EL}-SW^{PL}

All failure mechanisms along the IN^{EL}-SW^{PL} path are illustrated in Figure 4-15. The failure mechanisms can be established based on 3 possible cases of kinematic modes, $\hat{j}$, achieved in plastic state due to limited connectors elongation capacity. Failure mechanisms I, II and III are define for $\hat{j} = \tilde{j}$, IV, V and VI are defined for $\tilde{j} + 1 \leq \hat{j} \leq m - 1$ and VII is defined for $\hat{j} = m$.

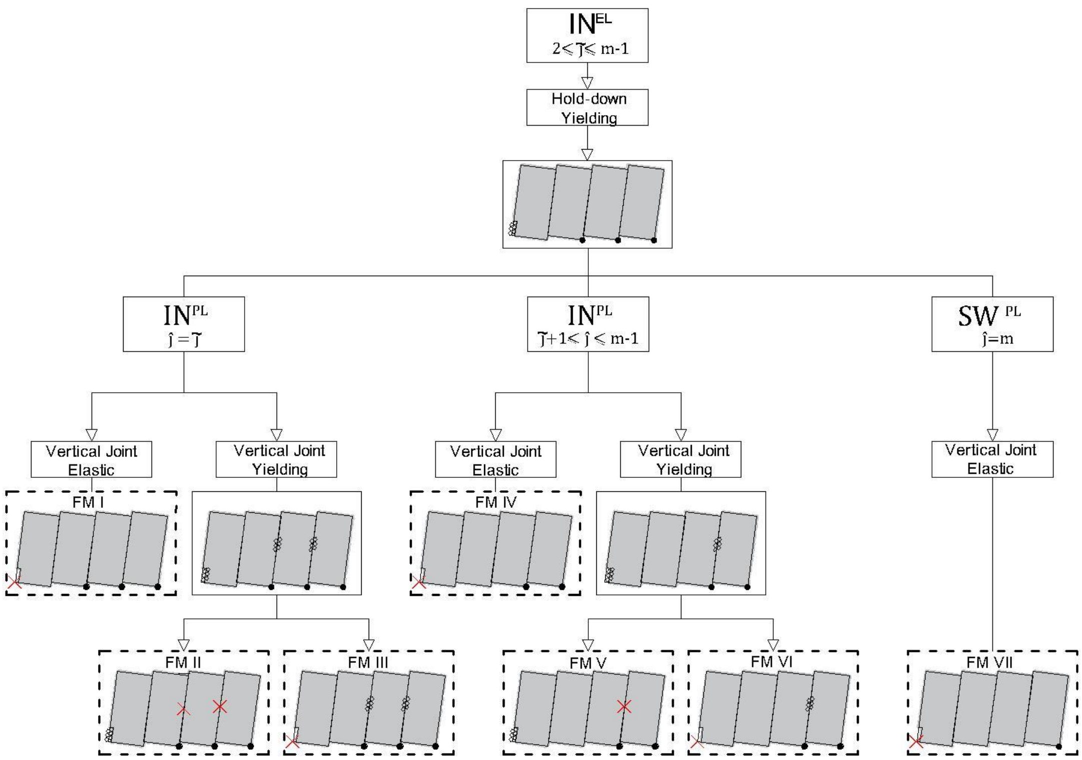

Figure 4-15: Definition of Failure Mechanism for IN^{EL}-SW^{PL}

The subsequent sections will follow the structure presented in Figure 4-15, starting by describing the elastic state in CP and IN behaviour (Section 4.4.1), followed by a description of the plastic states in the IN^{PL} ($\hat{j} = \tilde{j}$), IN^{PL} ($1 \leq \hat{j} \leq m - 1$) and SW^{PL} behaviour in Sections 4.4.2, 4.4.3 and 4.4.4, respectively.

4.4.1 CP and IN behaviour in Elastic State

As mentioned before, the first point in the force-displacement relationship of the wall for all cases is the activation force, which was previously defined by Equation (6) and discussed in Section 3.2.

The first segment of the force-displacement relationship in limited by the change between kinematic mode 1 and 2 and is denoted, $F_t^{el,1}$, presented in Equation (1). The first transitional force is associated with the following displacement:

$$\Delta_{h,t}^{el,1} = \frac{F_t^{el,1} - F_q}{k_H^{el,1}} \quad (80)$$

The intermediate displacements of the wall for any kinematic mode j^* in the range of $[2, \tilde{\jmath}]$, associated with intermediate transitional forces F_t^{el,j^*}, are the sum of the lateral displacement of the wall in kinematic mode 1 and the incremental displacement to achieve all intermediate kinematic modes (2 to $\tilde{\jmath}$). The expression is shown in Equation (81).

$$\Delta_{h,t}^{el,j^*} = \frac{F_t^{el,1} - F_q}{k_H^{el,1}} + \sum_{j^*=2}^{\tilde{\jmath}} \frac{F_t^{el,j^*} - F_t^{el,j^*-1}}{k_H^{el,j^*}} \quad (81)$$

The last elastic segment (Figure 4-13) is limited by the transitional force to achieve kinematic mode $\tilde{\jmath}$ and the elastic strength in kinematic mode $\tilde{\jmath}$, $R_{w,h}^{el,\tilde{\jmath}}$, as expressed in Equation (8). Therefore, the associated elastic displacement of case IN^{EL}-SW^{PL} and is expressed in Equation (82):

$$\Delta_h^{el} = \frac{R_{w,h}^{el,\tilde{\jmath}} \cdot h^2}{b^2 \cdot k_h'^{\,el,\tilde{\jmath}}} - \frac{q \cdot h}{2 \cdot k_h'^{\,el,\tilde{\jmath}}} \cdot \frac{\left(m + \tilde{\jmath} \cdot (\tilde{\jmath} - 1)\right) \cdot n \cdot k_c + (\tilde{\jmath} - 1) \cdot (m - \tilde{\jmath}) \cdot k_h}{n \cdot k_c + (\tilde{\jmath} - 1) \cdot k_h} \quad (82)$$

Where $k_h'^{\,el,\tilde{\jmath}}$ is the equivalent hold-down tensile stiffness for IN behaviour with $\tilde{\jmath} = j^*$.

$$k_h'^{\,el,\tilde{\jmath}} = \frac{n \cdot k_c \cdot [(\tilde{\jmath} + m\tilde{\jmath} - m) \cdot k_h + (m - \tilde{\jmath}) \cdot n \cdot k_c]}{n \cdot k_c + (\tilde{\jmath} - 1) \cdot k_h} \quad (83)$$

4.4.2 IN Behaviour Region for Kinematic Mode $\hat{j} = \tilde{\jmath}$ in Plastic State, Failure Mechanisms $I - III$

As can be seen in Figure 4-16, IN^{PL} is defined by the limits represented with the yielding of the hold-down, and the transitional force to achieve kinematic mode $\tilde{\jmath} + 1$, $F_t^{pl,\tilde{\jmath}}$. This transition force defines the state where the $\tilde{\jmath}^{th}$ panel is no longer in contact with the ground, i.e. the reaction of panel $\tilde{\jmath}$ is equal to zero (Figure 4-17).

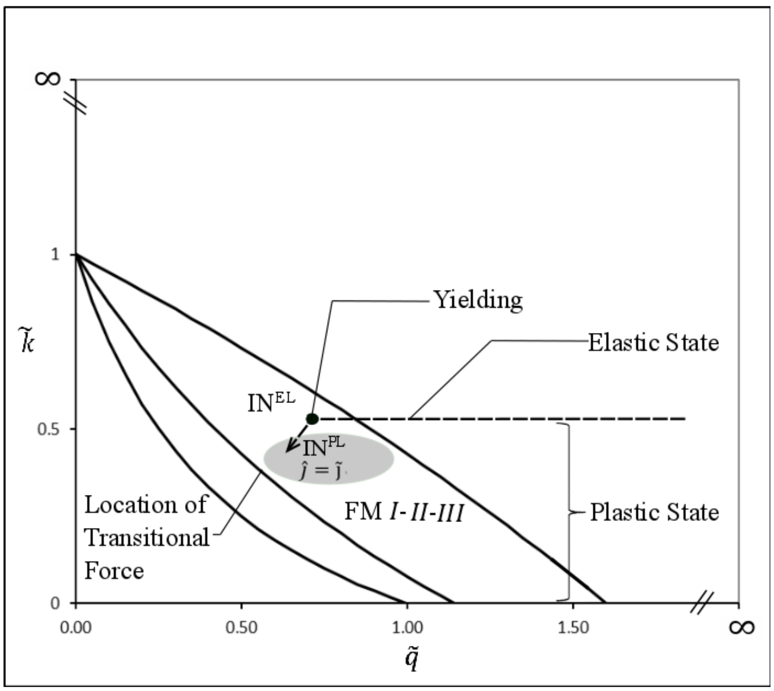

Figure 4-16: Behaviour Region IN^{PL} with $\tilde{\jmath}$ for Kinematic Path of Case IN^{EL}-SW^{PL}

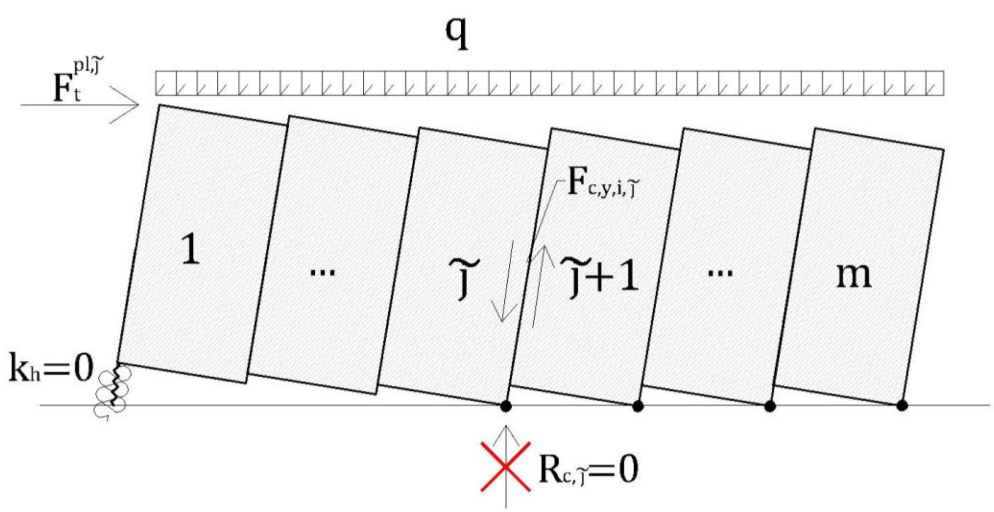

Figure 4-17: Transition from kinematic mode $\tilde{\jmath}$ to $\tilde{\jmath}+1$

The increase in lateral force, $F_t^{pl,\tilde{\jmath}} - R_{w,h}^{el,\tilde{\jmath}}$, that leads to kinematic mode $\tilde{\jmath}$ (i.e. $R_{c,\tilde{\jmath}} = 0$), is expressed using static equilibrium, as shown in Equation (84):

$$F_t^{pl,\tilde{\jmath}} - R_{w,h}^{el,\tilde{\jmath}} = \frac{R_{c,\tilde{\jmath}} \cdot b \cdot (m - \tilde{\jmath})}{h} \quad (84)$$

Where $R_{c,\tilde{\jmath}}$ is calculated considering static equilibrium of the $\tilde{\jmath}^{th}$ panel as:

$$R_{c,\tilde{\jmath}} = r_h + q \cdot b \cdot \tilde{\jmath} - n \cdot F_{c,y,i,\tilde{\jmath}} \quad (85)$$

Additionally, the forces in the panel joint between panel $\tilde{\jmath}$ and $\tilde{\jmath}+1$, $F_{c,y,i,\tilde{\jmath}}$, are required to be calculated when the wall is under a lateral force equivalent to the elastic strength, $R_{w,h}^{el,\tilde{\jmath}}$ (Casagrande et al. 2017).

$$F_{c,y,i,\tilde{\jmath}} = \frac{R_{w,h}^{el,\tilde{\jmath}} \cdot h}{n \cdot b} \cdot \frac{n \cdot k_c + (\tilde{\jmath}-1) \cdot k_h}{(\tilde{\jmath} + m \cdot \tilde{\jmath} - m) \cdot k_h + (m - \tilde{\jmath}) \cdot n \cdot k_c} - \frac{q \cdot b}{2 \cdot n} \cdot \frac{[m + \tilde{\jmath} \cdot (\tilde{\jmath}-1)] \cdot n \cdot k_c + (\tilde{\jmath}-1) \cdot (m - \tilde{\jmath}) \cdot k_h}{(\tilde{\jmath} + m \cdot \tilde{\jmath} - m) \cdot k_h + (m - \tilde{\jmath}) \cdot n \cdot k_c} \quad (86)$$

The total transitional force between kinematic mode $\tilde{\jmath}$ and $\tilde{\jmath}+1$ is expressed in Equation (87) as the sum of the elastic strength achieved in kinematic mode $\tilde{\jmath}$, $R_{w,h}^{el,\tilde{\jmath}}$, and the increase in force defined in Equation (84).

$$F_t^{pl,\tilde{\jmath}} = R_{w,h}^{el,\tilde{\jmath}} + \frac{R_{c,\tilde{\jmath}} \cdot b \cdot (m-\tilde{\jmath})}{h} \quad (87)$$

The total lateral displacement of the wall related to the transitional force defined in Equation (87), can be written as the sum of the elastic displacement and the displacement associated with the increase in force causing a shift to kinematic mode $\tilde{\jmath}+1$ from the elastic strength:

$$\Delta_{h,t}^{pl,\tilde{\jmath}} = \Delta_h^{el} + \frac{F_t^{pl,\tilde{\jmath}} - R_{w,h}^{el,\tilde{\jmath}}}{k_H^{pl,\tilde{\jmath}}} = \Delta_h^{el} + \frac{R_{c,\tilde{\jmath}} \cdot h}{n \cdot k_c \cdot b} \quad (88)$$

The equivalent hold-down stiffness in the plastic state for kinematic mode $\tilde{\jmath}$ is written in a similar fashion to that in the elastic state (Eq. 83) but without the contribution of the hold-down, $k_h'^{\,pl,\tilde{\jmath}} = k_h'^{\,el,\tilde{\jmath}}(k_h = 0)$. Therefore, the equivalent lateral stiffness of the wall is expressed as:

$$k_H^{pl,\tilde{\jmath}} = \frac{k_h'^{\,pl,\tilde{\jmath}} \cdot b^2}{h^2} = \frac{(m-\tilde{\jmath}) \cdot n \cdot k_c \cdot b^2}{h^2} \quad (89)$$

The transitional force, $F_t^{pl,\tilde{\jmath}}$ and its associated displacement cannot be attained in failure mechanisms I, II and III due to limited elongation capability in the connectors (see Figure 4-15). These failure mechanisms are achieved when the wall remains in kinematic mode $\tilde{\jmath}$ following the yielding of the hold-down. Attaining failure mechanism I is ensured by the following two conditions: a) failure of the hold-down is reached while the wall remains in kinematic mode $\tilde{\jmath}$ (Eq. 90), and b) the failure of the hold-down is reached prior to the yielding of the panel joints (Eq. 91):

$$d_{u,h} < V_0^{pl,\tilde{j}} = d_{y,h} + \frac{\tilde{j} \cdot R_{c,\tilde{j}}}{n \cdot k_c} \quad (90)^{A}$$

$$d_{y,c} > V_c^{pl,\tilde{j}} = V_c^{el,\tilde{j}} + \frac{(d_{u,h} - d_{y,h})}{\tilde{j}} \quad (91)$$

Where $V_0^{pl,\tilde{j}}$ is the total displacement of the hold-down in kinematic mode $\tilde{j}$ for the IN behaviour in the plastic state. It is expressed as the sum of the yielding displacement of the hold-down and the displacement of the hold-down to achieve kinematic mode $\tilde{j}$.

$V_c^{el,\tilde{j}}$ is the total elongation of vertical joints related to achievement of the elastic strength in kinematic mode $\tilde{j}$. Therefore, Equation (92) presents the summation of elongation of the vertical joints for kinematic mode 1, the incremental displacement for each subsequent kinematic mode up to $\tilde{j} - 1$ and the elongation related to the achievement of the elastic strength in kinematic mode $\tilde{j}$.

$$V_c^{el,\tilde{j}} =$$

$$\frac{b}{h \cdot {k'}_h^{el,1}} \cdot \left(\frac{F_t^{el,1} \cdot h^2}{b^2} - \frac{qmh}{2}\right) + \sum_{j=2}^{\tilde{j}-1} \frac{\left(F_t^{el,j} - F_t^{el,j-1}\right) \cdot h}{b \cdot [(j + m \cdot j - m) \cdot k_h + (m - j) \cdot n \cdot k_c]} + \frac{\left(R_{w,h}^{el,\tilde{j}} - F_t^{el,\tilde{j}-1}\right) \cdot h}{b \cdot [(\tilde{j} + m \cdot \tilde{j} - m) \cdot k_h + (m - \tilde{j}) \cdot n \cdot k_c]} \quad (92)$$

The plastic strength of the wall under these conditions can be written as the sum of the elastic strength and the interpolation between the elastic strength and the transitional force between kinematic modes $\tilde{j}$ and $\tilde{j} + 1$ governed by the ultimate displacement of the hold-down.

$$R_w^{pl,I} = R_{w,h}^{el,\tilde{j}} + \left(F_t^{pl,\tilde{j}} - R_{w,h}^{el,\tilde{j}}\right) \cdot \frac{d_{u,h} - d_{y,h}}{V_0^{pl,\tilde{j}} - d_{y,h}} \quad (93)$$

The lateral displacement in kinematic mode $\tilde{j}$ in the plastic state is controlled by the ultimate displacement of the hold-down for failure mechanism I.

$$\Delta_h^{u,I} = \Delta_h^{pl} = \Delta_h^{el} + \frac{h}{\tilde{j} \cdot b} \cdot \left(d_{u,h} - d_{y,h}\right) \quad (94)$$

The associated ductility for this failure mechanism is expressed as:

$$\mu_w{}^I = \frac{\Delta_h^{u,I}}{\Delta_h^{el}} \quad (95)$$

Failure mechanism II and III also occur in kinematic mode ȷ̃, but where the wall's plastic strength is governed by yielding in the vertical joints. Attaining failure mechanism II and III is ensured by the following two conditions: a) the yielding displacement of the vertical joints occurs prior to achieving the displacement in the connectors associated with the transitional force $F_t^{pl,\tilde{\jmath}}$ (Eq. 96), and b) yielding displacement of the vertical joints is reached prior to the ultimate displacement of the hold-down as expressed in equation (Eq. 97):

$$d_{y,c} < V_c^{el,\tilde{\jmath}} + \frac{R_{c,\tilde{\jmath}}}{n \cdot k_c} \quad (96)^A$$

$$d_{u,h} > d_{y,h} + \tilde{\jmath} \cdot \left(d_{y,c} - V_c^{el,\tilde{\jmath}}\right) \quad (97)^A$$

The plastic strength of the wall for failure mechanisms II and III occurs when the panel joints yield. Therefore, the wall resistance can be expressed as the sum of the elastic strength and interpolation of the increase of force to achieve kinematic mode $\tilde{\jmath} + 1$ that is governed by the yielding displacement of the panel joints:

$$R_w^{pl,II} = R_w^{pl,III} = R_{w,h}^{el,\tilde{\jmath}} + \left(F_t^{pl,\tilde{\jmath}} - R_{w,h}^{el,\tilde{\jmath}}\right) \cdot \frac{n \cdot k_c \left(d_{y,c} - V_c^{el,\tilde{\jmath}}\right)}{R_{c,\tilde{\jmath}}} \quad (98)^A$$

The total displacement at the plastic strength for both failure mechanisms II and III is governed by the yield displacement of the vertical joint.

$$\Delta_h^{pl,II} = \Delta_h^{pl,III} = \Delta_h^{el} + \frac{R_w^{pl,II,III} - R_{w,h}^{el,\tilde{\jmath}}}{k_H^{pl,\tilde{\jmath}}} = \frac{r_c \cdot h}{k_c \cdot b} = d_{y,c} \cdot \frac{h}{b} \quad (99)$$

The ultimate displacements for failure mechanism II and III are characterized by failure in the vertical joints and in the hold-down, respectively. Failure mechanism II is expressed as the ultimate displacement for vertical joint and the panel aspect ratio whereas failure mechanism III is the sum of elastic displacement and the allowable elongation from yielding to ultimate displacement of the hold-down in relation with the segment of the wall with uplifted panels.

$$\Delta_h^{u,II} = \frac{h}{b} \cdot d_{u,c} \quad (100)$$

$$\Delta_h^{u,III} = \Delta_h^{el} + \frac{h}{\tilde{j} \cdot b}\left(d_{u,h} - d_{y,h}\right) \quad (101)$$

The ductility for failure mechanism II and III can be expressed as:

$$\mu_w{}^{II} = \frac{\Delta_h^{u,II}}{\Delta_h^{el}} \quad (102)$$

$$\mu_w{}^{III} = \frac{\Delta_h^{u,III}}{\Delta_h^{el}} \quad (103)$$

4.4.3 IN Behaviour Region for kinematic mode $\tilde{\mathbf{j}} + \mathbf{1} \leq \hat{\boldsymbol{j}} \leq \boldsymbol{m}$ in Plastic State, Failure Mechanisms $\boldsymbol{IV} - \boldsymbol{VI}$

Figure 4-18 illustrates the region for failure mechanisms $IV - VI$, which starts with kinematic mode $\tilde{j} + 1$ and ends with the achievement of SW behaviour or a kinematic mode in between. This particular behaviour is attained when the ductility of the connectors is sufficient to extend the wall beyond kinematic mode $\tilde{j}$.

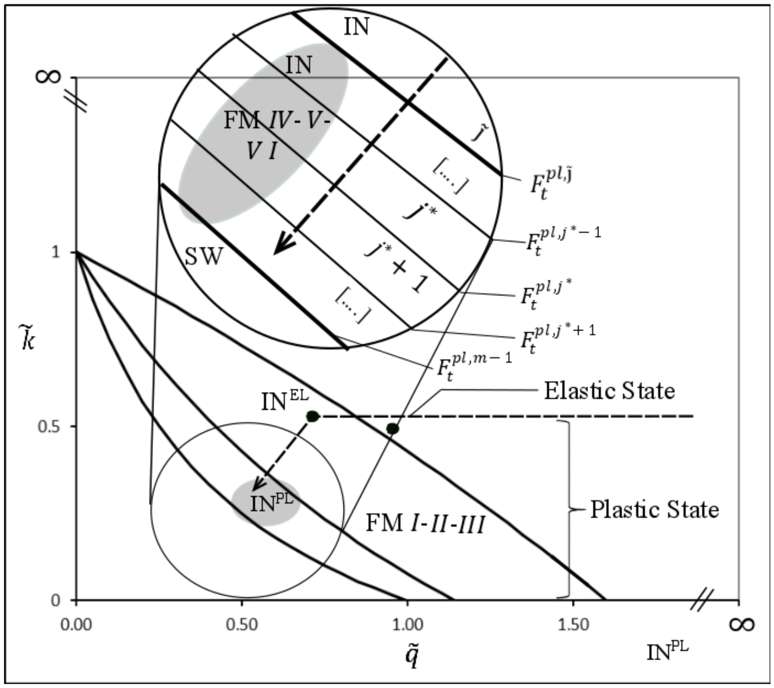

Figure 4-18: Behaviour Region IN^{PL} with $\tilde{j} = [2, m-1]$ for Kinematic Path of Case IN^{EL}-SW^{PL}

The development of the force-displacement curve follows the procedure outlined in Figure 4-19. As indicated in Figure 4-19, the value of j^* is increased between $\tilde{j}+1$ and $m-1$.

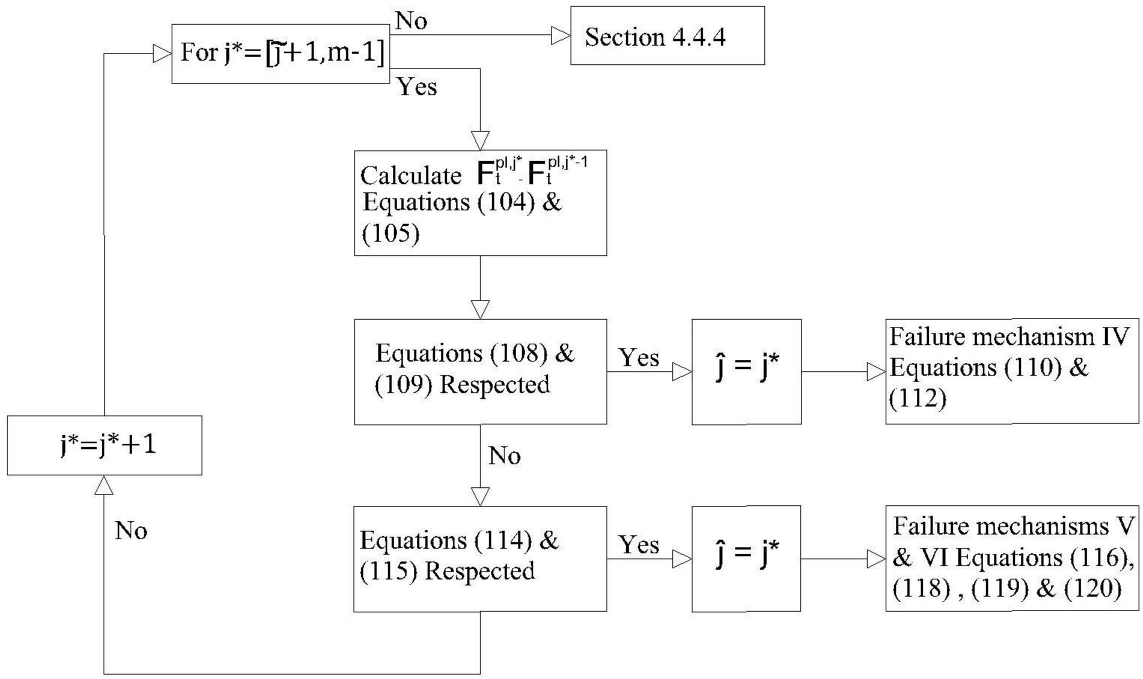

Figure 4-19: Steps to solve IN Behaviour Region of Case IN^{EL}-SW^{PL}, Failure Mechanisms IV-VI

The transitional forces and associated displacements for kinematic mode j^* and $j^* + 1$ are calculated to define the limits surrounding kinematic mode j^*. The transitional forces to attain modes j^* and $j^* + 1$ are denoted F_t^{pl,j^*-1} and F_t^{pl,j^*}, respectively. Through static equilibrium, the increase in lateral force between two adjacent kinematic modes can be expressed as:

$$F_t^{pl,j^*} - F_t^{pl,j^*-1} = \frac{R_{c,j^*} \cdot b}{h}(m - j^*) = \frac{q \cdot b^2}{h}(m - j^*) \quad (104)$$

Where the reaction force of the j^{*th} panel only considers the vertical load applied on the panel because the stiffness of the panels not in contact with ground (from 1 to j^*) is equal to zero in this segment of the wall since the hold-down has yielded and the wall stiffness is assumed as springs in series representing the hold-down and vertical joint. Therefore, the lateral forces are transferred to the next panels in contact with the ground and the reaction force takes the following expression using static equilibrium:

$$R_{c,j^*} = q \cdot b \quad (105)$$

The total transitional force at the point where the wall changes from kinematic mode j^* to kinematic mode $j^* + 1$ is:

$$F_t^{pl,j^*} = F_t^{pl,\tilde{\jmath}} + \sum_{j=\tilde{\jmath}+1}^{j^*} \frac{q \cdot b^2}{h} (m - j) \quad (106)$$

The total lateral displacement for kinematic mode j^* associated with transitional force consist of the elastic displacement, the displacement to develop kinematic mode $\tilde{\jmath}$ and the incremental displacement to fully develop kinematic mode j between $\tilde{\jmath} + 1$ and j^* . It is expressed in Equation (107).

$$\Delta_{h,t}^{pl,j^*} = \Delta_h^{el} + \frac{R_{c,\tilde{\jmath}} \cdot h}{n \cdot k_c \cdot b} + \sum_{j=\tilde{\jmath}+1}^{j^*} \frac{q \cdot h}{n \cdot k_c} \quad (107)^{A}$$

Failure mechanism IV is characterized by the failure of the hold-down in kinematic mode j^* attained before the yielding of the vertical joints, as expressed in Equation (108). Equation (109) shows that the ultimate displacement of the hold-down in failure mechanism IV is bounded by the deformation to fully develop kinematic mode $j^* - 1$ and j^*. This is expressed through the following two conditions:

$$d_{y,c} > V_c^{el,\tilde{\jmath}} + \frac{R_{c,\tilde{\jmath}}}{n \cdot k_c} + \sum_{j=\tilde{\jmath}+1}^{j^*-1} \frac{q \cdot b}{n \cdot k_c} + \frac{1}{j^*} \cdot \left[d_{u,h} - d_{y,h} - \frac{\tilde{\jmath} \cdot R_{c,\tilde{\jmath}}}{n \cdot k_c} - \sum_{j=\tilde{\jmath}+1}^{j^*-1} \frac{j \cdot q \cdot b}{n \cdot k_c} \right] \quad (108)^{A}$$

$$d_{y,h} + \frac{\tilde{\jmath} \cdot R_{c,\tilde{\jmath}}}{n \cdot k_c} + \sum_{j=\tilde{\jmath}+1}^{j^*-1} \frac{j \cdot q \cdot b}{n \cdot k_c} \leq d_{u,h} < d_{y,h} + \frac{\tilde{\jmath} \cdot R_{c,\tilde{\jmath}}}{n \cdot k_c} + \sum_{j=\tilde{\jmath}+1}^{j^*} \frac{j \cdot q \cdot b}{n \cdot k_c} \quad (109)^{A}$$

If both conditions (i.e. Eq.108 and 109) are met, then j^* and $\hat{j}$ are equal and become associated with the final kinematic mode in the plastic state.

The plastic strength for failure mechanism IV is calculated by adding the $\tilde{\jmath}^{th}$ transitional force, $F_t^{pl,\tilde{\jmath}}$, the increase of force required to fully develop kinematic mode $j^* = [2, \hat{j}-1]$ and an interpolation of the increase of force to achieve kinematic mode $\hat{j}+1$ that is governed by the ultimate displacement of the hold-down. The plastic strength associated with kinematic mode $\hat{j}$ resulting in the failure of the hold-down is presented in Equation (110) from interpolation.

$$R_w^{pl,IV} = F_t^{pl,\tilde{\jmath}} + \sum_{j=\tilde{\jmath}+1}^{\hat{j}-1} \frac{q \cdot b^2}{h}(m - j) + \left(\frac{d_{u,h} - V_0^{pl,\hat{j}}}{\left(\frac{\hat{j} \cdot q \cdot b}{n \cdot k_c}\right)} \right) \cdot \frac{q \cdot b^2}{h}(m - \hat{j}) \quad (110)$$

Where $V_0^{pl,\hat{j}}$ is the total hold-down elongation attained in mode $\hat{j}$.

$$V_0^{pl,\hat{j}} = d_{y,h} + \frac{\tilde{\jmath} \cdot R_{c,\tilde{\jmath}}}{n \cdot k_c} + \sum_{j=\tilde{\jmath}+1}^{\hat{j}-1} \frac{j \cdot q \cdot b}{n \cdot k_c} \quad (111)^{A}$$

The ultimate displacement of the wall in failure mechanism IV is the sum of the lateral displacement of the wall in elastic state (kinematic mode 1 to $\tilde{\jmath}$), the incremental displacement in kinematic mode $\tilde{\jmath}$ in the plastic state, the incremental displacement to achieve all intermediate kinematic modes ($\tilde{\jmath}+1$ to $\hat{j}-1$) and the displacement in the final kinematic mode $\hat{j}$ governed by failure in the hold-down. The expression is shown in Equation (112).

$$\Delta_h^{u,IV} = \Delta_h^{pl,IV} = \Delta_h^{el} + \frac{R_{c,\tilde{\jmath}} \cdot h}{n \cdot k_c \cdot b} + \sum_{j=\tilde{\jmath}+1}^{\hat{j}-1} \frac{q \cdot h}{n \cdot k_c} + \frac{h}{\hat{j} \cdot b}\left(d_{u,h} - V_0^{pl,\hat{j}}\right) \quad (112)^{A}$$

The ductility of the wall can be developed as:

$$\mu_w{}^{IV} = \frac{\Delta_h^{u,IV}}{\Delta_h^{el}} \quad (113)$$

Failure mechanisms V and VI occurs when the vertical joints yield in kinematic mode j^* prior the failure of the hold-down, as expressed in Equation (114). Equation (115) shows that the yielding displacement of the vertical joints in failure mechanism V and VI is bounded by the deformation to fully develop kinematic mode $j^* - 1$ and j^*.

$$d_{u,h} > d_{y,h} + \frac{\tilde{\jmath} \cdot R_{c,\tilde{\jmath}}}{n \cdot k_c} + \sum_{j=\tilde{\jmath}+1}^{j^*-1} \frac{j \cdot q \cdot b}{n \cdot k_c} + j^* \cdot \left[d_{y,c} - V_c^{el,\tilde{\jmath}} - \frac{R_{c,\tilde{\jmath}}}{n \cdot k_c} - \sum_{j=\tilde{\jmath}+1}^{j^*-1} \frac{q \cdot b}{n \cdot k_c} \right] \quad (114)^{A}$$

$$V_c^{el,\tilde{\jmath}} + \frac{R_{c,\tilde{\jmath}}}{n \cdot k_c} + \sum_{j=\tilde{\jmath}+1}^{j^*-1} \frac{q \cdot b}{n \cdot k_c} \leq d_{y,c} < V_c^{el,\tilde{\jmath}} + \frac{R_{c,\tilde{\jmath}}}{n \cdot k_c} + \sum_{j=\tilde{\jmath}+1}^{j^*} \frac{q \cdot b}{n \cdot k_c} \quad (115)^{A}$$

The plastic strength of failure mechanism V and VI is the sum of the first transitional force, $F_t^{pl,1}$, the increase of force required fully develop kinematic mode $j^* = [2, \hat{\jmath} - 1]$ and the interpolation of the increase of force in kinematic mode $\hat{\jmath}$ that is governed by the yielding displacement of the panel joints.

$$R_w^{pl,V} = R_w^{pl,VI} = F_t^{pl,\tilde{\jmath}} + \sum_{j=\tilde{\jmath}+1}^{\hat{\jmath}-1} \frac{q \cdot b^2}{h} (m - j) + \left(\frac{d_{y,c} - V_c^{pl,\hat{\jmath}}}{\left(\frac{q \cdot b}{n \cdot k_c} \right)} \right) \cdot \frac{q \cdot b^2}{h} (m - \hat{\jmath}) \quad (116)$$

Where $V_c^{pl,\hat{\jmath}}$ is the total elongation of fasteners in vertical joints $\hat{\jmath}$ to $m - 1$ attained in mode $\hat{\jmath}$ and is shown Equation (117).

$$V_c^{pl,\hat{\jmath}} = V_c^{el,\tilde{\jmath}} + \frac{R_{c,\tilde{\jmath}}}{n \cdot k} + \sum_{\tilde{\jmath}+1}^{\hat{\jmath}-1} \frac{q \cdot b}{n \cdot k_c} \quad (117)^{A}$$

The plastic displacement of the wall in failure mechanism V and VI is the sum of the lateral displacement of the wall in kinematic mode $\tilde{\jmath}$, the incremental displacement to develop all intermediate kinematic modes ($\tilde{\jmath} + 1$ to $\hat{\jmath} - 1$) and the displacement in the final kinematic mode $\hat{\jmath}$ governed by yielding of the vertical joints. The expression is shown in Equation (118).

$$\Delta_h^{pl,V,VI} = \Delta_h^{el} + \frac{R_{c,\tilde{\jmath}} \cdot h}{n \cdot k_c \cdot b} + \sum_{j=\tilde{\jmath}+1}^{\hat{\jmath}-1} \frac{q \cdot h}{n \cdot k_c} + \frac{R_w^{pl,V,VI} - F_t^{pl,\hat{\jmath}}}{k_H^{pl,\hat{\jmath}}} = \frac{h}{b} \cdot d_{y,c} \quad (118)$$

The ultimate displacements for failure mechanism V and VI are characterized by failure in the vertical joints and the hold-down, respectively. It can be expressed as the ultimate displacement of the vertical joint and the wall panel aspect ratio for Equation (119). Equation (120) is developed as the sum the elastic displacement (up to kinematic mode $\tilde{\jmath}$), the incremental displacement to fully develop kinematic mode $\tilde{\jmath}$, the incremental displacement associated with all kinematic mode $\tilde{\jmath}+1$ to $\hat{\jmath}-1$ and the displacement in the final kinematic mode $\hat{\jmath}$ governed by failure in the hold-down.

$$\Delta_h^{u,V} = \frac{h}{b} \cdot d_{u,c} \quad (119)$$

$$\Delta_h^{u,VI} = \Delta_h^{el} + \frac{R_{c,\tilde{\jmath}} \cdot h}{n \cdot k_c \cdot b} + \sum_{j=\tilde{\jmath}+1}^{\hat{\jmath}-1} \frac{q \cdot h}{n \cdot k_c} + \frac{h}{\hat{\jmath} \cdot b}\left(d_{u,h} - V_0^{pl,\hat{\jmath}}\right) \quad (120)^{A}$$

The ductility for kinematic modes V and VI are expressed in Equations (121) and (122), respectively.

$$\mu_w{}^{V} = \frac{\Delta_h^{u,V}}{\Delta_h^{el}} \quad (121)$$

$$\mu_w{}^{VI} = \frac{\Delta_h^{u,VI}}{\Delta_h^{el}} \quad (122)$$

4.4.4 SW Behaviour State in Plastic State, Failure Mechanisms VII

As shown in Figure 4-17, SW behaviour is achieved when kinematic mode m is reached.

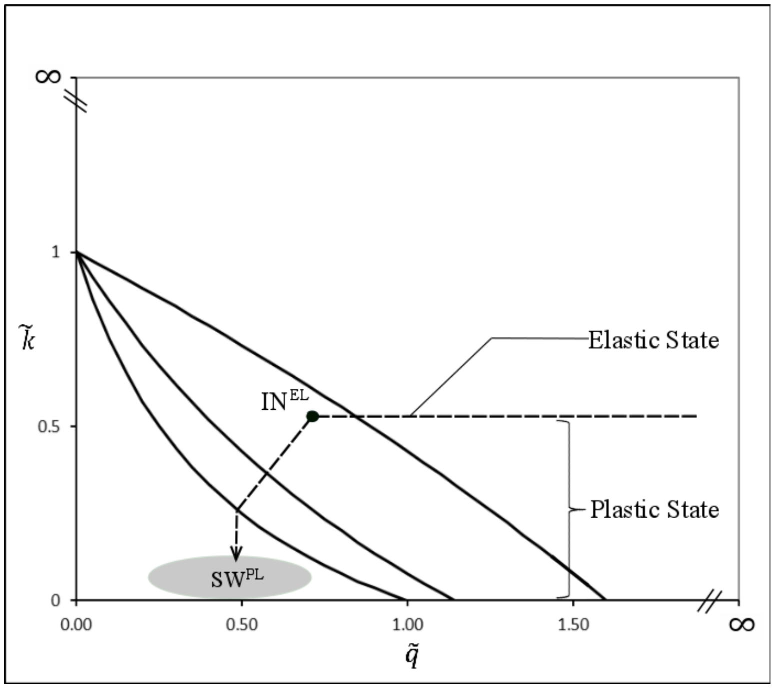

Figure 4-20: Behaviour Region SW^{PL} for Kinematic Path of Case IN^{EL}-SW^{PL}

The plastic strength of the wall is equal to the transitional force, $F_t^{pl,m-1}$, and can be obtained by static equilibrium:

$$R_w^{pl,VII} = F_t^{pl,m-1} = R_{w,h}^{el,\tilde{j}} + \frac{R_{c,\tilde{j}} \cdot b \cdot (m-\tilde{j})}{h} + \sum_{j=\tilde{j}+1}^{m-1} \frac{q \cdot b^2}{h}(m - \mathrm{j}) = \frac{r_h \cdot B}{h} + \frac{q \cdot B^2}{2 \cdot h} \quad (123)$$

The wall displacement associated with the plastic strength is the summation of the plastic deformation attained in kinematic mode $\tilde{j}$ and the incremental displacement for each subsequent kinematic mode up to $m - 1$:

$$\Delta_h^{pl,VII} = \Delta_{h,t}^{pl,\tilde{j}} + \sum_{j=\tilde{j}+1}^{m-1} \frac{F_t^{pl,j} - F_t^{pl,j-1}}{k_H^{pl,j}} = \Delta_h^{el} + \frac{R_{c,\tilde{j}} \cdot h}{n \cdot k_c \cdot b} + \sum_{j=\tilde{j}+1}^{m-1} \frac{q \cdot h}{n \cdot k_c} \quad (124)^{A}$$

For the wall to achieve the SW behaviour in the plastic state in failure mechanism VII, the panel joint between the $m - 1^{\text{th}}$ and m^{th} panels must remain elastic.

$$d_{y,c} > V_c^{el,\tilde{\jmath}} + \frac{R_{c,\tilde{\jmath}}}{n \cdot k_c} + \sum_{j=\tilde{\jmath}+1}^{m-1} \frac{q \cdot b}{n \cdot k_c}$$ (125)[A]

The ultimate lateral displacement of the wall is only dependant on the hold-down elongation since no additional load is applied to the elastic vertical joint. The elongation in hold-down for the SW behaviour, $V_0^{pl,m}$, is calculated as:

$$V_0^{pl,m} = d_{y,h} + \frac{\tilde{\jmath} \cdot R_{c,\tilde{\jmath}}}{n \cdot k_c} + \sum_{j=\tilde{\jmath}+1}^{m-1} \frac{j \cdot q \cdot b}{n \cdot k_c}$$ (126)[A]

Ensuring the hold-down's ultimate displacement is larger than the required elongation to reach SW behaviour can be expressed as:

$$d_{u,h} \geq V_0^{pl,m}$$ (127)

The ultimate displacement of the wall in failure mechanism VII is the sum of the lateral displacement of the wall in kinematic mode $\tilde{\jmath}$, the incremental displacement to develop all intermediate kinematic modes ($\tilde{\jmath} + 1$ to $m - 1$) and the displacement in the final kinematic mode m governed by failure in the hold-down. The expression is shown in Equation (128).

$$\Delta_h^{u,VII} = \Delta_{h,t}^{pl,\tilde{\jmath}} + \sum_{\mathrm{j}=\tilde{\jmath}+1}^{m-1} \frac{q \cdot h}{n \cdot k_c} + \frac{h}{B} \cdot \left(d_{u,h} - V_0^{pl,m}\right)$$ (128)[A]

The ductility associated with the ultimate potential displacement in SW behaviour results the following for failure mechanism VII:

$$\mu_w{}^{VII} = \frac{\Delta_h^{u,VII}}{\Delta_h^{el}}$$ (129)

CHAPTER 5 - Development of the Analytical Model to Achieve CP as Final Behaviour

5.1 General

Three possible failure paths can lead to the final CP behaviour after attaining elastic yield in CP, SW or IN behaviour, as seen in Figure 5-1. The final CP behaviour is achieved due to yielding of vertical joints prior to yielding in the hold-down. The wall may not develop full CP behaviour in the plastic phase due to insufficient displacement capacity in the connectors, which will also be covered in this chapter.

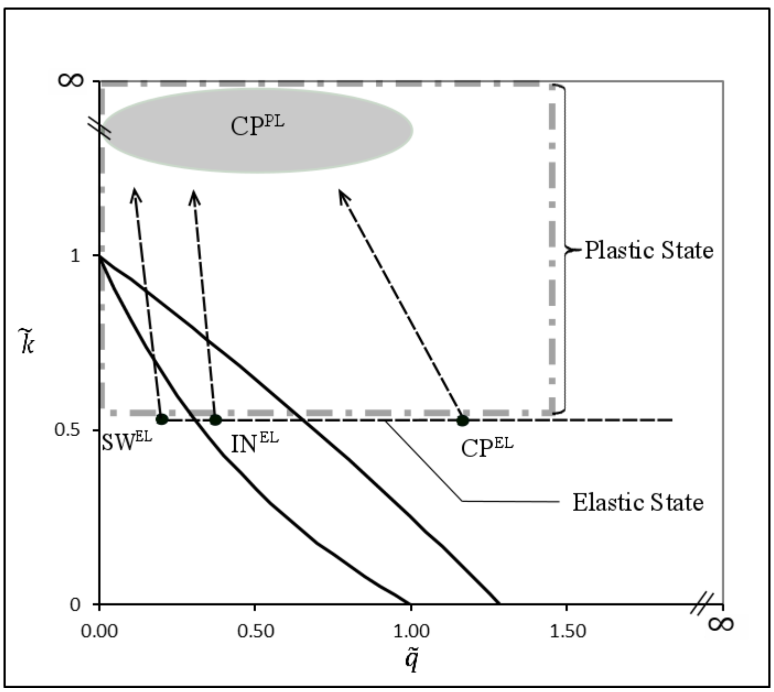

Figure 5-1: Kinematic Paths to Achieve CP Behaviour

Achieving CP behaviour is ensured by the condition shown in Equation (130) for any kinematic mode $\tilde{j}$.

$R_{w,h}^{el,\tilde{j}} > R_{w,c}^{el,\tilde{j}}$ (130)

In order to achieve CP behaviour in the elastic state, the elastic strength of the wall related to vertical joint yielding in the CP behaviour ($\tilde{j} = 1$) is required to be less than the transition force between kinematic mode 1 and 2 in the elastic state, as expressed in the following condition.

$R_{w,c}^{el,1} < F_t^{el,1} \ or \ \tilde{k} > 1$ (131)

The SW kinematic behaviour in the elastic state is achieved when the elastic strength of the wall related to vertical joint yielding in the SW behaviour ($\tilde{j} = m$) is larger than the final transitional force prior to attaining kinematic mode m in the elastic state.

$R_{w,c}^{el,m} > F_t^{el,m-1}$ (132)

Finally, the IN behaviour in the elastic state is achieved when the elastic strength of the wall related to hold-down yielding in the IN behaviour ($\tilde{j} = [2, m-1]$) is between the transitional forces defining the intermediate kinematic modes immediately before and after the mode under consideration, i.e. for $\tilde{j} = j^*$.

$F_t^{el,j^*-1} < R_{w,c}^{el,j^*} < F_t^{el,j^*}$ (133)

5.2 Model development for the CP^{EL}-CP^{PL} Case

This case is ensured by the inequalities presented in Equations (130) and (131), and the behaviour regions are presented in the general force-displacement curve shown in Figure 5-2 and associated kinematic path in Figure 5-3.

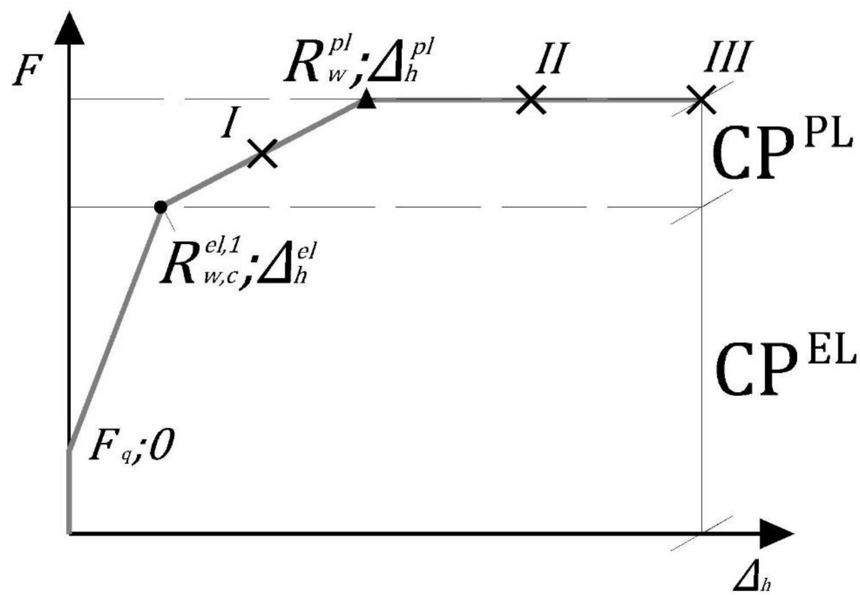

Figure 5-2: General Elasto-Plastic Force-Displacement Curve for Kinematic Path CP^{EL}-CP^{PL}

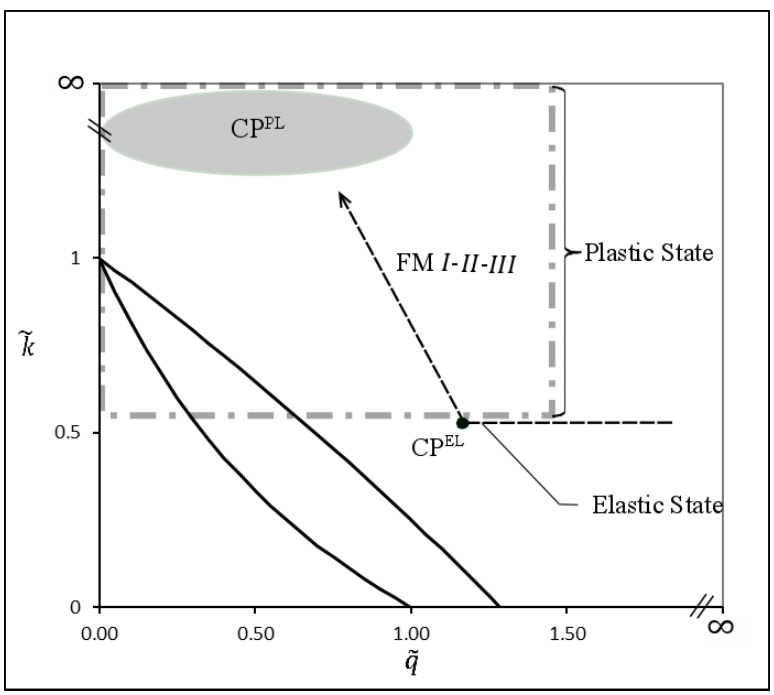

Figure 5-3:Behaviour Region of failure Mechanism for CP^{EL}-SW^{PL}

Different failure mechanisms (i.e. $I - III$) can be defined depending only on the sequence of failure of the connectors. All failure mechanisms along the CP^{EL}-CP^{PL} path are illustrated in Figure 5-4.

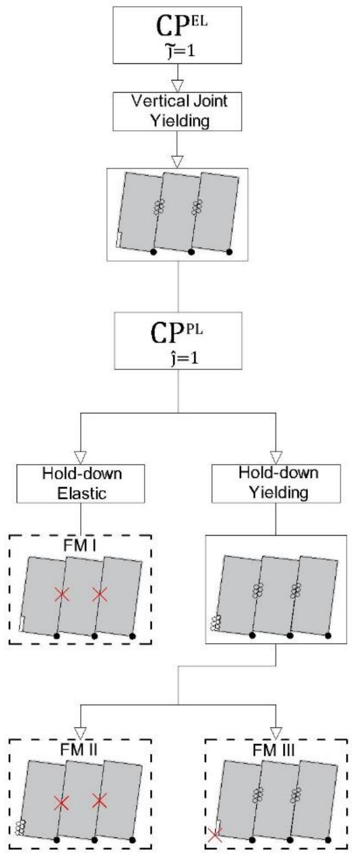

Figure 5-4: Definition of Failure Mechanism for CP^{EL}-CP^{PL}

The subsequent sections will follow the structure presented in Figure 5-4, starting with describing the elastic state in CP behaviour (Section 5.2.1), followed by a description of the plastic states in the CP behaviour in Sections 5.2.2.

5.2.1 CP Behaviour in Elastic State

The first point in the force-displacement relationship of the wall for all failure mechanisms is the activation force, as defined by Equation (6) and discussed in Section 3.2.

The elastic strength of the wall associated with the vertical joints yield strength in kinematic mode 1, $R_{w,c}^{el,1}$, can be described as (same as Equation (4) in Section 3.2):

$$R_{w,h}^{el,1} = r_c \cdot \frac{{k'_h}^{el,1} \cdot b}{k_c \cdot h} + F_q \quad (134)$$

The top horizontal displacement of the wall associated with the elastic strength, Δ_h^{el}, can be written as a function of the vertical elongation in the vertical joint, $d_{y,c}$:

$$\Delta_h^{el} = \frac{R_{w,c}^{el,1} - F_q}{k_H^{el,1}} = \frac{r_c \cdot {k'_h}^{el,1} \cdot b}{k_c \cdot h} \cdot \frac{h^2}{{k'_h}^{el,1} \cdot b^2} = \frac{r_c \cdot h}{k_c \cdot b} = d_{y,c} \cdot \frac{h}{b} \quad (135)$$

5.2.2 Plastic CP Behaviour Region, Failure Mechanism $I - III$

As can be seen in Figure 5-3, CP^{PL} region starts at the point where the panel joints yield. The tension force in the hold-down at the point where the panel joints yield can be calculated according to the equation presented in Casagrande et al. 2017:

$$T^{el,1} = \left(\frac{R_{w,c}^{el,1} \cdot h^2}{b^2} - \frac{q \cdot m \cdot h}{2}\right) \cdot \frac{k_h \cdot b}{{k'_h}^{el,1} \cdot h} \quad (136)$$

The increase in the hold-down force between the point where the panel joint connection yields and the point where the hold-down yields, $t^{pl,1}$, takes the following form according to Casagrande et al. (2017):

$$t^{pl,1} = \left(\frac{(R_w^{pl} - R_{w,c}^{el,1}) \cdot h^2}{b^2} - \frac{q \cdot m \cdot h}{2}\right) \cdot \frac{k_h \cdot b}{{k'_h}^{pl,1} \cdot h} = \frac{(R_w^{pl} - R_{w,c}^{el,1}) \cdot h}{b} \quad (137)$$

Where, the equivalent hold-down stiffness in the plastic state, prior to the yielding of the hold-down, is equal to the hold-down stiffness.

$${k'_h}^{pl,1} = {k'_h}^{el,1}(k_c = 0) = k_h \quad (138)$$

The total force in the hold-down at the point of the yielding (r_h) is the sum of the lateral force achieving panel joint yielding (Eq. 136) and the additional lateral force to achieve hold-down yielding (Eq.137). It is noteworthy to mention that the expressions dealing with the increase in force are independent of the activation force. As such, if q is considered in the elastic expression of the hold-down force, $T^{el,1}$, it should not be included in the force increase expressions.

$$r_h = T^{el,1} + t^{pl,1} = \left(\frac{R_{w,c}^{el,1} \cdot h^2}{b^2} - \frac{qmh}{2}\right) \cdot \frac{k_h \cdot b}{k_h^{\prime\, el,1} \cdot h} + \frac{(R_w^{pl} - R_{w,c}^{el,1}) \cdot h}{b} \quad (139)$$

The increase in lateral force in the plastic state to attain hold-down yield can be written as:

$$R_w^{pl} - R_{w,c}^{el,1} = \frac{b}{h} \cdot \left(r_h - \frac{r_c \cdot k_h}{k_c}\right) \quad (140)$$

The plastic strength, R_w^{pl} (at the yielding of the hold-down) might not be attained in failure mechanisms *I* due to the limited deformation capacity in the vertical joints (see Fig. 5-4). This failure mechanism is achieved when the wall remains in the CP behaviour following the failure of the panel joints. Attaining failure mechanism *I* is ensured by the following condition, where the ultimate elongation in vertical joints is reached prior to the yielding of the hold-down.

$$d_{u,c} < d_{y,h} \quad (141)$$

The plastic strength of the wall under this condition can be written as the sum of the elastic strength and the increase of force governed by the ultimate displacement of the vertical joints, using interpolation between the points of yield and ultimate displacement for the panel joints:

$$R_w^{pl,I} = R_{w,c}^{el,1} + \frac{b}{h} \cdot \left(r_h - \frac{r_c \cdot k_h}{k_c}\right) \cdot \frac{d_{u,c} - d_{y,c}}{d_{y,h} - d_{y,c}} \quad (142)$$

The total lateral displacement for failure mechanism I (Eq. 143) occurs in CP behaviour in the plastic state and is controlled only by the ultimate displacement of the vertical joints.

$$\Delta_h^{u,I} = \Delta_h^{pl,I} = \Delta_h^{el} + \frac{R_w^{pl,I} - R_{w,c}^{el,1}}{k_H^{pl,1}} = d_{u,c} \cdot \frac{h}{b} \quad (143)$$

The ductility of the wall for failure mechanism I is defined only by the ductility in the vertical joints, and can be expressed as:

$$\mu_w{}^I = \frac{\Delta_h^{u,I}}{\Delta_h^{el}} = \frac{d_{u,c}}{d_{y,c}} = \mu_c \quad (144)$$

The condition required to ensure yielding of the hold-down and to attain failure mechanism II and III is that the yielding displacement of the hold-down occurs prior to achieving the ultimate displacement in the vertical joints. Therefore:

$$d_{u,c} > d_{y,h} \quad (145)$$

The total plastic strength of the wall for these failure mechanisms can be expressed as the sum of the elastic strength and the increase of force needed to achieve yielding of the hold-down:

$$R_w^{pl,II} = R_w^{pl,III} = R_{w,c}^{el,1} + \left(R_w^{pl} - R_{w,c}^{el,1}\right) = \frac{b}{h}\left(r_h + r_c \cdot (m-1) \cdot n + \frac{q \cdot m \cdot b}{2}\right) \quad (146)^{A}$$

The total displacement at the plastic strength for both failure mechanisms II and III is governed by the yield displacement of the hold-down.

$$\Delta_h^{pl,II} = \Delta_h^{pl,III} = \Delta_h^{el} + \frac{R_w^{pl,II,III} - R_{w,c}^{el,1}}{k_H^{pl,1}} = d_{y,h} \cdot \frac{h}{b} \quad (147)$$

Where the equivalent lateral stiffness of wall developed as:

$$k_H^{pl,1} = \frac{k_h'^{\,pl,1} \cdot b^2}{h^2} = \frac{k_h \cdot b^2}{h^2} \quad (148)$$

The ultimate displacements for failure mechanism II and III are characterized by failure in the vertical joints and in the hold-down, respectively. They can be expressed as the ultimate displacement for each connector and the wall panel aspect ratio.

$$\Delta_h^{u,II} = \frac{h}{b} \cdot d_{u,c} \quad (149)$$

$$\Delta_h^{u,III} = \frac{h}{b} \cdot d_{u,h} \quad (150)$$

The ductility for failure mechanism II and III can be expressed as:

$$\mu_w{}^{II} = \frac{\Delta_h^{u,II}}{\Delta_h^{el}} = \frac{d_{u,c}}{d_{y,c}} = \mu_c \quad (151)$$

$$\mu_w{}^{III} = \frac{\Delta_h^{u,III}}{\Delta_h^{el}} = \frac{d_{u,h}}{d_{y,c}} = \mu_h \cdot \frac{d_{y,h}}{d_{y,c}} \quad (152)$$

5.3 Model Development for the SW^{EL}-CP^{PL} Case

This case is achieved through the SW behaviour in the elastic state and the CP behaviour in the final plastic state and is ensured by the inequalities presented in Equations (130) and (132). When failure mechanisms VII and $VIII$ (Figure 5-5) cannot be achieved, the behaviour of the wall depends on the limitation in the ductility of the individual connectors. Therefore, from the elastic state, the wall may only attain the plastic SW region or only reach the plastic state in the IN region. The different behaviour regions for which the wall may reach its ultimate capacity are presented in the general force-displacement curve shown in Figure 5-5 and associated kinematic path in Figure 5-6.

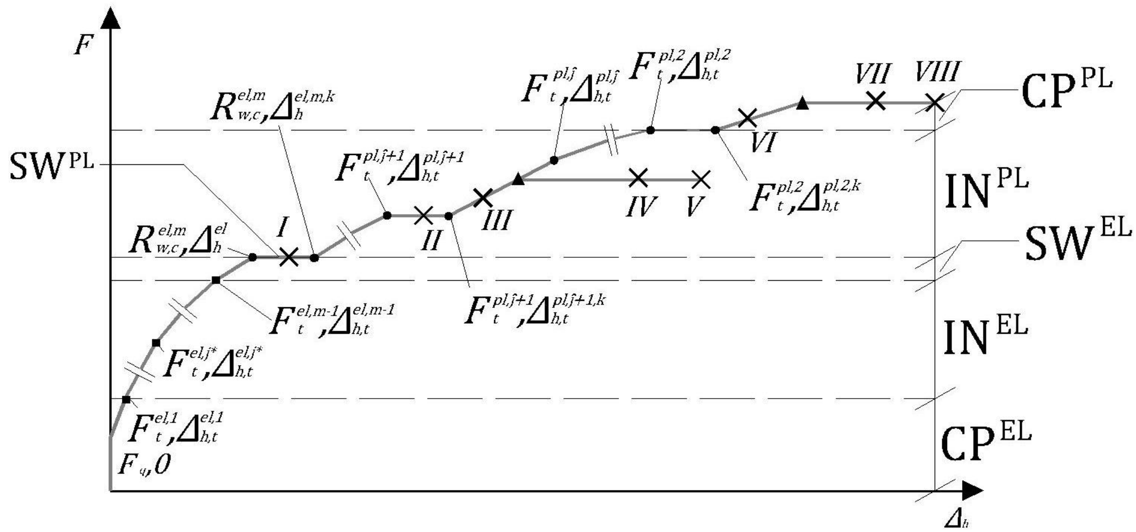

Figure 5-5: General Elasto-Plastic Force-Displacement Curve for Kinematic Path SW^{EL}-CP^{PL}

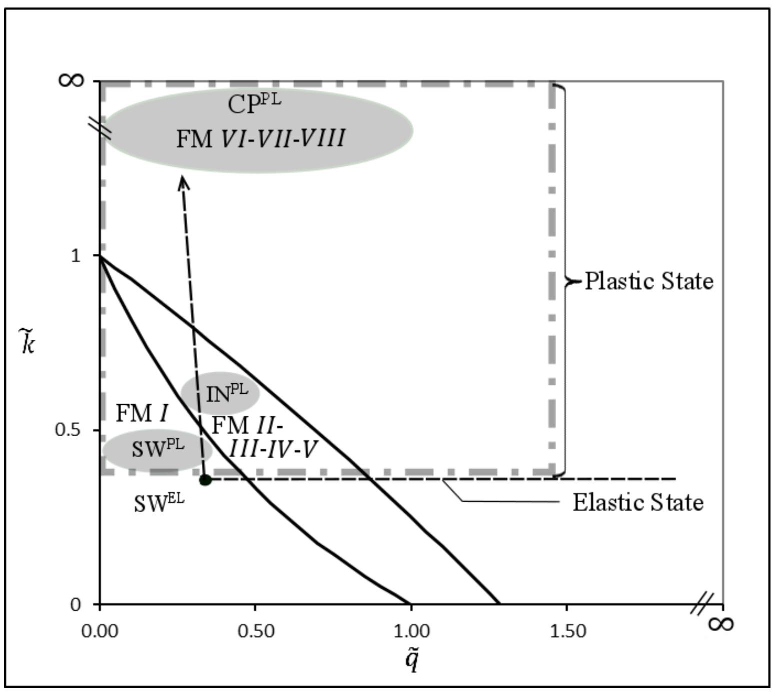

Figure 5-6:Behaviour Region of failure Mechanism for SW^{EL}-CP^{PL}

The mechanism to attain the plastic SW or IN regions is illustrated in Figure 5-7. From this figure, it can be observed that the wall changes kinematic mode from higher to lower mode number. This is achieved through yielding in the panel joints (i.e. sliding in the panels relative to one another). This is done progressively starting with the highest panel joint number joining the first panel in contact with ground ($j^* + 1$) with the lifted panel immediately adjacent (j^*). This constitutes a condition for which the wall would be in mode j^* when the lifted panel reattaches. All panels to the right of the reattached panel are not included in the wall stiffness. In other words, the wall is reduced to only the panels to the left of the first panel in contact with ground (i.e. 1 to j^*).

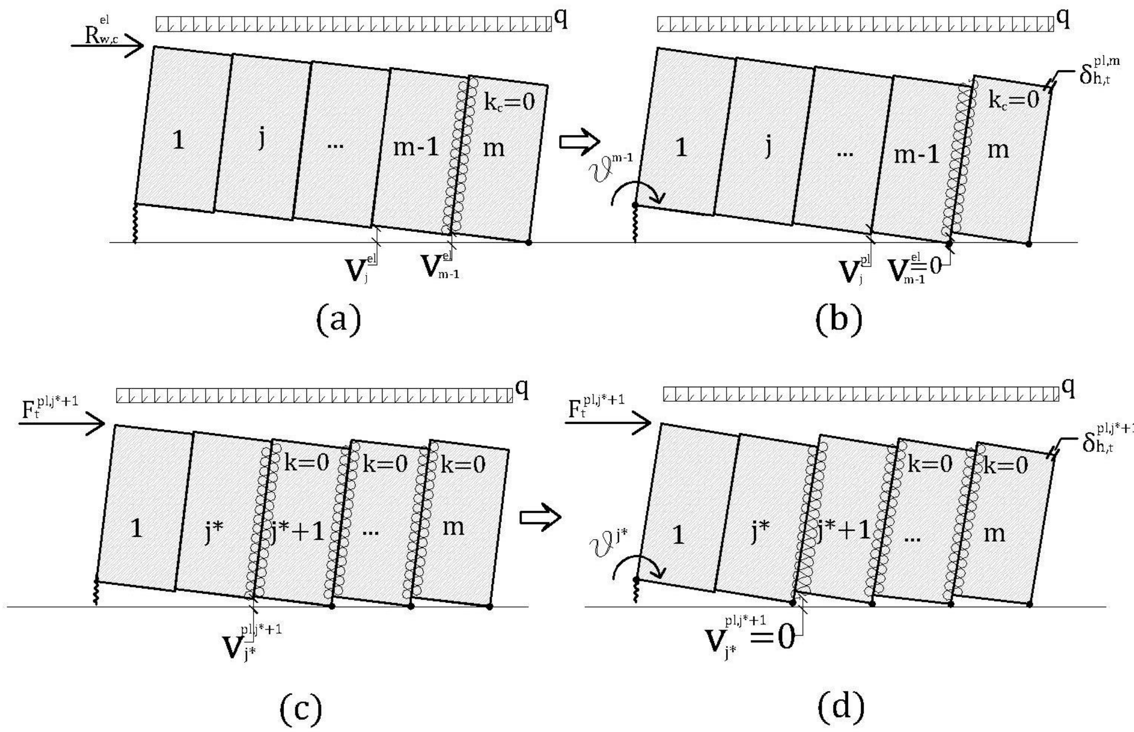

Figure 5-7: Transition between kinematic mode (a) m and (b) $m-1$ and general transition between kinematic mode (c) j^*+1 and (d) j^*

All failure mechanisms along the SW^{EL}-CP^{PL} path are illustrated in Figure 5-8.

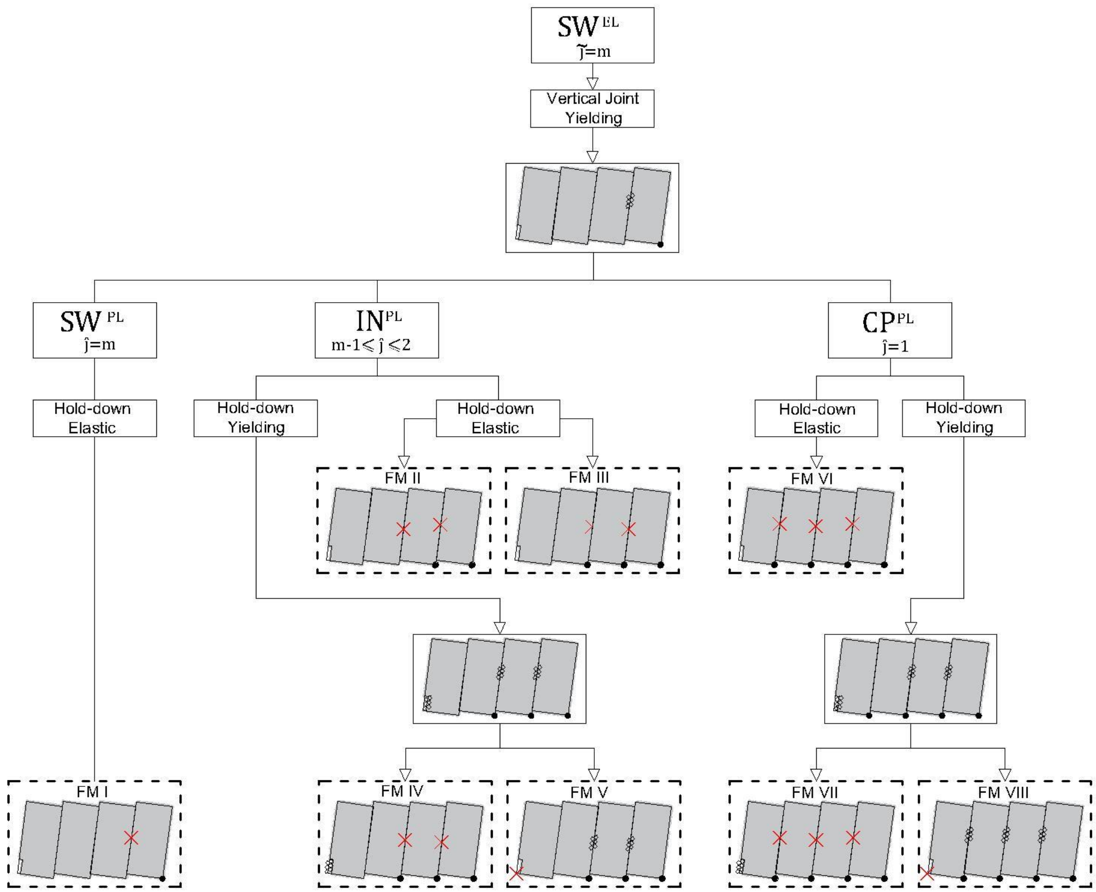

Figure 5-8: Definition of Failure Mechanism for SW^{EL}-CP^{PL}

It can be observed that when the hold-down remains elastic, the wall failure is governed by failure in the vertical joint(s). However, yielding of the hold-down in the IN^{PL} and CP^{PL} regions would lead to ultimate failure in ether hold-down or vertical joint.

The subsequent sections will follow the structure presented in Figure 5-8, starting by describing the elastic state (Section 5.3.1) until achieving SW behaviour, followed by a description of the plastic states in the SW^{PL} in Section 5.3.2. Section 5.3.3 presents the equations governing the upper limit of the IN behaviour as seen in Figure 5-7b to help describe the transition between the SW and IN behaviours. The failure mechanisms that could occur in kinematic mode $m-1$ are presented in Section 5.3.4 and expressed as a function of j^*. Finally, Section 5.3.5 presents the solutions for CP^{PL} behaviour and the associates failure mechanisms.

5.3.1 SW Behaviour in Elastic State

The wall transitions from CP^{EL} to SW^{EL} and remains SW^{EL} region by progressive lifting of the CLT panels between panel 1 and $m-1$. The value of the transitional force associated with kinematic mode j^* where $1 \le j^* \le m-1$ was presented in Equation (1) in Section 3.2. The associated transitional displacement achieved at kinematic mode j^*, $\Delta_{h,t}^{el,j^*}$, is developed as the sum of the displacements associated with the increase of force resulting in a change of kinematic modes prior to achieving j^*.

$$\Delta_{h,t}^{el,j^*} = \frac{F_t^{el,1} - F_q}{k_H^{el,1}} + \sum_{j=2}^{j^*} \frac{F_t^{el,j} - F_t^{el,j-1}}{k_H^{el,j}} \quad (153)$$

Where the equivalent lateral stiffness of the wall in the elastic state for mode j is written as:

$$k_H^{el,j} = \frac{{k'}_h^{el,j} \cdot b^2}{h^2} \quad (154)$$

The equivalent hold-down tensile stiffness for the elastic state of kinematic mode j^* is expressed as:

$${k'}_h^{el,j} = \frac{n \cdot k_c \cdot [(j + m \cdot j - m) \cdot k_h + (m-j) \cdot n \cdot k_c]}{n \cdot k_c + (j-1) \cdot k_h} \quad (155)$$

The elastic strength of the wall associated with the vertical joint yield strength in kinematic mode m, $R_{w,c}^{el,m}$, (same as Equation 10 in section 3.2) can be described as:

$$R_{w,c}^{el,m} = \frac{r_c \cdot n \cdot b \cdot \alpha_{(m)}}{h \cdot m \cdot \tilde{k}} + \frac{q \cdot b^2 \cdot \rho_{(m)}}{2 \cdot h} = \frac{r_c \cdot n \cdot b \cdot m}{h} + \frac{q \cdot b^2 \cdot (2m - m^2)}{2 \cdot h} \quad (156)$$

Where the expression for the elastic displacement is taken from Casagrande et al. (2017):

$$\Delta_h^{el} = \left(\frac{R_{w,c}^{el,m} \cdot h^2}{b^2} - \frac{q \cdot m^2 \cdot h}{2} \cdot \frac{k_h'^{\,el,m}}{k_h}\right) \cdot \frac{1}{m^2 \cdot k_h'^{\,el,m}} \quad (157)$$

The equivalent hold-down tensile stiffness is expressed as a system of springs in series as:

$$k_h'^{\,el,m} = \left(\frac{1}{k_h} + \frac{m-1}{n \cdot k_c}\right)^{-1} \quad (158)$$

5.3.2 Plastic SW Behaviour Region, Failure Mechanism *I*

As can be seen in Figure 5-9, SW^{PL} is enclosed by the yielding of vertical joint $m-1$ (transition from elastic to plastic state, Eq.156), and the transition between kinematic mode m and $m-1$ (between SW and IN behaviours), as illustrated in Figure 5-7a and 5-7b.

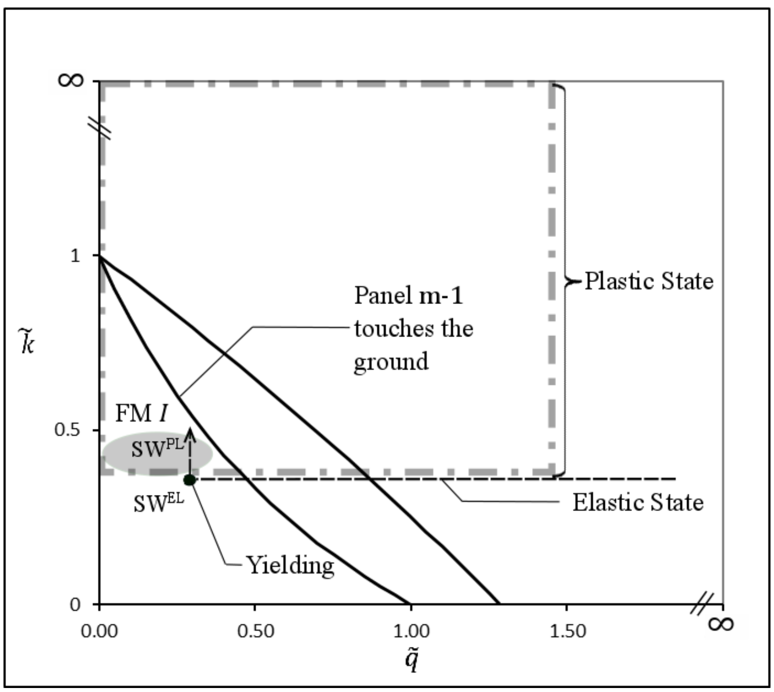

Figure 5-9: SW^{PL} behaviour region of Case SW^{EL}-CP^{PL}

The vertical displacement of the lower right joint of panel j for $[1, m-1]$ is calculated for the SW behaviour at the elastic strength as seen in Equation (159) with m panels (i.e. prior to the sliding and reattachment of panel $m-1$). The vertical displacements calculated in Equation (159) are required to obtain the lateral displacement of the wall (Casagrande et al. 2017).

$$v_j^{el,m} = \left[\frac{R_{w,c}^{el,m} \cdot h}{m \cdot b \cdot k_h \cdot n \cdot k_c}(n \cdot k_c - k_h) - \frac{q \cdot m \cdot b}{2 \cdot k_h}\left(\frac{k_h}{n \cdot k}(j-1)+1\right)\right] \cdot \frac{m-j}{m} \quad (159)$$

Kinematic mode $m-1$ is only reached when the $(m-1)^{th}$ panel reattaches with ground. The last panel not in contact with ground, $m-1$, will drop from the initial elevation calculated in the elastic state in kinematic mode m, $v_{m-1}^{el,m}$ (see Figure 5-7a). A variation of the angle of rotation would be attained, $\vartheta'^{\,m-1}$, since hold-down elongation remains the same, as presented in the Figure 5-7b.

$$\vartheta'^{\,m-1} = \frac{v_{m-1}^{el,m}}{(m-1) \cdot b} \quad (160)$$

The reattachment of panel $m-1$ with ground, cause by the sliding between panel m and $m-1$, leads to a change in elevation for the point of rotations of the remaining panels, $v_j^{pl,m-1}$ for $j=[1, m-2]$. The elevation of the point of rotation for panel $m-1$ is assumed to be 0 as it reattaches with ground.

$$v_j^{pl,m-1} = v_j^{el,m} - \vartheta'^{\,m-1} \cdot j \cdot b \quad (161)$$

The reattachment of panel $m-1$ has the effect of increasing the horizontal displacement of the wall without any increase in force. The increase in displacement between kinematic mode m and $m-1$ can be expressed as:

$$\delta_{h,t}^{pl,m} = \vartheta'^{\,m-1} \cdot h \quad (162)$$

The total displacement, $\Delta_{h,t}^{pl,m,k}$, is transitional displacement between kinematic model m and $m-1$, expressed as the elastic displacement and the increase in horizontal displacement due to the mode change (Eq. 162). k relates to the changes of kinematic mode.

$$\Delta_{h,t}^{pl,m,k}= \Delta_{h}^{el} + \delta_{h,t}^{pl,m} \quad (163)$$

The transitional displacement, $\Delta_{h,t}^{pl,m,k}$ may not be attained in failure mechanisms I due to limited displacement capacity in the vertical joint (see Fig. 5-8). This failure mechanism is achieved when the wall remains in the SW behaviour following the yielding of the vertical joint. Attaining failure mechanism I is ensured by the following two conditions: a) failure of the vertical joint is reached while the wall remains in SW behaviour, (Eq. 164), and b) the failure of vertical joint $m-1$ is reached prior to the yielding of the hold-down (Eq. 165):

$$\frac{b}{h} \cdot \Delta_{h}^{el}< d_{u,c} < \frac{b}{h} \cdot \Delta_{h,t}^{pl,m,k} \quad (164)$$

$$d_{y,h} > V_{0}^{el,m} = \frac{1}{k_h}\left(\frac{R_{w,c}^{el,m} \cdot h}{b \cdot m} - \frac{q \cdot b \cdot m}{2}\right) \quad (165)^{A}$$

The plastic strength is equal to the elastic strength defined in Equation (156).

$$R_{w,c}^{pl,I} = R_{w,c}^{el,m} \quad (166)$$

The total lateral displacement for failure mechanism I (Eq. 167) occurs in kinematic mode m in the plastic state and is controlled only by the ultimate displacement of vertical joint.

$$\Delta_{h}^{u,I}= \Delta_{h}^{pl,II}= \frac{h}{b} \cdot d_{u,c} \quad (167)$$

The ductility resulting this failure mechanism can be defined as:

$\mu_w{}^I = \frac{\Delta_h^{u,I}}{\Delta_h^{el}}$ (168)

5.3.3 Solution for Plastic IN Behaviour Region in kinematic mode $m-1$

This section presents kinematic mode $m-1$ to facilitate the understsand of the solutions in the IN behaviour presented in Section 5.3.4. Kinematic mode $m-1$ is attained when the trasitional displacement associated with a change in kinematic mode, $\Delta_{h,t}^{pl,m,k}$, is achieved. Figure 5-10 illustrates the regions for all kinematic modes in the IN behaviour associated with failure mechanisms $II-V$. The increase of force and displacement for mode $m-1$ only is covered in this section, whereas the solution for failure mechanisms $II-V$ is covered in section 5.3.4.

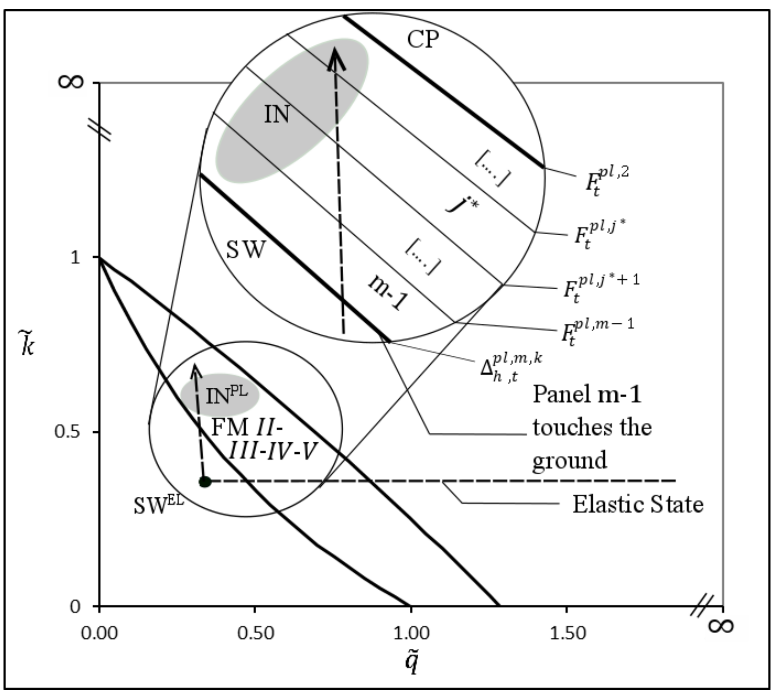

Figure 5-10: IN Behaviour Region with Kinematic Mode $m-1$ for Case SW^EL-CP^PL

At the point of reattachment of panel $m-1$ with ground, the wall is considered to only consist of $m-1$ panels. The force required to attain the yielding of vertical joint $m-2$ (Eq.

169) consists of the elastic strength contribution for a system with m panels, $R_{w,c}^{el,m}$ (obtained from Eq. 156) and the lateral force increase required to yield the $m-2$ joint, $f^{pl,m-1}$ (Fig. 5-11). $f^{pl,m-1}$ relates to increase of force in kinematic mode $m-1$ to attain the yielding of joint $m-2$.

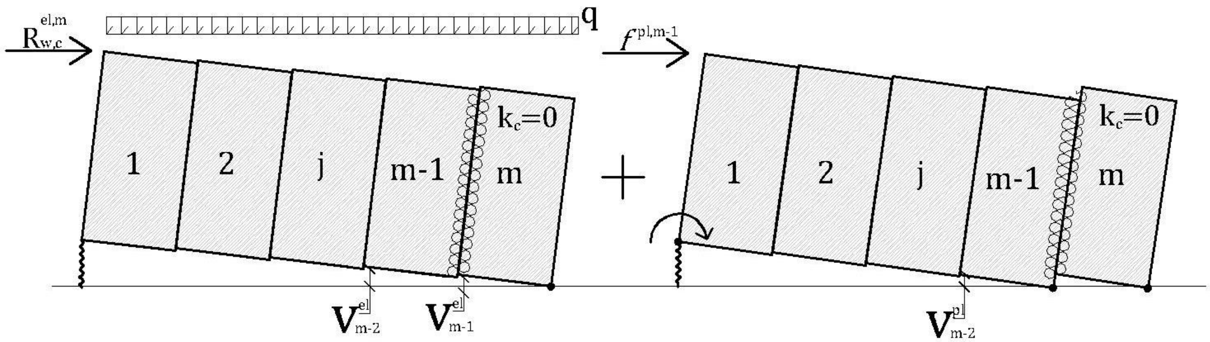

Figure 5-11: Effect of increase of force on vertical joint $m-2$

$$r_c = F_{c,y,\mathrm{i},m-2}(F = R_{w,c}^{el,m}, m = m) + F_{c,y,i,m-2}(f^{pl,m-1}, m = m-1, q = 0) \quad (169)$$

Where

$$F_{c,y,i,j} = \frac{1}{n} \cdot \left[\frac{F \cdot h}{b \cdot m} - \frac{q \cdot b \cdot (m-2 \cdot j)}{2}\right] \quad (170)$$

$F_{c,y,i,j}$ applies for single wall (SW) behaviour only, and its use here is appropriate since the $m-1$ vertical joint has yielded and does not contribute to the wall stiffness.

The strength of the vertical joint is expressed as the force in the joint at the elastic strength and the increase of lateral force to attain yielding of $m-2$ th joint.

$$r_c = \frac{1}{n} \cdot \left[\frac{R_{w,c}^{el,m} \cdot h}{b \cdot m} - \frac{q \cdot b \cdot (m-2 \cdot (m-2))}{2}\right] + \frac{1}{n} \cdot \frac{f^{pl,m-1} \cdot h}{b \cdot (m-1)} \quad (171)$$

The increase of force to attain yielding in the $m-2$ th joint is:

$$f^{pl,m-1} = \frac{b\cdot(m-1)\cdot n\cdot r_c}{h} - \frac{R_{w,c}^{el,m}\cdot(m-1)}{m} + \frac{q\cdot b^2\cdot(m-1)\cdot(-m+4)}{2\cdot h} \quad (172)^{A}$$

The total lateral load resisted at the yielding of the $m-2$ vertical joint can be expressed as:

$$F_t^{pl,m-1} = R_{w,c}^{el,m} + f^{pl,m-1} \quad (173)$$

The total plastic displacement of the wall for kinematic mode $m-1$ is the sum of the elastic lateral displacement, the displacement associated with the drop of panel $m-1$ and the increase of force to achieve the yielding of vertical joint $m-2$:

$$\Delta_{h,t}^{pl,m-1} = \Delta_h^{el} + \delta_{h,t}^{pl,m} + \frac{f^{pl,m-1}}{k_H^{pl,m-1}} \quad (174)$$

Where the equivalent lateral stiffness of the wall is calculated using $m-1$ panels:

$$k_H^{pl,m-1} = \frac{{k'}_h^{pl,m-1} \cdot b^2\cdot(m-1)^2}{h^2} \quad (175)$$

The equivalent hold-down tensile stiffness for SW behaviour with $m-1$ panels prior to the yielding of the $m-2^{th}$ panel joint can be expressed as springs in series for the hold-down and vertical joint connections:

$${k'}_h^{pl,m-1} = \left(\frac{1}{k_h} + \frac{(m-1)-1}{n\cdot k_c}\right)^{-1} = \left(\frac{1}{k_h} + \frac{m-2}{n\cdot k_c}\right)^{-1} \quad (176)$$

The increase of lateral force, $f^{pl,m-1}$, leads to an increase in vertical displacement of the panels not in contact with ground. The total vertical displacement in vertical joint j, for $1 \leq j \leq m-2$., ${v'}_j^{pl,m-1}$ can be expressed as the sum of the displacement achieved at elastic strength, the adjustment (reduction) due to the panel drop to achieve kinematic mode $m-1$, and the increase due to the lateral force $f^{pl,m-1}$. Equation (177) is the same than Equation (159) and since the input is an incremental force, the vertical load is neglected.

$$v_j'^{\,pl,m-1} = v_j^{pl,m-1} + \left\{\frac{f^{pl,m-1} \cdot h}{(m-1) \cdot b \cdot k_h \cdot n \cdot k_c}(n \cdot k_c - k_h)\right\} \cdot \frac{((m-1)-j)}{(m-1)} \qquad (177)$$

5.3.4 Plastic IN Behaviour Region, Failure Mechanism II, III, IV and V

Figure 5-12 illustrates the region for failure mechanisms $II - V$, which starts with the transitional force F_t^{pl,j^*+1} achieved and the drop of panel $j^* + 1$ and ends with transitional force F_t^{pl,j^*} achieved and when panel j^* reattached to the ground. The IN regions ends with the achievement of CP behaviour and Figure 5-12 illustrates the regions for all kinematic modes in the IN behaviour associated with failure mechanisms $II - V$.

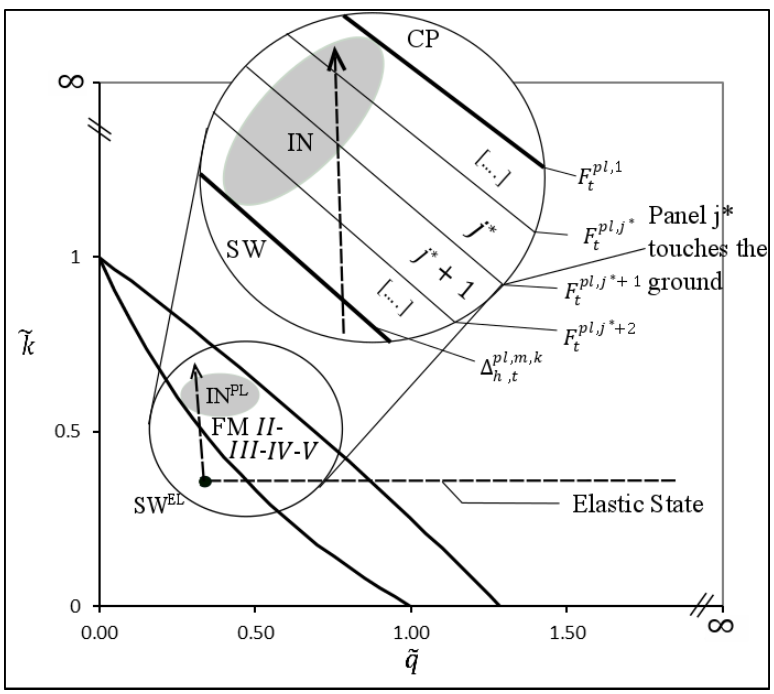

Figure 5-12: Kinematic Path of Case SW^EL-CP^PL for Plastic State in IN behaviour

The development of the force-displacement curve follows the procedure outlined in Figure 5-13. As indicated in Figure 5-13, the value of j^* is decreased between $m-1$ (also covered in the previous section) and 2.

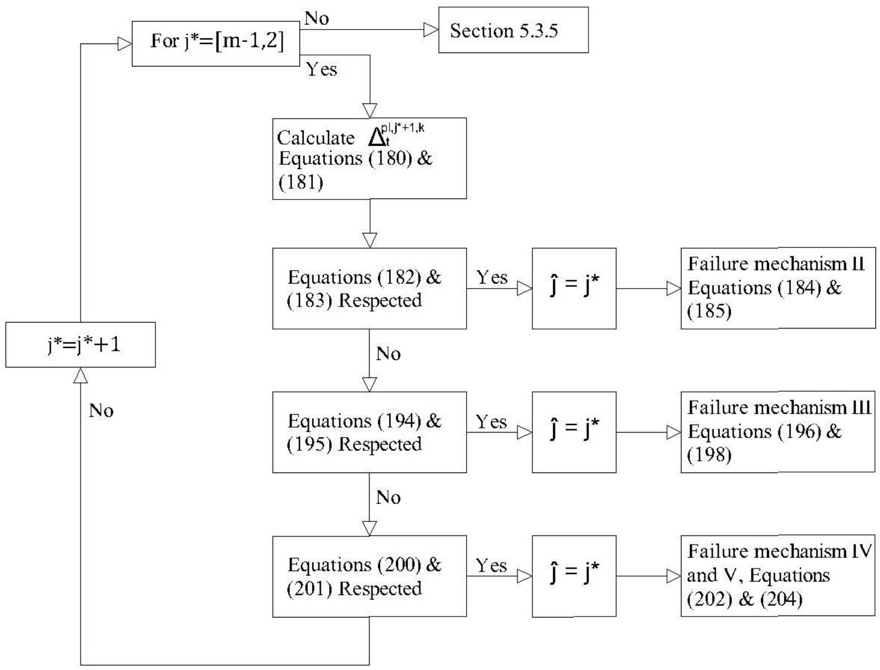

Figure 5-13: Steps to Solve IN Behaviour Region of Case SW^{EL}-CP^{PL}, Failure Mechanisms II-V

Kinematic mode j^* is only reached when the j^{*th} panel reattaches with ground. The last panel not in contact with ground, j^*, will drop from the adjusted value under the increase of lateral force resulting the yielding of joint j^* in the plastic state in kinematic mode j^*+1, $v'^{pl,j^*+1}_{j^*}$ (see Figure 5-7c). A variation in the angle of rotation would be attained, ϑ'^{j^*}, since hold-down elongation remains the same, as presented in the Figure 5-7d.

$$\vartheta'^{j^*} = \frac{v'^{pl,j^*+1}_{j^*}}{j^* \cdot b} \quad (178)$$

The reattachment of panel j^* with ground, cause by the sliding between panel $j^* + 1$ and j^* (see Figure 5-7c and 5-7d), leads to a change in elevation for the point of rotations of the remaining panels, v_j^{pl,j^*} for $j = [1, j^* - 1]$. The elevation of the point of rotation for panel j^* is assumed to be 0 as it reattaches with ground.

$$v_j^{pl,j^*} = v_j'^{\,pl,j^*+1} - \vartheta'^{\,j^*} \cdot j \cdot b = v_j^{el,m} - \sum_{i=j^*}^{m-1} \vartheta^i \cdot j \cdot b + \sum_{i=j^*+1}^{m-1} \left\{ \frac{f^{pl,i} \cdot h}{i \cdot b \cdot k_h \cdot n \cdot k_c} (n \cdot k_c - k_h) \right\} \cdot \frac{(i-j)}{i} \quad (179)$$

Where $v_j'^{\,pl,j^*+1}$, is the elevation of panel corrected with the increase of lateral load in kinematic model $j^* + 1$ expressed in the general form in Equation (201) and firstly calculated for kinematic mode $m - 1$ in Equation (177). The reattachment of panel j^* has the effect of increasing the horizontal displacement of the wall without any increase in force. The increase in displacement between kinematic mode $j^* + 1$ and j^*can be expressed as:

$$\delta_{h,t}^{pl,j^*+1} = \vartheta'^{\,j^*} \cdot h \quad (180)$$

The total displacement of the wall when panel j^* reattaches with the ground is the sum of the elastic displacement, the incremental displacement related to previous panel drop associated with kinematic modes m to $j^* + 1$ and the incremental displacement to fully developed the previous kinematic modes ($m - 1$ to $j^* + 1$). This displacement is still under the previous transitional force, F_t^{pl,j^*+1} , and the expression is shown in Equation (181).

$$\Delta_{h,t}^{pl,j^*+1,k} = \Delta_h^{el} + \sum_{j=j^*+1}^{m} \delta_{h,t}^{pl,j} + \sum_{j=j^*+1}^{m-1} \frac{f^{pl,j}}{k_H^{pl,j}} = \Delta_{h,t}^{pl,j^*+1} + \delta_{h,t}^{pl,j^*+1} \quad (181)$$

The transitional displacement, $\Delta_{h,t}^{pl,j^*+1,k}$ may not be attained in failure mechanisms II due to limited displacement capacity in the vertical joint (see Fig. 5-8). This failure mechanism is achieved when the wall remains in the SW behaviour following the yielding of the vertical joint. Attaining failure mechanism II is ensured by the following two conditions: a) failure of the vertical joint is reached while the wall remains in kinematic mode $j^* + 1$, (Eq. 182), and b) the failure of vertical joints j^* to $m - 1$ is reached prior to the yielding of the hold-down (Eq. 183):

$$\frac{b}{h} \cdot \Delta_{h,t}^{pl,j^*+1} < d_{u,c} < \frac{b}{h} \cdot \Delta_{h,t}^{pl,j^*+1,k} \quad (182)$$

$$d_{y,h} > \frac{1}{k_h}\left[\left(\frac{R_{w,c}^{el,m} \cdot h}{b \cdot m} - \frac{q \cdot b \cdot m}{2}\right) + \sum_{j=j^*-1}^{m-1} \frac{f^{pl,j} \cdot h}{b \cdot j}\right] \text{(183)}^{\mathrm{A}}$$

If both conditions (182) and (183) are met, then j^* becomes associated with the final kinematic mode in the plastic state, $\hat{j}$, as presented in Figure 5-13.

The plastic strength is defined as the transitional force F_t^{pl,j^*+1} previously established.

$$R_{w,c}^{pl,I} = F_t^{pl,j^*+1} \quad (184)$$

The total lateral displacement for failure mechanism II (Eq. 185) occurs in kinematic mode $j^* + 1$ in the plastic state and is controlled only by the ultimate displacement of vertical joints j^* to $m - 1$.

$$\Delta_h^{u,II} = \Delta_h^{pl,II} = \frac{h}{b} \cdot d_{u,c} \quad (185)$$

The ductility resulting this failure mechanism can be defined as:

$$\mu_w{}^{II} = \frac{\Delta_h^{u,II}}{\Delta_h^{el}} \quad (186)$$

At the point of reattachment of panel j^* with ground, the wall is considered to only consist of j^* panels. Therefore, the increase of force that would lead to the next transitional force, F_t^{pl,j^*}, is dependant on the force in the $j^* - 1$ joint. The force required to attain the yielding of vertical joint $j^* - 1$ (Eq. 169) consists of the elastic strength contribution for a system with m panels, $R_{w,c}^{el,m}$ (obtained from Equation 156), the increase of lateral force to yield the previous vertical joint j for $m - 2 \leq j \leq j^*$ in a system with j panels, $f^{pl,j}$, and the lateral force increase required to yield the $j^* - 1$ joint, f^{pl,j^*} (Fig. 5-11). f^{pl,j^*}relates to increase of force in kinematic mode j^* to attain the yielding of joint $j^* - 1$.

$$r_c = F_{c,y,i,j^*-1}\left(F = R_{w,c}^{el,\tilde{j}}, m = m\right) + \sum_{j=j^*+1}^{m-1} F_{c,y,i,j^*-1}\left(F = f^{pl,j}, m = j, q = 0\right) + F_{c,y,i,j^*-1}\left(F = f^{pl,j^*}, m = j^*, q = 0\right) \quad (187)$$

Where the force in vertical joint uses the equation for SW behaviour stated in Equation (170). Therefore, the equation for increase of lateral force f^{pl,j^*} to lead to the yielding of the $j^* - 1^{th}$ vertical joint is written:

$$f^{pl,j^*} = \frac{b \cdot j^*}{h} \cdot \left[n \cdot r_c + \frac{qb\left(m - 2(j^* - 1)\right)}{2}\right] - j^* \cdot \left[\frac{R_{w,c}^{el,m}}{m} + \sum_{j=j^*+1}^{m-1} \frac{f^{pl,j}}{j}\right] \text{(188)}^{\text{A}}$$

Where, $f^{pl,j}$ is defined as the force causing yielding in vertical joints between kinematic mode $m - 1$ to $j^* + 1$. The increase of force leading to the first joint yielding in the plastic state $(m - 2)$, $f^{pl,m-1}$, was calculated in Equation (173). Therefore, the lateral load applied on top of the wall is calculated following as shown in this expression:

$$F_t^{pl,j^*} = F_t^{pl,j^*+1} + f^{pl,j^*} = R_{w,c}^{el,m} + \sum_{j=j^*+1}^{m-1} f^{pl,j} + f^{pl,j^*} \quad (189)$$

The transitional plastic displacement of the wall for the development of kinematic mode j^* is the sum of the elastic displacement, the incremental displacement related to previous panel drop associated with kinematic modes m to j^*+1 and the incremental displacement related to the full development of the previous kinematic modes ($m-1$ to j^*+1) and, now, including kinematic mode j^*.

$$\Delta_{h,t}^{pl,j^*} = \Delta_{h,t}^{pl,j^*+1,k} + \frac{f^{pl,j^*}}{k_H^{pl,j^*}} = \Delta_h^{el} + \sum_{j=j^*+1}^{m} \delta_{h,t}^{pl,j} + \sum_{j=j^*}^{m-1} \frac{f^{pl,j}}{k_H^{pl,j}} \quad (190)$$

Where the equivalent lateral stiffness of the wall is calculated using j^* panels:

$$k_H^{pl,j^*} = \frac{k_h'^{pl,j^*} \cdot b^2 \cdot j^{*2}}{h^2} \quad (191)$$

The equivalent hold-down tensile stiffness is written for SW behaviour with j^* panels in the wall before the j^*-1^{th} connection yield:

$$k_h'^{pl,j^*} = \left(\frac{1}{k_h} + \frac{j^*-1}{n \cdot k_c}\right)^{-1} \quad (192)$$

Additionally, with the increase of lateral force f^{pl,j^*}, that led to the yielding of vertical joint j^*-1, new values of panel joint elevation are calculated in term of the lateral force for joint j in the domain of $[1, j^*-2]$.

$$v_j'^{pl,j^*} = v_j^{pl,j^*} + \left\{\frac{f^{pl,j^*} \cdot h}{j^* \cdot b \cdot k_h \cdot n \cdot k_c}(n \cdot k_c - k_h)\right\} \cdot \frac{(j^*-j)}{j^*} =$$

$$v_j^{el,m} - \sum_{i=j^*}^{m-1} \vartheta^i \cdot j \cdot b + \sum_{i=j^*}^{m-1} \left\{\frac{f^{pl,i} \cdot h}{i \cdot b \cdot k_h \cdot n \cdot k_c}(n \cdot k_c - k_h)\right\} \cdot \frac{(i-j)}{i} \quad (193)$$

Failure mechanism III is characterized by the failure in vertical joints in kinematic mode j^* attained prior the yielding of the hold-down as expressed in Equation (194). $f'^{pl,\hat{j}}$ is defined as the increase in force attained from the point where panel j^* reattaches with ground and is expressed in Equation (197). Equation (195) shows that the ultimate displacement of the vertical joint in failure mechanism III is bounded by the transitional deformation in the vertical joints to achieve kinematic mode j^* and the displacement resulting in the failure of the vertical joints up to $j^* - 1$. This is expressed through the following two conditions:

$$d_{y,h} > \frac{1}{k_h}\left[\left(\frac{R_{w,c}^{el,m} \cdot h}{b \cdot \tilde{j}} - \frac{q \cdot b \cdot \tilde{j}}{2}\right) + \sum_{j=\hat{j}+1}^{m-1} \frac{f^{pl,j} \cdot h}{b \cdot j} + \frac{f'^{\,pl,\hat{j}} \cdot h}{b \cdot \hat{j}}\right] \quad (194)$$
[A]

$$\frac{b}{h} \cdot \Delta_{h,t}^{pl,j^*+1,k} < d_{u,c} < \frac{b}{h} \cdot \Delta_{h,t}^{pl,j^*} \quad (195)$$

If both conditions (194) and (195) are met, j^* becomes associated with the final kinematic mode in the plastic state, $\hat{j}$, as presented in Figure 5-13.

The plastic strength for failure mechanism III is calculated by adding the elastic strength, the increase of force required to fully develop kinematic mode $j^* = [m - 1, \hat{j} + 1]$ and the increase of force in kinematic mode $\hat{j}$ governed by the failure in vertical joints.

$$R_w^{pl,III} = F_t^{pl,j^*+1} + f'^{\,pl,\hat{j}} = R_{w,c}^{el,m} + \sum_{j=\hat{j}+1}^{m-1} f^{pl,j} + f'^{\,pl,\hat{j}} \quad (196)$$

Where $f'^{\,pl,\hat{j}}$ is the increase of force in kinematic mode $\hat{j}$ governed by the rupture of vertical joint j in the range of $[\hat{j}, m - 1]$.

$$f'^{\,pl,\hat{j}} = k_H^{pl,\hat{j}} \cdot \left(\frac{h}{b} \cdot d_{u,c} - \Delta_{h,t}^{pl,\hat{j}+1,k}\right) \quad (197)$$

The lateral displacement of the wall is associated with the failure of the vertical joint and developed as:

$$\Delta_h^{u,III} = \Delta_h^{pl,III} = \frac{h}{b} \cdot d_{u,c} \quad (198)$$

The ductility is defined as:

$$\mu_w{}^{III} = \frac{\Delta_h^{u,III}}{\Delta_h^{el}} \quad (199)$$

Failure mechanisms IV and V occurs when the hold-down yield in kinematic mode j^* prior the failure of the vertical joints, as expressed in Equation (200). The wall displacement related to the yielding of hold-down, $\Delta_h^{pl,IV,V}$ can be found in Equation (204). Equation (201) ensures that the yielding displacement of the hold-down for failure mechanism IV and V is bounded by the deformation to fully develop kinematic mode $j^* + 1$ and j^*.

$$d_{u,c} > \frac{b}{h} \cdot \Delta_h^{pl,IV,V} \quad (200)$$

$$\frac{1}{k_h}\left[\left(\frac{R_{w,c}^{el,m} \cdot h}{b \cdot m} - \frac{q \cdot b \cdot m}{2}\right) + \sum_{j=j^*+1}^{m-1} \frac{f^{pl,j} \cdot h}{b \cdot j}\right] < d_{y,h} < \frac{1}{k_h}\left[\left(\frac{R_{w,c}^{el,m} \cdot h}{b \cdot m} - \frac{q \cdot b \cdot m}{2}\right) + \sum_{j=j^*}^{m-1} \frac{f^{pl,j} \cdot h}{b \cdot j}\right]$$

(201)[A]

If both conditions (200) and (201) are met, j^* becomes associated with the final kinematic mode in the plastic state, $\hat{j}$ as presented in Figure 5-13

The plastic strength for failure mechanism IV and V is calculated by adding the elastic strength, the increase of force required to fully develop kinematic mode $j^* = [m-1, \hat{j}+1]$ and the increase of force in kinematic mode $\hat{j}$ governed by the yielding of the hold-down.

$$R_w^{pl,IV,V} = F_t^{pl,j^*+1} + f'^{\,pl,\hat{j}} = R_{w,c}^{el,m} + \sum_{j=\hat{j}+1}^{m-1} \frac{f^{pl,j}}{k_H^{pl,j}} + f'^{\,pl,\hat{j}} \quad (202)$$

Where $f'^{\,pl,\hat{j}}$ is the increase of force in kinematic mode $\hat{j}$ governed by the yielding of the hold-down and has been developed from interpolation as:

$$f'^{\,pl,\hat{j}} = \hat{j} \cdot \left[\frac{b}{h}\left(r_h + \frac{q \cdot b \cdot m}{2}\right) - \frac{R_{w,c}^{el,m}}{m} - \sum_{j=\hat{j}+1}^{m-1} \frac{f^{pl,j}}{j}\right] \quad (203)[A]$$

The plastic displacement of the wall in failure mechanism IV and V is the sum of the lateral displacement of the wall in elastic state, the incremental displacement related to previous panel drop associated with kinematic modes m to $\hat{j}+1$, the incremental displacement related to the full development of the previous kinematic modes $m-1$ to $\hat{j}+1$ and the incremental displacement related to kinematic mode $\hat{j}$ governed by the hold-down yield. The expression is shown in Equation (204):

$$\Delta_h^{pl,IV,V} = \Delta_{h,t}^{pl,\hat{j}+1,k} + \frac{f'^{\,pl,\hat{j}}}{k_H^{pl,\hat{j}}} = \Delta_h^{el} + \sum_{j=\hat{j}+1}^{m} \delta_{h,t}^{pl,j} + \sum_{j=\hat{j}+1}^{m-1} \frac{f^{pl,j}}{k_H^{pl,j}} + \frac{f'^{\,pl,\hat{j}}}{k_H^{pl,\hat{j}}} \quad (204)$$

The ultimate displacements for failure mechanism IV and V are characterized by failure in the vertical joints and the hold-down, respectively. It can be expressed as the ultimate displacement of the vertical joint and the wall panel aspect ratio as expressed in Equation (205). Equation (206) is developed the sum of the lateral displacement of the wall in elastic state, the incremental displacement related to previous panel drop associated with kinematic modes m to $\hat{j}+1$, the incremental displacement related to the full development of the previous kinematic modes $m-1$ to $\hat{j}+1$, the incremental displacement related to kinematic mode $\hat{j}$ governed by the hold-down yield and the incremental displacement to achieve the ultimate displacement capacity of the hold-down.

$$\Delta_h^{u,IV} = \frac{h}{b} \cdot d_{u,c} \quad (205)$$

$$\Delta_h^{u,V} = \Delta_h^{pl,V} + \frac{h}{\hat{j} \cdot b} \cdot (d_{u,h} - d_{y,h}) = \Delta_h^{el} + \sum_{j=\hat{j}+1}^{m} \delta_{h,t}^{pl,j} + \sum_{j=\hat{j}+1}^{m-1} \frac{f^{pl,j}}{k_H^{pl,j}} + \frac{f'^{\,pl,\hat{j}}}{k_H^{pl,\hat{j}}} + \frac{h}{\hat{j} \cdot b} \cdot (d_{u,h} - d_{y,h}) \quad (206)$$

Therefore, the ductility for failure mechanism IV and V are:

$$\mu_w{}^{IV} = \frac{\Delta_h^{u,IV}}{\Delta_h^{el}} \quad (207)$$

$$\mu_w{}^{V} = \frac{\Delta_h^{u,V}}{\Delta_h^{el}} \quad (208)$$

5.3.5 Plastic CP Behaviour Region, Failure Mechanism $VI, VII, VIII$

As can be seen in Figure 5-14, CP^{PL} is defined by the limits represented by the reattachment of panel 1 with the ground and the yielding of the hold-down until failure is achieved.

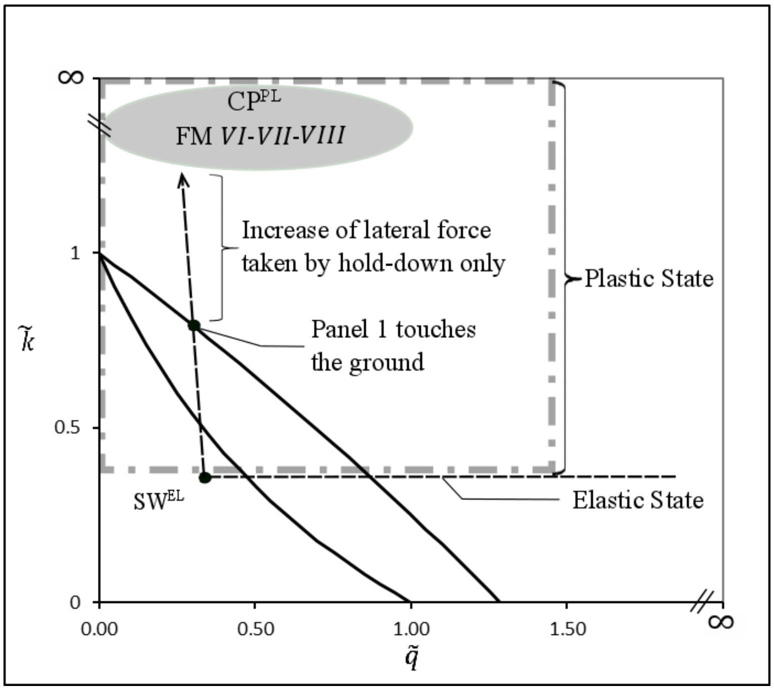

Figure 5-14: CP^{PL} behaviour region of Case SW^{EL}-CP^{PL}

Kinematic mode 1 is only reached when the first panel reattaches with ground. The last panel not in contact with ground, 1, will drop from the adjusted value under the increase of lateral force resulting the yielding of joint 1 in the plastic state in kinematic mode 2, $v'^{\,pl,j^*=2}_{j=1}$. A variation in the angle of rotation would be attained, $\vartheta'^{\,j^*=1}$, since hold-down elongation remains the same.

$$\vartheta'^{\,j^*=1} = \frac{v'^{\,pl,j^*=2}_{j=1}}{b} \quad (209)$$

Where:

$$v'^{\,pl,j^*=2}_{j=1} = v_j^{el,m} - \sum_{i=2}^{m-1} \vartheta^i \cdot j \cdot b + \sum_{i=2}^{m-1} \left\{ \frac{f^{pl,i} \cdot h}{i \cdot b \cdot k_h \cdot n \cdot k_c} (n \cdot k_c - k_h) \right\} \cdot \frac{(i-j)}{i} \quad (210)$$

The reattachment of panel 1 has the effect of increasing the horizontal displacement of the wall without any increase in force. The increase in displacement between kinematic mode 2 and 1can be expressed as:

$$\delta_{h,t}^{pl,2} = \vartheta'^{\,j^*=1} \cdot h \quad (211)$$

The total displacement of the wall when panel 1 reattaches with the ground is the sum of the elastic displacement, the incremental displacement related to previous panel drop associated with kinematic modes m to 2 and the incremental displacement to fully developed the previous kinematic modes $m-1$ to 2. This displacement is still under the previous transitional force, $F_t^{pl,2}$, and the expression is shown in Equation (212).

$$\Delta_{h,t}^{pl,2,k} = \Delta_{h,t}^{pl,2} + \delta_{h,t}^{pl,2} = \Delta_h^{el} + \sum_{j=m}^{2} \delta_{h,t}^{pl,j} + \sum_{j=2}^{m-1} \frac{f^{pl,j}}{k_H^{pl,j}} \quad (212)$$

The failure mechanism for which the first vertical joint would fail during this panel's drop is follows the same steps covered in 5.3.5 for Equations (182) to (186).

At the point of reattachment of panel 1 with ground, the wall is considered to only consist of 1 panel with only the hold-down for elastic connector. At this point, the total force in the hold-down consists of the elastic strength contribution for a system with m panels, $R_{w,c}^{el,m}$ (obtained from Equation 156), and the increase of lateral force to yield the previous vertical joint j for $m-2 \leq j \leq 2$ in a system with j panels, $f^{pl,j}$. Equation (213) determine the allowable increase of lateral force to achieve the yield of the hold-down

$$f^{pl,1} = \frac{b}{h} \cdot r_h - \left[\frac{R_{w,c}^{el,m}}{m} - \frac{q \cdot b^2 \cdot m}{2 \cdot h} + \sum_{j=2}^{m-1} \frac{f^{pl,j}}{j}\right] \quad (213)^{A}$$

The plastic strength of the wall is calculated as the sum of the elastic strength, the increase of force required fully develop kinematic mode $j^* = [m-1, 2]$ and the increase of force in kinematic mode 1 governed by the yielding of the hold-down. It can be simplified according to static equilibrium as:

$$R_w^{pl,VII,VIII} = F_t^{pl,2} + f^{pl,1} = R_{w,c}^{el,m} + \sum_{j=2}^{m-1} f^{pl,j} + f^{pl,1} = \frac{b}{h}\left(r_h + r_c \cdot (m-1) \cdot n + \frac{q \cdot m \cdot b}{2}\right)$$

(214)

The total displacement of the wall when achieving its plastic strength is the sum of the elastic displacement, the incremental displacement related to previous panel drop associated with kinematic modes m to 2 and the incremental displacement to fully developed the previous kinematic modes ($m-1$ to 2) and now including the increase of force that resulted in the hold-down yield.

$$\Delta_h^{pl} = \Delta_{h,t}^{pl,2,k} + \frac{f^{pl,1}}{k_H^{pl,1}} = \Delta_h^{el} + \sum_{j=2}^{m} \delta_{h,t}^{pl,j} + \sum_{j=2}^{m-1} \frac{f^{pl,j}}{k_H^{pl,j}} + \frac{f^{pl,1}}{k_H^{pl,1}} \quad (215)$$

Where, the equivalent lateral stiffness of the wall is calculated using 1 panel:

$$k_H^{pl,1} = \frac{k_h \cdot b^2}{h^2} \quad (216)$$

And where the equivalent hold-down tensile stiffness is defined assigning $k_c = 0$ as all joints have yield.

$$k'^{pl,1}_h = k_h + (m-1)\cdot n \cdot k_c = k_h \quad (217)$$

Failure mechanism VI is characterized by the failure in vertical joints in kinematic mode 1 attained prior the yielding of the hold-down as expressed in equation (218). $f'^{pl,\hat{j}}$ is defined as the increase in force attained from the point where panel 1 reattaches with ground and is expressed in Equation (221). Equation (219) shows that the ultimate displacement of the vertical joint in failure mechanism VI is bounded by the transitional deformation in the vertical joints to achieve kinematic mode 1and the displacement resulting the yield in the hold-down. This is expressed through the following two conditions:

$$d_{y,h} > \frac{1}{k_h}\left[\left(\frac{R^{el,m}_{w,c}\cdot h}{b\cdot m} - \frac{q\cdot b\cdot m}{2}\right) + \sum_{j=2}^{m-1}\frac{f^{pl,j}\cdot h}{b\cdot j} + \frac{f'^{pl,1}\cdot h}{b}\right] \quad (218)^{A}$$

$$\frac{b}{h}\cdot \Delta^{pl,2,k}_{h,t} < d_{u,c} < \frac{b}{h}\cdot \Delta^{pl}_{h} \ (219)$$

If both conditions (218) and (219) are met, j^* becomes associated with the final kinematic mode in the plastic state, $\hat{j}$, as presented in Figure 5-13.

The plastic strength for failure mechanism VI is calculated by adding the elastic strength, the increase of force required fully develop kinematic mode $j^* = [m-1, 2]$ and the increase of force in kinematic mode 1 governed by the failure in vertical joints.

$$R^{pl,VI}_{w} = F^{pl,2}_{t} + f'^{pl,1} = R^{el,m}_{w,c} + \sum_{j=2}^{m-1}\frac{f^{pl,j}}{k^{pl,j}_{H}} + f'^{pl,1} \quad (220)$$

Where $f'^{pl,\hat{j}}$ is the increase of force in kinematic mode 1 governed by the failure in vertical joints.

$$f'^{pl,1} = k^{pl,1}_{H}\cdot\left(\frac{h}{b}\cdot d_{u,c} - \Delta^{pl,2,k}_{h,t}\right) \quad (221)$$

The lateral displacement of the wall is associated with the failure of the vertical joint and developed as:

$$\Delta_h^{u,VI} = \Delta_h^{pl,VI} = \frac{h}{b} \cdot d_{u,c} \quad (222)$$

Therefore, the ductility is, per definition, expressed as:

$$\mu_w{}^{VI} = \frac{\Delta_h^{u,VI}}{\Delta_h^{el}} \quad (223)$$

Failure mechanism VII and $VIII$ are characterized by the yielding of the hold-down occurs prior the failure in vertical joint as expressed in Equation (224). Equation (225) shows that the yielding displacement of the hold-down in VII and $VIII$ occurs in kinematic mode 1. This is expressed through the following two conditions:

$$d_{u,c} > \frac{b}{h} \cdot \Delta_h^{pl} \quad (224)$$

$$d_{y,h} > \frac{1}{k_h} \cdot \left[\frac{R_{w,c}^{el,m} \cdot h}{b \cdot m} - \frac{q \cdot b \cdot m}{2} + \sum_{j=2}^{m-1} \frac{f^{pl,j} \cdot h}{b \cdot j} \right] \quad (225)^{A}$$

If both conditions (224) and (225) are met, then, kinematic mode 1 becomes associated with the final kinematic mode in the plastic state, $\hat{j}$, (Fig.5-13) and the wall achieve the plastic strength, $R_w^{pl,VII,VIII}$, and displacement, Δ_h^{pl}, stated in Equation (214) and (215) respectively.

The ultimate displacements for failure mechanism VII and $VIII$ are characterized by failure in the vertical joints and in the hold-down, respectively. They are both expressed as the connectors ultimate displacement and the panel aspect ratio.

$$\Delta_h^{u,VII} = \frac{h}{b} \cdot d_{u,c} \quad (226)$$

$$\Delta_h^{u,VIII} = \frac{h}{b} \cdot d_{u,h} \quad (227)$$

Therefore, the ductility is presented for both failure mechanism as:

$$\mu_w{}^{VII} = \frac{\Delta_h^{u,VII}}{\Delta_h^{el}} \quad (228)$$

$$\mu_w{}^{VIII} = \frac{\Delta_h^{u,VIII}}{\Delta_h^{el}} \quad (229)$$

5.4 Model Development for Case IN^{EL}-CP^{PL}

This case is achieved through the IN behaviour in the elastic state and the CP behaviour in the final plastic state and is ensured by the inequalities presented in Equations (130) and (133). As shown in Figure 5-16, the behaviour regions are presented as CP behaviour (CP^{EL}) and IN behaviour (IN^{EL}) both in the elastic state until kinematic mode j̃ is achieved. The wall starts at CP behaviour in the elastic phase, and the panels progressively lift starting with panel 1 to j̃, thereby achieving IN behaviour.

The procedure to develop the $IN^{EL}CP^{PL}$ follows in principle that of the $SW^{EL}CP^{PL}$ with the exception that for the $SW^{EL}CP^{PL}$ case, the wall rotates about one global rotation point and at the yield strength, the stiffness of the wall is equal to zero (represented by a plateau in the force-displacement graph) until the next panel reattaches with ground. For the $IN^{EL}CP^{PL}$ case, yielding occurs in all panel joints higher than panel j̃ at the elastic strength, leading to a rotation of panels 1 to j̃ in SW behaviour about the point of rotation in panel j̃. This means that the wall segment consisting of panels 1 to j̃ would maintain some level of stiffness.

When failure mechanisms IX and X (Figure 5-16) cannot be achieved, the behaviour of the wall depends on the limitation in the ductility of the individual connectors. Therefore, from the elastic state, the wall may possess limited ductility and therefore remain in the IN behaviour for kinematic mode $\hat{j} = \tilde{j}$ or achieve an inferior value of kinematic mode, $\hat{j}$, in the range of $\tilde{j} - 1 \leq \hat{j} \leq 2$. CP behaviour and the associated failure mechanisms IX and X are achieved if the ductility of each individual connectors is sufficient. The different behaviour regions for which the wall may reach its ultimate capacity are presented in the general force-displacement curve shown in Figure 5-15 and associated kinematic path in Figure 5-16.

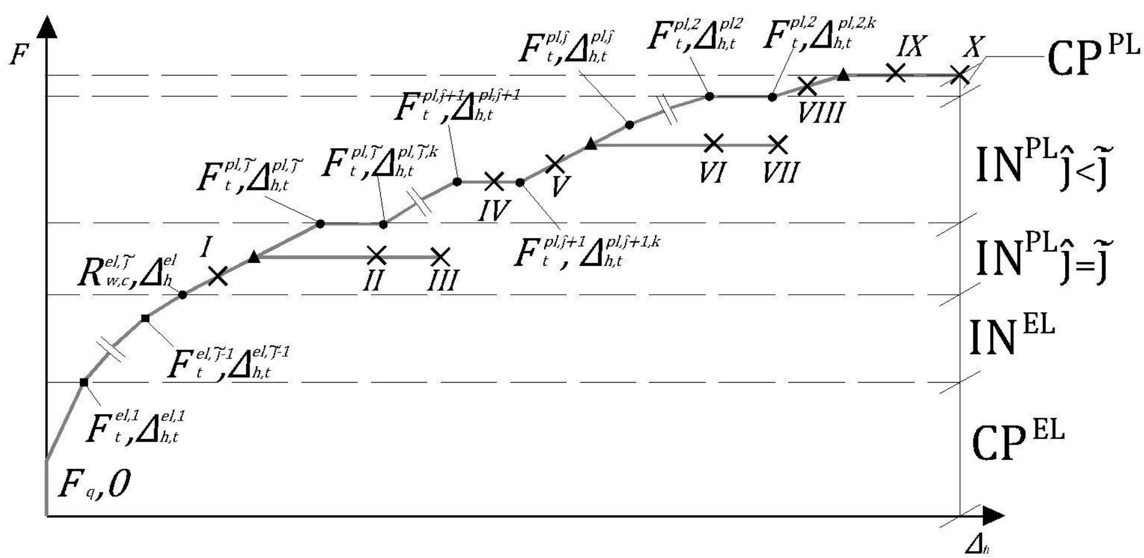

Figure 5-15: General Elasto-Plastic Force-Displacement Curve for Kinematic Path IN^{EL}-CP^{PL}

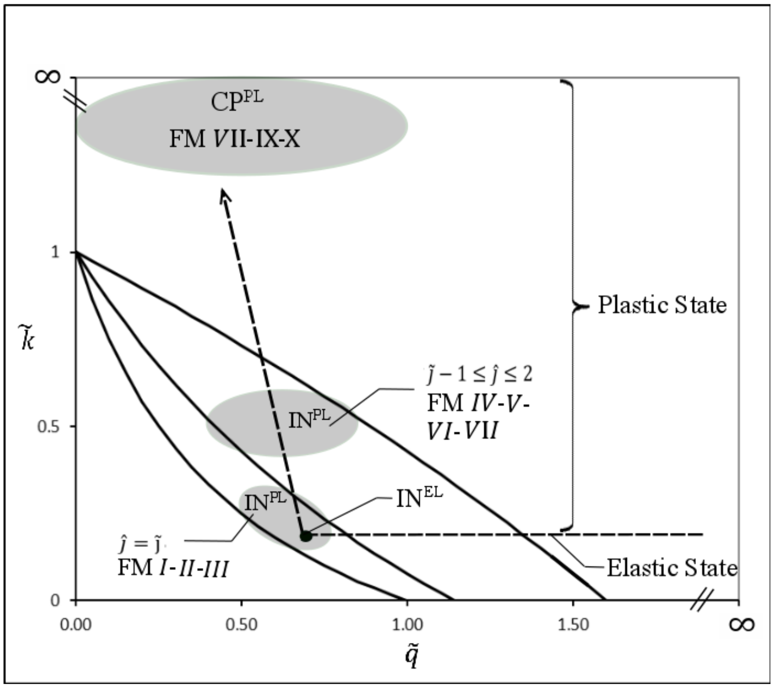

Figure 5-16: Behaviour Region of Case IN^{EL}-CP^{PL}

All failure mechanism along the IN^{EL}-CP^{PL} path are illustrated in Figure 5-17. The failure mechanisms can be established based on three possible cases of kinematic modes, $\hat{j}$, achieved in plastic state due to limited connectors elongation capacity. Failure mechanisms I, II and III are define for $\hat{j} = \tilde{j}$, IV through VII are defined for of $\tilde{j} - 1 \le \hat{j} \le 2$ and $VIII$, IX and X are defined for $\hat{j} = 1$.

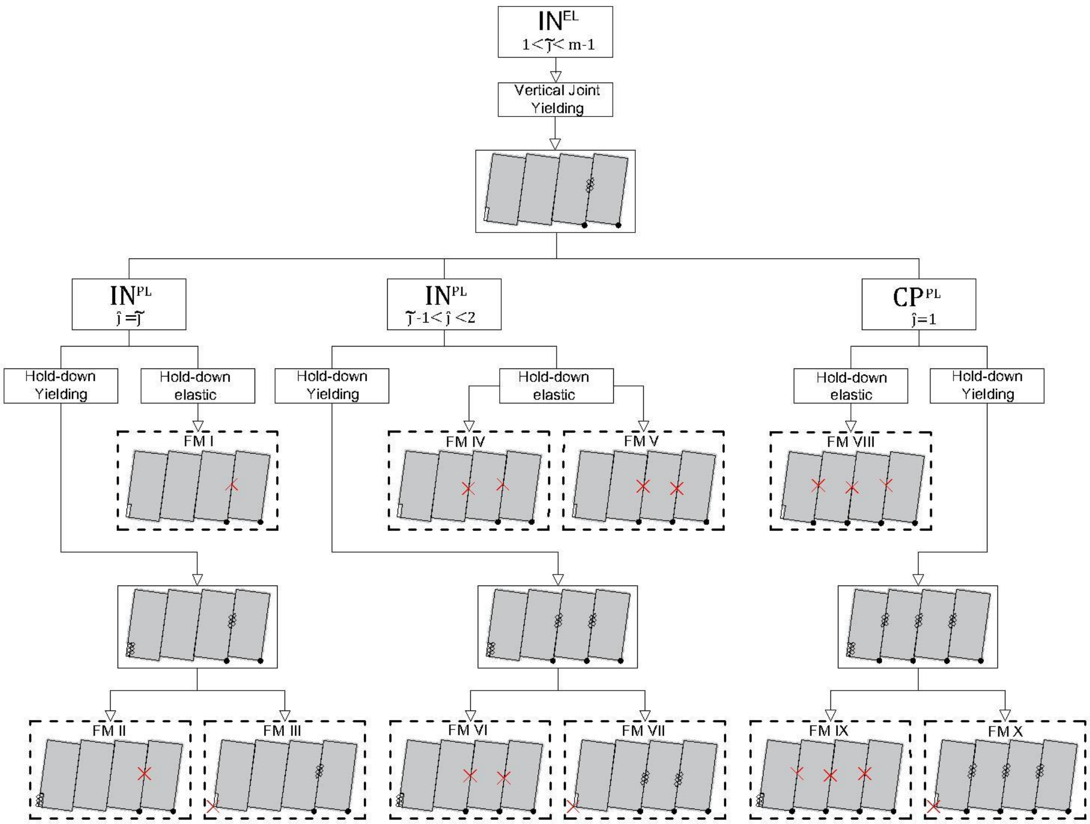

Figure 5-17: Definition of Failure Mechanism for IN^{EL}-CP^{PL}

The subsequent sections will follow the structure presented in Figure 5-17, starting by describing the elastic state in CP and IN behaviour (Section 5.4.1), followed by a description of the plastic states in the IN^{PL} ($\hat{j} = \tilde{j}$), IN ($1 \leq \hat{j} \leq m - 1$) and SW behaviour in Sections 5.4.2, 5.4.3 and 5.4.4, respectively.

5.4.1 CP and IN behaviour in Elastic State

The first point in the force-displacement relationship of the wall for all cases is the activation force, as defined by Equation (6) and discussed in Section 3.2.

The first segment of the force-displacement relationship in limited by the change between kinematic mode 1 and 2 and is denoted, $F_t^{el,1}$ presented in Equation (1). The first transitional force is associated with the following displacement:

$$\Delta_{h,t}^{el,1} = \frac{F_t^{el,1} - F_q}{k_H^{el,1}} \quad (230)$$

The intermediate displacements of the wall for any kinematic mode j^* in the range of $[2, \tilde{\jmath}]$, associated with intermediate transitional forces F_t^{el,j^*}, are the sum of the lateral displacement of the wall in CP behaviour and the incremental displacement to achieve all intermediate kinematic modes 2 to $\tilde{\jmath}$. The expression is shown in Equation (231).

$$\Delta_{h,t}^{el,j^*} = \frac{F_t^{el,1} - F_q}{k_H^{el,1}} + \sum_{j^*=2}^{\tilde{\jmath}} \frac{F_t^{el,j^*} - F_t^{el,j^*-1}}{k_H^{el,j^*}} \quad (231)$$

The last elastic segment (Figure 5-16) is limited by the transitional force to achieve kinematic mode $\tilde{\jmath}$ and the elastic strength in kinematic mode $\tilde{\jmath}$, $R_{w,h}^{el,\tilde{\jmath}}$, as expressed in Equation (8) of section 3.2. Therefore, the associated elastic displacement of case IN^{EL}-CP^{PL} has been developed in Casagrande et al. (2017) as:

$$\Delta_h^{el} = \frac{R_{w,h}^{el,\tilde{\jmath}} \cdot h^2}{b^2 \cdot k_h'^{\,el,\tilde{\jmath}}} - \frac{q \cdot h}{2 \cdot k_h'^{\,el,\tilde{\jmath}}} \cdot \frac{\left(m + \tilde{\jmath} \cdot (\tilde{\jmath} - 1)\right) \cdot n \cdot k_c + (\tilde{\jmath} - 1) \cdot (m - \tilde{\jmath}) \cdot k_h}{n \cdot k_c + (\tilde{\jmath} - 1) \cdot k_h} \quad (232)$$

Where $k_h'^{\,el,\tilde{\jmath}}$ is the equivalent hold-down tensile stiffness for IN behaviour with $\tilde{\jmath} = j^*$.

$$k_h'^{\,el,\tilde{\jmath}} = \frac{n \cdot k_c \cdot [(\tilde{\jmath} + m\tilde{\jmath} - m) \cdot k_h + (m - \tilde{\jmath}) \cdot n \cdot k_c]}{n \cdot k_c + (\tilde{\jmath} - 1) \cdot k_h} \quad (233)$$

5.4.2 IN Behaviour Region for Kinematic Mode $\hat{j} = \tilde{\jmath}$ in Plastic State, Failure Mechanisms $I - III$

As can be seen in Figure 5-18, $\mathrm{IN}^{\mathrm{PL}}$ is defined by the limits represented with the yielding of the vertical joint in kinematic mode $\tilde{\jmath}$, and the transitional force to achieve kinematic mode $\tilde{\jmath}-1$, $F_t^{pl,\tilde{\jmath}}$. The transitional force, $F_t^{pl,\tilde{\jmath}}$ defines the state at which panel $\tilde{\jmath}-1$ reattaches with ground as shown in Figure 5-19.

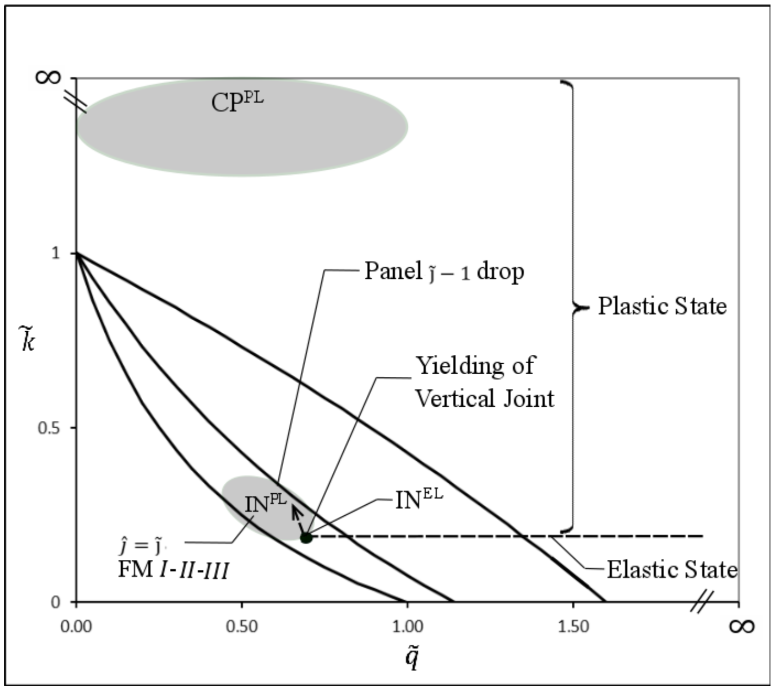

Figure 5-18:Behaviour Region $\mathrm{IN}^{\mathrm{PL}}$ of Case $\mathrm{IN}^{\mathrm{EL}}$-$\mathrm{CP}^{\mathrm{PL}}$

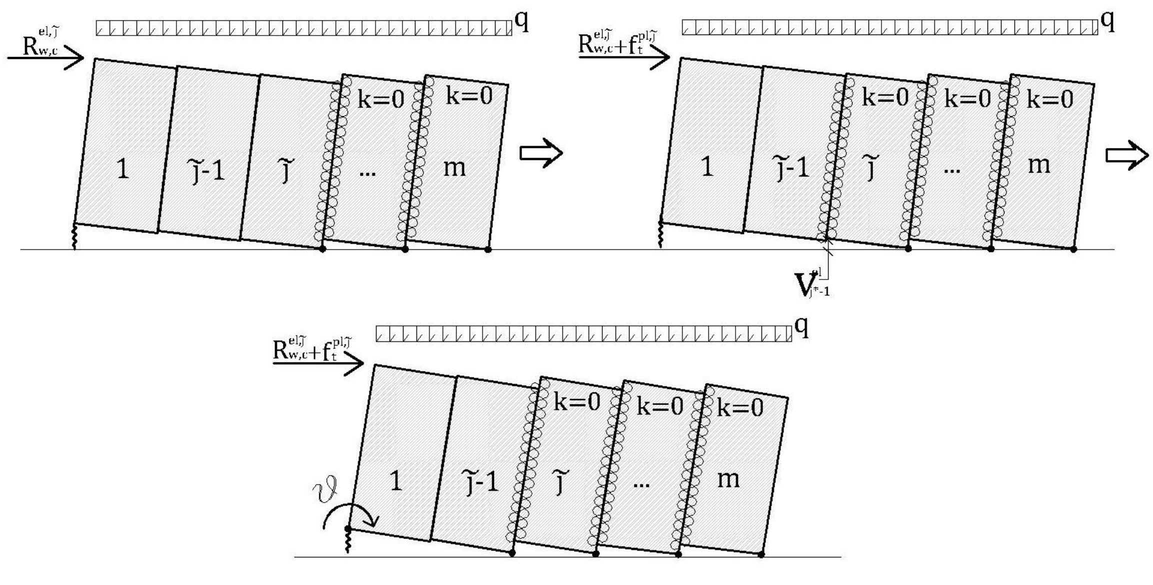

Figure 5-19: Transition from Elastic Kinematic Mode $\tilde{j}$ to Plastic Kinematic Mode $\tilde{j}$ and $\tilde{j}-1$ in Case IN^{EL}-CP^{PL}

The vertical displacement of the lower right joint of panel j for $[1, \tilde{j}-1]$ is calculated to determine the drop of panel in the domain of 1 to $\tilde{j}-1$. The elevation of uplifted panel j are calculated using IN behaviour equations provided in Casagrande et al. (2017).

$$v_j^{el,\tilde{j}} = \frac{R_{w,c}^{el,\tilde{j}}\cdot h}{n\cdot k_c\cdot b}\cdot\frac{(\tilde{j}-j)\cdot(n\cdot k_c-k_h)}{(\tilde{j}+m\cdot\tilde{j}-m)\cdot k_h+(m-\tilde{j})\cdot n\cdot k_c} - \frac{q\cdot b}{2\cdot n\cdot k_c}\cdot\frac{\tilde{j}^2\cdot(m-j)\cdot[(j-1)\cdot k_h+n\cdot k_c]-j^2\cdot(m-\tilde{j})\cdot[(\tilde{j}-1)\cdot k_h+n\cdot k_c]}{(\tilde{j}+m\cdot\tilde{j}-m)\cdot k_h+(m-\tilde{j})\cdot n\cdot k_c}$$

(234)

The wall, in kinematic mode $\tilde{j}$, can resist additional lateral force, $f^{pl,\tilde{j}}$, to achieve the yielding of the $\tilde{j}-1^{th}$ joint. The force required to attain the yielding of vertical joint $\tilde{j}-1$ (Eq. 235) consists of the elastic strength contribution for a system with $\tilde{j}$ panels, $R_{w,c}^{el,\tilde{j}}$, and the increase of lateral force required to yield the $\tilde{j}-1$ joint, $f^{pl,\tilde{j}}$ (Fig. 5-20).

$$r_c = F_{c,y,\mathrm{i},\tilde{j}-1}(F = R_{w,c}^{el,\tilde{j}}, m = \tilde{j}) + F_{c,y,\mathrm{i},\tilde{j}-1}(f^{pl,\tilde{j}}, m = \tilde{j}, q = 0) \quad (235)$$

Where the force vertical joints resulting the achievement of elastic strength in IN behaviour is written per Casagrande et al. (2017) as:

$$F_{c,y,i,j} = \frac{R_{w,c}^{el,\tilde{j}} \cdot h}{n \cdot b} \cdot \frac{\tilde{j} \cdot k_h}{(\tilde{j}+m \cdot \tilde{j}-m) \cdot k_h + (m-\tilde{j}) \cdot n \cdot k_c} - \frac{q \cdot b}{2 \cdot n} \cdot \frac{\tilde{j}^2 \cdot m \cdot k_h - 2 \cdot (\tilde{j}-1) \cdot [(\tilde{j}+m \cdot \tilde{j}-m) \cdot k_h + (m-\tilde{j}) \cdot n \cdot k_c]}{(\tilde{j}+m \cdot \tilde{j}-m) \cdot k_h + (m-\tilde{j}) \cdot n \cdot k_c} \quad (236)$$

The force in vertical joints in the plastic state (i.e. increase of force, $f^{pl,\tilde{j}}$) is calculated using the equation of SW behaviour (Eq.170) with $\tilde{j}$ panels as the other panel from $\tilde{j}+1$ to m have yielded and do not influence the stiffness of the elastic wall segment. The increase of lateral force in kinematic mode can be expressed the following way:

$$f^{pl,\tilde{j}} = \frac{b \cdot \tilde{j}}{h}\left[n \cdot r_c + \frac{qb}{2} \cdot \frac{\tilde{j}^2 \cdot m \cdot k_h - 2 \cdot (\tilde{j}-1) \cdot [(\tilde{j}+m \cdot \tilde{j}-m) \cdot k_h + (m-\tilde{j}) \cdot n \cdot k_c]}{(\tilde{j}+m \cdot \tilde{j}-m) \cdot k_h + (m-\tilde{j}) \cdot n \cdot k_c}\right] - \frac{R_{w,c}^{el,\tilde{j}} \cdot \tilde{j}^2 \cdot k_h}{(\tilde{j}+m \cdot \tilde{j}-m) \cdot k_h + (m-\tilde{j}) \cdot n \cdot k_c}$$

(237)[A]

Therefore, the total lateral load applied on top of the wall is calculated following the following expression:

$$F_t^{pl,\tilde{j}} = R_{w,c}^{el,\tilde{j}} + f^{pl,\tilde{j}} \quad (238)$$

The transitional plastic displacement of the wall for the development of kinematic mode $\tilde{j}$ is the sum of the elastic lateral displacement and the increase of displacement related to the yielding of vertical joint $\tilde{j}-1$:

$$\Delta_{h,t}^{pl,\tilde{j}} = \Delta_h^{el} + \frac{f^{pl,\tilde{j}}}{k_H^{pl,\tilde{j}}} \quad (239)$$

Where the equivalent lateral stiffness of the wall is calculated using $\tilde{j}$ panels:

$$k_H^{pl,\tilde{j}} = \frac{k_h'^{\,pl,\tilde{j}} \cdot b^2 \cdot \tilde{j}^2}{h^2} \quad (240)$$

The equivalent hold-down tensile stiffness is written for a single wall behaviour with $\tilde{\jmath}$ panels:

$$k_h'^{\,pl,\tilde{\jmath}} = \left(\frac{1}{k_h} + \frac{\tilde{\jmath}-1}{n \cdot k_c}\right)^{-1} \quad (241)$$

Additionally, with the increase of lateral force $f^{pl,\tilde{\jmath}}$, that led to the yielding of vertical joint $\tilde{\jmath}-1$, new values of panel joint elevation are calculated in term of the lateral force for joint j in the domain of $[1, \tilde{\jmath}-1]$

$$v_j'^{\,pl,\tilde{\jmath}} = v_j^{el,\tilde{\jmath}} + \left\{\frac{f^{pl,\tilde{\jmath}} \cdot h}{\tilde{\jmath} \cdot b \cdot k_h \cdot n \cdot k_c}(n \cdot k_c - k_h)\right\} \cdot \frac{(\tilde{\jmath}-j)}{\tilde{\jmath}} \quad (242)$$

Failure mechanism I is characterized by the failure in vertical joints $[\tilde{\jmath}, m-1]$ in kinematic mode $\tilde{\jmath}$ attained prior the yielding of the hold-down as expressed in Equation (243). $f'^{\,pl,\hat{\jmath}}$ is defined as the increase in force attained from the point where the vertical joints $[\tilde{\jmath}, m-1]$ yields and is expressed in Equation (246). Equation (244) shows that the ultimate displacement of the vertical joint in failure mechanism I is bounded by the deformation in the vertical joints at the elastic strength and the displacement resulting in the failure of the vertical joints up to $\tilde{\jmath}-1$. This is expressed through the following two conditions:

$$d_{y,h} > \frac{1}{k_h} \cdot \left[\left(\frac{R_{w,c}^{el,\tilde{\jmath}} \cdot h}{b} - \frac{q \cdot b \cdot m \cdot \tilde{\jmath}}{2}\right) \cdot \frac{\tilde{\jmath} \cdot k_h}{(\tilde{\jmath} + m \cdot \tilde{\jmath} - m) \cdot k_h + (m-\tilde{\jmath}) \cdot n \cdot k_c} + \frac{f'^{\,pl,\tilde{\jmath}} \cdot h}{b \cdot \tilde{\jmath}}\right] \quad (243)^{A}$$

$$\frac{b}{h} \cdot \Delta_h^{el} < d_{u,c} < \frac{b}{h} \cdot \Delta_{h,t}^{pl,\tilde{\jmath}} \quad (244)$$

If both conditions (243) and (244) are met, $\tilde{\jmath}$ becomes associated with the final kinematic mode in the plastic state, $\hat{\jmath}$.

The plastic strength for failure mechanism I is calculated by adding the elastic strength to the increase of force in kinematic mode $\hat{j}$ governed by the failure in vertical joints $\tilde{j}-1$ to $m-1$.

$$R_w^{pl,I} = R_{w,c}^{el,\tilde{j}} + f'^{\,pl,\hat{j}} \qquad (245)$$

Where $f'^{\,pl,\hat{j}}$ is the increase of force in kinematic mode $\hat{j}$ governed by the rupture of vertical joints $\tilde{j}-1$ to $m-1$.

$$f'^{\,pl,\hat{j}} = k_H^{pl,\tilde{j}} \cdot \left(\frac{h}{b} \cdot d_{u,c} - \Delta_h^{el}\right) \quad (246)$$

The lateral displacement of the wall associated with the rupture of the vertical joint is developed according to the ultimate displacement of the connector.

$$\Delta_h^{u,I} = \Delta_h^{pl,I} = \frac{h}{b} \cdot d_{u,c} \quad (247)$$

The ductility is expressed in term of its definition as:

$$\mu_w{}^I = \frac{\Delta_h^{u,I}}{\Delta_h^{el}} \quad (248)$$

Failure mechanisms II and III occurs when the hold-down yield in kinematic mode $\tilde{j}$ prior the failure of the vertical joints as expressed in Equation (249). $\Delta_h^{pl,II,III}$ is the plastic displacement resulting in the yielding of the hold-down as presented in Equation (253). Equation (250) ensures that the yielding displacement of the hold-down for failure mechanisms II and III is smaller than the elongation required to achieve kinematic model $\tilde{j}-1$. $f'^{\,pl,\hat{j}}$ is expressed in Equation (252). This is expressed through the following two conditions:

$$d_{u,c} > \frac{b}{h} \cdot \Delta_h^{pl,II,III} \qquad (249)$$

$$d_{y,h} < \frac{1}{k_h} \cdot \left[\left(\frac{R_{w,c}^{el,\tilde{j}} \cdot h}{b} - \frac{q \cdot b \cdot m \cdot \tilde{j}}{2}\right) \cdot \frac{\tilde{j} \cdot k_h}{(\tilde{j} + m \cdot \tilde{j} - m) \cdot k_h + (m - \tilde{j}) \cdot n \cdot k_c} + \frac{f^{\,pl,\tilde{j}} \cdot h}{b \cdot \tilde{j}}\right] \qquad (250)^{A}$$

If both conditions (249) and (250) are met, $\tilde{j}$ becomes associated with the final kinematic mode in the plastic state, $\hat{j}$.

The plastic strength for failure mechanism II and III is calculated by adding the elastic strength and the increase of force in kinematic mode $\hat{j}$ governed by the yielding of the hold-down.

$$R_w^{pl,II,III} = R_{w,c}^{el,\tilde{j}} + f'^{\,pl,\hat{j}} \qquad (251)$$

Where $f'^{\,pl,\hat{j}}$ is the increase of force in model $\hat{j}$ governed by the yielding of the hold-down from interpolation and can be expressed as:

$$f'^{\,pl,\hat{j}} = \left(\frac{r_h - T^{el,\tilde{j}}}{t^{pl,\tilde{j}}}\right) f^{pl,\tilde{j}} = \frac{r_h \cdot b \cdot \tilde{j}}{h} - \frac{\tilde{j}^2 \cdot k_h}{(\tilde{j} + m \cdot \tilde{j} - m) \cdot k_h + (m - \tilde{j}) \cdot n \cdot k_c}\left[R_{w,c}^{el,\tilde{j}} - \frac{q \cdot b^2 \cdot m \cdot \tilde{j}}{2 \cdot h}\right] \qquad (252)^{A}$$

The plastic displacement of the wall in failure mechanism II and III is the sum of the lateral displacement of the wall in elastic state and the lateral displacement associated with the increase of force resulting the yielding of the hold-down is written as:

$$\Delta_h^{pl,II,III} = \Delta_h^{el} + \frac{f'^{\,pl,\hat{j}}}{k_H^{pl,\tilde{j}}} \qquad (253)$$

The ultimate displacements for failure mechanism II and III are characterized by failure in the vertical joints and the hold-down, respectively. It can be expressed as the ultimate displacement of the vertical joint and the wall panel aspect ratio for Equation (254). Equation

(255) is developed as the sum of the plastic lateral displacement and the allowable increase of lateral displacement governed by the failure of the hold-down.

$$\Delta_h^{u,II} = \frac{h}{b} \cdot d_{u,c} \quad (254)$$

$$\Delta_h^{u,III} = \Delta_h^{pl,III} + \frac{h}{\tilde{j} \cdot b} \cdot (d_{u,h} - d_{y,h}) \quad (255)$$

Therefore, the ductility for those two failure mechanisms is expressed as:

$$\mu_w{}^{II} = \frac{\Delta_h^{u,II}}{\Delta_h^{el}} \quad (256)$$

$$\mu_w{}^{III} = \frac{\Delta_h^{u,III}}{\Delta_h^{el}} \quad (257)$$

5.4.3 IN Behaviour Region for Kinematic Mode $\tilde{j} - 1 < \hat{j} < 2$ in Plastic State, Failure Mechanisms $IV - VII$

Figure 5-20 illustrates the region for failure mechanisms $IV - VII$, which starts with the transitional force F_t^{pl,j^*+1} achieved and the drop of panel $j^* + 1$ and ends with transitional force F_t^{pl,j^*} achieved and when panel j^* reattached to the ground for $j^* \leq \tilde{j} - 1$. The IN regions ends with the achievement of CP behaviour.

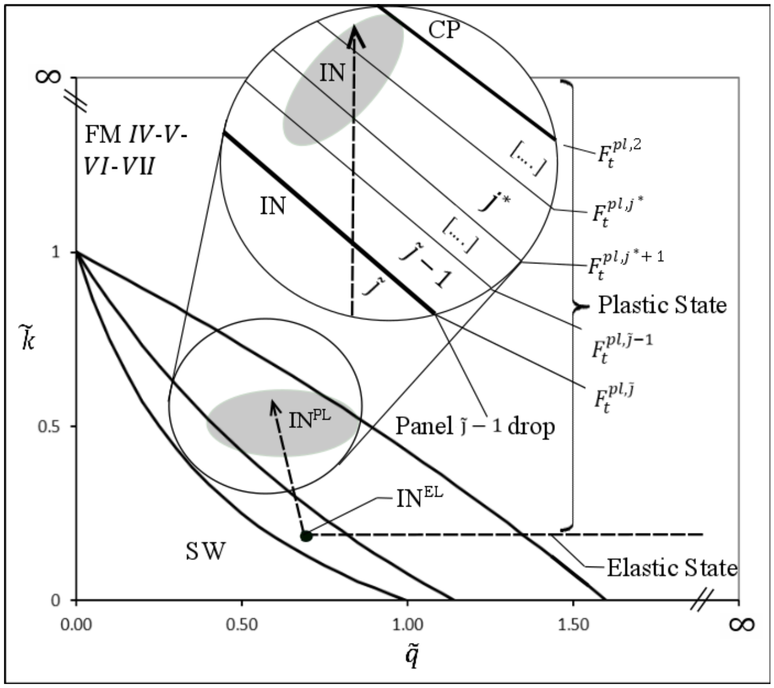

Figure 5-20: IN Behaviour Region for $\tilde{j}-1<\hat{j}<2$

The development of the force-displacement curve follows the procedure outlined in Figure 5-21. As indicated in Figure 5-21, the value of j^* is decreased between $\tilde{j}-1$ and 2 until a failure mechanism prevail the wall behaviour in a final kinematic mode $\hat{j}$ or the kinematic mode m is achieved.

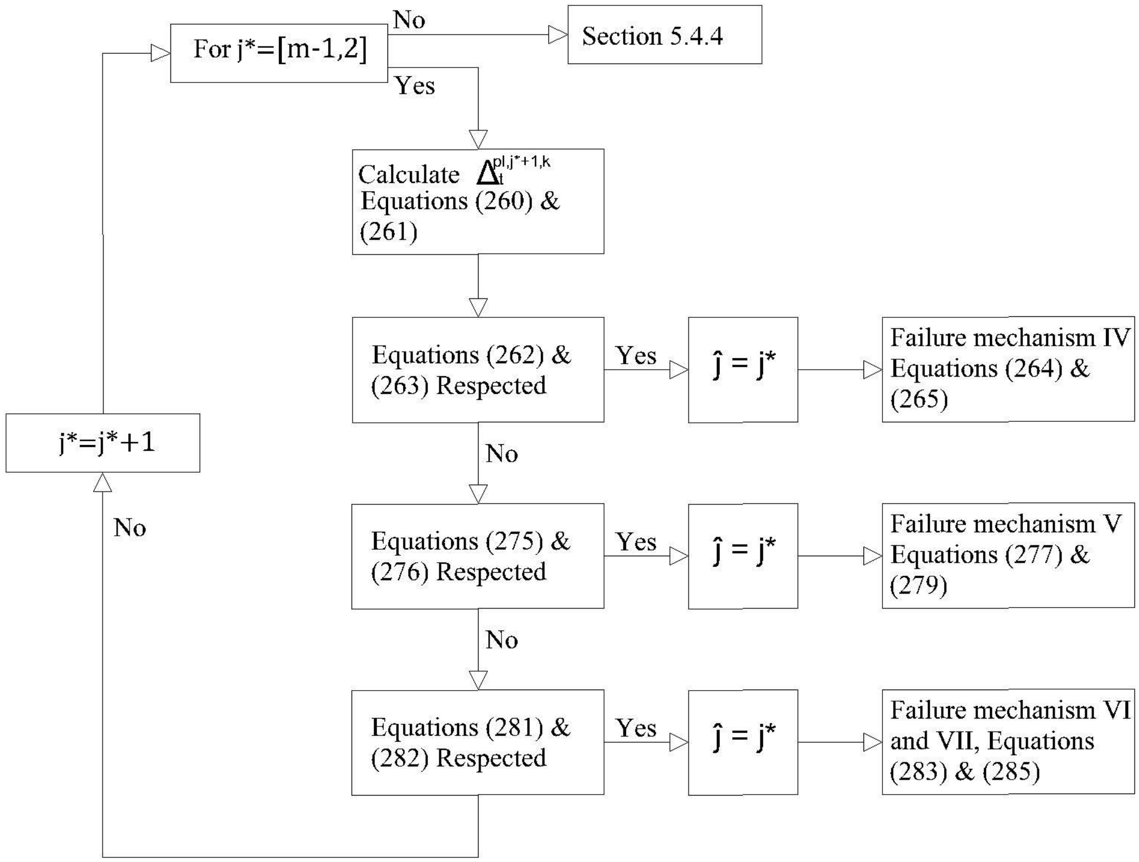

Figure 5-21: Steps to Solve IN Behaviour Region of Case IN^{EL}-CP^{PL}, Failure Mechanisms IV-VII

Kinematic mode j^* is only reached when the j^{*th} panel reattaches with ground. The last panel not in contact with ground, j^*, will drop from the adjusted value under the increase of lateral force resulting the yielding of joint j^* in the plastic state in kinematic mode j^*+1 , $v_{j^*}^{\prime\, pl,j^*+1}$ (calculated in Eq.242). A new angle of rotation would be attained, $\vartheta'^{\,j^*}$, since hold-down elongation remains the same.

The following equation allows to get the variation of angle of rotation due to rigid motion around the hold-down according to the elevation achieved by the j^{*th} panel in kinematic mode j^*+1 (previous kinematic mode).

$$\vartheta'^{\,j^*} = \frac{v'^{\,pl,j^*+1}_{j^*}}{j^* \cdot b} \quad (258)$$

The reattachment of panel j^* with ground, caused by the sliding between panel j^*+1 and j^* leads to a change in elevation for the point of rotations of the remaining panels, v_j^{pl,j^*} for $j=[1,j^*-1]$. The elevation of the point of rotation for panel j^* is assumed to be 0 as it reattaches with ground.

$$v_j^{pl,j^*} = v'^{\,pl,j^*+1}_j - \vartheta'^{\,j^*} \cdot j \cdot b = v_j^{el,m} - \sum_{i=j^*}^{\tilde{j}-1} \vartheta^i \cdot j \cdot b + \sum_{i=j^*+1}^{\tilde{j}} \left\{ \frac{f^{pl,i} \cdot h}{i \cdot b \cdot k_h \cdot n \cdot k_c} (n \cdot k_c - k_h) \right\} \cdot \frac{(i-j)}{i} \quad (259)$$

Where $v'^{\,pl,j^*+1}_j$, is the elevation of panel corrected with the increase of lateral load in kinematic model j^*+1 expressed in Equation (274) in the general form but was previously expressed in Equation (242) for kinematic mode $\tilde{j}$. The reattachment of panel j^* has the effect of increasing the horizontal displacement of the wall without any increase in force. The increase in displacement between kinematic mode j^*+1 and j^*can be expressed as:

$$\delta_{h,t}^{pl,j^*+1} = \vartheta'^{\,j^*} \cdot h \quad (260)$$

The total displacement of the wall when panel j^* reattaches with the ground is the sum the elastic displacement, the incremental displacement related to previous panel drop associated with kinematic modes $\tilde{j}-1$ to j^*+1 and the incremental displacement to fully developed the previous kinematic modes $\tilde{j}$ to j^*+1. This displacement is still under the previous transitional force, F_t^{pl,j^*+1} , and the expression is shown in Equation (261).

$$\Delta_{h,t}^{pl,j^*+1,k} = \Delta_{h,t}^{pl,j^*+1} + \delta_{h,t}^{pl,j^*+1} = \Delta_h^{el} + \sum_{j=j^*+1}^{\tilde{j}-1} \delta_{h,t}^{pl,j} + \sum_{j=j^*+1}^{\tilde{j}} \frac{f^{pl,j}}{k_H^{pl,j}} \quad (261)$$

The transitional displacement, $\Delta_{h,t}^{pl,j^*+1,k}$ might not be attained in failure mechanisms IV. Attaining failure mechanism IV is ensured by the following two conditions: a) failure of the vertical joint is reached while in transitional displacement between kinematic mode j^*+1 and j^* due to the drop of panel j^* (Eq. 262), and b) the failure of vertical joints j^* to m is reached prior to the yielding of the hold-down (Eq. 263):

$$\frac{b}{h} \cdot \Delta_{h,t}^{pl,j^*+1} < d_{u,c} < \frac{b}{h} \cdot \Delta_{h,t}^{pl,j^*+1,k} \quad (262)$$

$$d_{y,h} > \frac{1}{k_h} \cdot \left[\left(\frac{R_{w,c}^{el,\tilde{j}} \cdot h}{b} - \frac{q \cdot b \cdot m \cdot \tilde{j}}{2} \right) \cdot \frac{\tilde{j} \cdot k_h}{(\tilde{j}+m \cdot \tilde{j}-m) \cdot k_h + (m-\tilde{j}) \cdot n \cdot k_c} + \sum_{j=j^*}^{\tilde{j}} \frac{f^{pl,j} \cdot h}{b \cdot j} \right] \quad (263)^{A}$$

If both conditions (262) and (263) are met, j^* becomes associated with the final kinematic mode in the plastic state, $\hat{j}$ as presented in Figure 5-22.

In that case, the plastic strength would be defined as the transitional force between kinematic behaviour as no increase of force had occurred during the displacement:

$$R_w^{pl,IV} = F_t^{pl,\hat{j}} \quad (264)$$

The total lateral displacement for failure mechanism IV (Eq. 265) occurs in kinematic mode j^*+1 in the plastic state and is controlled only by the ultimate displacement of vertical joints j^* to $m-1$.

$$\Delta_h^{u,IV} = \Delta_h^{pl,IV} = \frac{h}{b} \cdot d_{u,c} \quad (265)$$

Therefore, the ductility is expressed in the next equation:

$$\mu_w{}^{IV} = \frac{\Delta_h^{u,IV}}{\Delta_h^{el}} \quad (266)$$

The force required to attain the yielding of vertical joint $j^* - 1$ (Eq. 267) consists of the elastic strength contribution for a system with $\tilde{j}$ panels, $R_{w,c}^{el,\tilde{j}}$ (obtained from Equation 156), the increase of lateral force to yield the previous vertical joint j for $\tilde{j} - 1 \leq j \leq j^*$ in a system with j panels, $f^{pl,j}$, and the lateral force increase required to yield the $j^* - 1$ joint, f^{pl,j^*}. f^{pl,j^*}relates to increase of force in kinematic mode j^* to attain the yielding of joint $j^* - 1$.

$$r_c = F_{c,y,i,j^*-1}\left(F = R_{w,c}^{el,\tilde{j}}, m = \tilde{j}\right) + \sum_{j=j^*+1}^{\tilde{j}-1} F_{c,y,i,j^*-1}\left(F = f^{pl,j}, m = j, q = 0\right) +$$
$$F_{c,y,i,j^*-1}\left(F = f^{pl,j^*}, m = j^*, q = 0\right) \quad (267)$$

Where, for the force distribution in vertical joint $j^* - 1$, the effect of elastic strength has to consider the wall in IN behaviour as shown in Equation (268) according to Casagrande et al. (2017). However, the effect of all other increase of lateral forces on vertical joint $j^* - 1$ can be calculated according to an SW behaviour (Eq.170) with j number of panels for $\tilde{j} - 1 \leq j \leq j^*$.

$$F_{c,y,i,j} = \frac{F \cdot h}{n \cdot b} \cdot \frac{j^* \cdot k_h}{(j^* + m \cdot j^* - m) \cdot k_h + (m - j^*) \cdot n \cdot k_c} - \frac{q \cdot b}{2 \cdot n} \cdot \frac{{j^*}^2 \cdot m \cdot k_h - 2 \cdot j \cdot [(j^* + m \cdot j^* - m) \cdot k_h + (m - j^*) \cdot n \cdot k_c]}{(j^* + m \cdot j^* - m) \cdot k_h + (m - j^*) \cdot n \cdot k_c} \quad (268)$$

Therefore, the equation of increase of lateral force f^{pl,j^*} to lead to the yielding of the $j^* - 1^{th}$ vertical joint is written as:

$f^{pl,j^*} =$

$$\frac{b \cdot j^*}{h} \cdot \left[n \cdot r_c + \frac{qb}{2} \cdot \frac{\tilde{j}^2 \cdot m \cdot k_h - 2 \cdot (j^* - 1)[(j^* + m \cdot j^* - m) \cdot k_h + (m - j^*) \cdot n \cdot k_c]}{[(j^* + m \cdot j^* - m) \cdot k_h + (m - j^*) \cdot n \cdot k_c]} \right] - j^* \cdot$$

$$\left[\frac{\tilde{j} \cdot R_{w,c}^{el,\tilde{j}} \cdot k_h}{[(\tilde{j} + m \cdot \tilde{j} - m) \cdot k_h + (m - \tilde{j}) \cdot n \cdot k_c]} + \sum_{j=j^*+1}^{\tilde{j}} \frac{f^{pl,j}}{j} \right] \quad (269)^{A}$$

Where, $f^{pl,j}$ is the force that yielded the previous vertical joint j for kinematic mode $\tilde{j} - 1$ to $j^* + 1$. The increase of force leading to the first joint yielding in the plastic state $\tilde{j} - 1$, $f^{pl,\tilde{j}}$, was calculated in Equation (237). Therefore, the lateral load applied on top of the wall is calculated following as the sum of the elastic strength, the increase of force to fully develop kinematic mode j for $\tilde{j} \leq j \leq j^* + 1$ and to fully develop kinematic mode j^*.

$$F_t^{pl,j^*} = F_t^{pl,j^*+1} + f^{pl,j^*} = R_{w,c}^{el,\tilde{j}} + \sum_{j=j^*+1}^{\tilde{j}} f^{pl,\tilde{j}} + f^{pl,j^*} \quad (270)$$

The transitional plastic displacement of the wall for the development of kinematic mode j^* is of the elastic displacement, the incremental displacement related to previous panel drop associated with kinematic modes $\tilde{j} - 1$ to $j^* + 1$ and the incremental displacement related to the full development of the previous kinematic modes ($\tilde{j}$ to $j^* + 1$) and, now, kinematic mode j^*.

$$\Delta_{h,t}^{pl,j^*} = \Delta_{h,t}^{pl,j^*+1,k} + \frac{f^{pl,j^*}}{k_H^{pl,j^*}} = \Delta_h^{el} + \sum_{j=j^*+1}^{\tilde{j}-1} \delta_{h,t}^{pl,j} + \sum_{j=j^*+1}^{\tilde{j}} \frac{f^{pl,j}}{k_H^{pl,j}} + \frac{f^{pl,j^*}}{k_H^{pl,j^*}} \quad (271)$$

Where the equivalent lateral stiffness of the wall is calculated using j^* panels:

$$k_H^{pl,j^*} = \frac{k_h'^{\,pl,j^*} \cdot b^2 \cdot j^{*2}}{h^2} \quad (272)$$

The equivalent hold-down tensile stiffness is written for a single wall behaviour with j^* panels in the wall before the $j^* - 1^{th}$ connection yield:

$$k_h'^{\,pl,j^*} = \left(\frac{1}{k_h} + \frac{j^*-1}{n\cdot k_c}\right)^{-1} \quad (273)$$

Additionally, with the increase of lateral force f^{pl,j^*}, that led to the yielding of connection j^*-1, new values of joints elevation are calculated in term of the lateral force for joint j in the domain of $[1, j^*-2]$

$$v_j'^{\,pl,j^*} = v_j^{pl,j^*} + \left\{\frac{f^{pl,j^*}\cdot h}{j^*\cdot b\cdot k_h\cdot n\cdot k_c}(n\cdot k_c - k_h)\right\}\cdot\frac{(j^*-j)}{j^*} =$$

$$v_j^{el,m} - \sum_{i=j^*}^{\tilde{j}-1}\vartheta^i\cdot j\cdot b + \sum_{i=j^*}^{\tilde{j}}\left\{\frac{f^{pl,i}\cdot h}{i\cdot b\cdot k_h\cdot n\cdot k_c}(n\cdot k_c - k_h)\right\}\cdot\frac{(i-j)}{i} \quad (274)$$

Failure mechanism V is characterized by the failure in vertical joints in kinematic mode j^* attained prior the yielding of the hold-down as expressed in Equation (275). $f'^{\,pl,\hat{j}}$ is defined as the increase in force attained from the point where panel j^* reattaches with ground and is expressed in Equation (278). Equation (276) shows that the ultimate displacement of the vertical joint in failure mechanism V is bounded by the deformation in vertical joint achieving kinematic mode j^* and the displacement resulting the yield in the next vertical joint, j^*-1, This is expressed through the following two conditions:

$$d_{y,h} > \frac{1}{k_h}\cdot\left[\left(\frac{R_{w,c}^{el,\tilde{j}}\cdot h}{b} - \frac{q\cdot b\cdot m\cdot\tilde{j}}{2}\right)\cdot\frac{\tilde{j}\cdot k_h}{(\tilde{j}+m\cdot\tilde{j}-m)\cdot k_h+(m-\tilde{j})\cdot n\cdot k_c} + \sum_{j=\hat{j}+1}^{\tilde{j}}\frac{f^{pl,j}\cdot h}{b\cdot j} + \frac{f'^{\,pl,\hat{j}}\cdot h}{b\cdot\hat{j}}\right] \quad (275)^{A}$$

$$\frac{b}{h}\cdot\Delta_{h,t}^{pl,j^*+1,k} < d_{u,c} < \frac{b}{h}\cdot\Delta_{h,t}^{pl,j^*} \quad (276)$$

If both conditions (275) and (276) are met, j^* becomes associated with the final kinematic mode in the plastic state, $\hat{j}$ as presented in Figure 5-22.

The plastic strength for failure mechanism V is calculated by adding the elastic strength, the increase of force required fully develop kinematic mode $j^* = [\tilde{j}, \hat{j}+1]$ and the increase of force in kinematic mode $\hat{\jmath}$ governed by the failure in vertical joint. The plastic strength associated with kinematic mode $\hat{\jmath}$ resulting in the failure of the vertical joint is presented in Equation (277).

$$R_w^{pl,V} = F_t^{pl,j^*+1} + f'^{\,pl,\hat{\jmath}} = R_{w,c}^{el,\tilde{\jmath}} + \sum_{j=\hat{\jmath}+1}^{\tilde{\jmath}} f^{pl,\tilde{\jmath}} + f'^{\,pl,\hat{\jmath}} \quad (277)$$

Where $f'^{\,pl,\hat{\jmath}}$ is the increase of force in kinematic mode $\hat{\jmath}$ governed by the rupture of vertical joints $\hat{\jmath}$ to $m-1$ and can be expressed from interpolation as:

$$f'^{\,pl,\hat{\jmath}} = k_H^{pl,\hat{\jmath}} \cdot \left(\frac{h}{b} \cdot d_{u,c} - \Delta_{h,t}^{pl,\hat{\jmath}+1,k}\right) \quad (278)$$

The lateral displacement of the wall is associated with the failure of the vertical joint and developed as:

$$\Delta_h^{u,V} = \Delta_h^{pl,V} = \frac{h}{b} \cdot d_{u,c} \quad (279)$$

Therefore, the ductility is:

$$\mu_w{}^V = \frac{\Delta_h^{u,III}}{\Delta_h^{el}} \quad (280)$$

Failure mechanisms VI and VII occurs when the hold-down yield in kinematic mode j^* prior the failure of the vertical joints as expressed in Equation (281). The wall displacement related to the yielding of hold-down, $\Delta_h^{pl,VI,VII}$, can be found in Equation (204). Equation (282) ensures that the yielding displacement of the hold-down in failure mechanism VI and VII is bounded by the deformation to fully develop kinematic mode $j^* + 1$ and j^*.

$$d_{u,c} > \frac{b}{h} \cdot \Delta_h^{pl,VI,VII} \quad (281)$$

$$\frac{1}{k_h}\cdot\left[\left(\frac{R_{w,c}^{el,\tilde{\jmath}}\cdot h}{b}-\frac{q\cdot b\cdot m\cdot \tilde{\jmath}}{2}\right)\cdot\frac{\tilde{\jmath}\cdot k_h}{(\tilde{\jmath}+m\cdot\tilde{\jmath}-m)\cdot k_h+(m-\tilde{\jmath})\cdot n\cdot k_c}+\sum_{j=j^*+1}^{\tilde{\jmath}}\frac{f^{pl,j}\cdot h}{b\cdot j}\right] < d_{y,h} < \frac{1}{k_h}\cdot\left[\left(\frac{R_{w,c}^{el,\tilde{\jmath}}\cdot h}{b}-\frac{q\cdot b\cdot m\cdot \tilde{\jmath}}{2}\right)\cdot\frac{\tilde{\jmath}\cdot k_h}{(\tilde{\jmath}+m\cdot\tilde{\jmath}-m)\cdot k_h+(m-\tilde{\jmath})\cdot n\cdot k_c}+\sum_{j=j^*}^{\tilde{\jmath}}\frac{f^{pl,j}\cdot h}{b\cdot j}\right] \quad (282)^{A}$$

If both conditions (281) and (282) are met, j^* becomes associated with the final kinematic mode in the plastic state, $\hat{\jmath}$ as presented in Figure 5-22.

The plastic strength for failure mechanism VI and VII is calculated by adding the elastic strength, the increase of force required fully develop kinematic mode $j^* = [m-1, \hat{\jmath}+1]$ and the increase of force in kinematic mode $\hat{\jmath}$ governed by the yielding of the hold-down.

$$R_w^{pl,VI,VII} = F_t^{pl,\hat{\jmath}+1} + f'^{\,pl,\hat{\jmath}} = R_{w,c}^{el,\tilde{\jmath}} + \sum_{j=\hat{\jmath}+1}^{\tilde{\jmath}} f^{pl,\tilde{\jmath}} + f'^{\,pl,\hat{\jmath}} \quad (283)$$

Where $f'^{\,pl,\hat{\jmath}}$ is the increase of force in kinematic mode $\hat{\jmath}$ governed by the yielding of the hold-down and has been developed from interpolation as:

$$f'^{\,pl,\hat{\jmath}} = \hat{\jmath}\cdot\left[\frac{b}{h}\left(r_h-\frac{\tilde{\jmath}\cdot k_h}{(\tilde{\jmath}+m\cdot\tilde{\jmath}-m)\cdot k_h+(m-\tilde{\jmath})\cdot n\cdot k_c}\cdot\left(\frac{R_{w,c}^{el,\tilde{\jmath}}\cdot h}{b}-\frac{q\cdot b\cdot m\cdot\tilde{\jmath}}{2}\right)\right)-\sum_{j=\hat{\jmath}+1}^{\tilde{\jmath}}\frac{f^{pl,j}}{j}\right] \quad (284)^{A}$$

The plastic displacement of the wall in failure mechanism VI and VII is the sum of the lateral displacement of the wall in elastic state, the incremental displacement related to previous panel drop associated with kinematic modes $\tilde{\jmath}-1$ to $\hat{\jmath}+1$, the incremental displacement related to the full development of the previous kinematic modes $\tilde{\jmath}$ to $\hat{\jmath}+1$ and, the incremental displacement related to kinematic mode j^* governed by the hold-down yield. The expression is shown in Equation (285).

$$\Delta_h^{pl,VI,VII} = \Delta_{h,t}^{pl,\hat{\jmath}+1,k} + \frac{f'^{\,pl,\hat{\jmath}}}{k_H^{pl,\hat{\jmath}}} = \Delta_h^{el} + \sum_{j=j^*+1}^{\tilde{\jmath}-1}\delta_{h,t}^{pl,j} + \sum_{j=\hat{\jmath}+1}^{\tilde{\jmath}}\frac{f^{pl,j}}{k_H^{pl,j}} \quad (285)$$

The ultimate displacements for failure mechanism VI and VII are characterized by failure in the vertical joints and the hold-down, respectively. It can be expressed as the ultimate displacement of the vertical joint and the wall panel aspect ratio for Equation (286). Equation (287) is developed as the sum of the plastic lateral displacement and the allowable increase of lateral displacement governed by the failure of the hold-down.

$$\Delta_h^{u,IV} = \frac{h}{b} \cdot d_{u,c} \quad (286)$$

$$\Delta_h^{u,V} = \Delta_h^{pl,V} + \frac{h}{\hat{j} \cdot b} \cdot (d_{u,h} - d_{y,h}) \quad (287)$$

Therefore, the ductility for mode of failure VI and VII are:

$$\mu_w{}^{IV} = \frac{\Delta_h^{u,IV}}{\Delta_h^{el}} \quad (288)$$

$$\mu_w{}^{V} = \frac{\Delta_h^{u,V}}{\Delta_h^{el}} \quad (289)$$

5.4.4 Plastic CP Behaviour Region, Failure Mechanism VII, IX, X

As can be seen in Figure 5-22, CP^{PL} is defined by the limits represented by the reattachment of panel 1 with the ground and the yielding of the hold-down until failure is achieved.

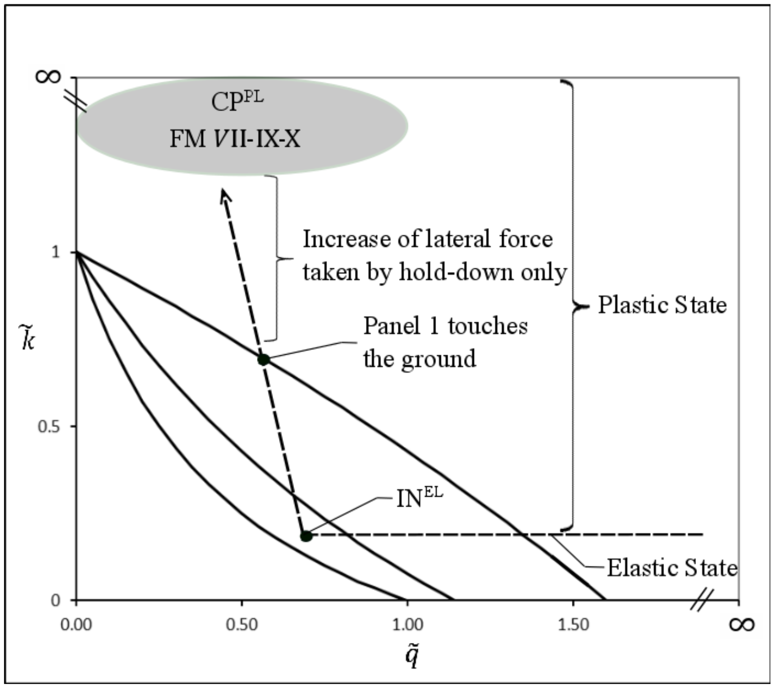

Figure 5-22: CP behaviour Region of Case IN^{EL}-CP^{PL}

Kinematic mode 1 is only reached when the first panel reattaches with ground. The last panel not in contact with ground, 1, will drop from the adjusted value under the increase of lateral force resulting the yielding of joint 1 in the plastic state in kinematic mode 2, $v'^{\,pl,j^*=2}_{j=1}$. A variation of the angle of rotation would be attained, $\vartheta'^{\,j^*=1}$, since hold-down elongation remains the same.

$$\vartheta'^{\,j^*=1} = \frac{v'^{\,pl,j^*=2}_{j=1}}{b} \quad (290)$$

Where

$$v'^{\,pl,j^*=2}_{j=1} = v^{el,m}_{j} - \sum_{i=2}^{\tilde{j}-1} \vartheta^{i} \cdot j \cdot b + \sum_{i=2}^{\tilde{j}} \left\{ \frac{f^{pl,i} \cdot h}{i \cdot b \cdot k_h \cdot n \cdot k_c} (n \cdot k_c - k_h) \right\} \cdot \frac{(i-j)}{i} \quad (291)$$

The reattachment of panel 1 has the effect of increasing the horizontal displacement of the wall without any increase in force. The increase in displacement between kinematic mode 2 and 1 can be expressed as:

$$\delta_{h,t}^{pl,2} = \vartheta'^{\,j^*=1} \cdot h \quad (292)$$

The total displacement of the wall when panel 1 enters in contact with the ground is the sum of the elastic displacement, the incremental displacement related to previous panel drop associated with kinematic modes $\tilde{j}-1$ to 2 and the incremental displacement to fully developed the previous kinematic modes $\tilde{j}$ to 2. This displacement is still under the previous transitional force, $F_t^{pl,2}$, and the expression is shown in Equation (293).

$$\Delta_{h,t}^{pl,2,k} = \Delta_{h,t}^{pl,2} + \delta_{h,t}^{pl,2} = \Delta_h^{el} + \sum_{j=2}^{\tilde{j}-1} \delta_{h,t}^{pl,j} + \sum_{j=2}^{\tilde{j}} \frac{f^{pl,j}}{k_H^{pl,j}} \quad (293)$$

The failure mechanism for which the first vertical joint would yield during the panel's drop is covered in 5.4.3 for Equations (262) through (266).

At the point of reattachment of panel 1 with ground, the wall is considered to only consist of 1 panel with only the hold-down to resist additional lateral force. At this point, the total force in the hold-down consists of the elastic strength contribution for a system with $\tilde{j}$ panels, $R_{w,c}^{el,\tilde{j}}$ (obtained from Eq.156), and the increase of lateral force to yield the previous vertical joint j for $m-2 \leq j \leq 2$ in a system with j panels, $f^{pl,j}$. Equation (294) determine the allowable increase of tension force in the hold-down before achieving the hold-down strength, r_h, according to the equations established in Casagrande et al. (2017).

$$t^{pl,j^*=1} = r_h - \left[\left(\frac{R_{w,c}^{el,\tilde{j}} \cdot h}{b} - \frac{q \cdot b \cdot m \cdot \tilde{j}}{2} \right) \cdot \frac{\tilde{j} \cdot k_h}{(j^*+m \cdot j^*-m) \cdot k_h + (m-j^*) \cdot n \cdot k_c} + \sum_{j=2}^{\tilde{j}} \frac{f^{pl,j} \cdot h}{b \cdot j} \right] \quad (294)^{A}$$

Where, for the calculation of forces in the hold-down, the effect of elastic strength must consider the wall in IN behaviour as shown in Equation (295) according to Casagrande et al. (2017). However, the effect of all other increase of lateral forces on the hold-down can be calculated according to an SW behaviour with j number of panels for $\tilde{j}-1 \leq j \leq 2$.

$$T^{el,\tilde{j}} = \left(\frac{R_{w,c}^{el,\tilde{j}} \cdot h}{b} - \frac{q \cdot b \cdot m \cdot \tilde{j}}{2}\right) \cdot \frac{\tilde{j} \cdot k_h}{(\tilde{j}+m \cdot \tilde{j}-m) \cdot k_h+(m-\tilde{j}) \cdot n \cdot k_c} \quad (295)$$

Therefore, the increase of lateral force leading to the yielding of the hold-down is expressed as:

$$f^{pl,1} = \frac{b}{h} \cdot r_h - \left[\left(R_{w,c}^{el,\tilde{j}} - \frac{q \cdot b^2 \cdot m \cdot \tilde{j}}{2 \cdot h}\right) \cdot \frac{\tilde{j} \cdot k_h}{(j^*+m \cdot j^*-m) \cdot k_h+(m-j^*) \cdot n \cdot k_c} + \sum_{j=2}^{\tilde{j}} \frac{f^{pl,j}}{j}\right] \quad (296)^{A}$$

The plastic strength of the wall, leading to failure mechanism IX and X is calculated as the sum of the elastic strength, the increase of force required fully develop kinematic mode $j^* = [\tilde{j}, 2]$ and the increase of force in kinematic mode 1 governed by the yielding of the hold-down.

$$R_w^{pl,IX,X} = F_t^{pl,2} + f^{pl,1} = R_{w,c}^{el,\tilde{j}} + \sum_{j=2}^{\tilde{j}} f^{pl,\tilde{j}} + f^{pl,1} = \frac{b}{h}\left(r_h + r_c \cdot (m-1) \cdot n + \frac{q \cdot m \cdot b}{2}\right)$$

(297)

The total displacement of the wall when achieve its plastic strength is the sum of the elastic displacement, the incremental displacement related to previous panel drop associated with kinematic modes $\tilde{j}-1$ to 2 and the incremental displacement to fully developed the previous kinematic modes $\tilde{j}$ to 2 and now including the increase of force that resulted in the hold-down yield.

$$\Delta_h^{pl} = \Delta_{h,t}^{pl,2,k} + \frac{f^{pl,1}}{k_H^{pl,1}} = \Delta_h^{el} + \sum_{j=2}^{\tilde{j}-1} \delta_{h,t}^{pl,j} + \sum_{j=1}^{\tilde{j}} \frac{f^{pl,j}}{k_H^{pl,j}} \quad (298)$$

Where the equivalent lateral stiffness of the wall is calculated using 1 panel:

$$k_H^{pl,1} = \frac{k_h \cdot b^2}{h^2} \quad (299)$$

Failure mechanism $VIII$ is characterized by the failure in vertical joints previously yielded in kinematic mode 1 attained prior the yielding of the hold-down as expressed in Equation (300). $f'^{\,pl,\hat{j}}$ is defined as the increase in force attained from the point where panel 1 reattaches with ground and is expressed in Equation (303). Equation (301) shows that the ultimate displacement of the vertical joint in failure mechanism $VIII$ is bounded by the transitional deformation in the vertical joints to achieve kinematic mode 1and the displacement resulting the yield in the hold-down. This is expressed through the following two conditions:

$$d_{y,h} > \frac{1}{k_h} \cdot \left[\left(\frac{R_{w,c}^{el,\tilde{j}} \cdot h}{b} - \frac{q \cdot b \cdot m \cdot \tilde{j}}{2} \right) \cdot \frac{\tilde{j} \cdot k_h}{(\tilde{j} + m \cdot \tilde{j} - m) \cdot k_h + (m - \tilde{j}) \cdot n \cdot k_c} + \sum_{j=2}^{\tilde{j}} \frac{f^{pl,j} \cdot h}{b \cdot j} + \frac{f'^{\,pl,1} \cdot h}{b} \right] \quad (300)^{A}$$

$$\frac{b}{h} \cdot \Delta_{h,t}^{pl,2,k} < d_{u,c} < \frac{b}{h} \cdot \Delta_h^{pl} \quad (301)$$

If both conditions (300) and (301) are met, then, kinematic mode 1 becomes associated with the final kinematic mode in the plastic state, $\hat{j}$.

The plastic strength for failure mechanism $VIII$ is calculated by adding the elastic strength, the increase of force required fully develop kinematic mode $j^* = [\tilde{j}, 2]$ and the increase of force in kinematic mode 1 governed by the failure in vertical joint. The plastic strength associated with kinematic mode 1 with a failure of the vertical joint is presented in Equation (302).

$$R_w^{pl,VIII} = F_t^{pl,2} + f'^{\,pl,1} = R_{w,c}^{el,\tilde{j}} + \sum_{j=2}^{\tilde{j}} f^{pl,\tilde{j}} + f'^{\,pl,1} \quad (302)$$

$f'^{pl,1}$ is the increase of force in kinematic mode 1 governed by the rupture of vertical joint and can be expressed from interpolation as:

$$f'^{pl,1} = k_H^{pl,1} \cdot \left(\frac{h}{b} \cdot d_{u,c} - \Delta_{h,t}^{pl,2,k}\right) \quad (303)$$

The lateral displacement of the wall is associated with the failure of the vertical joint and developed as:

$$\Delta_h^{u,VIII} = \frac{h}{b} \cdot d_{u,c} \quad (304)$$

The ductility takes the following form:

$$\mu_w{}^{VIII} = \frac{\Delta_h^{u,VI}}{\Delta_h^{el}} \quad (305)$$

Failure mechanism IX and X are characterized by the yielding of the hold-down prior the failure in vertical joint as expressed in Equation (306). Equation (307) shows that the yielding displacement of the hold-down in IX and X should commence kinematic mode 1. This is expressed through the following two conditions:

$$d_{u,c} > \frac{b}{h} \cdot \Delta_h^{pl} \quad (306)$$

$$d_{y,h} > \frac{1}{k_h} \cdot \left[\left(\frac{R_{w,c}^{el,\tilde{j}} \cdot h}{b} - \frac{q \cdot b \cdot m \cdot \tilde{j}}{2}\right) \cdot \frac{\tilde{j} \cdot k_h}{(\tilde{j} + m \cdot \tilde{j} - m) \cdot k_h + (m - \tilde{j}) \cdot n \cdot k_c} + \sum_{j=2}^{\tilde{j}} \frac{f^{pl,j} \cdot h}{b \cdot j}\right] \quad (307)^{A}$$

If both conditions (306) and (307) are met, then, kinematic mode 1 becomes associated with the final kinematic mode in the plastic state, $\hat{j}$ and the wall achieve the plastic strength, R_w^{pl}, and the plastic displacement, Δ_h^{pl}, stated in Equation (297) and (298) respectively

The ultimate displacements for failure mechanism IX and X are characterized by failure in the vertical joints and in the hold-down, respectively. They are both expressed as the connectors ultimate displacement and the panel aspect ratio.

$$\Delta_h^{u,IX} = \frac{h}{b} \cdot d_{u,c} \quad (308)$$

$$\Delta_h^{u,X} = \frac{h}{b} \cdot d_{u,h} \quad (309)$$

Therefore, the ductility is presented for both failure mechanism as:

$$\mu_w{}^{IX} = \frac{\Delta_h^{u,IX}}{\Delta_h^{el}} \quad (310)$$

$$\mu_w{}^{X} = \frac{\Delta_h^{u,X}}{\Delta_h^{el}} \quad (311)$$

CHAPTER 6 - Validation of the Analytical Procedure by means of Numerical Modelling

A numerical model was developed using the commercially available software SAP2000 (Computers and Structures Inc., 2014) to validate the proposed analytical procedure reported in Chapter 4 and 5. The rocking behaviour of 3- and 4-panel CLT shearwalls was analysed for different properties of connectors such as stiffness, strength, and ultimate displacements and the results were compared with those obtained using the proposed model for different failure mechanisms. The force-displacement curves obtained from the numerical model were developed using displacement controlled non-linear static analysis, by first applying the vertical load followed by subjecting the wall to a horizontal displacement.

The CLT panels were modelled using perfectly rigid shell elements (i.e. the stiffness of the shell element has been increased with modifier to neglect the deformation in panels) with restricted degree of freedom making it behave as a membrane element. The panels were connected to each other with 2-dimensional spring element representing the fasteners in the vertical joints. The pattern of shell elements showed in Figure 6-1 has been developed to allow the 2-dimensional spring element to be located with the appropriate spacing (i.e spacing between fasteners) and assign gap-element throughout the panel width.

The effect of sliding was accounted for by modelling horizontal joint restraint at bottom right corner of the wall and thereby simulating the effect of angle brackets. A joint constraint was applied on the top points of the panels to simulate the diaphragm effect. The bottom face of the CLT panels was restrained by means of vertical gap-elements with a high axial compression stiffness (set to 100 kN/m) that allows uplift motion. The hold-down connection was modelled with a non-linear spring element with a specified stiffness for tensile and a high axial stiffness on the compressive side (i.e. to behave like gap element with 100 kN/m). All model components are presented in Figure 6-1.

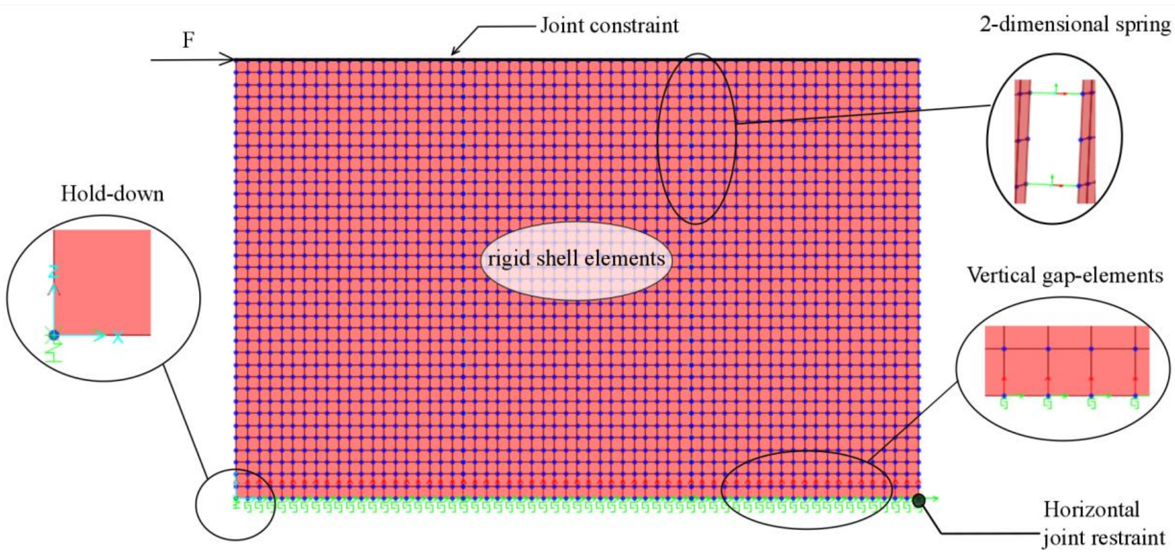

Figure 6-1: Modelling of a 3-panel wall

The general behaviour assigned on hold-down and fasteners for the numerical analysis is presented in Figure 6-2.

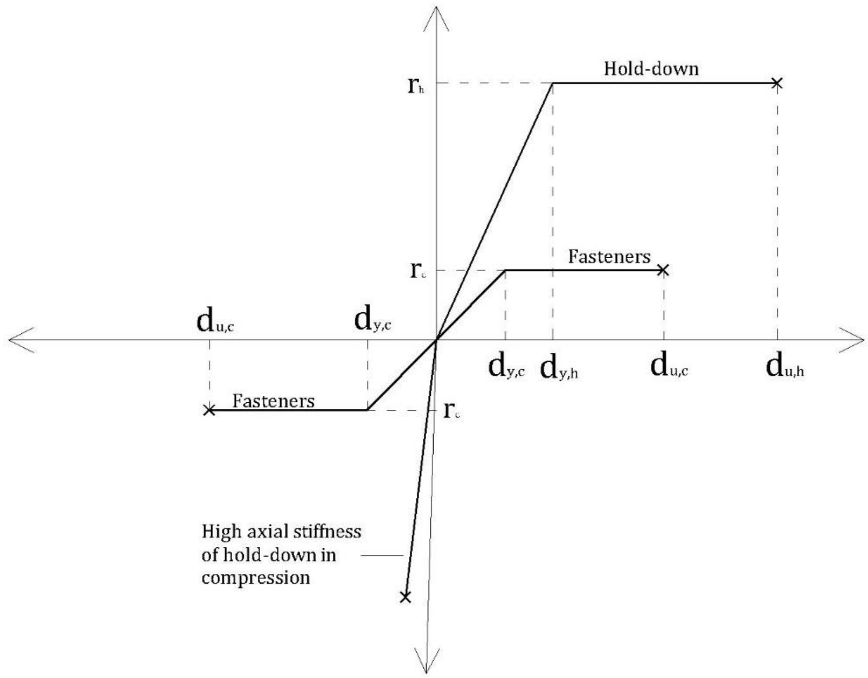

Figure 6-2: Behaviour of Connectors Modelled

The height h and the panel length b of the wall were assumed to be 2.7 m and 1.4 m, respectively. The fastener spacing in the panel-to-panel vertical joint, s, was selected as 150 mm (n=18). Different values of vertical load q are applied on the walls depending on the case under consideration.

Table 6-1 presents the different cases used in the comparison for the validation of the SW behaviour. This includes kinematic paths where the wall transition from SW, IN and CP behaviours in the elastic phase to SW in the plastic phase and include all the failure mechanisms within each path. Table 6-1 also presents the mechanical properties of hold-down and vertical-joint fasteners as well as the value of the vertical load q used in the comparison.

Table 6-1: Properties of connectors and variable for the modelling of cases achieving SW behaviour

Case	FM	*m*	Hold-down				Vertical joint				q [kN/m]
			K_h [kN/m]	r_h [kN]	$d_{y,h}$ [mm]	$d_{u,h}$ [mm]	k [kN/m]	r_c [kN]	$d_{y,c}$ [mm]	$d_{u,c}$ [mm]	
CP^{EL}-SW^{PL}	*I*	3	10000	10.0	1.00	2.00	700	5.0	7.14	20.00	15.0
	II	3	10000	40.0	4.00	20.00	700	4.0	5.71	15.00	40.0
	III	3	10000	40.0	4.00	15.00	700	4.0	5.71	20.00	40.0
	IV	3	10000	10.0	1.00	4.00	700	5.0	7.14	8.00	15.0
	V	3	10000	10.0	1.00	15.00	700	5.0	7.14	8.50	35.0
	VI	3	10000	10.0	1.00	15.00	700	5.0	7.14	12.00	35.0
	VII	3	10000	10.0	1.00	9.00	700	5.0	7.14	20.00	15.0
SW^{EL}-SW^{PL}	*I*	3	6000	40.0	6.67	23.33	700	14.0	20.00	30.00	5.0
IN^{EL}-SW^{PL}	*I*	3	6000	25.0	4.17	6.00	700	14.0	20.00	30.00	15.0
	II	3	2000	14.0	7.00	30.00	800	6.0	7.50	16.00	53.0
	III	3	2000	14.0	7.00	20.00	800	6.0	7.50	16.00	53.0
	IV	4	2000	25.0	12.50	16.50	700	8.5	12.14	16.00	40.0
	V	4	2000	25.0	12.50	35.00	700	8.5	12.14	13.50	40.0
	VI	4	2000	25.0	12.50	20.00	700	8.5	12.14	13.50	40.0
	VII	4	6000	25.0	4.17	12.00	700	14.0	20.00	30.00	15.0

Table 6-2 presents the comparison between the analytical procedure and the numerical model for all cases outlined in Table 6-1, for elastic and plastic strengths, elastic and plastic displacements as well as ultimate displacement.

Table 6-2: Comparative Results Between Analytical and Numerical Model for the Achievement of SW Behaviour

Case	FM	*Ratio between proposed Analytical Model and Numerical Analysis*				
		R_w^{el}	Δ_h^{el}	R_w^{pl}	Δ_h^{pl}	Δ_h^{u}
CP^{EL}-SW^{PL}	*I*	0.996	1.000	0.998	1.000	1.001
	II	0.997	1.001	0.995	0.995	0.992
	III	1.000	1.003	0.997	0.999	0.998
	IV	1.000	0.965	0.995	0.998	0.998
	V	0.993	0.990	0.996	0.999	0.997
	VI	0.996	1.000	0.997	0.995	0.998

	VII	0.991	0.995	0.992	0.989	0.996
SW^{EL}-SW^{PL}	*I*	0.989	0.991	0.989	0.991	0.997
IN^{EL}-SW^{PL}	*I*	1.004	1.003	0.995	0.992	0.992
	II	0.995	1.003	0.997	0.992	0.995
	III	1.003	0.996	0.997	0.982	0.992
	IV	0.997	0.996	0.994	0.997	0.997
	V	0.987	1.008	0.986	1.001	0.998
	VI	0.986	0.996	0.986	1.003	0.995
	VII	1.001	1.000	0.990	0.977	1.011

It can be seen from Table 6-2 that the maximum difference between the proposed model and the numerical analysis is 0.0305, which indicate the proposed model's suitability to express the wall behaviour for all possible failure mechanisms. Graphical examples of the model fit are also illustrated in Figure 6-3 for failure mechanism VII, VII and I for Case CP^{EL}-SW^{PL}, IN^{EL}-SW^{PL} and SW^{EL}-SW^{PL} respectively. Again, it can be seen that the behaviour obtained from the proposed analytical model matches almost perfectly with that obtained from the numerical analysis.

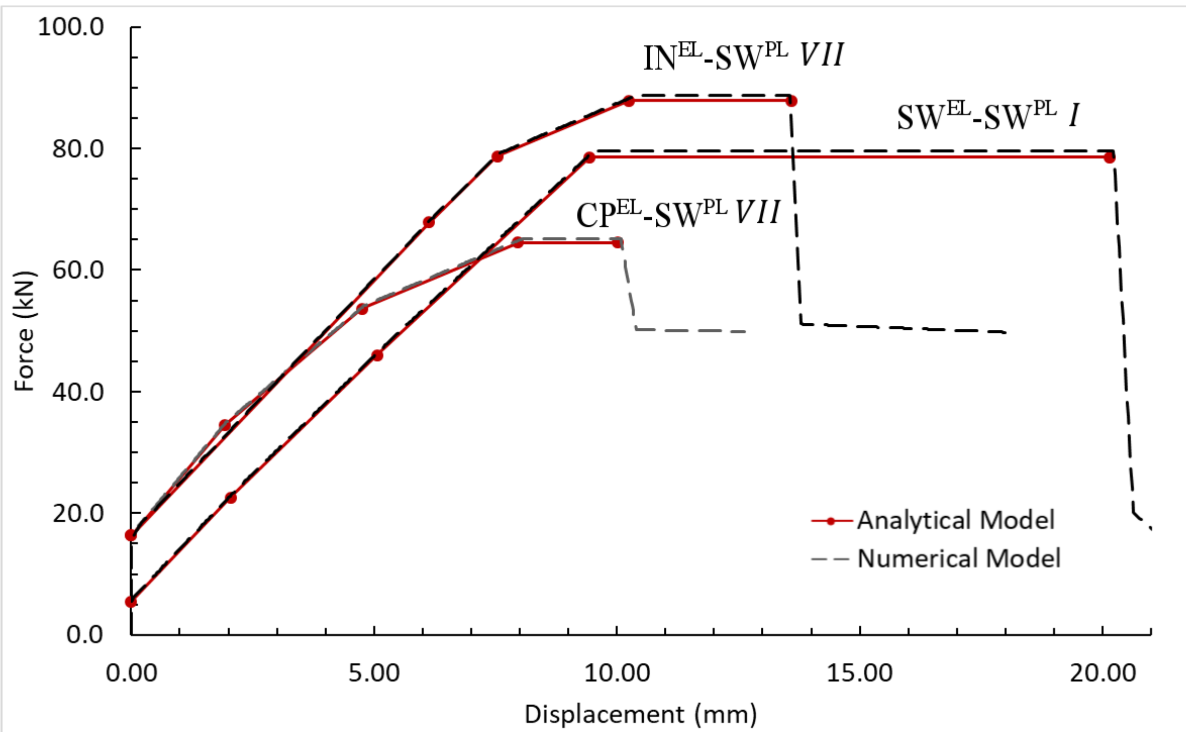

Figure 6-3: Comparison Between Numerical and Analytical Model in the Achievement of SW behaviour

Table 6-3 presents the different cases used in the comparison for the validation of the CP behaviour, and includes kinematic paths where the wall was in CP, IN and SW behaviours in the elastic phase. Table 6-4 presents the comparison between the analytical procedure and the numerical model for all cases outlined in Table 6-3.

Table 6-3: Properties of connectors and variable for the modelling of cases achieving CP behaviour

Case	FM	*m*	Hold-down				Vertical joint				q [kN/m]
			K_h [kN/m]	r_h [kN]	$d_{y,h}$ [mm]	$d_{u,h}$ [mm]	k [kN/m]	r_c [kN]	$d_{y,c}$ [mm]	$d_{u,c}$ [mm]	
$CP^{EL}CP^{PL}$	*I*	3	15000	100.0	6.67	12.00	700	2.0	2.86	5.00	8.0
	II	3	15000	100.0	6.67	15.00	700	2.0	2.86	7.78	8.0
	III	3	15000	100.0	6.67	11.93	700	2.0	2.86	15.00	8.0
$SW^{EL}CP^{PL}$	*I*	3	6000	100.0	16.67	20.00	700	5.0	7.14	8.50	8.0
	II	3	6000	100.0	16.67	20.00	700	5.0	7.14	12.00	8.0
	III	3	6000	100.0	16.67	20.00	700	5.0	7.14	9.30	8.0
	IV	3	6000	70.0	11.67	20.00	700	5.0	7.14	12.00	8.0
	V	3	6000	70.0	11.67	20.00	700	5.0	7.14	13.50	8.0
	VI	3	6000	100.0	16.67	20.00	700	5.0	7.14	14.00	8.0
	VII	3	6000	100.0	16.67	20.00	700	5.0	7.14	18.00	8.0
	VIII	3	6000	100.0	16.67	18.00	700	5.0	7.14	20.00	8.0
$IN^{EL}CP^{PL}$	*I*	4	6000	150.0	25.00	30.00	700	8.0	11.43	12.20	15.0
	II	4	6000	95.0	15.83	20.00	700	8.0	11.43	12.50	15.0
	III	4	6000	95.0	15.83	20.00	700	8.0	11.43	14.00	15.0
	IV	4	6000	150.0	25.00	30.00	700	8.0	11.43	13.00	15.0
	V	4	5500	150.0	27.27	30.00	700	8.0	11.43	14.50	15.0
	VI	4	6000	110.0	18.33	30.00	700	8.0	11.43	15.00	15.0
	VII	4	6000	110.0	18.33	20.00	700	8.0	11.43	16.00	15.0
	VIII	4	6000	150.0	25.00	30.00	700	8.0	11.43	24.00	15.0
	IX	4	6000	150.0	25.00	30.00	700	8.0	11.43	26.00	15.0
	X	4	6000	150.0	25.00	28.00	700	8.0	11.43	30.00	15.0

Table 6-4: Comparative Results Between Analytical and Numerical Model for the Achievement of CP Behaviour

Cases	FM	*Ratio between the proposed Analytical Model and Numerical Analysis*				
		R_w^{el}	Δ_h^{el}	R_w^{pl}	Δ_h^{pl}	Δ_h^{u}
$CP^{EL}CP^{PL}$	*I*	0.997	1.000	0.995	0.997	0.997
	II	0.987	0.980	0.995	0.992	0.996
	III	1.003	1.009	0.994	0.992	1.000
$SW^{EL}CP^{PL}$	*I*	1.000	0.999	1.000	1.011	1.011
	II	1.000	1.000	1.000	0.995	0.993
	III	1.001	1.001	0.999	0.998	0.998

	IV	0.998	1.002	0.999	0.982	0.991
	V	1.001	1.004	0.999	0.991	0.992
	VI	1.001	0.998	1.007	0.997	0.997
	VII	1.001	0.997	0.998	0.996	0.997
	VIII	1.001	0.998	0.998	1.000	0.997
$IN^{EL}CP^{PL}$	*I*	1.002	1.002	1.003	0.999	0.999
	II	1.001	0.997	0.995	0.997	0.994
	III	0.992	0.991	0.995	0.994	1.000
	IV	1.002	1.005	1.000	0.997	0.996
	V	0.998	1.000	1.007	0.999	0.999
	VI	0.998	1.000	1.002	0.992	0.998
	VII	0.998	1.000	0.997	0.995	0.987
	VIII	0.996	0.999	1.002	0.998	0.998
	XI	0.992	0.993	1.000	1.001	0.998
	XI	1.001	1.005	1.002	1.000	0.998

Again, it can be observed from Table 6-4 the match between the proposed analytical model and the numerical analysis is reasonable, with maximum difference of 0.020. Graphical examples of the model fit are also illustrated in Figure 6-4 failure mechanism III, X and $VIII$ of Case CP^{EL}-CP^{PL}, IN^{EL}-CP^{PL} and SW^{EL}-CP^{PL} respectively.

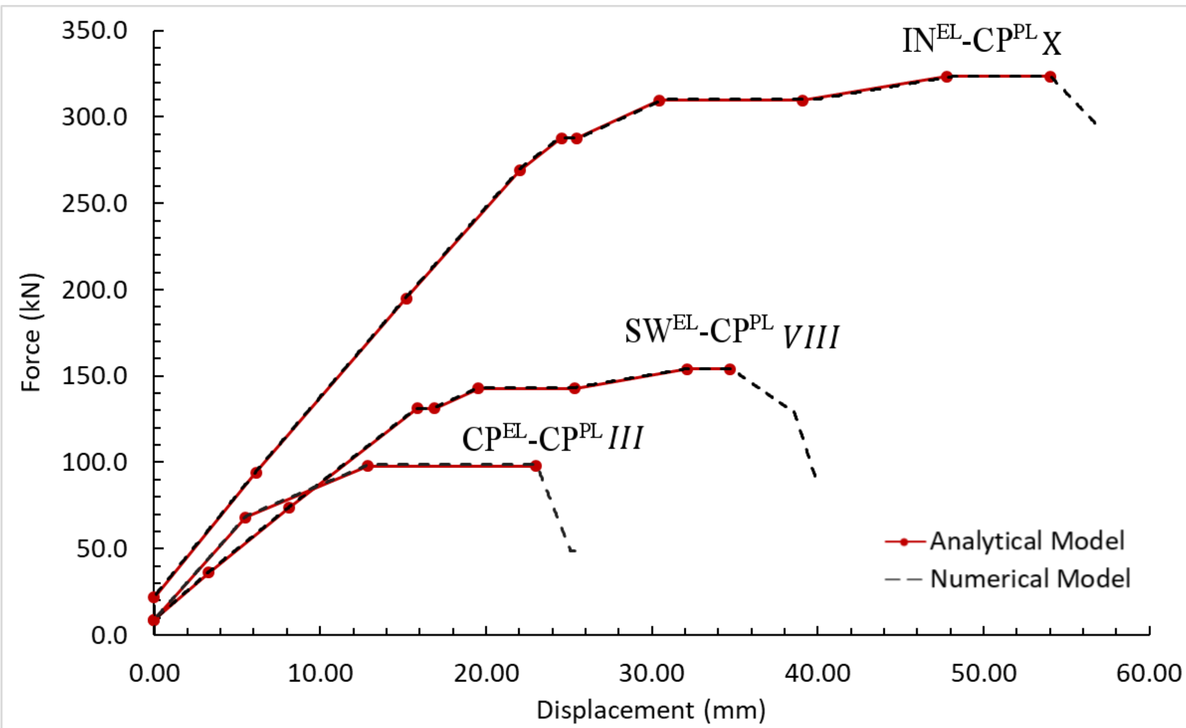

Figure 6-4: Comparison Between Numerical and Analytical Model in the Achievement of CP behaviour

It can be concluded that the analytical model is capable of predicting the behaviour of multi-panel shearwalls with reasonable accuracy. The slight difference between the analytical and numerical models can be attributed to the fact that the numerical model is an approximation and to obtain exact solution, an infinite number of increments during the non-linear static analysis would have been required. Increasing analysis steps were not deemed necessary when balancing the time to perform the analysis with the accuracy required from an engineering perspective, especially for a material with significant variability in properties like wood. The assumption of small angle may also contribute as a source of error under larger lateral displacement.

CHAPTER 7 - Code Implications

7.1 Current design provisions

7.1.1 General design concepts

The current edition of the Canadian timber design standard (CSA 2014) has recently adopted design provisions for CLT shearwalls and diaphragms. The provisions for CLT shearwalls apply to platform-type constructions not exceeding 30 m in height (i.e. balloon framing is excluded from the design standard) and wall segments with aspect ratios (height-to-length) between 1:1 and 4:1. The standard also contains height limitation for seismic design. A height limit of 20 m is imposed for buildings in high seismic zones, where $I_E F_a S_a(0.2) > 0.75$.

The provisions in CSA O86 require that the shear resistance of CLT shearwalls and diaphragms be governed by their boundary connections, where each panel is assumed to act as a rigid body. The capacity is required to be analysed using suitable methods of mechanics. There is currently no established analytical procedures in the design standard that provides detailing for multi-panel CLT shearwalls. There is also no mention of the effect of gravity load on the shearwall behaviour. Based on the analytical model developed in the current study, a simplified analytical procedure for the purpose of design that incorporates well-defined kinematic modes and includes the effect of gravity loads is proposed. The design requirements are presented and illustrated through a numerical example in Section 7.3.

7.1.2 Seismic design considerations for CLT structures

The ductility (R_d) and over-strength (R_o) factors for CLT shearwalls are provided in the standard and take on the values of 2.0 and 1.5, respectively. The values are applicable if the energy is dissipated through moderately ductile connections, following the capacity design principles, and assuming that the wall panels act in rocking or in combination of rocking and sliding. CLT panels with aspect ratios (height-to-length) less than 1:1 or acting in sliding only can be designed with R_d R_o = 1.3, which is the minimum specified in the NBCC for a non-energy dissipative systems. Also, type 4 or 5 irregularities, as defined in the 2015 NBCC (in-plane discontinuity or out-of-plane offset), are not allowed in buildings with CLT as the seismic force resisting system (SFRS).

Following the principle of capacity based design, dissipative and non-dissipative connectors are identified. The design standard CSA O86 requires that inelastic deformations and energy dissipation occur in vertical joints, shear connections between the shearwalls and the foundations or floors underneath, and hold-down connections, except for continuous steel rods. For a connection to be considered as energy dissipative the following requirements need to be satisfied according to the CSA O86 standard (2014):

a) connections shall be designed so that a yielding mode governs the resistance;
b) connections shall be at least moderately ductile in the directions of the assumed rigid body motions of CLT panels; and
c) connections shall possess sufficient deformation capacity to allow for the CLT panels to develop their assumed deformation behaviour, such as rocking, sliding, or combination thereof.

Non-dissipative connections are designed to remain elastic under the force and displacement demands that are induced in them when the energy-dissipative connections reach the 95th percentile of their ultimate resistance or target displacement, in accordance with engineering principles of equilibrium and displacement compatibility.

Finally, deflections are determined using established methods of mechanics that are required to include panel sliding, rocking, and deformation of supports.

7.2 Design examples based on current design approaches

7.2.1 Determining the kinematic mode based on the analytical model

The examples outlined in this section deal with a two-panel wall due to the feasibility of implementing static equilibrium considerations using hand-calculations. As discussed in Chapters 4 and 5, only coupled-panel (CP) and single wall (SW) behaviours can be attained for a two-panel wall. The wall's final kinematic mode depends on the stiffness ratio of panel joints and hold-down as well as the ratio of vertical to lateral loads. Plotting the dimensionless stiffness ratio $\widetilde{k} = \frac{k_h}{n \cdot k_c}$ as a function of the dimensionless load ratio $\tilde{q} = \frac{q \cdot B^2}{2 \cdot F \cdot h}$ for a two-panel wall, the diagram in Figure 6-1 can be obtained. Depending on the relative stiffness between the hold-down and the panel joint, the value for the dimensionless stiffness ratio may be greater or smaller than unity. The implication of that will be discussed in the examples in Section 7.2.3.

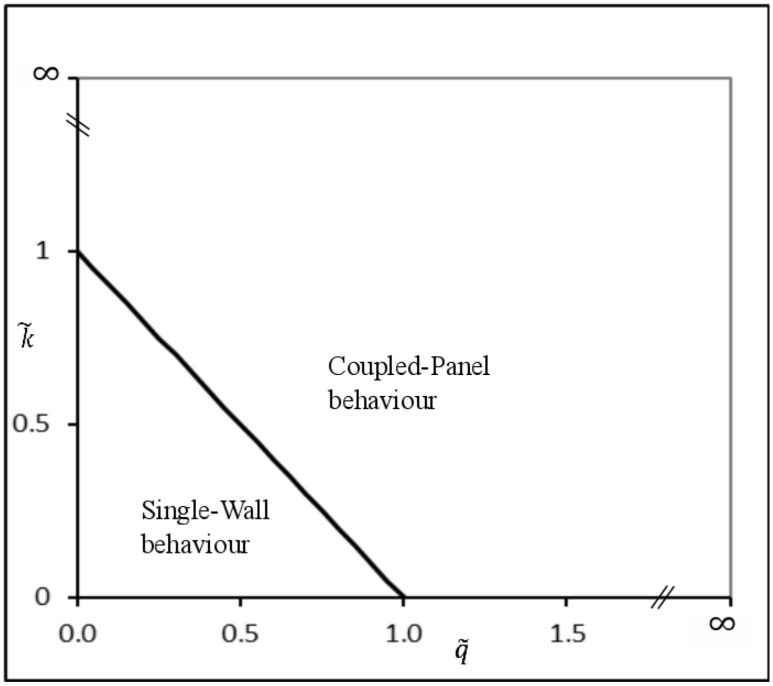

Figure 7-1: Kinematic Behaviour for m=2

7.2.2 Static equilibrium considerations

Due to the lack of analytical procedures, designers would resort to either complex models, where the CLT panel is assumed to be a rigid solid and the connections are considered as linear or non-linear springs, or simplified analysis methods such as static equilibrium.

The examples in this section investigate the validity of using static equilibrium to analyze and design a two-panel CLT shearwall and highlight the need for the analytical procedure. One limitation in this procedure is that the connections are assumed as rigid-plastic (the connection has infinite stiffness and infinite ductility) and as such several of the design requirements outlined in Section 7.1 cannot be checked or met. Another limitation is that the hold-down is assumed to resist the uplift force and the angle brackets contribute only to horizontal shear resistance. This is consistent with assumptions made in light frame wood shearwalls and also with observations made in experimental research studies (e.g. Popovski and Gavric 2016).

The two panels are assumed to have panel width b and height h. The panels are loaded with uniformly distributed gravity load q and a concentrated lateral load, F. The tensile resistance of the hold-down bracket and the vertical joints take on the values of r_h and r_c, respectively. n fasteners are assumed in the panel-to-panel connection.

For the SW behaviour the static equilibrium can be written for the case shown in Figure 7-2:

$$\sum M_o = q \cdot B \cdot \frac{B}{2} + T \cdot B - F \cdot h = 0$$

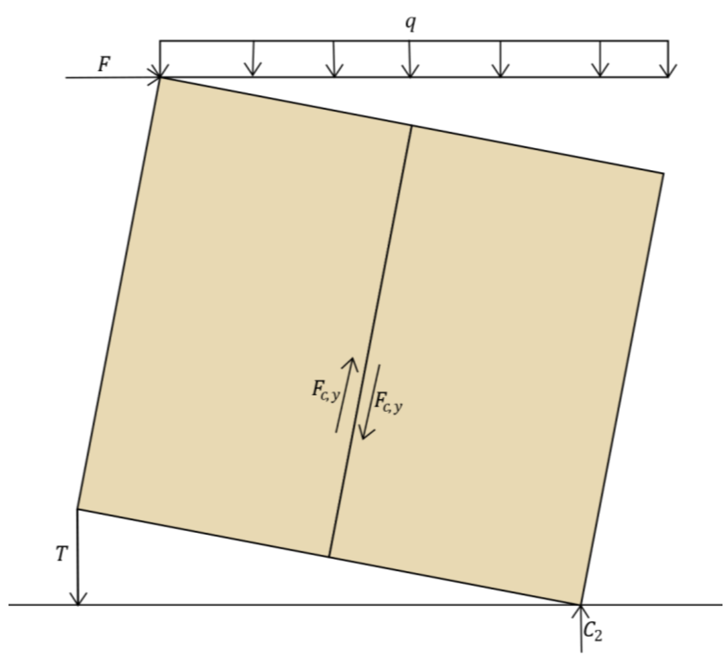

Figure 7-2: Static Equilibrium for 2-Panel Wall in SW Behaviour

The tension force in the hold-down can be expressed as:

$$T = \frac{F \cdot h}{B} - \frac{q \cdot B}{2}$$

Assuming that the hold-down attains its strength, r_h, the maximum lateral force acting on the wall is developed as:

$$F = \frac{r_h \cdot B}{h} + \frac{q \cdot B^2}{2h}$$

Performing the static equilibrium at the level of a single panel, the force acting in the vertical joint $F_{c,y}$ can be calculated as:

$$\sum F_y = F_{c,y} - q \cdot b - T = 0 \rightarrow F_{c,y} = q \cdot b + T$$

$$F_{c,y} = qb + \frac{F \cdot h}{B} - \frac{q \cdot B}{2} = \frac{F \cdot h}{B}$$

Rewriting the equation as function of the strength of a single vertical joint, r_c and the number of fasteners n in the vertical joint to determine the maximum lateral force F that can be applied on the wall results the following:

$$F_{c,y} = r_c \cdot n = \frac{F \cdot h}{B} \rightarrow F = \frac{r_c \cdot n \cdot B}{h}$$

The lateral force acting on the wall is taken as the minimum between the wall strength related to panel joint or hold-down:

$$R_w = Min\left(\frac{r_c \cdot n \cdot B}{h}, \frac{r_h \cdot B}{h} + \frac{q \cdot B^2}{2h}\right)$$

For the CP behaviour, the equilibrium equation can be written as:

$$\sum M_o = T \cdot 2 \cdot b + 2 \cdot q \cdot b^2 - F \cdot h - C_1 \cdot b = 0$$

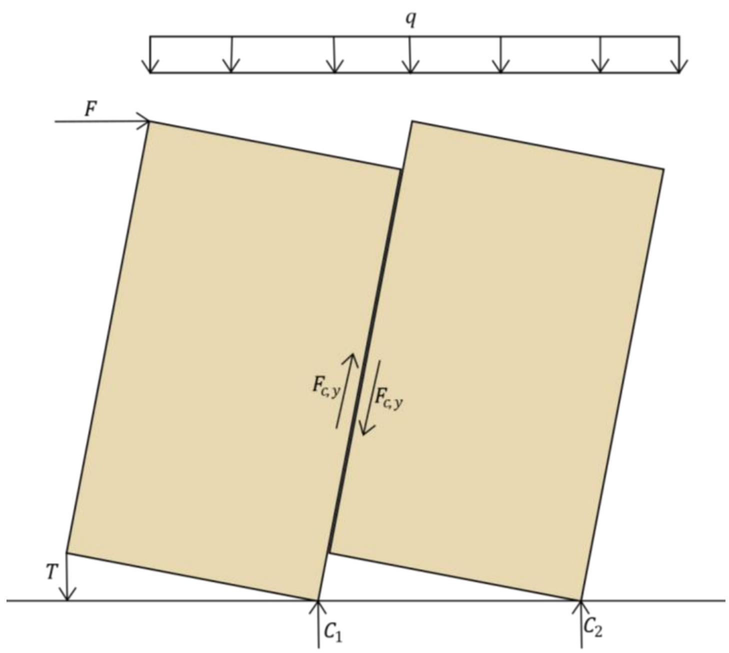

Figure 7-3:Static Equilibrium for 2-Panel Wall in CP Behaviour

The lateral force can be obtained as follows:

$$F = \frac{b}{h}(2 \cdot r_h + 2 \cdot q \cdot b - C_1)$$

Where C_1 is written from the equilibrium in the gravity direction to form the following equation.

$$\sum F_y = 0 \rightarrow C_1 = q \cdot b + T - F_{c,y}$$

The maximum lateral force applied on top of the wall can be written as a function of both the panel joint and hold-down strengths:

$$R_w = F = \frac{b}{h}(r_h + q \cdot b + n \cdot r_c)$$

7.2.3 Nummerical examples

Three examples are presented in this section. For all examples, a 2-panel CLT wall is assumed. The height of the wall is h =2.4m and the width of each panel is b =1.2m for a total wall width of B =2.4m. The vertical load applied on top of the wall is q =15 kN/m. A total of n=16 fasteners in each joint is assumed with a spacing of 150mm. Different values for the elastic stiffness and strength of the panel joint and hold-down are assumed. A summary of the values is presented in Table 7-1.

Table 7-1:Values for the elastic stiffness and strength

	k_c kN/m	k_h kN/m	r_c kN	r_h kN	$\tilde{k}$
Example 1	600	12,000	2.5	80.0	1.25
Example 2	600	5,000	10	50	0.52
Example 3	600	15,000	4.5	35	1.56

7.2.3.1 Example 1

In this example, the strength of the vertical joint fasteners, r_c, is 2.5 kN and the strength of the hold-down connection, r_h, is 80kN.

From the analytical model developed in Chapter 5, it was determined that kinematic model 1 ($\tilde{k}$>1) governs the behaviour of this wall. In this example, the panel joints will yield before the hold-down, after which the stiffness of the panel joints will be equal to zero and the dimensionless stiffness ratio will tend towards infinity, as shown in Figure 7-4. It can be determined through the analytical model that the walls strength is equal to 69.0 kN.

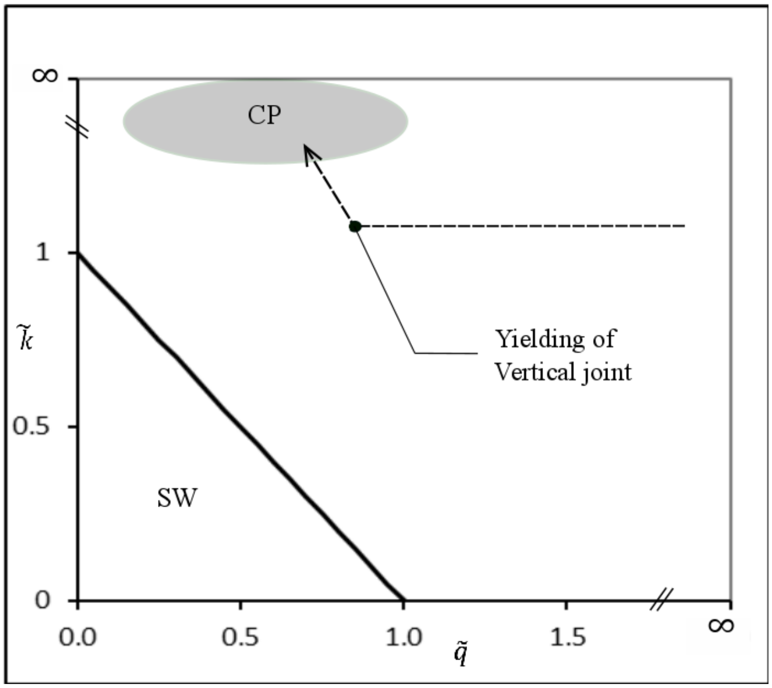

Figure 7-4: Kinematic Path of Example 1

Not being privy to this information a designer would evaluate both methods of static equilibrium described in Section 7.2.1 and obtain the following results:

$$CP\ behaviour: R_w = \frac{b}{h}(r_h + q \cdot b + n \cdot r_c) = \frac{1.2}{2.4}(80 + 16 \cdot 1.2 + 15 \cdot 2.5) = 69.0\ kN$$

$$SW\ behaviour: R_w = Min\left(\frac{r_c \cdot n \cdot B}{h}, \frac{r_h \cdot B}{h} + \frac{q \cdot B^2}{2h}\right)$$

$$= Min\left(\frac{2.5 \cdot 16 \cdot 2.4}{2.4}, \frac{80 \cdot 2.4}{2.4} + \frac{15 \cdot 2.4^2}{2 \cdot 2.4}\right) = Min(40.0\ kN, 98.0\ kN)$$

$$= 40.0\ kN$$

The designer would likely select the smaller of the two strength values because it provides conservative design. However, the selected design strength is close to half of the actual one, and that will lead to an uneconomical design. Had the designer known which kinematic mode the wall would behave in (here CP behaviour), static equilibrium would have yielded exact match with the analytical solution, as shown in Figure 7-5.

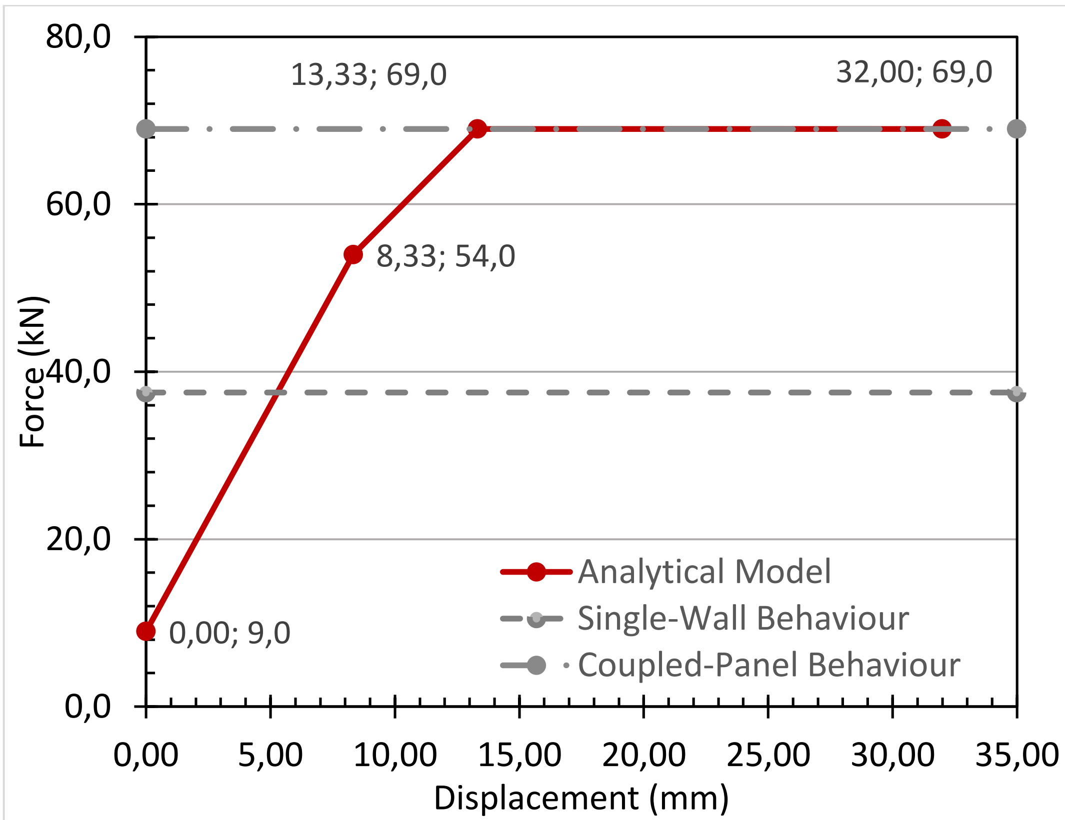

Figure 7-5: Comparison of Results Between Static Equilibrium and Analytical Procedures for Example 1

7.2.3.2 Example 2

In this example, the strength of the vertical joint, r_c, is 10 kN and the strength of the hold-down, r_h, is 50kN. For this example, the dimensionless stiffness ratio is calculated as $\tilde{k}$=0.52. From the analytical model, it can be determined that the kinematic path the wall will undergo is as shown in Figure 7-6, where the wall will start in the CP behaviour in the elastic phase and will transition to the SW behaviour in the plastic phase, which means the wall will behave in final kinematic mode 2. Using the analytical model from Chapter 5, the walls strength can be calculated to 68.0 kN.

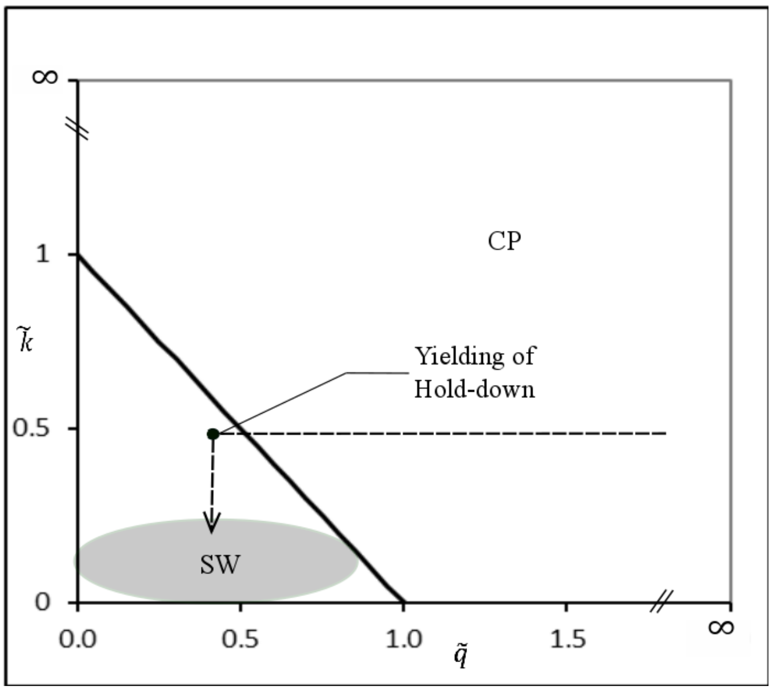

Figure 7-6: Kinematic Path for Example 2

From static equilibrium, one obtains:

$$CP\ behaviour: R_w = \frac{b}{h}(r_h + qb + nr_c) = \frac{1.2}{2.4}(50 + 15 \cdot 1.2 + 16 \cdot 10) = 114.0\ kN$$

$$SW\ behaviour: R_w = Min\left(\frac{r_c \cdot n \cdot B}{h}, \frac{r_h \cdot B}{h} + \frac{q \cdot B^2}{2h}\right)$$

$$= Min\left(\frac{10 \cdot 16 \cdot 2.4}{2.4}, \frac{50 \cdot 2.4}{2.4} + \frac{15 \cdot 2.4^2}{2 \cdot 2.4}\right) = Min(160.0\ kN, 68.0\ kN)$$

$$= 68.0\ kN$$

Simply assuming CP behaviour would in this case have led to a non-conservative solution that would overestimate the wall strength. Once again, static equilibrium would have provided exact match with the analytical solution if the kinematic mode was known, as shown in Figure 7-7. Selecting the smaller of the two values obtained from static equilibrium would again be conservative and (unintentionally) correct.

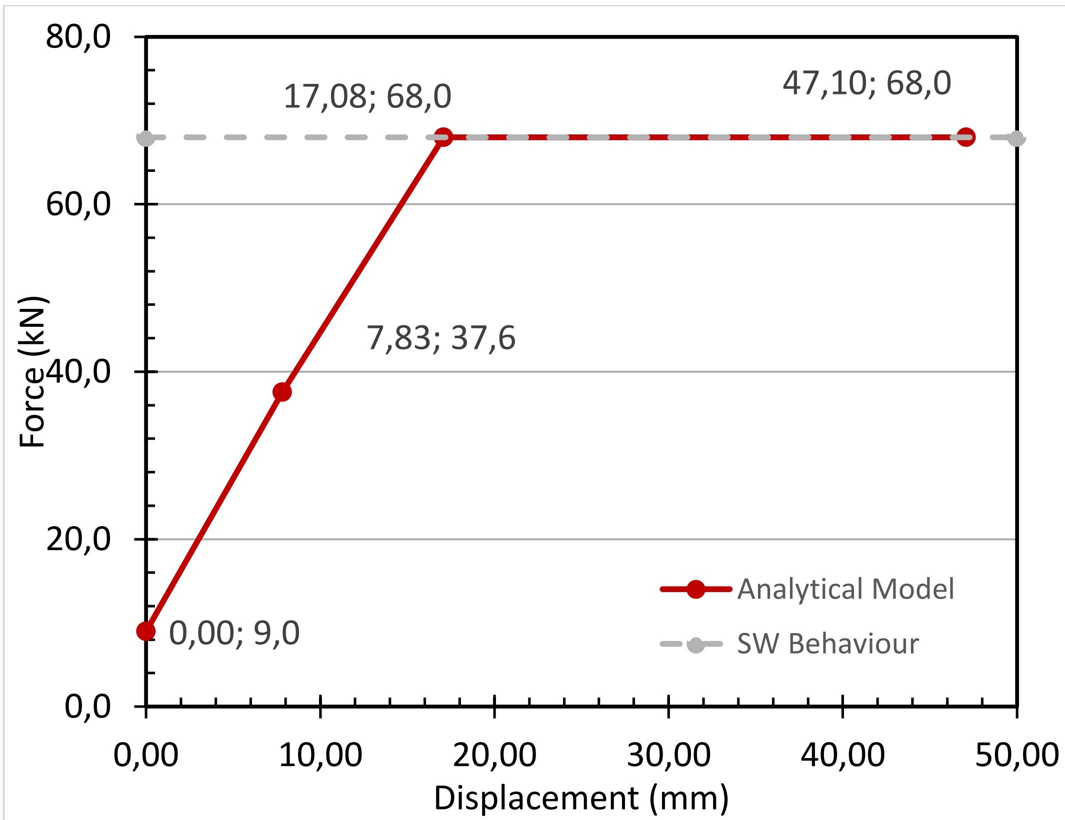

Figure 7-7:Comparison of Results Between Static Equilibrium and Analytical Procedures for Example 2

7.2.3.3 Example 3

In this example, the strength of the vertical joint, $\boldsymbol{r_c}$, is 4.5 kN and the strength of the hold-down, $\boldsymbol{r_h}$, is 35kN. The dimensionless stiffness ratio is larger than 1 ($\widetilde{\boldsymbol{k}}$=1.56), however the kinematic path the wall is different than that in example 1, as shown in Figure 7-8. The hold-down connection yields before the panel joint connection and the wall transitions to the SW behaviour in the plastic phase. The walls strength can be calculated to 58.1 kN.

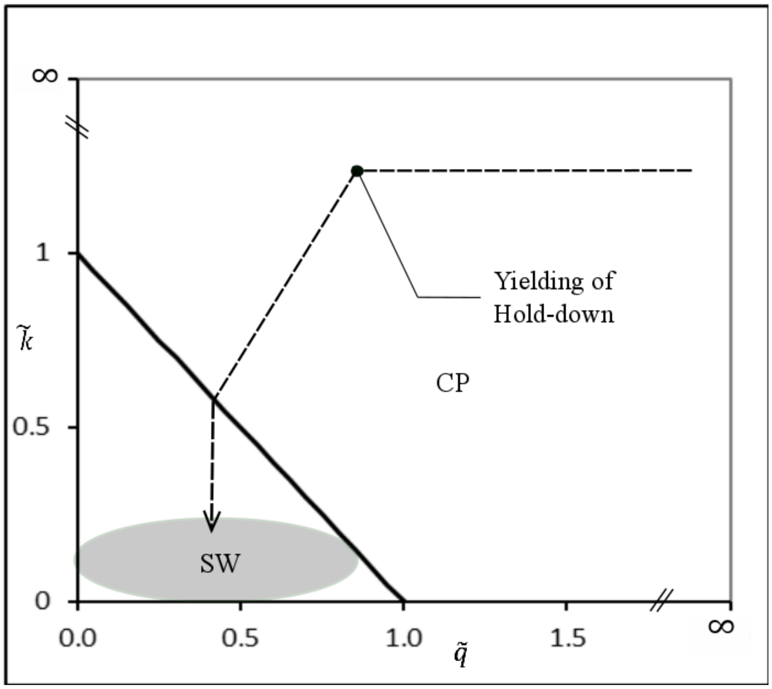

Figure 7-8: Kinematic Path for Example 3

Based on the erroneous rationale (assumed by some designers) that because the dimensionless stiffness ratio is larger than 1(i.e. stiff hold-down) then the behaviour will always be in CP mode, calculating the wall strength based on static equilibrium one obtains:

$$R_w = \frac{b}{h}(r_h + q \cdot b + n \cdot r_c) = \frac{1.2}{2.4}(35 + 16 \cdot 1.2 + 16 \cdot 4.5) = 62.5\ kN$$

In this case the designer would have over-estimated the wall strength, leading to a non-conservative design.

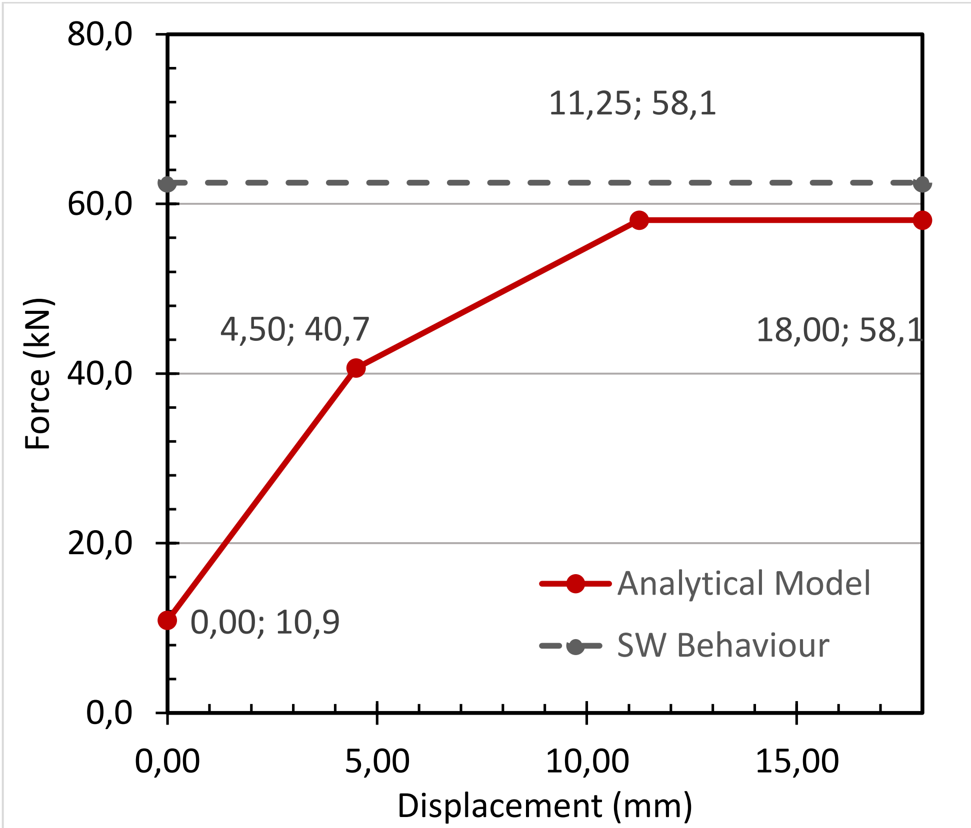

Figure 7-9: Force Displacement curve for kinematic model 1 with hold-down yielding

It can be observed that taking the minimum of the two wall strengths related to the CP and SW behaviour is sufficient and conservative for strength requirements. However, when considering the capacity based design concept to protect the dissipative connections and over design the non-dissipative connections as outlined in Section 7.1.2, chosing the minimum of the two strengths may lead to non-conservative design of the non-dissipative connectors. Knowledge about the failure mechanism is essential to perform adequate design. For this reason the following proposed requirements are presented as possible methodology for design of CLT shearwalls where well-defined and desired kinematic behaviours are attained.

7.3 Proposed simplified design methodology

7.3.1 General

Section 7.2 highlighted the limitation in the ability of the static equilibrium method in estimating the wall's lateral strength. The lack of knowledge about the wall behaviour led to possible over or under estimation of the strength. Furthermore, the static equilibrium also lacks the ability to estimate the initial stiffness, yield strength and diplacement, as well as the ultimate displacement and hence ductility. Therefore, based on the research presented in this thesis, two behaviours are proposed with emphasis on the CP or SW as final wall behaviour. The motivation for chosing the CP behaviour is the potential level of ductility attained since both panel joints and hold-down connections can yield, whereas higher initial stiffness and ultimate capacity can be attained in the SW behaviour.

More specifically, case SW^{EL}-SW^{PL} was selected from Chapter 4 due to its simplicity, (since only one failure mechanism is attained) and potential for higher wall stiffness and capacity.

Case CP^{EL}-CP^{PL} is also selected due to its simplicity and consistency in solution.

7.3.2 The SW model

The force-displacement curve for this case consist of a multi-linear segments with a decreasing stiffness until the achievement of the SW behaviour. Figure 7-10 shows the component of the force-displacement graph needed for the purpose of design, including the activation force, elastic and plastic strength with their associated displacement, initial stiffness and the ultimate displacement.

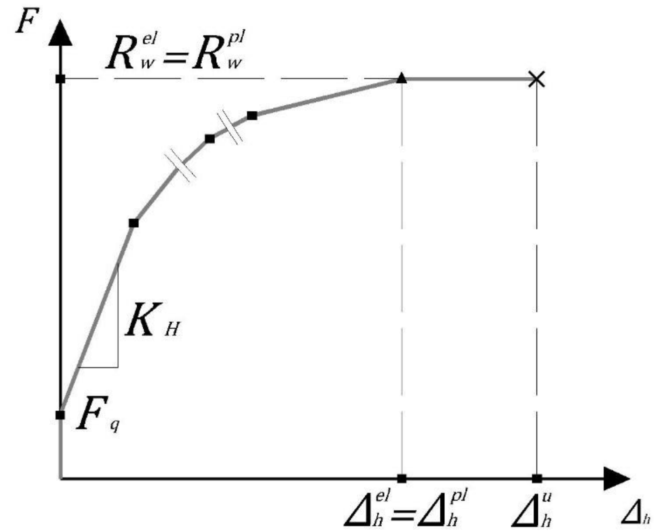

Figure 7-10: Variables of Force-Displacement Curve for SW Behaviour

The steps to be taken by the designer to determin all variables required are as follows:

1. Obtain connection data from manufacturer

The following information are needed from the fastener manufacturer obtained from test results: (a) fastners stiffness, (b) yield/ultimate strengths, (c) yield displacements, and (d) ultimate displacements. A force diplacement curve as that shown in Figure 7-11 contain the required information.

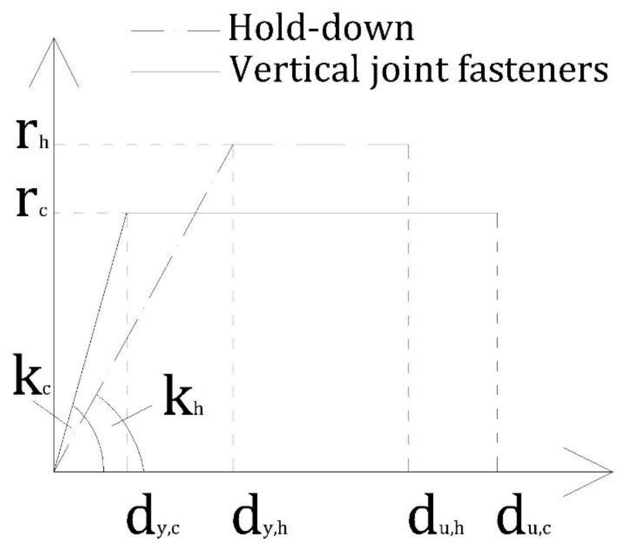

Figure 7-11: Connectors properties

2. Calculate activation force

The first point on the wall's force-displcacement curve is the activation force and it can be determined as:

$$F_q = \frac{q \cdot m \cdot b^2}{2 \cdot h}$$

Where q is the uniformly distributed vertical load applied on the wall, b is the panel width, m is the number of panel constituting the wall and h is the panel height.

3. Ensure SW behaviour

The requirements to acheive SW baheviour are:

$$\tilde{k} < 1$$

$$r_h + \frac{1}{2} \cdot q \cdot b \cdot (2m - 2) < n \cdot r_c$$

$$r_h + \frac{1}{2} \cdot q \cdot b \cdot m > \frac{q \cdot b \cdot m \cdot [\tilde{k} \cdot (m-2) + 1]}{2 \cdot (1 - \tilde{k})}$$

Where r_h and r_c are the strength of the hold-down and panel joint fasteners, respectively (see Fig. 7-11), n is the number of fasteners in each vertical joint. $\tilde{k}$ is the dimensionless stiffness ratio and shall be taken as:

$$\tilde{k} = \frac{k_h}{n \cdot k_c}$$

Where k_h and k_c are the stiffness of the hold-down and panel joint fasteners, respectively (Fig. 7-11).

4. Determine the wall strength

The wall strength shall be calculated as follows:

$$R_w^{el} = R_w^{pl} = \frac{1}{h} \cdot \left[r_h \cdot b \cdot m + \frac{1}{2} \cdot q \cdot b^2 \cdot m^2 \right]$$

5. Determine the wall elastic displacement

The wall elastic displacement shall be calculated as follows:

$$\Delta_h^{el} = \left(\frac{R_w^{pl} \cdot h^2}{b^2} - \frac{q \cdot m^2 \cdot h}{2} \cdot \frac{k_h'}{k_h} \right) \cdot \frac{1}{m^2 \cdot k_h'}$$

Where k_h' is defined as:

$$k_h' = \left(\frac{1}{k_h} + \frac{m-1}{n \cdot k_c} \right)^{-1}$$

6. Determine the wall's initial stiffness

The initial lateral stiffness of the wall shall be taken as:

$$k_H = \frac{b^2 \cdot [k_h + (m-1) \cdot n \cdot k_c]}{h^2}$$

7. Determine the wall's ultimate displacement due to rocking motion

The ultimate displacement for rocking motion shall be taken as:

$$\Delta_h^u = \Delta_h^{pl} + \frac{h}{m \cdot b} \cdot \left(d_{u,h} - d_{y,h}\right)$$

8. Determine the wall's displacement due to shear deformation

$$\Delta_a = \frac{R_w^{pl}}{K_A}$$

Where K_A is the equivalent shear stiffness of the wall provided by the angle brackets designed to stay elastic and it is expressed as:

$$K_{A,1} = \sum_{i=1}^{m} K_{a,i} = \frac{m \cdot b \cdot k_a}{s_a}$$

Where s_a is the spacing between each angle brackets and $K_{a,i}$ the shear stiffness of each individual bracket.

9. Determine the total ultimate wall's displacement due to shear and rocking

$$\Delta_w = \Delta_h^u + \Delta_a$$

7.3.3 Design example for SW behaviour

This example (same as example 2 in Section 7.2) presents a 2-panel wall for an expected SW behaviour. Each panel is of dimensions $b \times h$ respectively of $1.2m \times 2.4m$. The vertical joint is composed of 16 fasteners spaced at 150mm with the following properties provided by the manufacturer: $r_c = 10kN$, $k_c = 600kN/m\,(d_{y,c} = 16.67mm)$ and the ultimate displacement capacity of the individual fasteners is $d_{u,c} = 60.00mm$. The hold-down has the following properties: $r_h = 50kN$, $k_h = 5000kN/m$ ($d_{y,h} = 10.00\ mm$)and the ultimate displacement capacity of the hold-down is $d_{u,h} = 40.00mm$. Two angle brackets are installed to resist shear force in the middle of each panel. It is a non-dissipative connector (i.e. stay elastic until failure of the wall) with a shear stiffness of $9000kN/m$. The wall is also subjected to a uniformly distributed gravity load $q = 15\ kN/m$. The figure below illustrates the connection behaviour.

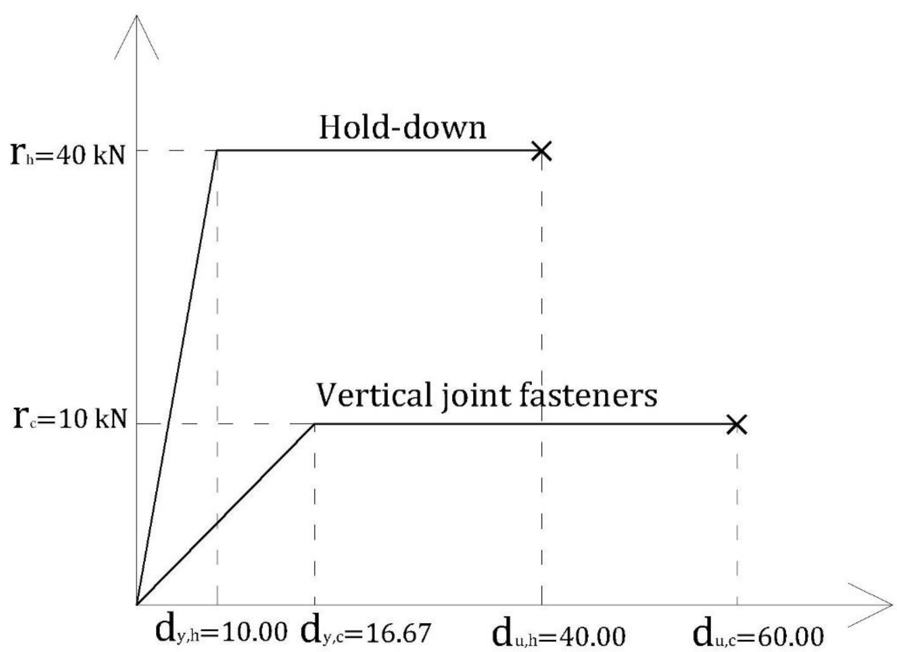

Figure 7-12: Properties of Connectors for Example Achieving SW Behaviour

The design requirements outlined in Section 7.3.2 are used to design the CLT wall in this example. Step 1 in the methodology is outlined in the problem statement and through Figure 7-12.

2. Calculate activation force

$$F_q = \frac{q \cdot m \cdot b^2}{2 \cdot h} = \frac{15 \cdot 2 \cdot 1.2^2}{2 \cdot 2.4} = 9kN$$

3. Ensure SW behaviour

Calculate the dimensionless stiffness ratio:

$$\tilde{k} = \frac{k_h}{n \cdot k_c} = \frac{5000}{16 \cdot 600} = 0.52 < 1$$

$$r_h + \frac{1}{2} \cdot q \cdot b \cdot (2m - 2) < n \cdot r_c$$
$$50 + \frac{1}{2} \cdot 15 \cdot 1.2 \cdot (2 \cdot 2 - 2) < 16 \cdot 10$$
$$68 < 160$$

The calculation of the second condition is:

$$r_h + \frac{1}{2} \cdot q \cdot b \cdot m > \frac{q \cdot b \cdot m \cdot [\tilde{k} \cdot (m-2)+1]}{2 \cdot (1-\tilde{k})}$$
$$50 + \frac{1}{2} \cdot 15 \cdot 1.2 \cdot 2 > \frac{15 \cdot 1.2 \cdot 2 \cdot [0.56 \cdot (2-2)+1]}{2 \cdot (1-0.56)}$$
$$68 > 40.9$$

Therefore, the requirement for SW behaviour have been confirmed.

4. Determine the wall strength

$$R_w^{pl} = \frac{1}{h} \cdot \left[r_h \cdot b \cdot m + \frac{1}{2} \cdot q \cdot b^2 \cdot m^2 \right] = \frac{1}{2.4} \cdot \left[50 \cdot 1.2 \cdot 2 + \frac{1}{2} \cdot 16 \cdot 1.2^2 \cdot 2^2 \right] = 68.0 kN$$

5. Determine the wall elastic displacement

$$k_h' = \left(\frac{1}{k_h} + \frac{m-1}{n \cdot k_c} \right)^{-1} = \left(\frac{1}{5000} + \frac{2-1}{16 \cdot 600} \right)^{-1} = 3288\ kN/m$$

$$\Delta_h^{el} = \left(\frac{R_w^{pl} \cdot h^2}{b^2} - \frac{q \cdot m^2 \cdot h}{2} \cdot \frac{k_h'}{k_h} \right) \cdot \frac{1}{m^2 \cdot k_h'} = \left(\frac{68.0 \cdot 2.4^2}{1.2^2} - \frac{15 \cdot 2^2 \cdot 2.4}{2} \cdot \frac{3288}{5000} \right) \cdot \frac{1}{2^2 \cdot 3288} = 17.1\ mm$$

6. Determine the wall's initial stiffness

$$k_H = \frac{b^2 \cdot [k_h + (m-1) \cdot n \cdot k_c]}{h^2} = \frac{1.2^2 \cdot [5000 + (2-1) \cdot 16 \cdot 600]}{2.4^2} = 3650 kN/m$$

7. Determine the wall's ultimate displacement

$$\Delta_h^u = \Delta_h + \frac{h}{B} \cdot \left(d_{u,h} - d_{y,h}\right) = 17.1\ mm + \frac{2.4}{2.4} \cdot (40 - 10) = 47.1\ mm$$

The wall rocking behaviour can be illustrated as shown in Figure 7-7 in section 7.2.3 with a comparison with the values of static equilibrium.

8. Determine the wall's displacement due to shear deformation

Determine the equivalent shear stiffness of the wall:

$$K_A = \sum_{i=1}^{m} K_{a,i} = \frac{m \cdot b \cdot k_a}{s_a} = K_{a,1} + K_{a,2} = 18{,}000\ kN/m$$

The displacement contribution from shear can be calculated.

$$\Delta_a = \frac{R_w^{pl}}{K_A} = \frac{68.0}{18{,}000} = 3.77mm$$

9. Determine the total ultimate wall's displacement due to shear and rocking

$$\Delta_w = 47.1 + 3.77 = 50.87mm$$

7.3.4 CP behaviour behaviour

The force-displacement curve for the CP behaviour consists of two linear segments. Figure 7-13 shows includes the required variable to fully described the wall behaviour including: the activation force, elastic and plastic strength with their associated displacement, the initial stiffness and the ultimate displacement.

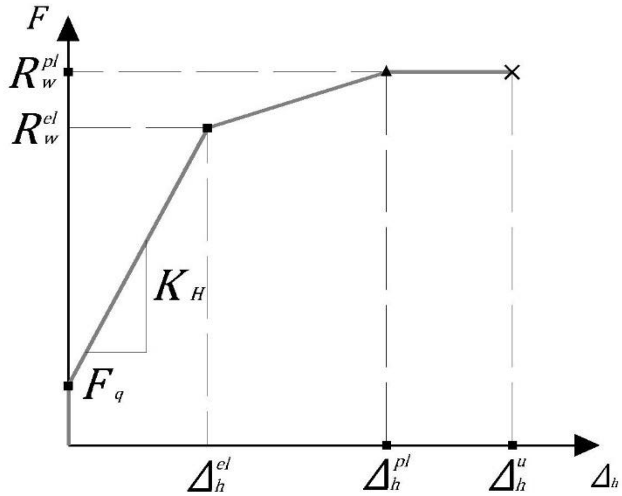

Figure 7-13:Variables of Force-Displacement Curve for CP Behaviour

The steps to be taken by the designer to determin all variables to achieve CP behaviour are as follows:

1. Obtain connection data from manufacturer (Figure 7-11)
2. Calculate activation force

$$F_q = \frac{q \cdot m \cdot b^2}{2 \cdot h}$$

Where q is the uniformly distributed vertical load applied on the wall, b is the panel width, m is the number of panel constituting the wall and h is the panel height.

3. Ensure CP behaviour

The requirements to acheive CP baheviour are:

$$d_{y,c} < d_{y,h}$$

$$d_{u,c} > d_{y,h}$$

Where $d_{y,c}$ and $d_{y,h}$ are the yield displacement of fasteners and hold-down respectively and $d_{u,c}$ and $d_{u,h}$ are the ultimate displacement of fasteners and hold-down respectively (Figure 7-11). In addition of the two previous condition, **only one of the next two conditions** shall be respected:

$$\tilde{k} > 1 \quad \textbf{or} \quad r_c \cdot \frac{k_h' \cdot b}{k_c \cdot h} + F_q < \frac{q \cdot b^2}{2h} \cdot \frac{(2-m) \cdot \tilde{k} + 3m - 2}{(1-\tilde{k})}$$

Where r_c and k_c are the strength and the stiffness of fasteners (Figure 7-11). $\tilde{k}$ is the dimensionless stiffness ratio and shall be taken as:

$$\tilde{k} = \frac{k_h}{n \cdot k_c}$$

k_h' is the equivalent hold-down stiffness and express as:

$$k_h' = k_h + (m-1) \cdot n \cdot k_c$$

4. Determine the wall elastic strength

The elastic strength shall be calculated as follows:

$$R_W^{el} = r_c \cdot \frac{k_h' \cdot b}{k_c \cdot h} + F_q$$

5. Determine the wall's initial stiffness

The initial lateral stiffness of the wall shall be taken as:

$$k_H = \frac{b^2 \cdot k_h'}{h^2}$$

6. Determine the wall elastic displacement

The wall yield displacement shall be calculated as follows:

$$\Delta_h^{el} = d_{y,c} \cdot \frac{h}{b}$$

7. Determine the wall plastic strength

The plastic strength shall be calculated as follows:

$$R_w^{pl} = \frac{b}{h}\left(r_h + n \cdot r_c \cdot (m-1) + \frac{q \cdot m \cdot b}{2}\right)$$

8. Determine the wall plastic displacement

The wall displacement when the yield of the both connector is achieves shall be calculated as follows:

$$\Delta_h^{pl} = d_{y,h} \cdot \frac{h}{b}$$

9. Determine the wall's ultimate displacement due to rocking motion

The ultimate displacement for rocking motion shall be taken as:

$$\Delta_h^{u} = min\left[\frac{h}{b} \cdot d_{u,c}, \frac{h}{b} \cdot d_{u,h}\right]$$

10. Determine the wall's displacement due to shear deformation

$$\Delta_a = \frac{R_w^{pl}}{K_A}$$

Where K_A is the equivalent shear stiffness of the wall expressed as:

$$K_{A,1} = \sum_{i=1}^{m} K_{a,i} = \frac{m \cdot b \cdot k_a}{s_a}$$

Where s_a is the spacing between each angle brackets and $K_{a,i}$ the shear stiffness of each individual bracket.

11. Determine the total ultimate wall's displacement due to shear and rocking

$$\Delta_w = \Delta_h^u + \Delta_a$$

7.3.5 Design example

This example (same as example 1 in Section 7.2) presents a 2-panel wall for an expected CP behaviour. Each panel is of dimensions $b \times h$ respectively of $1.2m \times 2.4m$. The vertical joint is composed of 15 fasteners with the following properties provided by the manufacturer: $r_c = 2.5kN$, $k_c = 600kN/m$ ($d_{y,c} = 4.17mm$) and the ultimate displacement capacity of the individual fasteners is $d_{u,c} = 16.00mm$. The hold-down has the following properties: $r_h = 80kN$, $k_h = 12{,}000kN/m$ ($d_{y,h} = 6.67\ mm$)and the ultimate displacement capacity of the hold-down is $d_{u,h} = 20.00mm$. Two angle brackets are to be installed to resist shear force in the middle of each panel. It is a non-dissipative connector (i.e. stay elastic until failure of the wall) with a shear stiffness of $9000kN/m$. The wall to design is under a uniformly distributed load $q = 15kN/m$.

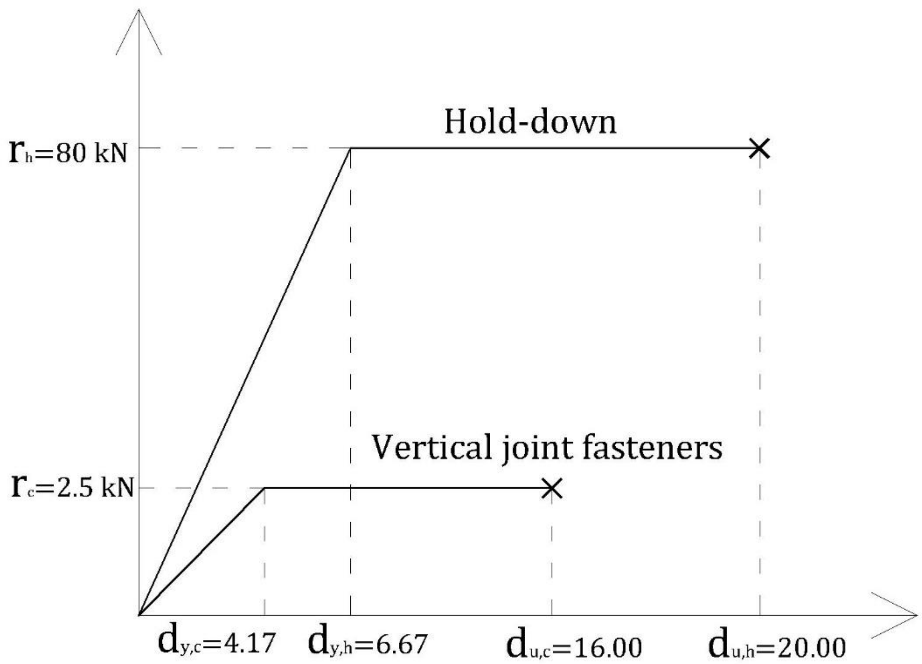

Figure 7-14: Properties of Connectors for Example Achieving CP Behaviour

The design requirements outlined in Section 7.3.4 are used to design the CLT wall in this example. Step 1 in the methodology is outlined in the problem statement and through Figure 7-14.

2. Calculate activation force

$$F_q = \frac{q \cdot m \cdot b^2}{2 \cdot h} = \frac{15 \cdot 2 \cdot 1.2^2}{2 \cdot 2.4} = 9kN$$

3. Ensure CP behaviour

$$d_{y,c} < d_{y,h}$$
$$4.17 < 6.67$$

$$d_{u,c} > d_{y,h}$$
$$12.00 > 6.67$$

$$\tilde{k} = \frac{k_h}{n \cdot k_c} > 1$$

$$\frac{k_h}{n \cdot k_c} = \frac{12{,}000}{16 \cdot 600} = 1.25 \quad \text{or} \quad r_c \cdot \frac{k_h' \cdot b}{k_c \cdot h} + F_q < \frac{q \cdot b^2}{2h} \cdot \frac{(2-m) \cdot \tilde{k} + 3m - 2}{(1-\tilde{k})}$$

$$ok$$

Since $\tilde{k} > 1$, it is not needed to check the other condition. The requirements for CP behaviour are confirmed.

4. Determine the wall elastic strength

$$k_h' = 12{,}000 + (2-1) \cdot 16 \cdot 600 = 21{,}600 kN/m$$

$$R_w^{el} = r_c \cdot \frac{{k_h'}^{el,1} \cdot b}{k_c \cdot h} + F_q = 2.5 \cdot \frac{21{,}600 \cdot 1.2}{600 \cdot 2.4} + 9 = 54.0\ kN$$

5. Determine the wall's initial stiffness

$$k_H = \frac{b^2 \cdot k_h'}{h^2} = \frac{1.2^2 \cdot 21{,}600}{2.4^2} = 5400 kN/m$$

6. Determine the wall elastic displacement

$$\Delta_h^{el} = d_{y,c} \cdot \frac{h}{b} = 4.17 \cdot \frac{2.4}{1.2} = 8.34 mm$$

7. Determine the wall plastic strength

$$R_w^{pl} = \frac{b}{h}\left(r_h + n \cdot r_c \cdot (m-1) + \frac{q \cdot m \cdot b}{2}\right) = \frac{1.2}{2.4}\left(80 + 16 \cdot 2.5 \cdot (2-1) + \frac{15 \cdot 2 \cdot 1.2}{2}\right) =$$

$$69.0 kN$$

8. Determine the wall plastic displacement

$$\Delta_h^{pl} = d_{y,h} \cdot \frac{h}{b} = 6.67 \cdot \frac{2.4}{1.2} = 13.34\ mm$$

9. Determine the wall's ultimate displacement due to rocking motion

The ultimate displacement for rocking motion shall be taken as:

$$\Delta_h^u = min\left[\frac{h}{b} \cdot d_{u,c}, \frac{h}{b} \cdot d_{u,h}\right] = min\left[\frac{2.4}{1.2} \cdot 16.00, \frac{2.4}{1.2} \cdot 20.00\right] = 32.00mm$$

Therefore, the ultimate displacement is governed by the ultimate displacement in the vertical joint. The values of strengths and rocking displacements are also found in Figure 7-5 in Section 7.2.

10. Determine the wall's displacement due to shear deformation

$$K_{A,1} = \sum_{i=1}^{m} K_{a,i} = \frac{m \cdot b \cdot k_a}{s_a} = K_{a,1} + K_{a,2} = 18{,}000\ kN/m$$

The displacement contribution from shear can be calculated.

$$\Delta_a = \frac{R_w^{pl}}{K_A} = \frac{69.0}{18{,}000} = 3.83mm$$

$$\Delta_w = 32.00 + 3.83 = 35.83mm$$

CHAPTER 8 - Conclusion

This thesis presents an analytical methodology to predict the behaviour of multi-panel CLT shearwalls. The research established that the behaviour of the wall is dependent on the panel aspect ratio, connectors' configuration and properties as well as gravity load. Six cases with a total of 36 different failure mechanisms were developed depending on the connectors' stiffness and strength properties. Two final wall behaviours were explored, namely single wall (SW) and couple panel (CP) behaviours. In general, it was found that the SW behaviour could be achieved if the yielding in the hold-down occurred prior to yielding in the panel joints and, inversely, CP behaviour was achieved if the yielding in the vertical joint occur prior to yielding in the hold-down.

The analytical model was compared with a numerical model, and the results showed that the proposed model was capable of describing the assumed behaviour with reasonable accuracy.

The current design provisions for CLT shearwalls were presented and the shortcomings related to identifying the failure mechanism highlighted. An investigation of the suitability of only using static equilibrium was undertaken, and it was shown that relying on the considerations of static equilibrium cannot always ensure reasonable prediction of the behaviour. It was further demonstrated that it was not feasible to check some of the design requirements by relying solely on static equilibrium. Simplified design provisions based on the current research were proposed with the aim to optimize the walls ductility (CP behaviour) or strength and stiffness (SW behaviour).

Future work is recommended to supplement the current study with a comprehensive experimental program in order to validate the model assumptions and demonstrate the physical meaning for some of the proposed kinematic modes and failure mechanisms. The proposed analytical model could be used to guide the development of such experimental program, especially in the selection of the test matrix.

References

ASTM E2126-11. Standard test methods for cyclic (reversed) load test for shear resistance of walls for buildings. West Conshohocken: ASTM International; 2011.

Casagrande, D., Doudak, G., Mauro, L., Polastri, A. (2017) "Analytical Approach to Establish the Elastic Behaviour of Multi-Panel CLT Shear-Walls Subjected to Lateral Loads" *ASCE Journal of Structural Engineering*

Casagrande, D., Rossi, S., Tomasi, R., and Mischi, G. (2016) "A predictive analytical model for the elasto-plastic behaviour of a light timber-frame shear-wall." *Construction and Building Materials,* Vol. 102, 1113-1126, doi: 0.1016/j.conbuildmat.2015.06.025.

Ceccotti, A., Lauriola, M.P., Pinna, M., and Sandhaas, C. (2006). "SOFIE project – cyclic tests on cross-laminated wooden panels." *Proceedings of World Conference on Timber Engineering (WCTE)*, Portland, USA.

Folz, B. and Filiatrault, A. (2001). "SAWS - Version 1.0, A Computer Program for the Seismic Analysis of Woodframe Structures", Structural Systems Research Project Report No. SSRP-2001/09, Dept. of Structural Engineering, UCSD, La Jolla, CA

Gavric, I., Fragiacomo M.., and Ceccotti A. (2015a). "Cyclic behavior of CLT wall systems: experimental tests and analytical prediction models." *ASCE Journal of Structural Engineering*, 141 (11).

Gavric, I., Fragiacomo, M.., Ceccotti, A., (2015b) "Cyclic behavior of typical screwed connections for cross-laminated (CLT) structures", European Journal of Wood and Wood Products, Vol 73(2), 179-191, doi:10.1007/s00107-014-0877-6.

Gavric, I., Fragiacomo, M.., Popovski, M., Ceccotti, A., (2013) "Behaviour of Cross-Laminated Timber Panels under Cyclic Loads", European Journal of Wood and Wood Products, Vol 73(2), 179-191, doi: 0.1007/978-94-007-7811-5_62

Hossain, A., Danzig, I., and Tannert, T. (2016) "Cross-Laminated Timber Shear Connections with Double-Angled Self-Tapping Screw Assemblies.", *Journal of Structural Engineering*, Vol 142, (11)

FPInnovation. (2011) "CLT Handbook", FPInnovations, Librairie and Archives Canada, Quebec, Canada, ISBN 978-0-86488-574-0

Lowes, L. and Mitra, N. (2004). "A Beam-Column Joint Model for Simulating the Earthquake Response of Reinforced Concrete Frames", Pacific Earthquake Engineering Research Center No. PEER-2003/10, College of Engineering, University of California, Berkeley, CA

Popovski. M., and Gavric. I. (2016). "Performance of a 2-story CLT house subjected to lateral loads." *Journal of Structural Engineering*, 142(4), E4015006(1-12), doi: 10.1061/(ASCE)ST.1943-541X.0001315.

Popovski, M., and Karacabeyli, E. (2011). "Seismic behaviour of cross-laminated timber structures." *Proceedings of World Conference on Timber Engineering (WCTE),* Vancouver, Canada, Volume 2, 2012, Pages 335-344.

Pozza, L., and Trutalli D. (2016). “An analytical formulation of q-factor for mid-rise CLT buildings based on parametric numerical analyses.” *Bulletin of Earthquake Engineering,* 10.1007/s10518-016-0047-9 2016.

Pozza, L., Scotta, R., Trutalli, D., Polastri, A., and Smith, I. (2016) “Experimentally based q-factor estimation of cross-laminated timber walls”. *Proceedings of the ICE - Structures and Buildings*, 169(7), 492-507, doi: 10.1680/jstbu.15.00009.

Sadeghi, M., and Smith, I. (2014) “Edge Connections for CLT Plates: In-Plane Shear Tests on Half-Lapped and single Spline Joints.”, *Proceedings of 9th World Conference on Timber Engineering (WCTE)*, Quebec City, Canada.

Shen, Y.I., Schneider, J., Tesfamariam, S., Stiemer, S. F., and Mu, Z.G. (2013) "Hysteresis behavior of bracket connection in cross-laminated-timber shear walls." *Construction and Building Materials,* Vol 48, 980–991, doi: 10.1016/j.conbuildmat.2013.07.050

Yasumura, M., Kobayashi, K, Okabe, M., Miyake, T., and Matsumoto, K. (2016). “Full-scale tests and numerical analysis of low-rise CLT structures under lateral loading.” *Journal of Structural Engineering*, 142(4), doi: 10.1061/(ASCE)ST.1943-541X.0001348.

Appendix

Equation (27)

$$F_t^{pl,1} = R_{w,h}^{el,1} + \left(F_t^{pl,1} - R_{w,h}^{el,1}\right)$$

$$F_t^{pl,1} = \frac{r_h \cdot {k'_h}^{el,1} \cdot b}{k_h \cdot h} + F_q + \frac{b \cdot (m-1)}{h} \cdot \left[r_h \cdot \left(1 - \frac{n \cdot k_c}{k_h}\right) + q \cdot b\right]$$

$$F_t^{pl,1} = \frac{r_h \cdot {k'_h}^{el,1} \cdot b}{k_h \cdot h} + \frac{q \cdot m \cdot b^2}{2h} + \frac{b \cdot (m-1) \cdot r_h}{h} \cdot \left(1 - \frac{n \cdot k_c}{k_h}\right) + \frac{qb^2 \cdot (m-1)}{h}$$

$$F_t^{pl,1} = \frac{r_h \cdot b}{h}\left[\frac{k_h + (m-1) \cdot n \cdot k_c}{k_h} - \frac{(m-1) \cdot n \cdot k_c}{k_h} + (m-1)\right] + \frac{qb^2}{2h}[m + 2(m-1)]$$

$$F_t^{pl,1} = \frac{r_h \cdot b}{h}\left[\frac{k_h}{k_h} + \frac{(m-1) \cdot n \cdot k_c}{k_h} - \frac{(m-1) \cdot n \cdot k_c}{k_h} + (m-1)\right] + \frac{qb^2}{2h}[3m-2]$$

$$F_t^{pl,1} = \frac{r_h \cdot b \cdot m}{h} + \frac{q \cdot b^2}{2h} \cdot (3m-2)$$

Equation (28)

$$\Delta_{h,t}^{pl,1} = \Delta_h^{el} + \frac{F_t^{pl,1} - R_{w,h}^{el,1}}{k_H^{pl,1}}$$

$$\Delta_{h,t}^{pl,1} = \frac{r_h \cdot h}{k_h \cdot b} + \frac{h^2}{(m-1) \cdot n \cdot k_c \cdot b^2} \cdot \frac{R_{c,1} \cdot b}{h} \cdot (m-1)$$

$$\Delta_{h,t}^{pl,1} = \frac{r_h \cdot h}{k_h \cdot b} + \frac{R_{c,1} \cdot h}{n \cdot k_c \cdot b}$$

$$\Delta_{h,t}^{pl,1} = \frac{r_h \cdot h}{k_h \cdot b} + \frac{h}{n \cdot k_c \cdot b} \cdot \left[r_h \cdot \left(1 - \frac{n \cdot k_c}{k_h}\right) + q \cdot b\right]$$

$$\Delta_{h,t}^{pl,1} = \frac{r_h \cdot h}{k_h \cdot b} - \frac{r_h \cdot h}{k_h \cdot b} + \frac{h \cdot r_h}{n \cdot k_c \cdot b} + \frac{q \cdot h}{n \cdot k_c}$$

$$\Delta_{h,t}^{pl,1} = \frac{r_h \cdot h}{k_h \cdot b} - \frac{r_h \cdot h}{k_h \cdot b} + \frac{h \cdot r_h}{n \cdot k_c \cdot b} + \frac{q \cdot h}{n \cdot k_c}$$

$$\Delta_{h,t}^{pl,1} = \frac{h}{b \cdot n \cdot k_c} \cdot (r_h + qb)$$

Equation (30)

$$V_0^{pl,1} = V_0^{el,1} + v_0^{pl,1}$$

Where $v_0^{pl,1}$ in the incremental elongation of hold-down in the plastic state of kinematic mode 1. According to Casagrande et al. (2017), the following is derived:

$$V_0^{el,1} = b \cdot \vartheta = b \cdot \frac{1}{k_h'^{\,el,1} \cdot h} \left(\frac{R_{w,h}^{el,1} \cdot h^2}{b^2} - \frac{q \cdot m \cdot h}{2} \right)$$

$$V_0^{el,1} = \frac{b}{k_h'^{\,el,1} \cdot h} \left(\frac{h^2}{b^2} \cdot \left[r_h \cdot \frac{k_h'^{\,el,1} \cdot b}{k_h \cdot h} + \frac{q \cdot m \cdot b^2}{2h} \right] - \frac{q \cdot m \cdot h}{2} \right)$$

$$V_0^{el,1} = \frac{b}{k_h'^{\,el,1} \cdot h} \left(\frac{h \cdot r_h \cdot k_h'^{\,el,1}}{b \cdot k_h} + \frac{q \cdot m \cdot h}{2} - \frac{q \cdot m \cdot h}{2} \right)$$

$$V_0^{el,1} = \frac{r_h}{k_h}$$

The increase of elongation in plastic state is expressed with the same equation without the contribution of the vertical load.

$$v_0^{pl,1} = \frac{b}{k_h'^{\,el,1} \cdot h} \left(\frac{\left(F_t^{pl,1} - R_{w,h}^{el,1}\right) \cdot h^2}{b^2} - \frac{q \cdot m \cdot h}{2} \right)$$

$$v_0^{pl,1} = \frac{b}{k_h'^{\,pl,1} \cdot h}\left(\frac{h^2}{b^2} \cdot \frac{R_{c,1} \cdot b}{h} \cdot (m-1) - 0\right)$$

$$v_0^{pl,1} = \frac{R_{c,1} \cdot (m-1)}{(m-1) \cdot n \cdot k_c}$$

$$v_0^{pl,1} = \frac{1}{n \cdot k_c}\left[r_h \cdot \left(1 - \frac{n \cdot k_c}{k_h}\right) + q \cdot b\right]$$

$$v_0^{pl,1} = \frac{r_h}{n \cdot k_c} - \frac{r_h}{k_h} + \frac{q \cdot b}{n \cdot k_c}$$

$$v_0^{pl,1} = \frac{1}{n \cdot k_c} \cdot (r_h + q \cdot b) - \frac{r_h}{k_h}$$

Therefore, the total elongation of the hold-down is:

$$V_0^{pl,1} = V_0^{el,1} + v_0^{pl,1}$$

$$V_0^{pl,1} = \frac{r_h}{k_h} + \frac{1}{n \cdot k_c} \cdot (r_h + q \cdot b) - \frac{r_h}{k_h}$$

$$V_0^{pl,1} = \frac{1}{n \cdot k_c} \cdot (r_h + q \cdot b)$$

Equation (35)

$$V_c^{pl,1} = V_c^{el,1} + v_c^{pl,1}$$

Because in kinematic mode 1, $V_c^{el,1} = V_0^{el,1}$ and $v_c^{pl,1} = v_0^{pl,1}$ because the elongation of the hold-down and fasteners are the same in CP behaviour as they have the same ratio of elongation. Therefore, the following is developed:

$$V_c^{pl,1} = \frac{1}{n \cdot k_c} \cdot (r_h + q \cdot b)$$

Equation (45)

$$F_t^{pl,j^*} = F_t^{pl,1} + \sum_{j=2}^{j^*}\left(F_t^{pl,j} - F_t^{pl,j-1}\right)$$

From Equation (27):

$$F_t^{pl,1} = \frac{r_h \cdot b \cdot m}{h} + \frac{q \cdot b^2}{2h} \cdot (3m - 2)$$

Therefore, continuing the derivation, the following is developed:

$$F_t^{pl,j^*} = \frac{r_h \cdot b \cdot m}{h} + \frac{q \cdot b^2}{2h} \cdot (3m - 2) + \sum_{j=2}^{j^*}\left(\frac{q \cdot b^2}{h}(m - j)\right)$$

$$F_t^{pl,j^*} = \frac{r_h \cdot b \cdot m}{h} + \frac{q \cdot b^2}{2h} \cdot (3m - 2) + \frac{q \cdot b^2}{h} \cdot \sum_{j=2}^{j^*}(m - j)$$

$$F_t^{pl,j^*} = \frac{r_h \cdot b \cdot m}{h} + \frac{q \cdot b^2}{2h}\left[(3m - 2) + 2 \cdot \sum_{j=2}^{j^*}(m - j)\right]$$

$$F_t^{pl,j^*} = \frac{r_h \cdot b \cdot m}{h} + \frac{q \cdot b^2}{2h}\left[(3m - 2) + 2 \cdot [m(j^* - 1) - 0.5 \cdot j^* \cdot (j^* + 1) + 1]\right]$$

$$F_t^{pl,j^*} = \frac{r_h \cdot b \cdot m}{h} + \frac{q \cdot b^2}{2h}[(3m - 2) + 2 \cdot m(j^* - 1) - j^* \cdot (j^* + 1) + 2]$$

$$F_t^{pl,j^*} = \frac{r_h \cdot b \cdot m}{h} + \frac{q \cdot b^2}{2h}[3m + 2m(j^* - 1) - j^*(j^* + 1)]$$

Equation (46)

$$\Delta_{h,t}^{pl,j^*} = \Delta_{h,t}^{pl,1} + \sum_{j=2}^{j^*} \frac{F_t^{pl,j} - F_t^{pl,j-1}}{k_H^{pl,j}}$$

$$\Delta_{h,t}^{pl,j^*} = \frac{h}{b \cdot n \cdot k_c} \cdot (r_h + qb) + \sum_{j=2}^{j^*} \left[\frac{q \cdot b^2}{h} (m - j) \cdot \frac{h^2}{(m-j) \cdot n \cdot k_c \cdot b^2} \right]$$

$$\Delta_{h,t}^{pl,j^*} = \frac{h \cdot r_h}{b \cdot n \cdot k_c} + \frac{q \cdot h}{n \cdot k_c} + \sum_{j=2}^{j^*} \left[\frac{q \cdot h}{n \cdot k_c} \right]$$

$$\Delta_{h,t}^{pl,j^*} = \frac{r_h}{b \cdot n \cdot k_c} + \sum_{j=1}^{j^*} \left[\frac{q \cdot h}{n \cdot k_c} \right]$$

$$\Delta_{h,t}^{pl,j^*} = \frac{h}{b} \cdot \frac{r_h}{n \cdot k_c} + \frac{q \cdot h \cdot j^*}{n \cdot k_c}$$

Equation (49)

$V_{\mathrm{c}}^{el,1} = \frac{r_h}{k_h}$ and $v_{\mathrm{c}}^{pl,1} = \frac{1}{n \cdot k_c} \cdot (r_h + q \cdot b) - \frac{r_h}{k_h}$ are established in Equation (35) of this Appendix.

$V_0^{el,1} = \frac{r_h}{k_h}$ and $v_0^{pl,1} = \frac{1}{n \cdot k_c} \cdot (r_h + q \cdot b) - \frac{r_h}{k_h}$ are established in Equation (30) of this Appendix.

The incremental of elongation through kinematic mode j^* can be develop as:

$$v_{\mathrm{c}}^{pl,j^*} = \frac{b}{k_h'^{\ pl,j^*} \cdot h} \left(\frac{\left(F_t^{pl,j^*} - F_t^{pl,j^*-1} \right) \cdot h^2}{b^2} - \frac{q \cdot m \cdot h}{2} \right)$$

$$v_{\mathrm{c}}^{pl,j^*} = \frac{b}{(m - j^*) \cdot n \cdot k_c \cdot h} \left(\frac{h^2}{b^2} \left(\frac{q \cdot b^2}{h} (m - j^*) \right) - 0 \right)$$

$$v_{\mathrm{c}}^{pl,j^*} = \frac{q \cdot b}{n \cdot k_c}$$

The incremental elongation of the hold-down through kinematic mode j^* can be develop as:

$$v_0^{pl,j^*} = \frac{j^* \cdot b}{k_h'^{\,pl,j^*} \cdot h}\left(\frac{\left(F_t^{pl,j^*} - F_t^{pl,j^*-1}\right) \cdot h^2}{b^2} - \frac{q \cdot m \cdot h}{2}\right)$$

$$v_0^{pl,j^*} = \frac{j^* \cdot q \cdot b}{n \cdot k_c}$$

Therefore, Equation (49) represents the sum of the elongation in kinematic mode 1 (for both plastic and elastic) and the incremental elongation due all kinematic mode up $j^* - 1$ and the incremental elongation in kinematic mode j^* governed by the hold-down develop by interpolation:

$$d_{y,c} > V_{\mathrm{c}}^{pl,1} + \sum_{j=2}^{j^*-1} v_{\mathrm{c}}^{pl,j} + v_{\mathrm{c}}^{pl,j^*} \cdot \frac{d_{u,h} - \left(V_0^{el,1} + v_0^{pl,1} + \sum_{j=2}^{j^*-1} v_0^{pl,j}\right)}{v_0^{pl,j^*}}$$

$$d_{y,c} > \frac{r_h}{n \cdot k_c} + \frac{q \cdot b}{n \cdot k_c} + \sum_{j=2}^{j^*-1} \frac{q \cdot b}{n \cdot k_c} + \frac{q \cdot b}{n \cdot k_c} \cdot \frac{d_{u,h} - \left(\frac{r_h}{n \cdot k_c} + \sum_{j=2}^{j^*-1} \frac{j \cdot q \cdot b}{n \cdot k_c}\right)}{\frac{j^* \cdot q \cdot b}{n \cdot k_c}}$$

$$d_{y,c} > \frac{r_h}{n \cdot k_c} + \frac{q \cdot b}{n \cdot k_c} + (j^* - 2)\frac{q \cdot b}{n \cdot k_c} + \frac{1}{j^*}\left[d_{u,h} - \frac{r_h}{n \cdot k_c} - \frac{(j^* - 1) \cdot j^*}{2} \cdot \frac{q \cdot b}{n \cdot k_c} + \frac{q \cdot b}{n \cdot k_c}\right]$$

$$d_{y,c} > \frac{r_h}{n \cdot k_c} + (j^* - 1)\frac{q \cdot b}{n \cdot k_c} + \frac{d_{u,h}}{j^*} - \frac{r_h}{j^* \cdot n \cdot k_c} - \frac{(j^* - 1) \cdot q \cdot b}{2 \cdot n \cdot k_c} + \frac{q \cdot b}{j^* \cdot n \cdot k_c}$$

$$d_{y,c} > \frac{r_h}{n \cdot k_c}\left(1 - \frac{1}{j^*}\right) + \frac{q \cdot b}{n \cdot k_c}\left[\frac{(j^* - 1)}{2} + \frac{1}{j^*}\right] + \frac{d_{u,h}}{j^*}$$

Equation (50)

$V_0^{el,1} = \frac{r_h}{k_h}$ and $v_0^{pl,1} = \frac{1}{n \cdot k_c} \cdot (r_h + q \cdot b) - \frac{r_h}{k_h}$ are established in Equation (30) of this Appendix.

$v_0^{pl,j^*} = \frac{j^* \cdot q \cdot b}{n \cdot k_c}$ is established in Equation (49) of this Appendix.

$$V_0^{el,1} + v_0^{pl,1} + \sum_{j=2}^{j^*-1} v_0^{pl,j} < d_{u,h} < V_0^{el,1} + v_0^{pl,1} + \sum_{j=2}^{j^*} v_0^{pl,j}$$

$$\frac{1}{n \cdot k_c} \cdot (r_h + q \cdot b) + \sum_{j=2}^{j^*-1} \frac{j \cdot q \cdot b}{n \cdot k_c} < d_{u,h} < \frac{1}{n \cdot k_c} \cdot (r_h + q \cdot b) + \sum_{j=2}^{j^*} \frac{j \cdot q \cdot b}{n \cdot k_c}$$

$$\frac{r_h}{n \cdot k_c} + \frac{1 \cdot q \cdot b}{n \cdot k_c} + \sum_{j=2}^{j^*-1} \frac{j \cdot q \cdot b}{n \cdot k_c} < d_{u,h} < \frac{r_h}{n \cdot k_c} + \frac{1 \cdot q \cdot b}{n \cdot k_c} + \sum_{j=2}^{j^*} \frac{j \cdot q \cdot b}{n \cdot k_c}$$

$$\frac{r_h}{n \cdot k_c} + \frac{q \cdot b}{n \cdot k_c} \sum_{j=1}^{j^*-1} j < d_{u,h} < \frac{r_h}{n \cdot k_c} + \frac{q \cdot b}{n \cdot k_c} \sum_{j=1}^{j^*} j$$

$$\frac{r_h}{n \cdot k_c} + \frac{q \cdot b}{n \cdot k_c} \cdot \frac{j^* \cdot (j^* - 1)}{2} < d_{u,h} < \frac{r_h}{n \cdot k_c} + \frac{q \cdot b}{n \cdot k_c} \cdot \frac{j^* \cdot (j^* + 1)}{2}$$

$$\frac{1}{n \cdot k_c} \left(r_h + \frac{j^* \cdot (j^* - 1) q \cdot b}{2} \right) < d_{u,h} < \frac{1}{n \cdot k_c} \left(r_h + \frac{j^* \cdot (j^* + 1) q \cdot b}{2} \right)$$

Equation (51)

$V_0^{el,1} = \frac{r_h}{k_h}$ and $v_0^{pl,1} = \frac{1}{n \cdot k_c} \cdot (r_h + q \cdot b) - \frac{r_h}{k_h}$ are established in Equation (30) of this Appendix.

$v_0^{pl,j^*} = \frac{j^* \cdot q \cdot b}{n \cdot k_c}$ is established in Equation (49) of this Appendix.

$$R_w^{pl,IV} = F_t^{pl,1} + \sum_{j=2}^{\hat{j}-1} F_t^{pl,j} - F_t^{pl,j-1} + \left(\frac{d_{u,h} - V_0^{pl,\hat{j}}}{v_0^{pl,\hat{j}}}\right) \cdot \left(F_t^{pl,\hat{j}} - F_t^{pl,\hat{j}-1}\right)$$

$$R_w^{pl,IV} = F_t^{pl,1} + \sum_{j=2}^{\hat{j}-1} \frac{q \cdot b^2}{h}(m - j) + \left(\frac{d_{u,h} - V_0^{pl,\hat{j}}}{\left(\frac{\hat{j} \cdot q \cdot b}{n \cdot k_c}\right)}\right) \cdot \frac{q \cdot b^2}{h}(m - \hat{j})$$

$$R_w^{pl,IV} = \frac{r_h \cdot b \cdot m}{h} + \frac{q \cdot b^2}{2h} \cdot (3m - 2) + \frac{q \cdot b^2 \cdot m \cdot (\hat{j} - 2)}{h} - \frac{q \cdot b^2 \cdot \hat{j}(\hat{j} - 1)}{2h} + \frac{q \cdot b^2}{h}$$
$$+ \left(\frac{d_{u,h} - \frac{r_h}{n \cdot k_c} - \frac{\hat{j} \cdot (\hat{j} - 1) \cdot q \cdot b}{2 \cdot n \cdot k_c}}{\left(\frac{\hat{j} \cdot q \cdot b}{n \cdot k_c}\right)}\right) \cdot \frac{q \cdot b^2}{h}(m - \hat{j})$$

$$R_w^{pl,IV} = \frac{r_h \cdot b \cdot m}{h} + \frac{q \cdot b^2}{2h} \cdot (3m - 2) + \frac{q \cdot b^2 \cdot m \cdot (\hat{j} - 2)}{h} - \frac{q \cdot b^2 \cdot \hat{j}(\hat{j} - 1)}{2h} + \frac{q \cdot b^2}{h}$$
$$+ \frac{d_{u,h} \cdot n \cdot k_c \cdot b \cdot (m - \hat{j})}{\hat{j} \cdot h} - \frac{r_h \cdot b \cdot (m - \hat{j})}{\hat{j} \cdot h} - \frac{(\hat{j} - 1)(m - \hat{j}) q \cdot b^2}{2 \cdot h}$$

$$R_w^{pl,IV} = \frac{r_h \cdot b}{h}\left[m + 1 - \frac{m}{\hat{j}}\right] + \frac{q \cdot b^2 \cdot m \cdot \hat{j}}{2 \cdot h} + \frac{d_{u,h} \cdot n \cdot k_c \cdot b \cdot (m - \hat{j})}{\hat{j} \cdot h}$$

Equation (52)

$V_0^{el,1} = \frac{r_h}{k_h}$ and $v_0^{pl,1} = \frac{1}{n \cdot k_c} \cdot (r_h + q \cdot b) - \frac{r_h}{k_h}$ are established in Equation (30) of this Appendix.

$v_0^{pl,j^*} = \frac{j^* \cdot q \cdot b}{n \cdot k_c}$ is established in Equation (49) of this Appendix.

$$V_0^{pl,\hat{j}} = V_0^{el,1} + v_0^{pl,1} + \sum_{j=2}^{\hat{j}} v_0^{pl,j}$$

$$V_0^{pl,\hat{j}} = \frac{1}{n \cdot k_c} \cdot (r_h + q \cdot b) + \sum_{j=2}^{\hat{j}} \frac{j \cdot q \cdot b}{n \cdot k_c}$$

$$V_0^{pl,\hat{j}} = \frac{r_h}{n \cdot k_c} + \frac{q \cdot b}{n \cdot k_c} \sum_{j=1}^{\hat{j}} j$$

$$V_0^{pl,\hat{j}} = \frac{r_h}{n \cdot k_c} + \frac{\hat{j} \cdot (\hat{j} - 1) \cdot q \cdot b}{2 \cdot n \cdot k_c}$$

Equation (53)

$\frac{F_t^{pl,j} - F_t^{pl,j-1}}{k_H^{pl,j}} = \frac{q \cdot h}{n \cdot k_c}$ is established in Equation (46) of this Appendix

Equation (53) can be developed.

$$\Delta_h^{u,IV} = \Delta_{h,t}^{pl,1} + \sum_{j=2}^{\hat{j}-1} \frac{F_t^{pl,j} - F_t^{pl,j-1}}{k_H^{pl,j}} + \frac{h}{\hat{j} \cdot b} \cdot \left(d_{u,h} - V_0^{pl,\hat{j}}\right)$$

$$\Delta_h^{u,IV} = \frac{h}{b}\left(\frac{r_h}{k_h} + \frac{R_{c,1}}{n \cdot k_c}\right) + \sum_{j=2}^{\hat{j}-1} \frac{q \cdot h}{n \cdot k_c} + \frac{h}{\hat{j} \cdot b} \cdot \left(d_{u,h} - V_0^{pl,\hat{j}}\right)$$

$$\Delta_h^{u,IV} = \frac{h}{b}\left(\frac{r_h}{k_h} + \frac{R_{c,1}}{n \cdot k_c}\right) + \frac{(\hat{j} - 2) q \cdot h}{n \cdot k_c} + \frac{h}{\hat{j} \cdot b} \cdot \left(d_{u,h} - V_0^{pl,\hat{j}}\right)$$

$$\Delta_h^{u,IV} = \frac{r_h \cdot h}{b \cdot n \cdot k_c} + \frac{q \cdot h}{n \cdot k_c} + \frac{(\hat{j} - 2) q \cdot h}{n \cdot k_c} + \frac{h}{\hat{j} \cdot b} \cdot \left(d_{u,h} - \frac{r_h}{n \cdot k_c} - \frac{\hat{j} \cdot (\hat{j} - 1) \cdot q \cdot b}{2 \cdot n \cdot k_c}\right)$$

$$\Delta_h^{u,IV} = \frac{r_h \cdot h}{b \cdot n \cdot k_c} + \frac{(\hat{j} - 1) q \cdot h}{n \cdot k_c} + \frac{d_{u,h} \cdot h}{\hat{j} \cdot b} - \frac{r_h \cdot h}{\hat{j} \cdot b \cdot n \cdot k_c} - \frac{(\hat{j} - 1) \cdot q \cdot h}{2 \cdot n \cdot k_c}$$

$$\Delta_h^{u,IV} = \frac{r_h \cdot h}{b \cdot n \cdot k_c} + \frac{(\hat{j} - 1) q \cdot h}{2 \cdot n \cdot k_c} + \frac{d_{u,h} \cdot h}{\hat{j} \cdot b} - \frac{r_h \cdot h}{\hat{j} \cdot b \cdot n \cdot k_c}$$

$$\Delta_h^{u,IV} = \frac{h}{b \cdot \hat{j}} \cdot \left[d_{u,h} + \frac{(\hat{j}\ - 1) \cdot r_h}{n \cdot k_c} + \frac{q \cdot b \cdot \hat{j}}{2 \cdot n \cdot k_c} (\hat{j} - 1) \right]$$

Equation (55)

$V_{\mathrm{c}}^{el,1} = \frac{r_h}{k_h}$ and $v_{\mathrm{c}}^{pl,1} = \frac{1}{n \cdot k_c} \cdot (r_h + q \cdot b) - \frac{r_h}{k_h}$ are established in Equation (35) of this Appendix.

$v_{\mathrm{c}}^{pl,j^*} = \frac{j^* \cdot q \cdot b}{n \cdot k_c}$ is established in Equation (49) of this Appendix.

$V_0^{el,1} = \frac{r_h}{k_h}$ and $v_0^{pl,1} = \frac{1}{n \cdot k_c} \cdot (r_h + q \cdot b) - \frac{r_h}{k_h}$ are established in Equation (30) of this Appendix.

$v_0^{pl,j^*} = \frac{j^* \cdot q \cdot b}{n \cdot k_c}$ is established in Equation (49) of this Appendix.

$$d_{u,h} > V_0^{el,1} + v_0^{pl,1} + \sum_{j=2}^{j^*-1} v_0^{pl,j} + v_0^{pl,j^*} \cdot \frac{d_{y,c} - \left(V_{\mathrm{c}}^{el,1} + v_{\mathrm{c}}^{pl,1} + \sum_{j=2}^{j^*-1} v_{\mathrm{c}}^{pl,j} \right)}{v_{\mathrm{c}}^{pl,j^*}}$$

$$d_{u,h} > \frac{r_h}{n \cdot k_c} + \frac{q \cdot b}{n \cdot k_c} + \sum_{j=2}^{j^*-1} \frac{j \cdot q \cdot b}{n \cdot k_c} + \frac{j^* \cdot q \cdot b}{n \cdot k_c} \cdot \frac{d_{y,c} - \left(\frac{r_h}{n \cdot k_c} + \sum_{j=1}^{j^*-1} \frac{q \cdot b}{n \cdot k_c} \right)}{\frac{q \cdot b}{n \cdot k_c}}$$

$$d_{u,h} > \frac{r_h}{n \cdot k_c} + \frac{q \cdot b}{n \cdot k_c} + \frac{(j^* - 1) \cdot j^* \cdot q \cdot b}{2 \cdot n \cdot k_c} - \frac{q \cdot b}{n \cdot k_c} + j^* \cdot \left[d_{y,c} - \frac{r_h}{n \cdot k_c} - \frac{(j^* - 1) \cdot q \cdot b}{n \cdot k_c} \right]$$

$$d_{u,h} > \frac{r_h}{n \cdot k_c} + \frac{(j^* - 1) \cdot j^* \cdot q \cdot b}{2 \cdot n \cdot k_c} + j^* \cdot d_{y,c} - \frac{j^* \cdot r_h}{n \cdot k_c} - \frac{(j^* - 1) \cdot q \cdot b \cdot j^*}{n \cdot k_c}$$

$$d_{u,h} > \frac{r_h}{n \cdot k_c} (1 - j^*) - \frac{(j^* - 1) \cdot j^* \cdot q \cdot b}{2 \cdot n \cdot k_c} + j^* \cdot d_{y,c}$$

Equation (56)

$V_{\mathrm{c}}^{el,1} = \frac{r_h}{k_h}$ and $v_{\mathrm{c}}^{pl,1} = \frac{1}{n \cdot k_c} \cdot (r_h + q \cdot b) - \frac{r_h}{k_h}$ are established in Equation (35) of this Appendix.

$v_{\mathrm{c}}^{pl,j^*} = \frac{j^* \cdot q \cdot b}{n \cdot k_c}$ is established in Equation (49) of this Appendix.

$$V_{\mathrm{c}}^{pl,1} + \sum_{j=2}^{j^*-1} v_{\mathrm{c}}^{pl,j^*} < d_{y,c} < V_{\mathrm{c}}^{pl,1} + \sum_{j=2}^{j^*} v_{\mathrm{c}}^{pl,j^*}$$

$$\frac{1}{n \cdot k_c} \cdot (r_h + q \cdot b) + \sum_{j=2}^{j^*-1} \frac{q \cdot b}{n \cdot k_c} < d_{y,c} < \frac{1}{n \cdot k_c} \cdot (r_h + q \cdot b) + \sum_{j=2}^{j^*} \frac{q \cdot b}{n \cdot k_c}$$

$$\frac{1}{n \cdot k_c} (r_h + (j^* - 1) qb) < d_{y,c} < \frac{1}{n \cdot k_c} (r_h + j^* qb)$$

Equation (57)

$V_{\mathrm{c}}^{el,1} = \frac{r_h}{k_h}$ and $v_{\mathrm{c}}^{pl,1} = \frac{1}{n \cdot k_c} \cdot (r_h + q \cdot b) - \frac{r_h}{k_h}$ are established in Equation (35) of this Appendix.

$v_{\mathrm{c}}^{pl,j^*} = \frac{j^* \cdot q \cdot b}{n \cdot k_c}$ is established in Equation (49) of this Appendix.

$$R_w^{pl,V} = R_w^{pl,VI} = F_t^{pl,1} + \sum_{j=2}^{\hat{j}-1} \frac{q \cdot b^2}{h} (m - j) + \left(\frac{d_{y,c} - V_c^{pl,\hat{j}}}{v_{\mathrm{c}}^{pl,\hat{j}}} \right) \cdot \frac{q \cdot b^2}{h} (m - \hat{j})$$

$$R_w^{pl,V} = R_w^{pl,VI} = F_t^{pl,1} + \sum_{j=2}^{\hat{j}-1} \frac{q \cdot b^2}{h} (m - j) + \left(\frac{d_{y,c} - V_c^{pl,\hat{j}}}{\left(\frac{q \cdot b}{n \cdot k_c} \right)} \right) \cdot \frac{q \cdot b^2}{h} (m - \hat{j})$$

$$R_w^{pl,V} = R_w^{pl,VI} = \frac{r_h \cdot b \cdot m}{h} + \frac{q \cdot b^2}{2h} \cdot (3m-2) + \frac{q \cdot b^2 \cdot m \cdot (\hat{j}-2)}{h} - \frac{q \cdot b^2 \cdot \hat{j}(\hat{j}-1)}{2h}$$
$$+ \frac{q \cdot b^2}{h} + \frac{q \cdot b^2 \cdot (m - \hat{j})}{h} \cdot \frac{n \cdot k_c}{q \cdot b} \left(\frac{r_c}{k_c} - \frac{1}{n \cdot k_c} [r_h + q \cdot b(\hat{j}-1)] \right)$$

$$R_w^{pl,V} = R_w^{pl,VI} = \frac{r_h \cdot b \cdot m}{h} + \frac{q \cdot b^2}{2h} \cdot (3m-2) + \frac{q \cdot b^2 \cdot m \cdot (\hat{j}-2)}{h} - \frac{q \cdot b^2 \cdot \hat{j}(\hat{j}-1)}{2h}$$
$$+ \frac{q \cdot b^2}{h} + \frac{b \cdot (m - \hat{j}) \cdot n \cdot k_c}{h} \cdot \left(\frac{r_c}{k_c} - \frac{1}{n \cdot k_c} [r_h + q \cdot b(\hat{j}-1)] \right)$$

$$R_w^{pl,V} = R_w^{pl,VI} = \frac{r_h \cdot b \cdot m}{h} + \frac{q \cdot b^2}{2h} \cdot (3m-2) + \frac{q \cdot b^2 \cdot m \cdot (\hat{j}-2)}{h} - \frac{q \cdot b^2 \cdot \hat{j}(\hat{j}-1)}{2h}$$
$$+ \frac{q \cdot b^2}{2} + \frac{b \cdot (m - \hat{j}) \cdot n \cdot r_c}{h} - \frac{r_h \cdot b \cdot (m - \hat{j})}{h} - \frac{b^2 \cdot q \cdot (\hat{j}-1)(m - \hat{j})}{h}$$

$$R_w^{pl,V} = R_w^{pl,VI} = \frac{r_h \cdot b}{h} [\hat{j}] + \frac{n \cdot r_c \cdot b}{h} [m - \hat{j}] + \frac{q \cdot b^2}{2 \cdot h} (m - \hat{j} + \hat{j}^2)$$

Equation (58)

$V_c^{el,1} = \frac{r_h}{k_h}$ and $v_c^{pl,1} = \frac{1}{n \cdot k_c} \cdot (r_h + q \cdot b) - \frac{r_h}{k_h}$ are established in Equation (35) of this Appendix.

$v_c^{pl,j^*} = \frac{j^* \cdot q \cdot b}{n \cdot k_c}$ is established in Equation (49) of this Appendix.

$$V_c^{pl,\hat{j}} = V_c^{el,1} + v_c^{pl,1} + \sum_{j=2}^{\hat{j}-1} v_c^{pl,j}$$

$$V_c^{pl,\hat{j}} = \frac{1}{n \cdot k_c} \cdot (r_h + q \cdot b) + \sum_{j=2}^{\hat{j}-1} \frac{q \cdot b}{n \cdot k_c}$$

$$V_c^{pl,\hat{j}} = \frac{1}{n \cdot k_c} \cdot (r_h + q \cdot b) + \frac{(\hat{j}-1) \cdot q \cdot b}{n \cdot k_c}$$

$$V_c^{pl,\hat{j}} = \frac{1}{n \cdot k_c}[r_h + q \cdot b(\hat{j}-1)]$$

Equation (61)

$\frac{F_t^{pl,j} - F_t^{pl,j-1}}{k_H^{pl,j}} = \frac{q \cdot h}{n \cdot k_c}$ is established in Equation (46) of this Appendix

$$\Delta_h^{u,VI} = \Delta_{h,t}^{pl,1} + \sum_{j=2}^{\hat{j}-1} \frac{F_t^{pl,j} - F_t^{pl,j-1}}{k_H^{pl,j}} + \frac{h}{\hat{j} \cdot b} \cdot \left(d_{u,h} - V_0^{pl,\hat{j}}\right)$$

$$\Delta_h^{u,IV} = \frac{h}{b}\left(\frac{r_h}{k_h} + \frac{R_{c,1}}{n \cdot k_c}\right) + \sum_{j=2}^{\hat{j}-1} \frac{q \cdot h}{n \cdot k_c} + \frac{h}{\hat{j} \cdot b} \cdot \left(d_{u,h} - V_0^{pl,\hat{j}}\right)$$

$$\Delta_h^{u,IV} = \frac{h}{b}\left(\frac{r_h}{k_h} + \frac{R_{c,1}}{n \cdot k_c}\right) + \frac{(\hat{j}-2) \cdot q \cdot h}{n \cdot k_c} + \frac{h}{\hat{j} \cdot b}\left(d_{u,h} - \frac{r_h}{n \cdot k_c} - \frac{\hat{j} \cdot (\hat{j}-1) \cdot q \cdot b}{2 \cdot n \cdot k_c}\right)$$

$$\Delta_h^{u,IV} = \frac{h \cdot r_h}{b \cdot n \cdot k_c} + \frac{q \cdot h}{n \cdot k_c} + \frac{(\hat{j}-2) \cdot q \cdot h}{n \cdot k_c} + \frac{h}{\hat{j} \cdot b}\left(d_{u,h} - \frac{r_h}{n \cdot k_c} - \frac{\hat{j} \cdot (\hat{j}-1) \cdot q \cdot b}{2 \cdot n \cdot k_c}\right)$$

$$\Delta_h^{u,IV} = \frac{h \cdot r_h}{b \cdot n \cdot k_c} + \frac{(\hat{j}-1) \cdot q \cdot h}{n \cdot k_c} + \frac{h \cdot d_{u,h}}{\hat{j} \cdot b} - \frac{h \cdot r_h}{\hat{j} \cdot b \cdot n \cdot k_c} - \frac{h \cdot q \cdot (\hat{j}-1)}{2 \cdot n \cdot k_c}$$

$$\Delta_h^{u,IV} = \frac{h \cdot r_h}{b \cdot n \cdot k_c} + \frac{q \cdot h \cdot (\hat{j}-1)}{2 \cdot n \cdot k_c} + \frac{h \cdot d_{u,h}}{\hat{j} \cdot b} - \frac{h \cdot r_h}{\hat{j} \cdot b \cdot n \cdot k_c}$$

$$\Delta_h^{u,VI} = \frac{h}{b \cdot \hat{j}} \cdot \left[d_{u,h} + \tilde{k}(\hat{j}-1)d_{y,h} + \frac{q \cdot b \cdot \hat{j}}{2 \cdot n \cdot k_c}(\hat{j}-1)\right]$$

Equation (65)

$\frac{F_t^{pl,j}-F_t^{pl,j-1}}{k_H^{pl,j}}=\frac{q\cdot h}{n\cdot k_c}$ is established in Equation (46) of this Appendix

$$\Delta_h^{pl,VII}=\Delta_{h,t}^{pl,1}+\sum_{j=2}^{m-1}\frac{F_t^{pl,j}-F_t^{pl,j-1}}{k_H^{pl,j}}$$

$$\Delta_h^{pl,VII}=\frac{h}{b\cdot n\cdot k_c}\cdot(r_h+qb)+\sum_{j=2}^{m-1}\frac{q\cdot h}{n\cdot k_c}$$

$$\Delta_h^{pl,VII}=\frac{r_h\cdot h}{b\cdot n\cdot k_c}+\frac{q\cdot h}{n\cdot k_c}+\sum_{j=2}^{m-1}\frac{q\cdot h}{n\cdot k_c}$$

$$\Delta_h^{pl,VII}=\frac{r_h\cdot h}{b\cdot n\cdot k_c}+\sum_{j=1}^{m-1}\frac{q\cdot h}{n\cdot k_c}$$

$$\Delta_h^{pl,VII}=\frac{r_h\cdot h}{b\cdot n\cdot k_c}+\frac{(m-1)q\cdot h}{n\cdot k_c}$$

$$\Delta_h^{pl,VII}=\frac{h}{b}\cdot\frac{r_h}{n\cdot k_c}+\frac{q\cdot h\cdot(m-1)}{n\cdot k_c}$$

Equation (66)

$V_{\mathrm{c}}^{el,1}=\frac{r_h}{k_h}$ and $v_{\mathrm{c}}^{pl,1}=\frac{1}{n\cdot k_c}\cdot(r_h+q\cdot b)-\frac{r_h}{k_h}$ are established in Equation (35) of this Appendix.

$v_{\mathrm{c}}^{pl,j^*}=\frac{j^*\cdot q\cdot b}{n\cdot k_c}$ is established in Equation (49) of this Appendix.

The panel joint between the $m-1^{\text{th}}$ and m^{th} panels must remain elastic until achieving SW behaviour.

$$d_{y,c} \geq V_{\text{c}}^{el,1} + v_{\text{c}}^{pl,1} + \sum_{j=2}^{m-1} v_{\text{c}}^{pl,j}$$

$$d_{y,c} \geq \frac{1}{n \cdot k_c} \cdot (r_h + q \cdot b) + \sum_{j=2}^{m-1} \frac{q \cdot b}{n \cdot k_c}$$

$$d_{y,c} \geq \frac{1}{n \cdot k_c} [r_h + q \cdot b \cdot (m-1)]$$

Equation (67)

$V_0^{el,1} = \frac{r_h}{k_h}$ and $v_0^{pl,1} = \frac{1}{n \cdot k_c} \cdot (r_h + q \cdot b) - \frac{r_h}{k_h}$ are established in Equation (30) of this Appendix.

$v_0^{pl,j^*} = \frac{j^* \cdot q \cdot b}{n \cdot k_c}$ is established in Equation (49) of this Appendix.

$$V_0^{pl,m} = V_0^{el,1} + v_0^{pl,1} + \sum_{j=2}^{m-1} v_0^{pl,j}$$

$$V_0^{pl,m} = \frac{1}{n \cdot k_c} (r_h + qb) + \sum_{j=2}^{m-1} \frac{j \cdot q \cdot b}{n \cdot k_c}$$

$$V_0^{pl,m} = \frac{1}{n \cdot k_c} \left[r_h + \frac{q \cdot b \cdot m \cdot (m-1)}{2} \right]$$

Equation (69)

$\frac{F_t^{pl,j} - F_t^{pl,j-1}}{k_H^{pl,j}} = \frac{q \cdot h}{n \cdot k_c}$ is established in Equation (46) of this Appendix

$$\Delta_h^{u,VII} = \Delta_{h,t}^{pl,1} + \sum_{j=2}^{m-1} \frac{F_t^{pl,j} - F_t^{pl,j-1}}{k_H^{pl,j}} + \frac{h}{m \cdot b} \cdot \left(d_{u,h} - V_0^{pl,m} \right)$$

$$\Delta_h^{u,VII} = \frac{h}{b \cdot n \cdot k_c} \cdot (r_h + qb) + \sum_{j=2}^{m-1} \frac{q \cdot h}{n \cdot k_c} + \frac{h}{m \cdot b} \cdot \left(d_{u,h} - V_0^{pl,m}\right)$$

$$\Delta_h^{u,VII} = \frac{r_h \cdot h}{b \cdot n \cdot k_c} + \frac{q \cdot h}{n \cdot k_c} + \sum_{j=2}^{m-1} \frac{q \cdot h}{n \cdot k_c} + \frac{h}{m \cdot b} \cdot \left(d_{u,h} - V_0^{pl,m}\right)$$

$$\Delta_h^{u,VII} = \frac{r_h \cdot h}{b \cdot n \cdot k_c} + \sum_{j=1}^{m-1} \frac{q \cdot h}{n \cdot k_c} + \frac{h}{m \cdot b} \cdot \left(d_{u,h} - V_0^{pl,m}\right)$$

$$\Delta_h^{u,VII} = \frac{r_h \cdot h}{b \cdot n \cdot k_c} + \frac{(m-1) \cdot q \cdot h}{n \cdot k_c} + \frac{h}{m \cdot b} \cdot \left(d_{u,h} - \frac{1}{n \cdot k_c}\left[r_h + \frac{q \cdot b \cdot m \cdot (m-1)}{2}\right]\right)$$

$$\Delta_h^{u,VII} = \frac{h}{m \cdot b} \cdot d_{u,h} - \frac{r_h \cdot h}{m \cdot b \cdot n \cdot k_c} - \frac{q \cdot (m-1) \cdot h}{2 \cdot n \cdot k_c} + \frac{r_h \cdot h}{b \cdot n \cdot k_c} + \frac{(m-1) \cdot q \cdot h}{n \cdot k_c}$$

$$\Delta_h^{u,VII} = \frac{h}{m \cdot b} \cdot d_{u,h} - \frac{r_h \cdot h}{m \cdot b \cdot n \cdot k_c} + \frac{r_h \cdot h}{b \cdot n \cdot k_c} + \frac{(m-1) \cdot q \cdot h}{2 \cdot n \cdot k_c}$$

$$\Delta_h^{u,VII} = \frac{h}{m \cdot b} \cdot d_{u,h} - \frac{r_h \cdot h}{m \cdot b \cdot n \cdot k_c} + \frac{m \cdot r_h \cdot h}{m \cdot b \cdot n \cdot k_c} + \frac{(m-1) \cdot q \cdot h}{2 \cdot n \cdot k_c}$$

$$\Delta_h^{u,VII} = \frac{h}{m \cdot b} \cdot d_{u,h} + \frac{(m-1) \cdot r_h \cdot h}{m \cdot b \cdot n \cdot k_c} + \frac{(m-1) \cdot q \cdot h}{2 \cdot n \cdot k_c}$$

$$\Delta_h^{u,VII} = \frac{h}{m \cdot b} \cdot d_{u,h} - \frac{h(m-1)}{m \cdot b} \frac{r_h}{n \cdot k_c} + \frac{q \cdot h \cdot (m-1)}{2 \cdot n \cdot k_c}$$

Equation (90)

Achieving the yielding of the hold-down in kinematic mode j̃ ensures the $V_0^{el,\tilde{j}} = d_{y,h}$. The increase of hold-down elongation to fully develop kinematic mode j̃ in plastic state is developed according to the equation in Casagrande et al. (2017):

$$v_0^{pl,\tilde{\jmath}} = \frac{\tilde{\jmath}}{[(\tilde{\jmath} + m \cdot \tilde{\jmath} - m) \cdot k_h + (m - \tilde{\jmath}) \cdot n \cdot k_c]} \left(\left(\frac{R_{c,\tilde{\jmath}} \cdot b \cdot (m - \tilde{\jmath})}{h} \right) \cdot \frac{h}{b} - \frac{q \cdot m \cdot h}{2} \right)$$

$$v_0^{pl,\tilde{\jmath}} = \frac{\tilde{\jmath}}{[(\tilde{\jmath} + m \cdot \tilde{\jmath} - m) \cdot k_h + (m - \tilde{\jmath}) \cdot n \cdot k_c]} \left(\left(\frac{R_{c,\tilde{\jmath}} \cdot b \cdot (m - \tilde{\jmath})}{h} \right) \cdot \frac{h}{b} - 0 \right)$$

$$v_0^{pl,\tilde{\jmath}} = \frac{\tilde{\jmath}}{[(m - \tilde{\jmath}) \cdot n \cdot k_c]} \left(\left(\frac{R_{c,\tilde{\jmath}} \cdot b \cdot (m - \tilde{\jmath})}{h} \right) \cdot \frac{h}{b} - 0 \right)$$

$$v_0^{pl,\tilde{\jmath}} = \frac{\tilde{\jmath} \cdot R_{c,\tilde{\jmath}}}{n \cdot k_c}$$

Therefore, Equation (90) is written as:

$$V_0^{pl,\tilde{\jmath}} = V_0^{el,\tilde{\jmath}} + v_0^{pl,\tilde{\jmath}}$$

$$V_0^{pl,\tilde{\jmath}} = d_{y,h} + \frac{\tilde{\jmath} \cdot R_{c,\tilde{\jmath}}}{n \cdot k_c}$$

Equation (96)

$$v_{\mathrm{c}}^{pl,\tilde{\jmath}} = \frac{1}{[(\tilde{\jmath} + m \cdot \tilde{\jmath} - m) \cdot k_h + (m - \tilde{\jmath}) \cdot n \cdot k_c]} \left(\left(\frac{R_{c,\tilde{\jmath}} \cdot b \cdot (m - \tilde{\jmath})}{h} \right) \cdot \frac{h}{b} - \frac{q \cdot m \cdot h}{2} \right)$$

$$v_{\mathrm{c}}^{pl,\tilde{\jmath}} = \frac{1}{[(m - \tilde{\jmath}) \cdot n \cdot k_c]} \left(\left(\frac{R_{c,\tilde{\jmath}} \cdot b \cdot (m - \tilde{\jmath})}{h} \right) \cdot \frac{h}{b} - 0 \right)$$

$$v_{\mathrm{c}}^{pl,\tilde{\jmath}} = \frac{R_{c,\tilde{\jmath}}}{n \cdot k_c}$$

Equation (96) can be develop as:

$$d_{y,c} < V_c^{el,\tilde{\jmath}} + v_{\mathrm{c}}^{pl,\tilde{\jmath}}$$

$$d_{y,c} < V_c^{el,\tilde{\jmath}} + \frac{R_{c,\tilde{\jmath}}}{n \cdot k_c}$$

Equation (97)

$V_c^{el,\tilde{\jmath}}$ and $v_c^{pl,\tilde{\jmath}} = \frac{R_{c,\tilde{\jmath}}}{n \cdot k_c}$ are established in Equation (96) of this Appendix.

$V_0^{el,\tilde{\jmath}} = d_{y,h}$ and $v_0^{pl,\tilde{\jmath}} = \frac{\tilde{\jmath} \cdot R_{c,\tilde{\jmath}}}{n \cdot k_c}$ are established in Equation (90) of this Appendix

The elongation in kinematic mode $\tilde{\jmath}$ until the yielding of vertical joints is written as an interpolation:

$$d_{u,h} > V_0^{el,\tilde{\jmath}} + v_0^{pl,\tilde{\jmath}} \cdot \frac{d_{y,c} - V_c^{el,\tilde{\jmath}}}{v_c^{pl,\tilde{\jmath}}}$$

$$d_{u,h} > V_0^{el,\tilde{\jmath}} + \frac{\tilde{\jmath} \cdot R_{c,\tilde{\jmath}}}{n \cdot k_c} \cdot \frac{d_{y,c} - V_c^{el,\tilde{\jmath}}}{\frac{R_{c,\tilde{\jmath}}}{n \cdot k_c}}$$

$$d_{u,h} > d_{y,h} + \tilde{\jmath} \cdot \left(d_{y,c} - V_c^{el,\tilde{\jmath}}\right)$$

Equation (98)

$V_c^{el,\tilde{\jmath}}$ and $v_c^{pl,\tilde{\jmath}} = \frac{R_{c,\tilde{\jmath}}}{n \cdot k_c}$ are established in Equation (96) of this Appendix.

$v_c^{pl,j^*} = \frac{q \cdot b}{n \cdot k_c}$ is established in Equation (49) of this Appendix.

$$R_w^{pl,II} = R_w^{pl,III} = R_{w,h}^{el,\tilde{\jmath}} + \left(F_t^{pl,\tilde{\jmath}} - R_{w,h}^{el,\tilde{\jmath}}\right) \cdot \frac{\left(d_{y,c} - V_c^{el,\tilde{\jmath}}\right)}{v_c^{pl,\tilde{\jmath}}}$$

$$R_w^{pl,II} = R_w^{pl,III} = R_{w,h}^{el,\tilde{\jmath}} + \left(F_t^{pl,\tilde{\jmath}} - R_{w,h}^{el,\tilde{\jmath}}\right) \cdot \frac{\left(d_{y,c} - V_c^{el,\tilde{\jmath}}\right)}{\frac{R_{c,\tilde{\jmath}}}{n \cdot k_c}}$$

$$R_w^{pl,II} = R_w^{pl,III} = R_{w,h}^{el,\tilde{\jmath}} + \left(F_t^{pl,\tilde{\jmath}} - R_{w,h}^{el,\tilde{\jmath}}\right) \cdot \frac{n \cdot k_c \left(d_{y,c} - V_c^{el,\tilde{\jmath}}\right)}{R_{c,\tilde{\jmath}}}$$

Equation (107)

It can be established that the change in generic kinematic mode j^* will increase the lateral displacement of the wall by the following:

$$\frac{F_t^{pl,j} - F_t^{pl,j-1}}{k_H^{pl,j}} = \left[\frac{q \cdot b^2}{h}(m - j^*)\right] \cdot \frac{h^2}{(m - j^*) \cdot n \cdot k_c \cdot b^2}$$

$$\frac{F_t^{pl,j} - F_t^{pl,j-1}}{k_H^{pl,j}} = \frac{q \cdot h}{n \cdot k_c}$$

Therefore, Equation (107) takes the following form:

$$\Delta_{h,t}^{pl,j^*} = \Delta_h^{el} + \frac{R_{c,\tilde{\jmath}} \cdot h}{n \cdot k_c \cdot b} + \sum_{j=\tilde{\jmath}+1}^{j^*} \frac{q \cdot h}{n \cdot k_c}$$

Equation (108)

$V_c^{el,\tilde{\jmath}}$ and $v_c^{pl,\tilde{\jmath}} = \frac{R_{c,\tilde{\jmath}}}{n \cdot k_c}$ are established in Equation (96) of this Appendix.

$V_0^{el,\tilde{\jmath}} = d_{y,h}$ and $v_0^{pl,\tilde{\jmath}} = \frac{\tilde{\jmath} \cdot R_{c,\tilde{\jmath}}}{n \cdot k_c}$ are established in Equation (90) of this Appendix

To develop this equation, it is required to know the incremental displacement of hold-down required for the development of kinematic mode larger than j̃.

$$v_0^{pl,j^*} = \frac{j^* \cdot b}{k_h'^{\;pl,j^*} \cdot h}\left(\frac{\left(F_t^{pl,j^*} - F_t^{pl,j^*-1}\right) \cdot h^2}{b^2} - \frac{q \cdot m \cdot h}{2}\right)$$

$$v_0^{pl,j^*} = \frac{j^* \cdot q \cdot b}{n \cdot k_c}$$

The incremental of elongation through kinematic mode j^* can be develop as:

$$v_{\mathrm{c}}^{pl,j^*} = \frac{b}{k_h'^{\,pl,j^*} \cdot h}\left(\frac{\left(F_t^{pl,j^*} - F_t^{pl,j^*-1}\right) \cdot h^2}{b^2} - \frac{q \cdot m \cdot h}{2}\right)$$

$$v_{\mathrm{c}}^{pl,j^*} = \frac{b}{(m - j^*) \cdot n \cdot k_c \cdot h}\left(\frac{h^2}{b^2}\left(\frac{q \cdot b^2}{h}(m - j^*)\right) - 0\right)$$

$$v_{\mathrm{c}}^{pl,j^*} = \frac{q \cdot b}{n \cdot k_c}$$

The yielding displacement, in this equation, has to be larger than the elongation required to achieve the ultimate displacement of hold-down in kinematic mode j^*.

$$d_{y,c} > V_c^{el,\tilde{\jmath}} + v_{\mathrm{c}}^{pl,\tilde{\jmath}} + \sum_{j=\tilde{\jmath}+1}^{j^*-1} v_{\mathrm{c}}^{pl,j} + v_{\mathrm{c}}^{pl,j^*} \cdot \frac{d_{u,h} - V_0^{el,\tilde{\jmath}} - v_0^{pl,\tilde{\jmath}} - \sum_{j=\tilde{\jmath}+1}^{j^*-1} v_0^{pl,j}}{v_0^{pl,j^*}}$$

$$d_{y,c} > V_c^{el,\tilde{\jmath}} + v_{\mathrm{c}}^{pl,\tilde{\jmath}} + \sum_{j=\tilde{\jmath}+1}^{j^*-1} \frac{q \cdot b}{n \cdot k_c} + \frac{q \cdot b}{n \cdot k_c} \cdot \frac{d_{u,h} - d_{y,h} - \frac{\tilde{\jmath} \cdot R_{c,\tilde{\jmath}}}{n \cdot k_c} - \sum_{j=\tilde{\jmath}+1}^{j^*-1} \frac{j \cdot q \cdot b}{n \cdot k_c}}{\frac{j^* \cdot q \cdot b}{n \cdot k_c}}$$

$$d_{y,c} > V_c^{el,\tilde{\jmath}} + \frac{R_{c,\tilde{\jmath}}}{n \cdot k_c} + \sum_{j=\tilde{\jmath}+1}^{j^*-1} \frac{q \cdot b}{n \cdot k_c} + \frac{1}{j^*} \cdot \left[d_{u,h} - d_{y,h} - \frac{\tilde{\jmath} \cdot R_{c,\tilde{\jmath}}}{n \cdot k_c} - \sum_{j=\tilde{\jmath}+1}^{j^*-1} \frac{j \cdot q \cdot b}{n \cdot k_c}\right]$$

Equation (109)

$V_0^{el,\tilde{\jmath}} = d_{y,h}$ and $v_0^{pl,\tilde{\jmath}} = \frac{\tilde{\jmath} \cdot R_{c,\tilde{\jmath}}}{n \cdot k_c}$ are established in Equation (90) of this Appendix

$v_0^{pl,j^*} = \frac{j^* \cdot q \cdot b}{n \cdot k_c}$ is established in Equation (108) of this Appendix.

$$V_0^{el,\tilde{\jmath}} + v_0^{pl,\tilde{\jmath}} + \sum_{j=\tilde{\jmath}+1}^{j^*-1} v_0^{pl,j} \leq d_{u,h} < V_0^{el,\tilde{\jmath}} + v_0^{pl,\tilde{\jmath}} + \sum_{j=\tilde{\jmath}+1}^{j^*} v_0^{pl,j}$$

$$d_{y,h} + \frac{\tilde{\jmath} \cdot R_{c,\tilde{\jmath}}}{n \cdot k_c} + \sum_{j=\tilde{\jmath}+1}^{j^*-1} \frac{j \cdot q \cdot b}{n \cdot k_c} \leq d_{u,h} < d_{y,h} + \frac{\tilde{\jmath} \cdot R_{c,\tilde{\jmath}}}{n \cdot k_c} + \sum_{j=\tilde{\jmath}+1}^{j^*} \frac{j \cdot q \cdot b}{n \cdot k_c}$$

Equation (111)

$V_0^{el,\tilde{\jmath}} = d_{y,h}$ and $v_0^{pl,\tilde{\jmath}} = \frac{\tilde{\jmath} \cdot R_{c,\tilde{\jmath}}}{n \cdot k_c}$ are established in Equation (90) of this Appendix

$v_0^{pl,j^*} = \frac{j^* \cdot q \cdot b}{n \cdot k_c}$ is established in Equation (108) of this Appendix.

$$V_0^{pl,\hat{\jmath}} = V_0^{el,\tilde{\jmath}} + v_0^{pl,\tilde{\jmath}} + \sum_{j=\tilde{\jmath}+1}^{\hat{\jmath}-1} v_0^{pl,j}$$

$$V_0^{pl,\hat{\jmath}} = d_{y,h} + \frac{\tilde{\jmath} \cdot R_{c,\tilde{\jmath}}}{n \cdot k_c} + \sum_{j=\tilde{\jmath}+1}^{\hat{\jmath}-1} \frac{j \cdot q \cdot b}{n \cdot k_c}$$

Equation (112)

$\frac{F_t^{pl,j} - F_t^{pl,j-1}}{k_H^{pl,j}} = \frac{q \cdot h}{n \cdot k_c}$ is established in Equation (107) of this Appendix

$$\Delta_h^{u,IV} = \Delta_h^{pl,IV} = \Delta_h^{el} + \frac{R_{c,\tilde{\jmath}} \cdot h}{n \cdot k_c \cdot b} + \sum_{j=\tilde{\jmath}+1}^{\hat{\jmath}-1} \frac{q \cdot h}{n \cdot k_c} + \frac{h}{\hat{\jmath} \cdot b}\left(d_{u,h} - V_0^{pl,\hat{\jmath}}\right)$$

Equation (114)

$V_c^{el,\tilde{\jmath}}$ and $v_c^{pl,\tilde{\jmath}} = \frac{R_{c,\tilde{\jmath}}}{n \cdot k_c}$ are established in Equation (96) of this Appendix.

$v_{\mathrm{c}}^{pl,j^*} = \frac{q \cdot b}{n \cdot k_c}$ is established in Equation (108) of this Appendix.

$V_0^{el,\tilde{\jmath}} = d_{y,h}$ and $v_0^{pl,\tilde{\jmath}} = \frac{\tilde{\jmath} \cdot R_{c,\tilde{\jmath}}}{n \cdot k_c}$ are established in Equation (90) of this Appendix

$v_0^{pl,j^*} = \frac{j^* \cdot q \cdot b}{n \cdot k_c}$ is established in Equation (108) of this Appendix.

$$d_{u,h} > V_0^{el,\tilde{\jmath}} + v_0^{pl,\tilde{\jmath}} + \sum_{j=\tilde{\jmath}+1}^{j^*-1} v_0^{pl,\mathrm{j}} + v_0^{pl,j^*} \cdot \frac{d_{y,c} - V_c^{el,\tilde{\jmath}} - v_{\mathrm{c}}^{pl,\tilde{\jmath}} - \sum_{j=\tilde{\jmath}+1}^{j^*-1} v_{\mathrm{c}}^{pl,\mathrm{j}}}{v_{\mathrm{c}}^{pl,j^*}}$$

$$d_{u,h} > d_{y,h} + \frac{\tilde{\jmath} \cdot R_{c,\tilde{\jmath}}}{n \cdot k_c} + \sum_{j=\tilde{\jmath}+1}^{j^*-1} \frac{j \cdot q \cdot b}{n \cdot k_c} + \frac{j^* \cdot q \cdot b}{n \cdot k_c} \cdot \frac{d_{y,c} - V_c^{el,\tilde{\jmath}} - \frac{R_{c,\tilde{\jmath}}}{n \cdot k_c} - \sum_{j=\tilde{\jmath}+1}^{j^*-1} \frac{q \cdot b}{n \cdot k_c}}{\frac{q \cdot b}{n \cdot k_c}}$$

$$d_{u,h} > d_{y,h} + \frac{\tilde{\jmath} \cdot R_{c,\tilde{\jmath}}}{n \cdot k_c} + \sum_{j=\tilde{\jmath}+1}^{j^*-1} \frac{j \cdot q \cdot b}{n \cdot k_c} + j^* \cdot \left[d_{y,c} - V_c^{el,\tilde{\jmath}} - \frac{R_{c,\tilde{\jmath}}}{n \cdot k_c} - \sum_{j=\tilde{\jmath}+1}^{j^*-1} \frac{q \cdot b}{n \cdot k_c} \right]$$

Equation (115)

$V_c^{el,\tilde{\jmath}}$ and $v_{\mathrm{c}}^{pl,\tilde{\jmath}} = \frac{R_{c,\tilde{\jmath}}}{n \cdot k_c}$ are established in Equation (96) of this Appendix.

$v_{\mathrm{c}}^{pl,j^*} = \frac{q \cdot b}{n \cdot k_c}$ is established in Equation (108) of this Appendix.

$$V_c^{el,\tilde{\jmath}} + v_{\mathrm{c}}^{pl,\tilde{\jmath}} + \sum_{j=\tilde{\jmath}+1}^{j^*-1} v_{\mathrm{c}}^{pl,\mathrm{j}} \leq d_{y,c} < V_c^{el,\tilde{\jmath}} + v_{\mathrm{c}}^{pl,\tilde{\jmath}} + \sum_{j=\tilde{\jmath}+1}^{j^*} v_{\mathrm{c}}^{pl,\mathrm{j}}$$

$$V_c^{el,\tilde{\jmath}} + \frac{R_{c,\tilde{\jmath}}}{n \cdot k_c} + \sum_{j=\tilde{\jmath}+1}^{j^*-1} \frac{q \cdot b}{n \cdot k_c} \leq d_{y,c} < V_c^{el,\tilde{\jmath}} + \frac{R_{c,\tilde{\jmath}}}{n \cdot k_c} + \sum_{j=\tilde{\jmath}+1}^{j^*} \frac{q \cdot b}{n \cdot k_c}$$

Equation (117)

$V_c^{el,\tilde{\jmath}}$ and $v_{\mathrm{c}}^{pl,\tilde{\jmath}} = \frac{R_{c,\tilde{\jmath}}}{n \cdot k_c}$ are established in Equation (96) of this Appendix.

$v_{\mathrm{c}}^{pl,j^*} = \frac{q \cdot b}{n \cdot k_c}$ is established in Equation (108) of this Appendix.

$$V_c^{pl,\hat{\jmath}} = V_c^{el,\tilde{\jmath}} + v_{\mathrm{c}}^{pl,\tilde{\jmath}} + \sum_{j=\tilde{\jmath}+1}^{\hat{\jmath}-1} v_{\mathrm{c}}^{pl,\mathrm{j}}$$

$$V_c^{pl,\hat{\jmath}} = V_c^{el,\tilde{\jmath}} + \frac{R_{c,\tilde{\jmath}}}{n \cdot k} + \sum_{\tilde{\jmath}+1}^{\hat{\jmath}-1} \frac{q \cdot b}{n \cdot k_c}$$

Equation (120)

$\frac{F_t^{pl,j} - F_t^{pl,j-1}}{k_H^{pl,j}} = \frac{q \cdot h}{n \cdot k_c}$ is established in Equation (107) of this Appendix

$$\Delta_h^{u,VI} = \Delta_h^{el} + \frac{R_{c,\tilde{\jmath}} \cdot h}{n \cdot k_c \cdot b} + \sum_{j=\tilde{\jmath}+1}^{\hat{\jmath}-1} \frac{q \cdot h}{n \cdot k_c} + \frac{h}{\hat{\jmath} \cdot b}\left(d_{u,h} - V_0^{pl,\hat{\jmath}}\right)$$

Equation (124)

$\frac{F_t^{pl,j} - F_t^{pl,j-1}}{k_H^{pl,j}} = \frac{q \cdot h}{n \cdot k_c}$ is established in Equation (107) of this Appendix

Therefore, Equation (124) is expressed as:

$\Delta_h^{pl,VII} = \Delta_{h,t}^{pl,\tilde{\jmath}} + \sum_{j=\tilde{\jmath}+1}^{m-1} \frac{F_t^{pl,j} - F_t^{pl,j-1}}{k_H^{pl,j}} = \Delta_h^{el} + \frac{R_{c,\tilde{\jmath}} \cdot h}{n \cdot k_c \cdot b} + \sum_{j=\tilde{\jmath}+1}^{m-1} \frac{q \cdot h}{n \cdot k_c}$

Equation (125)

$V_0^{el,\tilde{\jmath}} = d_{y,h}$ and $v_0^{pl,\tilde{\jmath}} = \frac{\tilde{\jmath} \cdot R_{c,\tilde{\jmath}}}{n \cdot k_c}$ are established in Equation (90) of this Appendix

$v_0^{pl,j^*} = \frac{j^* \cdot q \cdot b}{n \cdot k_c}$ is established in Equation (108) of this Appendix.

$$d_{y,c} > V_0^{el,\tilde{j}} + v_0^{pl,\tilde{j}} + \sum_{j=\tilde{j}+1}^{m-1} v_0^{pl,j}$$

$$d_{y,c} > V_c^{el,\tilde{j}} + \frac{R_{c,\tilde{j}}}{n \cdot k_c} + \sum_{j=\tilde{j}+1}^{m-1} \frac{q \cdot b}{n \cdot k_c}$$

Equation (126)

$V_0^{el,\tilde{j}} = d_{y,h}$ and $v_0^{pl,\tilde{j}} = \frac{\tilde{j} \cdot R_{c,\tilde{j}}}{n \cdot k_c}$ are established in Equation (90) of this Appendix

$v_0^{pl,j^*} = \frac{j^* \cdot q \cdot b}{n \cdot k_c}$ is established in Equation (108) of this Appendix.

$$V_0^{pl,m} = d_{y,h} + \frac{\tilde{j} \cdot R_{c,\tilde{j}}}{n \cdot k_c} + \sum_{j=\tilde{j}+1}^{m-1} \frac{j \cdot q \cdot b}{n \cdot k_c}$$

$$V_0^{pl,m} = d_{y,h} + \frac{\tilde{j} \cdot R_{c,\tilde{j}}}{n \cdot k_c} + \sum_{j=\tilde{j}+1}^{m-1} \frac{j \cdot q \cdot b}{n \cdot k_c}$$

Equation (128)

It can be established that the change in generic kinematic mode j^* will increase the lateral displacement of the wall by the following:

$$\frac{F_t^{pl,j} - F_t^{pl,j-1}}{k_H^{pl,j}} = \left[\frac{q \cdot b^2}{h}(m - j^*)\right] \cdot \frac{h^2}{(m - j^*) \cdot n \cdot k_c \cdot b^2}$$

$$\frac{F_t^{pl,j} - F_t^{pl,j-1}}{k_H^{pl,j}} = \frac{q \cdot h}{n \cdot k_c}$$

Therefore, Equation (128) is expressed as:

$$\Delta_h^{u,VII} = \Delta_{h,t}^{pl,\tilde{j}} + \sum_{j=\tilde{j}+1}^{m-1} \frac{q \cdot h}{n \cdot k_c} + \frac{h}{B} \cdot \left(d_{u,h} - V_0^{pl,m}\right)$$

Equation (146)

$$R_w^{pl,II} = R_w^{pl,III} = R_{w,c}^{el,1} + \left(R_w^{pl} - R_{w,c}^{el,1}\right)$$

$$R_w^{pl,II} = R_w^{pl,III} = r_c \cdot \frac{k_h'^{\,el,1} \cdot b}{k_c \cdot h} + \frac{q \cdot m \cdot b^2}{2 \cdot h} + \frac{b}{h} \cdot \left(r_h - \frac{r_c \cdot k_h}{k_c}\right)$$

$$R_w^{pl,II} = R_w^{pl,III} = r_c \cdot \frac{[k_h + (m-1) \cdot n \cdot k_c] \cdot b}{k_c \cdot h} + \frac{q \cdot m \cdot b^2}{2 \cdot h} + \frac{b}{h} \cdot \left(r_h - \frac{r_c \cdot k_h}{k_c}\right)$$

$$R_w^{pl,II} = R_w^{pl,III} = \frac{r_c \cdot [k_h + (m-1) \cdot n \cdot k_c] \cdot b}{k_c \cdot h} + \frac{q \cdot m \cdot b^2}{2 \cdot h} + \frac{r_h \cdot b}{h} - \frac{r_c \cdot b \cdot k_h}{h \cdot k_c}$$

$$R_w^{pl,II} = R_w^{pl,III} = \frac{r_c \cdot k_h \cdot b}{k_c \cdot h} + \frac{r_c \cdot (m-1) \cdot n \cdot k_c \cdot b}{k_c \cdot h} + \frac{q \cdot m \cdot b^2}{2 \cdot h} + \frac{r_h \cdot b}{h} - \frac{r_c \cdot b \cdot k_h}{h \cdot k_c}$$

$$R_w^{pl,II} = R_w^{pl,III} = \frac{r_c \cdot (m-1) \cdot n \cdot b}{h} + \frac{q \cdot m \cdot b^2}{2 \cdot h} + \frac{r_h \cdot b}{h}$$

$$R_w^{pl,II} = R_w^{pl,III} = \frac{b}{h}\left(r_h + r_c \cdot (m-1) \cdot n + \frac{q \cdot m \cdot b}{2}\right)$$

Equation (165)

The elongation of hold-down through kinematic 1 to m is expressed according to Casagrande et al. (2017):

$$V_0^{el,m} = \frac{1}{k_h}\left(\frac{R_{w,c}^{el,m} \cdot h}{b \cdot m} - \frac{q \cdot b \cdot m}{2}\right)$$

Therefore, Equation (165) is expressed as:

$$d_{y,h} > V_0^{el,m} = \frac{1}{k_h}\left(\frac{R_{w,c}^{el,m} \cdot h}{b \cdot m} - \frac{q \cdot b \cdot m}{2}\right)$$

Equation (172)

From Equation (171):

$$r_c = \frac{1}{n} \cdot \left[\frac{R_{w,c}^{el,m} \cdot h}{b \cdot m} - \frac{q \cdot b \cdot \left(m - 2 \cdot (m-2)\right)}{2}\right] + \frac{1}{n} \cdot \frac{f^{pl,m-1} \cdot h}{b \cdot (m-1)}$$

$$n \cdot r_c = \frac{R_{w,c}^{el,m} \cdot h}{b \cdot m} - \frac{q \cdot b \cdot \left(m - 2 \cdot (m-2)\right)}{2} + \frac{f^{pl,m-1} \cdot h}{b \cdot (m-1)}$$

$$\frac{f^{pl,m-1} \cdot h}{b \cdot (m-1)} = n \cdot r_c - \frac{R_{w,c}^{el,m} \cdot h}{b \cdot m} + \frac{q \cdot b \cdot \left(m - 2 \cdot (m-2)\right)}{2}$$

$$f^{pl,m-1} = \frac{b \cdot (m-1) \cdot n \cdot r_c}{h} - \frac{R_{w,c}^{el,m} \cdot (m-1)}{m} + \frac{q \cdot b^2 \cdot (m-1) \cdot (-m+4)}{2 \cdot h}$$

Equation (183)

$V_0^{el,m} = \frac{1}{k_h}\left[\left(\frac{R_{w,c}^{el,m} \cdot h}{b \cdot m} - \frac{q \cdot b \cdot m}{2}\right)\right]$ is established in Equation (165) of this Appendix.

The incremental elongation of hold-down in other kinematic mode j^* is

$$v_0^{pl,j^*} = \frac{1}{k_h}\left[\left(\frac{f^{pl,j^*} \cdot h}{b \cdot m} - \frac{q \cdot b \cdot m}{2}\right)\right]$$

$$v_0^{pl,j^*} = \frac{1}{k_h}\left[\left(\frac{f^{pl,j^*} \cdot h}{b \cdot j^*} - 0\right)\right]$$

$$v_0^{pl,j^*} = \frac{1}{k_h} \cdot \frac{f^{pl,j^*} \cdot h}{b \cdot j^*}$$

Therefore, condition state inequation (183) can be develop as:

$$d_{y,h} > V_0^{el,m} + \sum_{j=j^*-1}^{m-1} v_0^{pl,j^*}$$

$$d_{y,h} > \frac{1}{k_h}\left[\left(\frac{R_{w,c}^{el,m} \cdot h}{b \cdot m} - \frac{q \cdot b \cdot m}{2}\right) + \sum_{j=j^*-1}^{m-1} \frac{f^{pl,j} \cdot h}{b \cdot j}\right]$$

Equation (188)

From Equation (187):

$r_c = F_{c,y,i,j^*-1}\left(F = R_{w,c}^{el,\tilde{J}}, m = m\right) + \sum_{j=j^*+1}^{m-1} F_{c,y,i,j^*-1}\left(F = f^{pl,j}, m = j, q = 0\right) +$
$F_{c,y,i,j^*-1}\left(F = f^{pl,j^*}, m = j^*, q = 0\right)$

$$r_c = \frac{1}{n} \cdot \left[\frac{R_{w,c}^{el,m} \cdot h}{b \cdot m} - \frac{q \cdot b \cdot \left(m - 2 \cdot (m-2)\right)}{2}\right] + \sum_{j=j^*+1}^{m-1} \frac{1}{n} \cdot \frac{f^{pl,j} \cdot h}{b \cdot j} + \frac{1}{n} \cdot \frac{f^{pl,j^*} \cdot h}{b \cdot j^*}$$

$$\frac{f^{pl,j^*} \cdot h}{b \cdot j^*} = n \cdot r_c - \frac{R_{w,c}^{el,m} \cdot h}{b \cdot m} + \frac{q \cdot b \cdot \left(m - 2 \cdot (m-2)\right)}{2} - \sum_{j=j^*+1}^{m-1} \frac{f^{pl,j} \cdot h}{b \cdot j}$$

$$f^{pl,j^*} = \frac{n \cdot r_c \cdot b \cdot j^*}{h} - \frac{R_{w,c}^{el,m} \cdot j^*}{m} + \frac{q \cdot b^2 \cdot j^* \cdot \left(m - 2 \cdot (m-2)\right)}{2 \cdot h} - j^* \cdot \sum_{j=j^*+1}^{m-1} \frac{f^{pl,j}}{j}$$

$$f^{pl,j^*} = \frac{b \cdot j^*}{h} \cdot \left[n \cdot r_c + \frac{qb\left(m - 2(j^*-1)\right)}{2}\right] - j^* \cdot \left[\frac{R_{w,c}^{el,m}}{m} + \sum_{j=j^*+1}^{m-1} \frac{f^{pl,j}}{j}\right]$$

Equation (194)

$V_0^{el,m} = \frac{1}{k_h}\left[\left(\frac{R_{w,c}^{el,m} \cdot h}{b \cdot m} - \frac{q \cdot b \cdot m}{2}\right)\right]$ is established in Equation (165) of this Appendix.

$v_0^{pl,j^*} = \frac{1}{k_h} \cdot \frac{f^{pl,j^*} \cdot h}{b \cdot j^*}$ is established in Equation (183) of this Appendix.

$$d_{y,h} > V_0^{el,m} + \sum_{j=\hat{j}+1}^{m-1} v_0^{pl,j} + v_0^{pl,\hat{j}\prime}$$

$$d_{y,h} > \frac{1}{k_h}\left[\left(\frac{R_{w,c}^{el,m} \cdot h}{b \cdot \tilde{j}} - \frac{q \cdot b \cdot \tilde{j}}{2}\right) + \sum_{j=\hat{j}+1}^{m-1} \frac{f^{pl,j} \cdot h}{b \cdot j} + \frac{f'^{\,pl,\hat{j}} \cdot h}{b \cdot \hat{j}}\right]$$

Equation (201)

$V_0^{el,m} = \frac{1}{k_h}\left[\left(\frac{R_{w,c}^{el,m} \cdot h}{b \cdot m} - \frac{q \cdot b \cdot m}{2}\right)\right]$ is established in Equation (165) of this Appendix.

$v_0^{pl,j^*} = \frac{1}{k_h} \cdot \frac{f^{pl,j^*} \cdot h}{b \cdot j^*}$ is established in Equation (183) of this Appendix.

$$V_0^{el,m} + \sum_{j=j^*+1}^{m-1} v_0^{pl,j} < d_{y,h} < V_0^{el,m} + \sum_{j=j^*}^{m-1} v_0^{pl,j}$$

$$\frac{1}{k_h}\left[\left(\frac{R_{w,c}^{el,m} \cdot h}{b \cdot m} - \frac{q \cdot b \cdot m}{2}\right) + \sum_{j=j^*+1}^{m-1} \frac{f^{pl,j} \cdot h}{b \cdot j}\right] < d_{y,h}$$

$$< \frac{1}{k_h}\left[\left(\frac{R_{w,c}^{el,m} \cdot h}{b \cdot m} - \frac{q \cdot b \cdot m}{2}\right) + \sum_{j=j^*}^{m-1} \frac{f^{pl,j} \cdot h}{b \cdot j}\right]$$

Equation (203)

$V_0^{el,m} = \frac{1}{k_h}\left[\left(\frac{R_{w,c}^{el,m} \cdot h}{b \cdot m} - \frac{q \cdot b \cdot m}{2}\right)\right]$ is established in Equation (165) of this Appendix.

$v_0^{pl,j^*} = \frac{1}{k_h} \cdot \frac{f^{pl,j^*} \cdot h}{b \cdot j^*}$ is established in Equation (183) of this Appendix.

$$f'^{pl,\hat{j}} = f^{pl,\hat{j}} \cdot \frac{d_{u,h} - \left(V_0^{el,m} + \sum_{j=\hat{j}+1}^{m-1} v_0^{pl,j}\right)}{v_0^{pl,\hat{j}}}$$

$$f'^{pl,\hat{j}} = f^{pl,\hat{j}} \cdot \frac{d_{u,h} - \left(\frac{1}{k_h}\left[\left(\frac{R_{w,c}^{el,m} \cdot h}{b \cdot m} - \frac{q \cdot b \cdot m}{2}\right)\right] + \sum_{j=\hat{j}+1}^{m-1} \frac{1}{k_h} \cdot \frac{f^{pl,j} \cdot h}{b \cdot j}\right)}{\frac{1}{k_h} \cdot \frac{f^{pl,\hat{j}} \cdot h}{b \cdot \hat{j}}}$$

$$f'^{pl,\hat{j}} = \frac{k_h \cdot b \cdot \hat{j} \cdot d_{u,h}}{h} - \frac{k_h \cdot b \cdot \hat{j}}{h} \cdot \left(\frac{1}{k_h}\left[\left(\frac{R_{w,c}^{el,m} \cdot h}{b \cdot m} - \frac{q \cdot b \cdot m}{2}\right)\right] + \sum_{j=\hat{j}+1}^{m-1} \frac{1}{k_h} \cdot \frac{f^{pl,j} \cdot h}{b \cdot j}\right)$$

$$f'^{pl,\hat{j}} = \frac{r_h \cdot b \cdot \hat{j}}{h} - \frac{R_{w,c}^{el,m}}{m} - \sum_{j=\hat{j}+1}^{m-1} \frac{f^{pl,j}}{j} + \frac{q \cdot b^2 \cdot m}{2 \cdot \mathrm{h}}$$

$$f'^{pl,\hat{j}} = \hat{j} \cdot \left[\frac{b}{h}\left(r_h + \frac{q \cdot b \cdot m}{2}\right) - \frac{R_{w,c}^{el,m}}{m} - \sum_{j=\hat{j}+1}^{m-1} \frac{f^{pl,j}}{j}\right]$$

Equation (213)

From Casagrande et al. (2017):

$$T^{el,m} = \frac{R_{w,c}^{el,m} \cdot h}{b \cdot m} - \frac{q \cdot b \cdot m}{2}$$

$$t^{pl,j} = \frac{f^{pl,j} \cdot h}{b \cdot j}$$

Therefore, the following equality can be written to achieve the hold-down strength:

$$r_h = T^{el,m} + \sum_{j=2}^{m-1} t^{pl,j} + t^{pl,1}$$

$$r_h = \frac{R_{w,c}^{el,m} \cdot h}{b \cdot m} - \frac{q \cdot b \cdot m}{2} + \sum_{j=2}^{m-1} \frac{f^{pl,j} \cdot h}{b \cdot j} + t^{pl,1}$$

$$t^{pl,1} = r_h - \left[\frac{R_{w,c}^{el,m} \cdot h}{b \cdot m} - \frac{q \cdot b \cdot m}{2} + \sum_{j=2}^{m-1} \frac{f^{pl,j} \cdot h}{b \cdot j} \right]$$

$t^{pl,j} = \frac{f^{pl,j} \cdot h}{b \cdot j}$ is established in Equation (212) of this Appendix.

From Equation (212),

$$t^{pl,1} = r_h - \left[\frac{R_{w,c}^{el,m} \cdot h}{b \cdot m} - \frac{q \cdot b \cdot m}{2} + \sum_{j=2}^{m-1} \frac{f^{pl,j} \cdot h}{b \cdot j} \right]$$

Therefore:

$$\frac{f^{pl,1} \cdot h}{b} = r_h - \left[\frac{R_{w,c}^{el,m} \cdot h}{b \cdot m} - \frac{q \cdot b \cdot m}{2} + \sum_{j=2}^{m-1} \frac{f^{pl,j} \cdot h}{b \cdot j} \right]$$

$$f^{pl,1} = \frac{b}{h} \cdot r_h - \left[\frac{R_{w,c}^{el,m}}{m} - \frac{q \cdot b^2 \cdot m}{2 \cdot h} + \sum_{j=2}^{m-1} \frac{f^{pl,j}}{j} \right]$$

Equation (218)

$V_0^{el,m} = \frac{1}{k_h} \left[\left(\frac{R_{w,c}^{el,m} \cdot h}{b \cdot m} - \frac{q \cdot b \cdot m}{2} \right) \right]$ is established in Equation (165) of this Appendix.

$v_0^{pl,j^*} = \frac{1}{k_h} \cdot \frac{f^{pl,j^*} \cdot h}{b \cdot j^*}$ is established in Equation (183) of this Appendix.

$$d_{y,h} > V_0^{el,m} + \sum_{j=2}^{m-1} v_0^{pl,j} + v_0'^{\,pl,1}$$

$$d_{y,h} > \frac{1}{k_h}\left[\left(\frac{R_{w,c}^{el,m} \cdot h}{b \cdot m} - \frac{q \cdot b \cdot m}{2}\right) + \sum_{j=2}^{m-1} \frac{f^{pl,j} \cdot h}{b \cdot j} + \frac{f'^{\,pl,1} \cdot h}{b}\right]$$

Equation (225)

$V_0^{el,m} = \frac{1}{k_h}\left[\left(\frac{R_{w,c}^{el,m} \cdot h}{b \cdot m} - \frac{q \cdot b \cdot m}{2}\right)\right]$ is established in Equation (165) of this Appendix.

$v_0^{pl,j^*} = \frac{1}{k_h} \cdot \frac{f^{pl,j^*} \cdot h}{b \cdot j^*}$ is established in Equation (183) of this Appendix.

$$d_{y,h} > V_0^{el,m} + \sum_{j=2}^{m-1} v_0^{pl,j}$$

$$d_{y,h} > \frac{1}{k_h} \cdot \left[\frac{R_{w,c}^{el,m} \cdot h}{b \cdot m} - \frac{q \cdot b \cdot m}{2} + \sum_{j=2}^{m-1} \frac{f^{pl,j} \cdot h}{b \cdot j}\right]$$

Equation (237)

From Equation (235):

$$r_c = F_{c,y,\mathrm{i},\tilde{j}-1}(F = R_{w,c}^{el,\tilde{j}}, m = \tilde{j}) + F_{c,y,i,\tilde{j}-1}(f^{pl,\tilde{j}}, m = \tilde{j}, q = 0)$$

$$r_c = \frac{R_{w,c}^{el,\tilde{j}} \cdot h}{n \cdot b} \cdot \frac{\tilde{j} \cdot k_h}{(\tilde{j} + m \cdot \tilde{j} - m) \cdot k_h + (m - \tilde{j}) \cdot n \cdot k_c} - \frac{q \cdot b}{2 \cdot n}$$
$$\cdot \frac{\tilde{j}^2 \cdot m \cdot k_h - 2 \cdot (\tilde{j} - 1) \cdot [(\tilde{j} + m \cdot \tilde{j} - m) \cdot k_h + (m - \tilde{j}) \cdot n \cdot k_c]}{(\tilde{j} + m \cdot \tilde{j} - m) \cdot k_h + (m - \tilde{j}) \cdot n \cdot k_c} + \frac{f^{pl,\tilde{j}} \cdot h}{n \cdot b}$$

$$\frac{f^{pl,\tilde{j}} \cdot h}{n \cdot b} = r_c - \frac{R_{w,c}^{el,\tilde{j}} \cdot h}{n \cdot b} \cdot \frac{\tilde{j} \cdot k_h}{(\tilde{j} + m \cdot \tilde{j} - m) \cdot k_h + (m - \tilde{j}) \cdot n \cdot k_c} + \frac{q \cdot b}{2 \cdot n}$$
$$\cdot \frac{\tilde{j}^2 \cdot m \cdot k_h - 2 \cdot (\tilde{j} - 1) \cdot [(\tilde{j} + m \cdot \tilde{j} - m) \cdot k_h + (m - \tilde{j}) \cdot n \cdot k_c]}{(\tilde{j} + m \cdot \tilde{j} - m) \cdot k_h + (m - \tilde{j}) \cdot n \cdot k_c}$$

$$f^{pl,\tilde{j}} = \frac{b \cdot \tilde{j}}{h}\left[n \cdot r_c + \frac{qb}{2} \cdot \frac{\tilde{j}^2 \cdot m \cdot k_h - 2 \cdot (\tilde{j} - 1) \cdot [(\tilde{j} + m \cdot \tilde{j} - m) \cdot k_h + (m - \tilde{j}) \cdot n \cdot k_c]}{(\tilde{j} + m \cdot \tilde{j} - m) \cdot k_h + (m - \tilde{j}) \cdot n \cdot k_c}\right]$$

$$- \frac{R_{w,c}^{el,\tilde{j}} \cdot \tilde{j}^2 \cdot k_h}{(\tilde{j} + m \cdot \tilde{j} - m) \cdot k_h + (m - \tilde{j}) \cdot n \cdot k_c}$$

Equation (243)

From Casagrande et al. (2017), the elongation of hold-down through the elastic state is:

$$V_0^{el,\tilde{j}} = \frac{1}{k_h}\left(\frac{R_{w,c}^{el,\tilde{j}} \cdot h}{b} - \frac{q \cdot b \cdot m \cdot \tilde{j}}{2}\right) \cdot \frac{\tilde{j} \cdot k_h}{(\tilde{j} + m \cdot \tilde{j} - m) \cdot k_h + (m - \tilde{j}) \cdot n \cdot k_c}$$

The elongation through kinematic mode $j^*$for $[\,\tilde{j}, m - 1]$ is given with the same equation than for SW behaviour:

$$v_0^{pl,j^*} = \frac{1}{k_h} \cdot \frac{f^{pl,j^*} \cdot h}{b \cdot j^*}$$

Therefore, Equation 243 is written as:

$$d_{y,h} > V_0^{el,\tilde{j}} + v_0^{pl,\tilde{j}}$$

$$d_{y,h} > \frac{1}{k_h} \cdot \left[\left(\frac{R_{w,c}^{el,\tilde{j}} \cdot h}{b} - \frac{q \cdot b \cdot m \cdot \tilde{j}}{2}\right) \cdot \frac{\tilde{j} \cdot k_h}{(\tilde{j} + m \cdot \tilde{j} - m) \cdot k_h + (m - \tilde{j}) \cdot n \cdot k_c} + \frac{f'^{\,pl,\tilde{j}} \cdot h}{b \cdot \tilde{j}}\right]$$

Equation (250)

$V_0^{el,\tilde{j}} = \frac{1}{k_h}\left(\frac{R_{w,c}^{el,\tilde{j}} \cdot h}{b} - \frac{q \cdot b \cdot m \cdot \tilde{j}}{2}\right) \cdot \frac{\tilde{j} \cdot k_h}{(\tilde{j} + m \cdot \tilde{j} - m) \cdot k_h + (m - \tilde{j}) \cdot n \cdot k_c}$ is established in Equation (243) of this Appendix.

$v_0^{pl,j^*} = \frac{1}{k_h} \cdot \frac{f^{pl,j^*} \cdot h}{b \cdot j^*}$ is established in Equation (243) of this Appendix.

$$d_{y,h} < V_0^{el,\tilde{j}} + v_0^{pl,\tilde{j}}$$

$$d_{y,h} < \frac{1}{k_h} \cdot \left[\left(\frac{R_{w,c}^{el,\tilde{j}} \cdot h}{b} - \frac{q \cdot b \cdot m \cdot \tilde{j}}{2} \right) \cdot \frac{\tilde{j} \cdot k_h}{(\tilde{j} + m \cdot \tilde{j} - m) \cdot k_h + (m - \tilde{j}) \cdot n \cdot k_c} + \frac{f^{\,pl,\tilde{j}} \cdot h}{b \cdot \tilde{j}} \right]$$

Equation (252)

$V_0^{el,\tilde{j}} = \frac{1}{k_h} \left(\frac{R_{w,c}^{el,\tilde{j}} \cdot h}{b} - \frac{q \cdot b \cdot m \cdot \tilde{j}}{2} \right) \cdot \frac{\tilde{j} \cdot k_h}{(\tilde{j} + m \cdot \tilde{j} - m) \cdot k_h + (m - \tilde{j}) \cdot n \cdot k_c}$ is established in Equation (243) of this Appendix.

$v_0^{pl,j^*} = \frac{1}{k_h} \cdot \frac{f^{pl,j^*} \cdot h}{b \cdot j^*}$ is established in Equation (243) of this Appendix.

$$f'^{\,pl,\hat{j}} = f^{pl,\hat{j}} \cdot \frac{d_{u,h} - \left(V_0^{el,\tilde{j}} \right)}{v_0^{pl,\tilde{j}}}$$

$$f'^{\,pl,\hat{j}} = f^{pl,\hat{j}} \cdot \frac{d_{u,h} - \left(\frac{1}{k_h} \left(\frac{R_{w,c}^{el,\tilde{j}} \cdot h}{b} - \frac{q \cdot b \cdot m \cdot \tilde{j}}{2} \right) \cdot \frac{\tilde{j} \cdot k_h}{(\tilde{j} + m \cdot \tilde{j} - m) \cdot k_h + (m - \tilde{j}) \cdot n \cdot k_c} \right)}{\frac{1}{k_h} \cdot \frac{f^{pl,\tilde{j}} \cdot h}{b \cdot \tilde{j}}}$$

$$f'^{\,pl,\hat{j}} = \frac{k_h \cdot b \cdot \tilde{j} \cdot d_{u,h}}{h} - \frac{k_h \cdot b \cdot \tilde{j}}{h} \cdot \left(\frac{1}{k_h} \left(\frac{R_{w,c}^{el,\tilde{j}} \cdot h}{b} - \frac{q \cdot b \cdot m \cdot \tilde{j}}{2} \right) \cdot \frac{\tilde{j} \cdot k_h}{(\tilde{j} + m \cdot \tilde{j} - m) \cdot k_h + (m - \tilde{j}) \cdot n \cdot k_c} \right)$$

$$f'^{\,pl,\hat{j}} = \frac{r_h \cdot b \cdot \tilde{j}}{h} - \frac{\tilde{j}^2 \cdot k_h}{(\tilde{j} + m \cdot \tilde{j} - m) \cdot k_h + (m - \tilde{j}) \cdot n \cdot k_c} \left[R_{w,c}^{el,\tilde{j}} - \frac{q \cdot b^2 \cdot m \cdot \tilde{j}}{2 \cdot h} \right]$$

Equation (263)

$V_0^{el,\tilde{j}} = \frac{1}{k_h}\left(\frac{R_{w,c}^{el,\tilde{j}} \cdot h}{b} - \frac{q \cdot b \cdot m \cdot \tilde{j}}{2}\right) \cdot \frac{\tilde{j} \cdot k_h}{(\tilde{j} + m \cdot \tilde{j} - m) \cdot k_h + (m - \tilde{j}) \cdot n \cdot k_c}$ is established in Equation (243) of this Appendix.

$v_0^{pl,j^*} = \frac{1}{k_h} \cdot \frac{f^{pl,j^*} \cdot h}{b \cdot j^*}$ is established in Equation (243) of this Appendix.

$$d_{y,h} > V_0^{el,\tilde{j}} + \sum_{j=j^*}^{\tilde{j}} v_0^{pl,j}$$

$$d_{y,h} > \frac{1}{k_h} \cdot \left[\left(\frac{R_{w,c}^{el,\tilde{j}} \cdot h}{b} - \frac{q \cdot b \cdot m \cdot \tilde{j}}{2}\right) \cdot \frac{\tilde{j} \cdot k_h}{(\tilde{j} + m \cdot \tilde{j} - m) \cdot k_h + (m - \tilde{j}) \cdot n \cdot k_c} + \sum_{j=j^*}^{\tilde{j}} \frac{f^{pl,j} \cdot h}{b \cdot j}\right]$$

Equation (269)

From Equation (267)

$$r_c = F_{c,y,i,j^*-1}\left(F = R_{w,c}^{el,\tilde{j}}, m = \tilde{j}\right) + \sum_{j=j^*+1}^{\tilde{j}-1} F_{c,y,i,j^*-1}\left(F = f^{pl,j}, m = j, q = 0\right) + F_{c,y,i,j^*-1}\left(F = f^{pl,j^*}, m = j^*, q = 0\right)$$

$$r_c = \frac{R_{w,c}^{el,\tilde{j}} \cdot h}{n \cdot b} \cdot \frac{j^* \cdot k_h}{(j^* + m \cdot j^* - m) \cdot k_h + (m - j^*) \cdot n \cdot k_c} - \frac{q \cdot b}{2 \cdot n} \cdot \frac{j^{*2} \cdot m \cdot k_h - 2 \cdot j \cdot [(j^* + m \cdot j^* - m) \cdot k_h + (m - j^*) \cdot n \cdot k_c]}{(j^* + m \cdot j^* - m) \cdot k_h + (m - j^*) \cdot n \cdot k_c} + \sum_{j=j^*+1}^{\tilde{j}-1} \frac{f^{pl,j} \cdot h}{n \cdot b} + \frac{f^{pl,j^*} \cdot h}{n \cdot b}$$

$$\frac{f^{pl,j^*} \cdot h}{n \cdot b} = r_c - \frac{R_{w,c}^{el,\tilde{j}} \cdot h}{n \cdot b} \cdot \frac{j^* \cdot k_h}{(j^* + m \cdot j^* - m) \cdot k_h + (m - j^*) \cdot n \cdot k_c} + \frac{q \cdot b}{2 \cdot n}$$

$$\cdot \frac{{j^*}^2 \cdot m \cdot k_h - 2 \cdot j \cdot [(j^* + m \cdot j^* - m) \cdot k_h + (m - j^*) \cdot n \cdot k_c]}{(j^* + m \cdot j^* - m) \cdot k_h + (m - j^*) \cdot n \cdot k_c} - \sum_{j=j^*+1}^{\tilde{j}-1} \frac{f^{pl,j} \cdot h}{n \cdot b}$$

$$f^{pl,j^*} = \frac{b \cdot j^*}{h} \cdot \left[n \cdot r_c + \frac{qb}{2} \cdot \frac{\tilde{j}^2 \cdot m \cdot k_h - 2 \cdot (j^* - 1)[(j^* + m \cdot j^* - m) \cdot k_h + (m - j^*) \cdot n \cdot k_c]}{[(j^* + m \cdot j^* - m) \cdot k_h + (m - j^*) \cdot n \cdot k_c]} \right]$$

$$- j^* \cdot \left[\frac{\tilde{j} \cdot R_{w,c}^{el,\tilde{j}} \cdot k_h}{[(\tilde{j} + m \cdot \tilde{j} - m) \cdot k_h + (m - \tilde{j}) \cdot n \cdot k_c]} + \sum_{j=j^*+1}^{\tilde{j}-1} \frac{f^{pl,j}}{j} \right]$$

Equation (275)

$V_0^{el,\tilde{j}} = \frac{1}{k_h} \left(\frac{R_{w,c}^{el,\tilde{j}} \cdot h}{b} - \frac{q \cdot b \cdot m \cdot \tilde{j}}{2} \right) \cdot \frac{\tilde{j} \cdot k_h}{(\tilde{j} + m \cdot \tilde{j} - m) \cdot k_h + (m - \tilde{j}) \cdot n \cdot k_c}$ is established in Equation (243) of this Appendix.

$v_0^{pl,j^*} = \frac{1}{k_h} \cdot \frac{f^{pl,j^*} \cdot h}{b \cdot j^*}$ is established in Equation (243) of this Appendix.

$$d_{y,h} > V_0^{el,\tilde{j}} + \sum_{j=\hat{j}+1}^{\tilde{j}} v_0^{pl,j} + {v'}_0^{pl,j^*}$$

$$d_{y,h} > \frac{1}{k_h} \cdot \left[\left(\frac{R_{w,c}^{el,\tilde{j}} \cdot h}{b} - \frac{q \cdot b \cdot m \cdot \tilde{j}}{2} \right) \cdot \frac{\tilde{j} \cdot k_h}{(\tilde{j} + m \cdot \tilde{j} - m) \cdot k_h + (m - \tilde{j}) \cdot n \cdot k_c} \right.$$

$$\left. + \sum_{j=\hat{j}+1}^{\tilde{j}} \frac{f^{pl,j} \cdot h}{b \cdot j} + \frac{{f'}^{pl,\hat{j}} \cdot h}{b \cdot \hat{j}} \right]$$

Equation (282)

$V_0^{el,\tilde{\text{j}}} = \frac{1}{k_h}\left(\frac{R_{w,c}^{el,\tilde{\text{j}}} \cdot h}{b} - \frac{q \cdot b \cdot m \cdot \tilde{j}}{2}\right) \cdot \frac{\tilde{j} \cdot k_h}{(\tilde{j}+m \cdot \tilde{j}-m) \cdot k_h + (m-\tilde{j}) \cdot n \cdot k_c}$ is established in Equation (243) of this Appendix.

$v_0^{pl,j^*} = \frac{1}{k_h} \cdot \frac{f^{pl,j^*} \cdot h}{b \cdot j^*}$ is established in Equation (243) of this Appendix.

$$V_0^{el,\tilde{\text{j}}} + \sum_{j=j^*+1}^{\tilde{j}} v_0^{pl,j} < d_{y,h} < V_0^{el,\tilde{\text{j}}} + \sum_{j=j^*}^{\tilde{j}} v_0^{pl,j}$$

$$\frac{1}{k_h} \cdot \left[\left(\frac{R_{w,c}^{el,\tilde{\text{j}}} \cdot h}{b} - \frac{q \cdot b \cdot m \cdot \tilde{j}}{2}\right) \cdot \frac{\tilde{j} \cdot k_h}{(\tilde{j} + m \cdot \tilde{j} - m) \cdot k_h + (m - \tilde{j}) \cdot n \cdot k_c} + \sum_{j=j^*+1}^{\tilde{j}} \frac{f^{pl,j} \cdot h}{b \cdot j}\right] < d_{y,h}$$
$$< \frac{1}{k_h} \cdot \left[\left(\frac{R_{w,c}^{el,\tilde{\text{j}}} \cdot h}{b} - \frac{q \cdot b \cdot m \cdot \tilde{j}}{2}\right) \cdot \frac{\tilde{j} \cdot k_h}{(\tilde{j} + m \cdot \tilde{j} - m) \cdot k_h + (m - \tilde{j}) \cdot n \cdot k_c} + \sum_{j=j^*}^{\tilde{j}} \frac{f^{pl,j} \cdot h}{b \cdot j}\right]$$

Equation (284)

$V_0^{el,\tilde{\text{j}}} = \frac{1}{k_h}\left(\frac{R_{w,c}^{el,\tilde{\text{j}}} \cdot h}{b} - \frac{q \cdot b \cdot m \cdot \tilde{j}}{2}\right) \cdot \frac{\tilde{j} \cdot k_h}{(\tilde{j}+m \cdot \tilde{j}-m) \cdot k_h + (m-\tilde{j}) \cdot n \cdot k_c}$ is established in Equation (243) of this Appendix.

$v_0^{pl,j^*} = \frac{1}{k_h} \cdot \frac{f^{pl,j^*} \cdot h}{b \cdot j^*}$ is established in Equation (243) of this Appendix.

$$f'^{\,pl,\hat{j}} = f^{pl,\hat{j}} \cdot \frac{d_{u,h} - \left(V_0^{el,\tilde{\text{j}}} + \sum_{j=\hat{j}+1}^{\tilde{j}} v_0^{pl,j}\right)}{v_0^{pl,\hat{j}}}$$

$$f'^{\,pl,\hat{j}} = f^{pl,\hat{j}} \cdot \frac{d_{u,h} - \left(\frac{1}{k_h}\left(\frac{R_{w,c}^{el,\tilde{\text{j}}} \cdot h}{b} - \frac{q \cdot b \cdot m \cdot \tilde{j}}{2}\right) \cdot \frac{\tilde{j} \cdot k_h}{(\tilde{j} + m \cdot \tilde{j} - m) \cdot k_h + (m - \tilde{j}) \cdot n \cdot k_c} + \sum_{j=\hat{j}+1}^{\tilde{j}} \frac{1}{k_h} \cdot \frac{f^{pl,j^*} \cdot h}{b \cdot j^*}\right)}{\frac{1}{k_h} \cdot \frac{f^{pl,\hat{j}} \cdot h}{b \cdot \hat{j}}}$$

$$f'^{pl,\hat{j}} = \frac{k_h \cdot b \cdot \hat{j} \cdot d_{u,h}}{h} - \frac{k_h \cdot b \cdot \hat{j}}{h} \cdot \left(\frac{1}{k_h} \left(\frac{R_{w,c}^{el,\tilde{j}} \cdot h}{b} - \frac{q \cdot b \cdot m \cdot \tilde{j}}{2} \right) \cdot \frac{\tilde{j} \cdot k_h}{(\tilde{j} + m \cdot \tilde{j} - m) \cdot k_h + (m - \tilde{j}) \cdot n \cdot k_c} + \sum_{j=\hat{j}+1}^{\tilde{j}} \frac{1}{k_h} \cdot \frac{f^{pl,j^*} \cdot h}{b \cdot j^*} \right)$$

$$f'^{pl,\hat{j}} = \hat{j} \cdot \left[\frac{b}{h} \left(r_h - \frac{\tilde{j} \cdot k_h}{(\tilde{j} + m \cdot \tilde{j} - m) \cdot k_h + (m - \tilde{j}) \cdot n \cdot k_c} \cdot \left(\frac{R_{w,c}^{el,\tilde{j}} \cdot h}{b} - \frac{q \cdot b \cdot m \cdot \tilde{j}}{2} \right) \right) - \sum_{j=\hat{j}+1}^{\tilde{j}} \frac{f^{pl,j}}{j} \right]$$

Equation (294)

From Casagrande et al. (2017):

$$T^{el,\tilde{j}} = \left(\frac{R_{w,c}^{el,\tilde{j}} \cdot h}{b} - \frac{q \cdot b \cdot m \cdot \tilde{j}}{2} \right) \cdot \frac{\tilde{j} \cdot k_h}{(j^* + m \cdot j^* - m) \cdot k_h + (m - j^*) \cdot n \cdot k_c}$$

$$t^{pl,j} = \frac{f^{pl,j} \cdot h}{b \cdot j}$$

Therefore, the following equality can be written to achieve the hold-down strength:

$$r_h = T^{el,\tilde{j}} + \sum_{j=2}^{\tilde{j}} t^{pl,j} + t^{pl,1}$$

$$r_h = \left(\frac{R_{w,c}^{el,\tilde{j}} \cdot h}{b} - \frac{q \cdot b \cdot m \cdot \tilde{j}}{2} \right) \cdot \frac{\tilde{j} \cdot k_h}{(j^* + m \cdot j^* - m) \cdot k_h + (m - j^*) \cdot n \cdot k_c} + \sum_{j=2}^{\tilde{j}} \frac{f^{pl,j} \cdot h}{b \cdot j} + t^{pl,1}$$

$$t^{pl,1} = r_h - \left[\left(\frac{R_{w,c}^{el,\tilde{j}} \cdot h}{b} - \frac{q \cdot b \cdot m \cdot \tilde{j}}{2} \right) \cdot \frac{\tilde{j} \cdot k_h}{(j^* + m \cdot j^* - m) \cdot k_h + (m - j^*) \cdot n \cdot k_c} + \sum_{j=2}^{\tilde{j}} \frac{f^{pl,j} \cdot h}{b \cdot j} \right]$$

Equation (296)

$t^{pl,j} = \frac{f^{pl,j} \cdot h}{b \cdot j}$ is established in Equation (212) of this Appendix.

From Equation (293),

$t^{pl,1} = r_h - \left[\left(\frac{R_{w,c}^{el,\tilde{j}} \cdot h}{b} - \frac{q \cdot b \cdot m \cdot \tilde{j}}{2}\right) \cdot \frac{\tilde{j} \cdot k_h}{(j^* + m \cdot j^* - m) \cdot k_h + (m - j^*) \cdot n \cdot k_c} + \sum_{j=2}^{\tilde{j}} \frac{f^{pl,j} \cdot h}{b \cdot j}\right]$

Therefore:

$$\frac{f^{pl,1} \cdot h}{b} = r_h - \left[\left(\frac{R_{w,c}^{el,\tilde{j}} \cdot h}{b} - \frac{q \cdot b \cdot m \cdot \tilde{j}}{2}\right) \cdot \frac{\tilde{j} \cdot k_h}{(j^* + m \cdot j^* - m) \cdot k_h + (m - j^*) \cdot n \cdot k_c} + \sum_{j=2}^{\tilde{j}} \frac{f^{pl,j} \cdot h}{b \cdot j}\right]$$

$$f^{pl,1} = \frac{b}{h} \cdot r_h - \left[\left(R_{w,c}^{el,\tilde{j}} - \frac{q \cdot b^2 \cdot m \cdot \tilde{j}}{2 \cdot h}\right) \cdot \frac{\tilde{j} \cdot k_h}{(j^* + m \cdot j^* - m) \cdot k_h + (m - j^*) \cdot n \cdot k_c} + \sum_{j=2}^{\tilde{j}} \frac{f^{pl,j}}{j}\right]$$

Equation (300)

$V_0^{el,\tilde{j}} = \frac{1}{k_h}\left(\frac{R_{w,c}^{el,\tilde{j}} \cdot h}{b} - \frac{q \cdot b \cdot m \cdot \tilde{j}}{2}\right) \cdot \frac{\tilde{j} \cdot k_h}{(\tilde{j} + m \cdot \tilde{j} - m) \cdot k_h + (m - \tilde{j}) \cdot n \cdot k_c}$ is established in Equation (243) of this Appendix.

$v_0^{pl,j^*} = \frac{1}{k_h} \cdot \frac{f^{pl,j^*} \cdot h}{b \cdot j^*}$ is established in Equation (243) of this Appendix.

$$d_{y,h} > V_0^{el,\tilde{j}} + \sum_{j=2}^{\tilde{j}} v_0^{pl,j} + v_0'^{\,pl,1}$$

$$d_{y,h} > \frac{1}{k_h} \cdot \left[\left(\frac{R_{w,c}^{el,\tilde{\jmath}} \cdot h}{b} - \frac{q \cdot b \cdot m \cdot \tilde{\jmath}}{2} \right) \cdot \frac{\tilde{\jmath} \cdot k_h}{(\tilde{\jmath} + m \cdot \tilde{\jmath} - m) \cdot k_h + (m - \tilde{\jmath}) \cdot n \cdot k_c} + \sum_{j=2}^{\tilde{\jmath}} \frac{f^{pl,j} \cdot h}{b \cdot j} + \frac{f'^{\,pl,1} \cdot h}{b} \right]$$

Equation (307)

$V_0^{el,\tilde{\jmath}} = \frac{1}{k_h} \left(\frac{R_{w,c}^{el,\tilde{\jmath}} \cdot h}{b} - \frac{q \cdot b \cdot m \cdot \tilde{\jmath}}{2} \right) \cdot \frac{\tilde{\jmath} \cdot k_h}{(\tilde{\jmath} + m \cdot \tilde{\jmath} - m) \cdot k_h + (m - \tilde{\jmath}) \cdot n \cdot k_c}$ is established in Equation (243) of this Appendix.

$v_0^{pl,j^*} = \frac{1}{k_h} \cdot \frac{f^{pl,j^*} \cdot h}{b \cdot j^*}$ is established in Equation (243) of this Appendix.

$$d_{y,h} > V_0^{el,\tilde{\jmath}} + \sum_{j=2}^{\tilde{\jmath}} v_0^{pl,j}$$

$$d_{y,h} > \frac{1}{k_h} \cdot \left[\left(\frac{R_{w,c}^{el,\tilde{\jmath}} \cdot h}{b} - \frac{q \cdot b \cdot m \cdot \tilde{\jmath}}{2} \right) \cdot \frac{\tilde{\jmath} \cdot k_h}{(\tilde{\jmath} + m \cdot \tilde{\jmath} - m) \cdot k_h + (m - \tilde{\jmath}) \cdot n \cdot k_c} + \sum_{j=2}^{\tilde{\jmath}} \frac{f^{pl,j} \cdot h}{b \cdot j} \right]$$